Theoretical Analysis and Numerical Investigation of Atrium Fire Engineering Design Principles

by

Tsun Bong CHAN

A thesis submitted in partial fulfilment for the requirements

for the degree of Doctor of Philosophy

at the

University of Central Lancashire

May 2024

Title:

“Theoretical Analysis and Numerical Investigation of Atrium Fire Engineering Design Principles”

Student Declaration

RESEARCH STUDENT DECLARATION FORM

Type of Award Doctor of Philosophy

School Engineering and Computing

*Sections marked * delete as appropriate*

1. Concurrent registration for two or more academic awards

Either *I declare that while registered as a candidate for the research degree, I have not been a registered candidate or enrolled student for another award of the University or other academic or professional institution

or ~~*I declare that while registered for the research degree, I was with the University's specific permission, a *registered candidate/*enrolled student for the following award:~~

_____

_____

2. Material submitted for another award

Either *I declare that no material contained in the thesis has been used in any other submission for an academic award and is solely my own work

or ~~*I declare that the following material contained in the thesis formed part of a submission for the award of:~~

_____

(state award and awarding body and list the material below):

_____

3. Collaboration

Where a candidate's research programme is part of a collaborative project, the thesis must indicate in addition clearly the candidate's individual contribution and the extent of the collaboration. Please state below:

_____

4. Use of a Proof-reader

Either ~~*The following third-party proof-reading service was used for this thesis _____ in accordance with the Policy on Proof-reading for Research Degree Programmes and the Research Element of Professional Doctorate Programmes.~~
~~A copy of the confirmatory statement of acceptance from that service has been lodged with the Academic Registry.~~

or *No proof-reading service was used in the compilation of this thesis.

Signature of Candidate _____

Print name: TSUN BONG CHAN

Abstract

In the project described in this thesis, computational fluid dynamics (CFD) was used comparatively with the traditional calculation approach to predict smoke behaviour in tall and long atrium geometries in order to review the empirical correlations used to this day. It is demonstrated that the empirical correlations specified in the regulations, design guides, and handbook for the industry, which were based on theory and experiments done for more than 30 to 45 years before, may not be applicable nowadays to large volumes and high atriums.

A number of correlations exist, related to cross-sectional area and height. Particular focus is made in one of the most widely used correlations for smoke mass flow rate and height defined in the National Fire Protection Association (NFPA). The constant, 0.28 used in NFPA 92: 2021 for smoke layer height applied in atrium design based on cross-sectional area is evaluated. A parametric study and the limits of applicability of the correlation are investigated by numerical analysis. A wide range of geometric characteristics, i.e., height, width, Sectional Aspect Ratio (SAR) and Plan Aspect Ratio (PAR) are investigated.

Based on the results of the current investigation, new constants are proposed to be used, namely 0.25 and 0.24 for 20-30 m and 40 m tall atrium respectively.

For long atriums, results from empirical equations for rectangular-base long atriums with different PAR have also been compared with a series of numerical simulations.

New constants 0.25 and 0.27 seem to better fit the numerical results for 10-20 m and 30-40 m long atriums. A simple table is presented for use by practitioner designers.

Current thesis results indicate that the constant is not universally applicable to atriums that are particularly high or long, and new correlations are applied with the aim of being used by fire safety engineers.

Some new results are also presented on the development of stratification in taller atria. There is an existing formula for this, valid for small atria, based upon the oxymoron of a temperature gradient. It was found that velocity profiles can identify where stratification will occur, and this influences the design strategy, such as not extracting gas above this height because it is not smoke.

Table of Contents

List of Tables

List of Figures

Nomenclature

Symbol	Quantity	Units
A	cross-sectional area	m^2
C	empirical constant	-
c_p	specific heat capacity of air at constant pressure	$kJ\ kg^{-1}K^{-1}$
g	acceleration due to gravity, 9.81	$m\ s^{-2}$
h	height of the opening	m
H	height of room	m
l_c	horizontal distance/separation	m
m	mass	$kg\ s^{-1}$
$\dot{m}$	mass flow rate	$kg\ s^{-1}$
n	empirical exponent	-
ρ_∞	density of ambient air	$kg\ m^{-3}$
P	pressure	Pa
q	total heat equivalent of room contents (fire load)	kJ
$\dot{Q}$	heat flow rate	kW
$\dot{Q}^*$	dimensionless heat release rate	-
T	temperature of smoke	℃ *or* K
T_0	ambient temperature	℃ *or* K
t	time	s
U	flow velocity	$m\ s^{-1}$
W	width of channel or opening	m
X	fraction of total heat flux	-
y	dimensionless height above floor, $y = z/H$	m
z	height above the floor, esp. smoke clearance height	m

Greek characters		
α_ε	entrainment coefficient	-
α	fire growth parameter	$kJ\ s^{-2}$
χ	combustion efficiency	-
σ	Stefan-Boltzmann constant, 5.67×10^{-11}	$kW\ m^{-2}\ K^{-4}$

ρ	Density	$kg\ m^{-3}$
τ	dimensionless time	-
ε	emissivity of smoky-hot layer	-
γ, δ	regression coefficients	-

Suffices	
B	balcony
b	burning rate
C	convective portion of heat flux, combustion
c	ceiling
d	discharge for a vertical opening
e	entrainment into fire plume
f	fire bed
fl	flame
g	hot/smoky gas layer
h	value at 'hot' location
i	at time of ignition
in	flow from cold location to hot location, esp. into a compartment
m	average value at a specific height along the centreline of plume
o, ∞	ambient value (outside enclosure)
out	flow from hot location to cold location, esp. out of an enclosure
p	plume
R	room, compartment floor-ceiling height
r	thermal radiation
s	horizontal separation of two fuels, spill plume
v	vent, window or doorway
1	virtual convective source of a fire plume

List of acronyms	
CFD	Computational Fluid Dynamics
FDS	Fire Dynamics Simulator
HRR	Heat Release Rate
PAR	Plan Aspect Ratio
PMV	Predicted Mean Vote index

NFPA	The National Fire Protection Association
SAR	Section Aspect Ratio

Acknowledgements

Firstly, I must thank you so much indeed for my advisors Dr. Eleni Asimakopoulou and Dr. Tony Graham.

I would like to thank my member of advisors, Dr. Andrei Chamchine, Dr. Weiming Liu, Dr. Champika Liyanage, and Dr. Jianqiang Mai. They have aided me as my friend, mentor, and advisors and give me invaluable intellectual guidance throughout this dissertation and enriching my knowledge, inspiring and sparked my interest in researching in the related area.

At the same time, I sincerely express my gratitude to all staff of School of Continuing and Professional Education (SCOPE) of the City University of Hong Kong regarding support and assistance for my study, in particular, the former programme leader – Mr. Fred Lau.

A special thanks to Dr. Jason Floyd, one of the authors of the Fire Dynamics Simulator User's Guide, takes time to answer my queries on fire source for FDS simulation result versus experimental data.

Finally, I would like to express my deepest thanks to my family. Their continuous support, patience and understanding throughout the course and this dissertation have assisted me to focus my study all these years. I would like to express my full-hearted gratitude to my family. Those all others that I have not addressed, and I hope that involve in my works will accept my implied thanks.

CHAPTER 1: Introduction

1.1 Scope and context

High-rise and tower buildings are commonly seen as a growing feature in cities. These buildings provide a controlled, convenient and comfortable environment. A large, open-spaced and glazed atrium is becoming a common design feature that allows architects to design outstanding works of art beyond interior design and also to consider external appearances. Despite this futuristic open-space concept, atria are ultimately a means to hold a greater population in a complicated and confined space in which fire has a chance of occurring.

The application of fire safety engineering primarily focuses on the evacuation of buildings in emergencies. Exploration of the effects of a fire on the evacuees and the structure of an unfamiliar building can help ensure that those affected are comfortable during stressful situations.

This project is concerned with the production, movement and effect of smoke when a fire occurs in an atrium.

When a fire occurs, the smoke generated fills the space, endangering the occupants and damaging public property. Smoke is regarded as a major threat to occupants, one which should be properly addressed using an appropriate smoke management system. In response, design codes and practices are informed by three sources of scientific research that should be used in synthesis. The first source is experimental measurement and empirical evaluation. The second is pen-and-paper calculation to review established formulae and standards. The third is the use of computational fluid dynamics (CFD) to simulate scenarios.

Full-scale experimentation is often expensive and pollutes the environment. When considering this, the scale of the laboratory also introduces conflict. Smaller-scale experimentation would be unrealistic and cannot simulate true results. Certain phenomena, such as boundary layers, make it difficult to place measuring devices precisely as a means of demonstrating accuracy, repeatability and generalizability with previously published works.

The pen-and-paper approach is generally accepted for simple atria and quasi-static conditions such as a carefully prescribed fire growth. The existing formulae have considered simple atria

in shopping malls, typically involving solutions of a single ordinary differential equation. As a result, previous equations have not considered the various shapes of an atrium, and thus the smoke layer cannot be determined accurately. Multiple design standards, such as NFPA 92,2021 [1], BRE 368,1999 [2], CIBSE Guide E,2010 [3] and, CIBSE TM19,1995 [4] have become standardised rules that have not changed resulting in a lack of modern updates to the formulae.

Computational fluid dynamics (CFD) [5] has become the predominant modern-day method available for engineers to explore atrium fires and calculate the effect of smoke. While it may still be beyond our abilities to specify the velocity and momentum of these fires and to manipulate individual particles in a macroscopic volume, current advancements allow simulations within an accuracy of ±10cm and a second-by-second simulation time of up to 15 minutes. This period is sufficient to capture large air flows and sub-scale estimations for realistic and valid predictions.

A vast number of iterations and convergence checks have been conducted using the latest FDS software build. However, this software does not include the most advanced sub-models of chemistry and physics compared to other CFD software, although it is sufficiently accurate for most fire-safety applications and is broadly accepted as an industrial standard. Although it was not applied during the creation of the design codes for predicting smoke fill, it is now widely used for confirmation purposes.

This project attempts to use CFD and the pen-and-paper approach to predict smoke behaviour in different sizes of atria in order to review the empirical correlations used to this day.

Modern atria are evolving into large and convoluted shapes and are made with increasingly novel materials. This project will consider various geometric aspects of an atrium, ranging from tall narrow (chimney-like) or wide flat structures, long narrow (corridor-like) layouts and atria that are wide or narrow in height above ground.

Such shapes provide a range of places for fire to occur and a range of places for ventilation systems to be implemented. Examples include doorways into and out of an atrium, such as an air-heater.

1.2 Aims and objectives

This project aims to employ CFD and the pen-and-paper approach to predict smoke behaviour in different sizes of atria and to re-evaluate and enhance the empirical formulae used in today's built environment. The sizes span the scale of modern atria.

More specifically, this thesis has five aims. First, it aims to analyse the physical mechanisms of smoke filling and smoke characteristics in atria. Second, it elaborates on research into the numerical tools and correlations used to predict smoke behaviour in atria. Third, it seeks to evaluate the effect of geometry and HRR on smoke-filling processes in atria. Fourth, it aims to exhibit the limitations of current methodologies for smoke filling when applied in atria. Finally, it seeks to develop a holistic methodology with improved practical implementation for smoke-filling calculations in atria.

The main objective of this study is to achieve the five aims, as a series of different tall and long atriums are considered:

(1) Literature review of empirical correlations for atria, plus types and configuration of atria;
(2) Literature review of design process;
(3) Literature review of experimental work on atria fires and smoke properties;
(4) Literature review of previous empirical correlations, with an emphasis on accurately estimating smoke layer, smoke-filling time and smoke production rate;
(5) Development of a numerical methodology using CFD to accurately simulate atrium smoke-filling;
(6) Data from past experimental data and fuel sources collected and compared with FDS for validation and verification;
(7) Parametric analysis of the effect of atrium geometric characteristics and HRR on smoke layer formation;
(8) Evaluation of empirical constants currently used in NFPA 92 for smoke layer height based on cross-sectional area; and
(9) Development of empirical calculations.

The project concludes with a list of factors that have an effect on atrium fires, such as height and constants used by practitioners in fire safety engineering.

1.3 Research Questions

This research raises the following questions:

(1) Are there any limitations to the contemporary concepts?

(2) Are there any complications with the current equations under review?

(3) Are there any problems with the calculation procedure?

(4) Does the mathematical formula for smoke spread accommodate the height and cross-sectional area of an atrium?

The findings of this study will examine the accuracy and appropriateness of using the same constants in the equations for various applications. They will also allow real-world designers to realistically assess the risks in atrium designs.

1.4 Structure of the thesis

Chapter 1 presents a general introduction of the background to the study, its aim and objectives, its methodology, and its value and contributions, along with a report outline structure and a summary of its main outcomes. **Chapter 2** is a literature review and examines both the codes used in the current fire safety design of atria, as well as the work that has been done using CFD. The chapter identifies the main problems that have been studied over time to estimate where the field is going and whether any missing or incomplete problems persist. The chapter also examines the different methodologies used to place that used within the current project. **Chapter 3** provides a methodological summary based on the results of the literature review. It explains how this project was taken to completion. **Chapter 4** elaborates upon the modelling procedure and explains how FDS works and how it was set up here. It also describes how a parametric study was formulated. **Chapter 5** evaluates the empirical correlations of smoke control and the development of empirical calculations. **Chapter 6** presents the conclusion of this study and possibilities for future work.

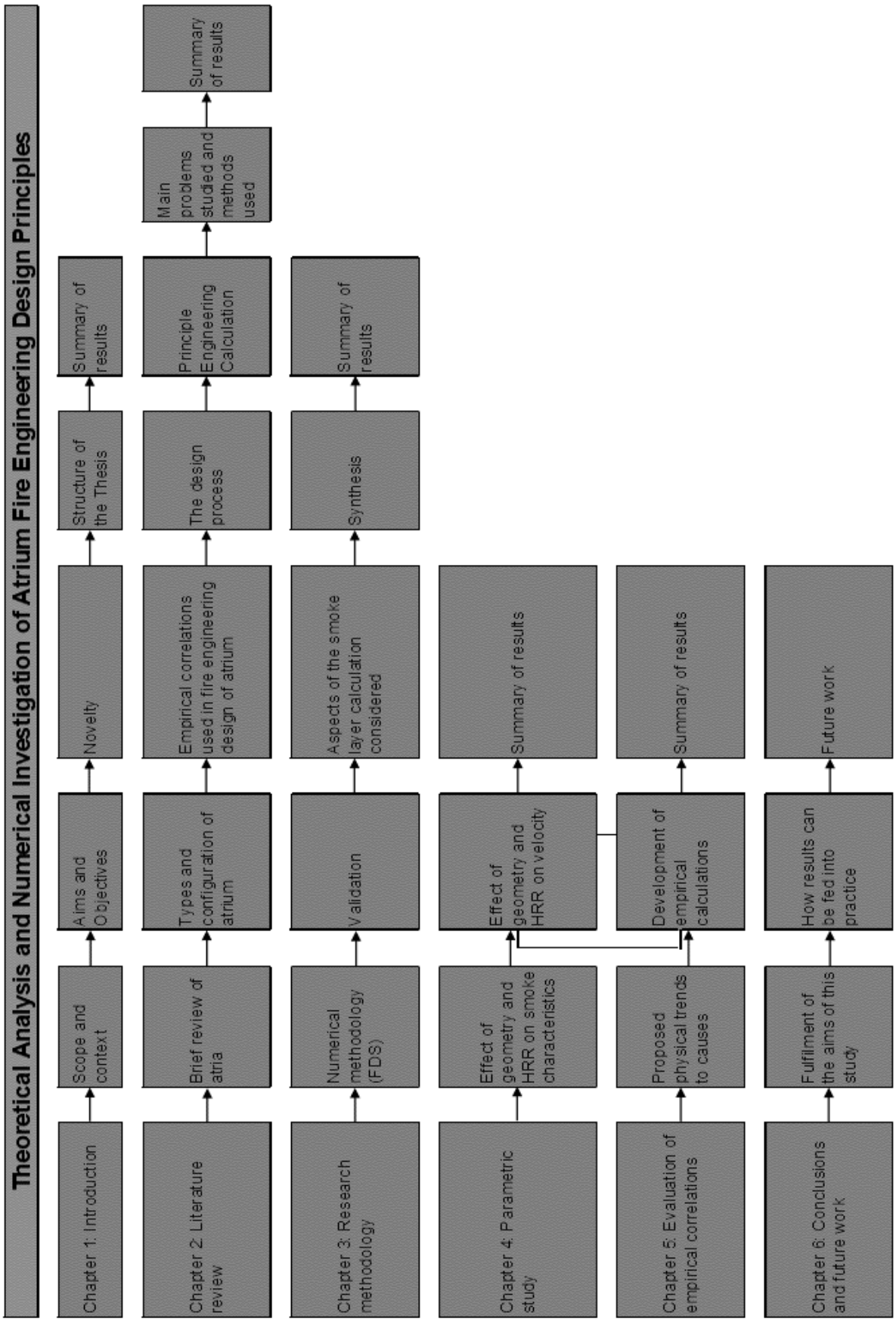

Figure 1-1 Structure of Thesis

The thesis includes a nomenclature section for the engineering formulae studied and a reference section listing the literature reviewed. An appendix also provides evidence of the simulations and data used to support the thesis argument.

1.5 Summary of results

This project looked at the safe design of atria, comparing established calculations with modern simulation techniques that offer significantly greater resolution and fundamental physics. It was found that some modification of the formulae could make significant improvements in limiting cases of fire, but that the established formulae had captured the main parameters to order-of-magnitude accuracy. Where discrepancies were found, the simulation approach offered physical explanations of whichever phenomena were not considered. The thesis concludes by suggesting corrections to the constants assumed for many years, as well as how allowances can be made for larger and more varied modern atria.

CHAPTER 2: Literature Review

2.1 Brief review of atria

In this chapter, the need for the study of smoke control is first established; the basic design process used around the world today is then described. Finally, the methods and problems under study are evaluated in order to arrive at the best way to achieve the project aims.

According to Our World in Data [6], the death rate from fire across the world in 2019 was 2 per 100,000, with a total death toll of 111,293. From the survey by NFPA, 2,730 civilian were killed in structure fire out of the total fire deaths of 3,500 in 2020, which accounted for 78% civilian loss in fire incident as shown in Table 2-1 [7]. The below Figure 2-1 shows the trend over the past 30 years from the data collected by Global Change Data Lab [6].

Figure 2-1 shows the number of deaths each year globally, extracted from a reliable data source Our World in Data [6]. The total is divided among age groups. The overall picture shows a significant decrease between 2005 and 2015, the bulk of which appears to be among the youngest people under 5. The birth rate is not shown, so this may or may not represent a constant fraction of the changing population.

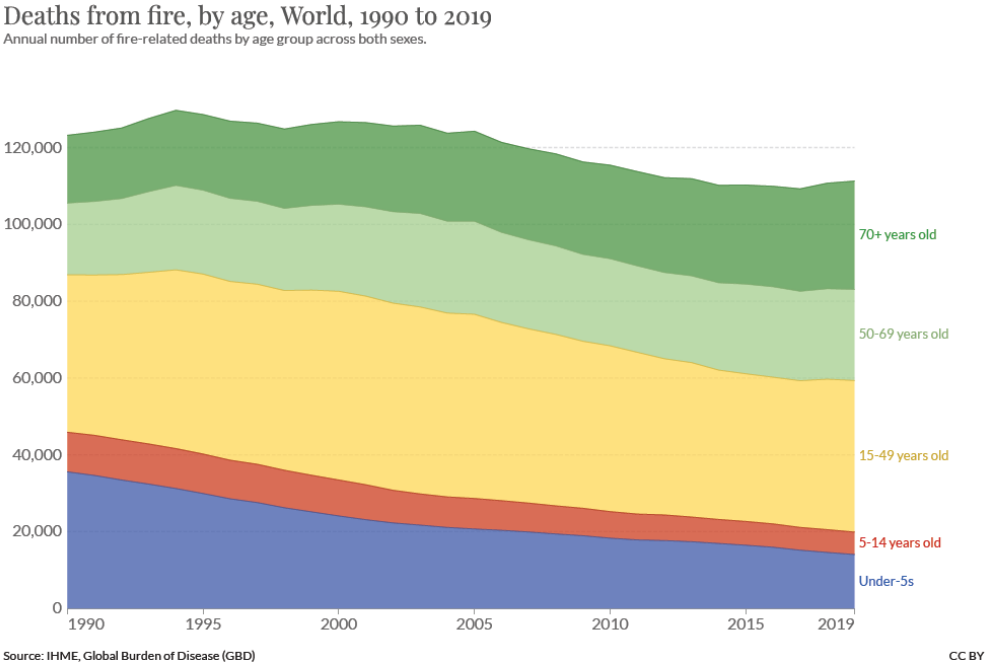

Figure 2-1 Global deaths from fire, by age, 1990 to 2019 [6]

Since we are not immortal, infallible or blessed with infinite resources for safety, some fire deaths are societally expected in even the most stable nations. However, a figure of around 100,000 per year is staggering and hard to consider societally acceptable. There may or may not have been some stagnation or event increase in fatalities since 2018; it is too soon to capture a long-term trend, and the world has undergone many changes, especially due to the Covid-19 pandemic. Nonetheless, it is sufficient to conclude that a significant reduction in fire-related deaths is desirable in all parts of the world. In the US, fire deaths in 2020 totalled 3,500, of which 2,730 were caused by structure fire with reference to NFPA's 2020 survey [7].

Figure 2-2 again shows decreasing fire deaths over several years compared to Figure 2-1. However, Figure 2-2 is for one nation, widely considered 'stable'. The death rate has almost halved, although it does not seem to have decreased further since 2001. Whatever social or political changes may have caused the drop, something more is now needed if 3,000 deaths per year are not to be permanently deemed acceptable.

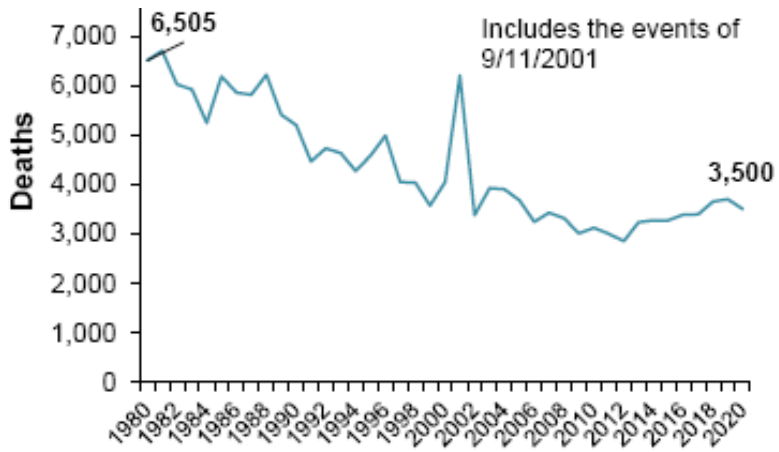

Figure 2-2 Civilian fire deaths by year [7]

Comparing Figure 2-1 and Figure 2-2, although they collect data on fire deaths in different ways, both show comparable decreasing trends and recent stagnation. Table 2-1 compares civilian deaths, injuries and property losses in the US in 2020. The salient point for this project is that structure fires make the greatest contribution in all cases. This is thought to be reflected in many countries, and it is sufficient evidence to focus the next generation of life-saving efforts on improving the fire safety engineering of the built environment. Although the death rate has dropped from 6,505 to 3,500, the elimination of fire risks remains the aim of all fire safety engineering design.

Table 2-1 Reported fires in 2020 by incident type extract from Fire Loss in the United States during 2020 – NFPA [7]

Incident Type	Fires		Civilian Deaths		Civilian Injuries		Property Loss (in millions)	
	No	%	No	%	No	%	US$	%
Fires in California Wildland - Urban Interface (WUI)							4,200	19
Structure Fire	490,500	35	2,730	78	13,000	86	12,107	55
Vehicle Fire	209,500	15	630	18	1,700	11	5,170	24
Outside and Other Fire	688,500	50	140	4	500	3	389	2
Total	1,388,500	100	3,500	100	15,200	100	21,866	100

Atria incorporated into commercial, industrial and any other type of premises are considered to have a high-risk profile due to population size and culpability of industry. Modern atria pose new challenges for fire safety design engineers; precaution and prevention of losing every single life and property are required. Therefore, the empirical correlations for calculation should be reliable to achieve this concern. The ultimate engineering target is the absolute control of an ever-increasing risk.

Contemporary atrium design usually has a large space either extra high or long. Regulations, codes of practice and industrial handbooks therefore set up the guidelines to the architectural design of atrium for smoke control.

There are well codified empirical correlations for the fire designers to follow. Research is continuing to update the ever improving the emerging discipline. The source for the empirical correlations prescribed in the NFPA92, 2021 [1], International Building Code (IBC), 2021 [8] , International standards and guides such as the International Standards Organisation ISO 23932-1, 2018 [9], CIBSE Guide E, Fire Engineering, 3rd Edition, Chartered Institute of Building Services Engineers (CIBSE), 2010 [3], BS 9999: Code of practice for fire safety in the design, management and use of buildings, British Standards Institution (BSI), 2017 [10], SFPE Handbook of Fire Protection Engineering, 5th Edition, Society of Fire Protection Engineers; Gaithersburg MD, 2016 [11]. Refereed journals, symposia and proceedings like International Conferences on Performance Base Design and Fire Safety are also as a referral.

However, many equations have been discovered by Morgan and Marshall (1975) [12] which comes from Law (1986) [13] in CIBSE Guide E 2010 [3], Thomas 1987 [14] included in BRE 368 1999 [2], Heskestad's model as given in Klote & Milke, 1992 [15] and demonstrated in NFPA 92B, 1991 [16], Poreh method set out in BRE 368 1999 over thirty to forty years for the mass flow rate in an enclosed fire compartment, these equations may not be applicable for the atria designs in the modern ages. Nowadays, some architects like Littlefair, P. (2002) [17], Moosavi, L. (2014) [18] , Wang, L., 2017 [19] have identified how aspect ratio may have an impact on energy efficiency in buildings and the effect of filling force by altering the ratio of an atrium. This would as a result affect the pulling force used to determine the movement of smoke. By having various aspect ratios in modern buildings, it can have an impact on the way ventilation works in a building.

According to a survey from Analysis of Atrium's Architectural Aspects in Office Buildings under Tropical Sky Conditions, 2010 [20], the most common atrium form is a centrally enclosed rectangular atrium or a linear atrium. The majority of atrium height is less than 5-storeys, at least one storey, and the tallest is 11-storey [20].

Atrium is a Latin word that refers to a main room or central court with a hearth since it causes the walls of the room to be covered with black soot as time elapses. The name "atrium" is typically referred as an ancient Roman house and later of a Christian Basilica. After 5000 years of development, it has been enveloped in households across ancient civilizations, classical civilizations, the Middle Ages, Renaissance civilizations, and modern civilizations. It experienced a revival in the middle of the 20th century.

However, in the modern era, its design has changed and resulted in glass walls and a roof which creates a common space interconnecting the adjacent galleries and stories within an atrium building. Atria and courtyards are commonly embedded in some buildings for natural ventilation and cooling purposes. Both atria and courtyards form centrepieces in buildings and connect them to the natural environment by providing natural ventilation and sunlight through the exchange of the internal and external air. Comparative analysis of a central atria and courtyard reveal that atrium with the same geometric dimensions, but a varied climate and glazing conditions provide higher energy efficiency as building height increase. On the other hand, an open courtyard to low-rise dwellings during summer and an atrium for the rest of the year, leads to an optimal balance between energy consumption and summer comfort in tough climates. In Italy at 700BC, a courtyard became a new design as atrium house which developed from the traditional form which can be traced back to 5000 years; the oldest form of courtyard residence known is from the ancient civilization at Kahun in Egypt. In

archaeological survey, a courtyard house was also found in Ur, Mesopotamia which dates back to 2000 BC as shown in Figure 2-3 (a). It was a simple square central courtyard [18] [21].

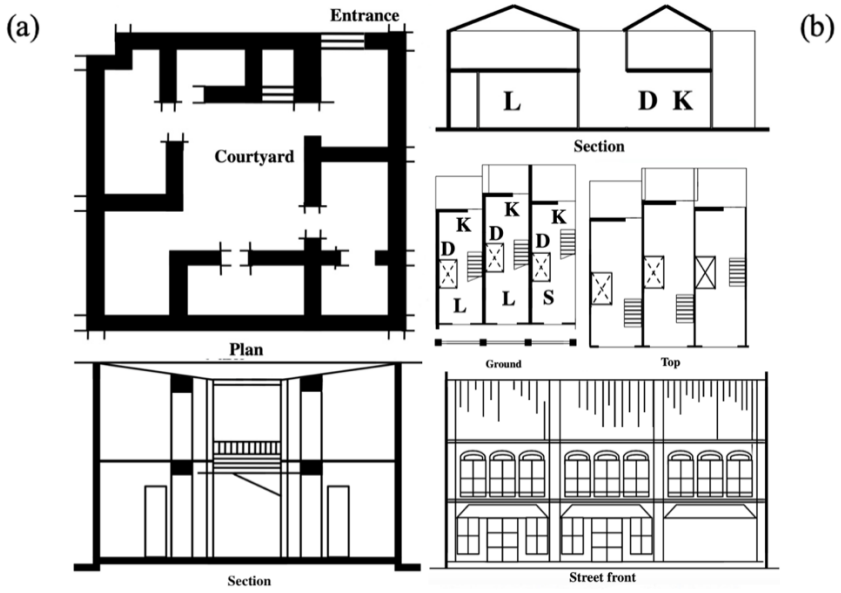

Figure 2-3 Section and plan of House of Ur, Mesopotamia (a), typical section, plan and elevation of Shop house design in Malaysia (b) [18]

Atrium has served not only as a climate regulator but also as a space for socialization with inhabitants of the building. In hot areas, courtyards are commonly utilized to fulfil this dual function. For instance, in the Tropics, courtyards provide natural ventilation and light for "Shop house" buildings such as the one in Figure 2-3 (b). The implementation of atria in the design of buildings for the modern era started during the Industrial Revolution since plate glass and structural elements like iron and steel were readily available. However, modern atria were not common until late 1950s and early 60s. The new form of atria originated from temperate climates in regions of high latitude where it provides an environmentally controllable room and natural sunlight or heat during winter.

With the increasing number of buildings with an atrium [22], especially in non-residential luxury buildings, the demand for ventilation systems to provide better air quality and thermal comfort for occupants has increased. This has consequently led to the employment of mechanical systems with high energy demand. Hence, in 1970s and early 80s, the environmental advantages of the atrium were considered anew as a post-oil crisis response to high-energy consumption in building designs. Nevertheless, the consideration was only

applied to atriums used in temperate climates. The direct application of temperate atrium solution to hotter climates caused significant problems which still need to be resolved. Thus, with the new energy efficient approach, natural ventilation, a potential environmental advantage of atria can be highlighted again.

2.2 Types and configuration of atrium

The design of an atrium is generally based on climatic conditions, architectural experiments, the expected level of thermal comfort, and the functions of the building. The placement of an atrium in a building is the main factor that determines the potential environmental advantages of an atrium in the building. There are four different shapes of atrium that form the main category of atria forms, which have been cited in literature based on the atrium location in the building as shown in Figure 2-4 [18] which was originally named by Hung and Chow (2001). Each form of atria has a particular environmental advantage that is chosen according to its ambient condition, expected ventilation, and daylight performance. For example, in temperate climates, in order to have more solar heat gained in winter and a more attractive view during different seasons, the atrium is attached to the building as a glazed façade Figure 2-4 (c). For the semi-enclosed type, Figure 2-4 (b) has only two glazing faces. When selecting an atrium for a hot and humid climate, the centralised atria Figure 2-4 (a) and linear atria Figure 2-4 (d) are the most effective types in minimising temperature fluctuations when compared to the rest. The performance of an atria attempts to provide neutral temperatures. Hence, the centralised and linear atria are the most common generic forms in use in hot regions.

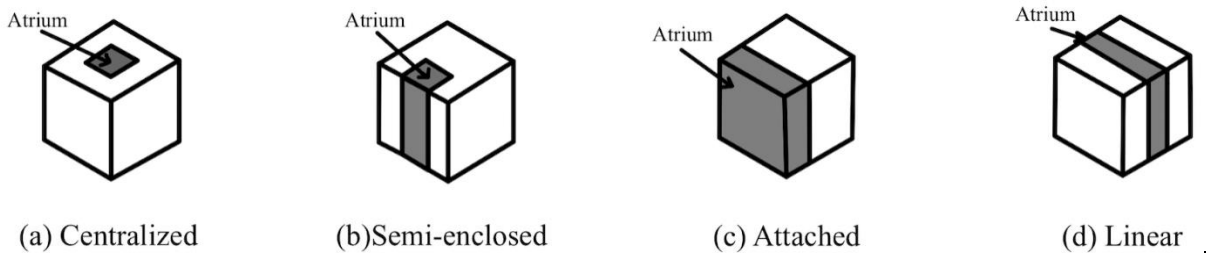

Figure 2-4 Four different generic forms of atrium and real samples, (a) Centralized, (b) semi-enclosed, (c) attached, (d) linear [18]

Figure 2-5 A sample of Closed Atrium Galleria Umberto I, Naples, Italy

Referring to Bednar (1986) [23], closed atrium is the most popular type of atrium. An example is the closed glass atrium of The Galleria Umberto I in Naples, Figure 2-5. It was built in the late 19th century and refurbished in the early 21st century. It is a place of interest, a meeting place and a passageway for easy access to nearby premises.

Based on the literature, in order to achieve the desired indoor thermal condition in naturally ventilated atria, two main design approaches have been cited.

(a) design atrium components and configurations

(b) implement appropriate ventilation techniques

These design parameters are mainly affected by external and internal variables. The efficiency of each parameter has been evaluated based on their influence in increasing the air flow rate and expected air flow pattern which consequently led to the improvement of thermal conditions and a decrease in energy consumption in an atrium. Figure 2-6 presents a list of the variables, ventilation techniques and their relationships with other design parameters in the structure of the recent design approaches to atria. This figure provides significance since it illustrates interdependencies among factors that influence passive design of atria.

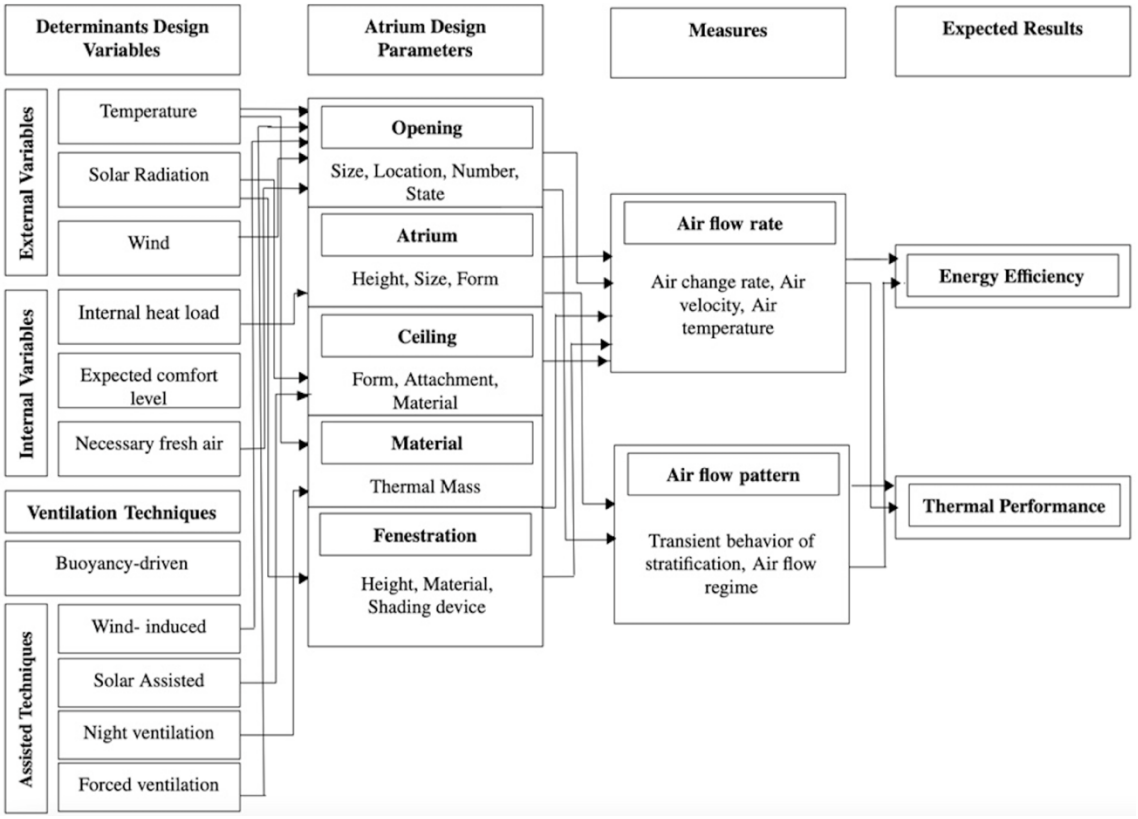

Figure 2-6 A map of design parameters and variables of atria [18]

2.2.1 Atrium geometry aspect ratio

The Plan Aspect Ratio and Sectional Aspect Ratio are two of the most influential parameters for atrium geometry. Both plan and sectional proportion affect smoke movement. The efficiency of pulling out the smoke mechanically decrease with an increase of height.

According to Bednar, 1986 [23], the Plan Aspect Ratio (PAR) is the ratio between the width (w) and length (l) whereas the Section Aspect Ratio (SAR) is the sectional proportion of atrium determined by the height-to-width portion. The atrium geometrical relationship in these two ratios is shown in Figure 2-7.

The PAR indicates whether the shape of atria is linear or square. Atria values below 0.4 are defined as linear atria. SAR ratio under 1.0 is a rectangular or linear atrium whereas when the figure is equal to 1.0 it is square.

A lower value of SAR indicates a shallower atrium. Atria with SAR lower than 1.0 are defined as a shallow atrium and when the SAR value is more than 2.0 it is a tall or narrow atrium.

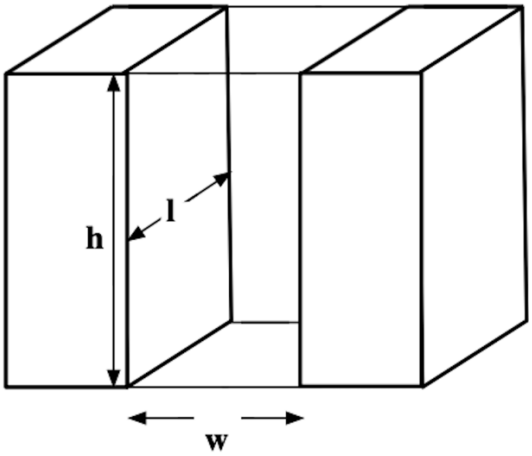

Figure 2-7 Atrium geometrical relationships

A survey in Malaysia shows that an enclosed rectangular-shaped atrium with shallower heights and flat roof profile is the most common form in atrium buildings [24]. From the study of energy efficiency, there was no significant difference between ratios of 1:2, 1:3 or 1:4. Whereas, the analysis of the Predicted Mean Vote index (PMV) shows that the atrium area ratio of 1:4 was closer to the thermal comfort specified zones in the atrium ratio [24] as shown in Figure 2-8 and Figure 2-9 .

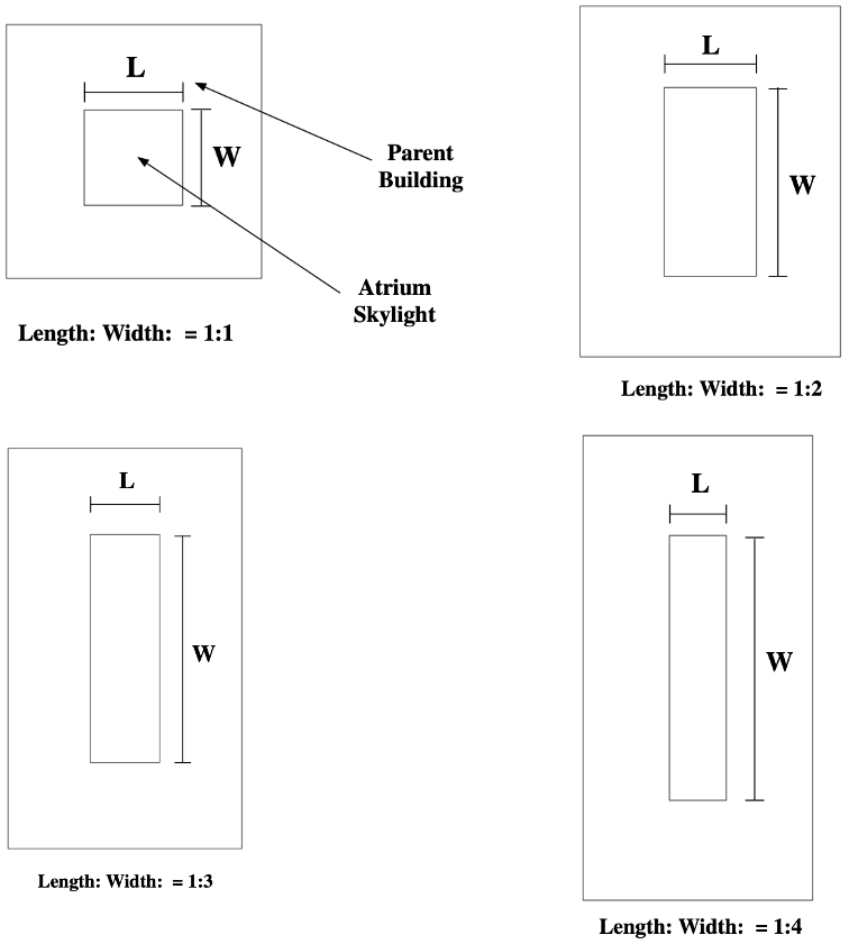

Figure 2-8 Different aspect ratios of atrium

Different aspect ratios of Atrium showing PAR change relating to the length and width in Figure 2-8 which demonstrate the Plan Aspect Ratio (PAR) of atrium is linear when it is more than 1:4.

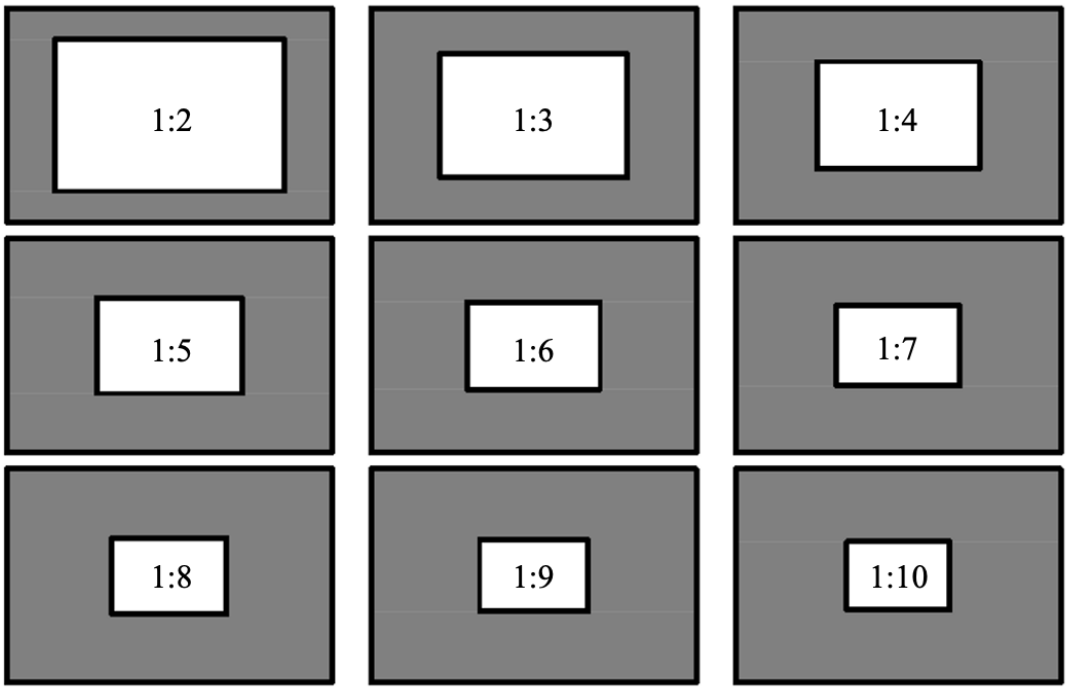

Figure 2-9 Different ratios of atrium (atrium area/total construction area) [24]

Figure 2-9 shows the daylight proportions in different aspects of the atrium ratios. The lower ratio has higher energy consumption. But from the result of the predicted mean vote index (PMV), the ratios 1:2, 1:3 and 1:4 do not have much difference in energy consumption, thermal comfort, or visual comfort.

Therefore, atrium ratios of 1:1, 1:2, 1:3, 1:4, 2:1, 3:1 and 4:1 are considered in this study with respect to popular modern architectural design, energy consumption, and the quality of environmental comfort.

2.3 Empirical correlations used in fire engineering design of atrium

Authoritative standards and codes of practice are critical when considering the efforts required achieving sufficient safety precautions and standards for protection when a fire is initiated. These standards are typically reviewed periodically and are updated and enhanced with newer findings.

Open-space concepts and atria designs are the current standards for modern building architecture and have been the focus nowadays. Atria has become more complex in relation to its geometrical designs which makes design guides and hand calculations imprecise when

predicting scenarios in which fire and smoke is developed. As a result, the use of performance-based design can help address these issues.

The fundamental design principle of smoke control is to reduce the impact of environmental circumstances such as temperature and pressure. These variables must be controlled as it determines smoke movement and as a result leads to the exposure of smoke and heat to occupants evacuating from the fire. Smoke control helps limit the spread of smoke and reduce the impact on civilians to prevent loss of life and damage to property.

Regulation and guidelines for smoke control in atrium have been adapted from different countries after the reintroduction of atrium designs to buildings from the 1960s. These concepts follow the fundamental criteria for fire development in enclosed compartments and the conservation equations, empirical formulae and correlations used for design in fire safety of the buildings.

From 1985, the NFPA Technical Committee in the United States recognized the requirement for smoke management in buildings. Following this, in 1991, the NFPA 92B [16] was published to introduce a Guide for Smoke Management in Malls, Atria and Large Areas and revisions have since been incorporated into the current version published in 2021. In the United Kingdom, CIBSE TM19, 1995 [4] gives a technical guide which addresses equations used in smoke. The Fire Research Station Publication BR258, 1994 [26] was also published to consider different design specifications for smoke control systems where exhaust ventilation may be required depending on the building arrangements.

The code of practice British Standards, BS5588: Part 7, 1997 [27], BS9999, 2017 [8], BS7974, 2019 [28], SFPE Handbooks, 2016 [11] have also provided an industrial guide for fire engineers to provide the most suitable designs for building architecture. The incorporation of fire and smoke management codes of practice provides safety and precautions to help aid evacuative procedures.

When considering the different variables that can influence the heat release rate of a fire, references from NFPA 92, 2021 [6], BRE 368, 1999 [2], CIBSE Guide E, 2010 [3], CIBSE TM19, 1995 [4] and the Method of Predicting Smoke Movement in Atria with Application to Smoke Management by Klote, 1994 [15] suggest that the fire load, diameter of the fuel base, geometry of the atrium, location of the fire source, and ventilation conditions are the key factors. As a result, these conditions must be addressed when fire engineers are designing a building to help maintain suitable parameters for atria designs.

Fire safety installations for a building include both passive and active provisions. Passive provision is something inert, like walls that prevent fire from spreading. In contrast, active provisions include heat detectors that require electricity to respond in the presence of fire. In previous years, fire safety was ensured by a series of prescriptive rules and inspections to ensure that it complied with the standard. Passive systems will generally comply, but the modern performance approach, otherwise known as the engineered solution, intends to allow architectural freedom compensated by a justified active approach. By allowing fire engineers to invest in a more active approach, it allows for design freedom and allows for intricate details previously unused.

However, all designs must meet with the regulations and code of practice issued by local government. References can be drawn in some international standards such as the ones from the United Kingdom and United States. Designers can use a range of arguments from simulation to case-precedent to justify their 'vision' calculation using equations that are very common. There are three main fire safety engineering approaches: equivalency, deterministic and probabilistic approach.

A tenable environment must be maintained in all the exit points and occupied spaces where civilians are situated in. This helps ensure that all personnel can have time to exit the area in a safe manner. The atrium must be equipped with an active or passive smoke control system to keep the accumulated smoke at least 1.83m above the floor for all means of egress for no less than 20 minutes as a mandatory requirement of atrium design in NFPA5000, Building Construction and Safety Code® , 2006 [29].

These are required to predict the entrainment of air flowing into the plume, mass flow rate of gases, and how computer fluid dynamics can be used for simulation of various fire scenarios for comparison against hand calculations.

Fires develop due to multiple factors including the materials present in an atrium which characterize fuel quantity and properties, ventilation (natural or mechanical), building geometry (volume and ceiling height), location of fire, and ambient conditions (temperature, wind, etc.). When considering a safe environment for occupants to stay in, it is crucial to consider all the factors that can affect how a fire can spread and allow for appropriate safety precautions to be taken into account.

2.4 The design process

Fire safety design can be performed using either of the two approaches discussed below. The first approach is the traditional method which utilizes a simple prescribed design code to demonstrate compliance with established norms. The later approach is the modern method which is also known as the engineering solution. This allows an architect to freely design without the use of prescriptive documents. They are only required to provide calculations, simulations, and evidence to state that functional safety is achieved.

The target design principle is to determine an effective and acceptable solution provided that tenable conditions are achieved for occupants in case of fire to limit the heat and smoke spread inside the premises. For the purpose of assessing quantitative modelling results, a tenability criteria is required in order to provide an indication in relation to the level of safety for the evacuation of occupants with respect to the heat and smoke conditions within the building.

In an atrium in particular, fire that is spread internally throughout the atrium is a relatively minor concern in comparison to the movement of hot and toxic gases. This is due to the fact that hot and toxic gases reside in the ceiling due to buoyancy and fill it in a downward motion to fill the volume of the atrium. Therefore, a properly designed smoke control system for atriums is critical and has been brought up as a concern in the UK Fire Research Station Publication BR258, 1994 [26]. This publication has provided design considerations for smoke control systems and also highlights the inclusion of exhaust ventilation depending on the type of building arrangement.

An atrium is defined as any space within a building that extends vertically for more than two floors. Examples include building lobbies, convenience stairs or social spaces that are frequently found in office buildings, malls, civic centres, and museums. In the event of a fire, smoke will quickly spread to other floors due to the nature of an atrium's design.

Smoke management in an atrium normally includes management of smoke within the large-volume spaces and any space that communicates with the large-volume spaces. A source of smoke is often a fire that has been lit in a large-volume space or within the communicating space. In providing fire safety for an atrium, utilizing smoke management would satisfy one or more of the following objectives pointed out in NFPA 92B, 2005 [16] and BS 5588: Part 7 [27] which are now updated to NFPA92, 2021 [6] and BS9999, 2017 [8] respectively:

- To maintain a tenable environment where all exit access and area of refuge access paths allow occupants to exit in sufficient time.
- To ensure that the smoke layer interface is maintained at a predetermined elevation.
- To assist the fire department personnel by approaching, locating, and extinguishing the fire.
- To limit the rise of the smoke layer temperature, toxic gas concentration, and the reduction of visibility.
- To limit the spread of smoke between the spaces that would occur as a result of leakage paths in a construction.

The above list appears to be explicit statements of the desired achievement goals for a smoke management system. Critical values for parameters used to assess the smoke hazard would be provided in various guides. For example, a safety smoke interface height is recommended to be higher than 3m for public buildings, and 2.5 m for non-public buildings in BS 5588: Part 7 [27] and BRE Report 368 [2]. Moreover, the smoke layer temperature of the gas should be lie between acceptable temperatures. The upper limit for smoke layer temperature is 200 ℃ to avoid painful heat radiation on lightly clad people beneath the smoke layer. In contrast, the low limit is more arbitrary, typically 20 ℃ above ambient to avoid loss of buoyancy. More critical values can be referenced in guides like CIBSE Guide E [3].

Tenability analysis should be performed to determine whether smoke is a hazard to occupants situated in the atria, as reported by Klote (1994) [15]. Guidance for developing an atrium smoke control system are given to designers in the United Kingdom under the British Standards BS 5588: Part 7 “Code of practice for the incorporation of atria in buildings” [27], CIBSE Guide E Fire engineering [3], the BRE Report 258 design approaches for smoke control in atrium buildings [26] and BRE Report 368 Design methodologies for smoke and heat exhaust ventilation [2]. In the United States, guidance on calculation procedures for the design of smoke in the atria are shown in NFPA 92B Guide for smoke management systems in malls, atria and large spaces [16] and the design book “Design of smoke management systems” [15].

British Standard 5588-7:1997 [27] gives guidance in relation to the incorporation of atria into new and existing buildings to ensure safety in the event of a fire or smoke spread. Building characteristics associated with the form and usage of atrium buildings that may affect fire risk include occupancy, atrium height, separation between atrium and associated floor areas, and fire load on atrium base. The occupancy category decision process is illustrated for a variety of occupant categories and atria. Strategies developed to prevent the flow of hot gases and

flames including fire-resisting and smoke retarding construction are identified in this document. Protection strategies such as evacuation, automatic fire detection, fire warning systems, smoke and heat ventilation, automatic suppression systems are discussed. Recommendations are made for smoke control and heat control systems. The atrium must be equipped with an active or passive smoke control system in order to keep the accumulated smoke at least 1.8m above the means of egress walking surface for no less than 20 minutes.

The fire safety requirements in an atrium can be summarized as follows:

(1) Construction requirements - the building shall be composed of non-combustible construction.

(2) Sprinklers (fire suppression) - the building shall contain sprinkler systems throughout.

(3) Lobbies - these are required at each level for exits that lead to an interconnected floor space. If an elevator shaft opens into the interconnected floor space and into storeys above it, lobbies are required to protect either by ensuring that the elevator door opening in the interconnected floor space is closed or the elevator door openings in the storeys above the interconnected floor space.

(4) Protected floor space - a protected floor space can be used to accommodate peak traffic during evacuation. It should be designed in a way that allows an exit to be within reach without requiring occupants to enter an interconnected floor space. It should also be separated from the interconnected floor space by a lobby.

(5) Intumescent - these shall be installed at each floor level, immediately adjacent to and surrounding the opening, to provide a smoke reservoir at the ceiling so that the smoke can be detected. Smoke seals must be at least 500mm deep, measured from the ceiling level to the bottom of the stop.

(6) Mechanical exhaust system - this type of system shall be provided to remove smoke from the interconnected floor space at a rate of four air changes per hour. Its purpose is to aid fire fighters in removing smoke and it is designed to be actuated manually by the responding fire department.

(7) Combustible content limit - the interconnected floor space shall be designed so that the combustible contents, excluding interior finishes, in those parts of the floor area in which the ceiling is more than 8m above the floor, are limited to no more than 16 g of combustible material (e.g., furnishings and items related to the occupancy) for each cubic metre of the interconnected floor space. This requirement is also referenced in the National Fire Code of Canada.

Atria are becoming more common worldwide. Standard guidance and the fire safety codes that currently exist may not be able to address specific fire safety concerns. For certain projects, it is appropriate to carry out a Qualitative Design Review (QDR) when developing the fire safety strategy - typically conducted in buildings that are taller than 50m. The QDR is defined in BS7974 2019 [28], as the initial stage of any engineering design by setting up the basic design parameters and the scope and objectives of the fire safety design. A performance-based approach may be the outcome from the QDR process. The typical timeframe in which a QDR meeting should be carried out is relatively early in the design process so that discussion outcomes can be incorporated into the design of the revised building. The intricacy of the design after various iterations can provide details that can be picked up by safety engineers for analysis to provide greater detail from broad concepts.

When considering the objectives of the fire safety design, the performance and suitability of design solutions proposed by respected fire safety engineers are considered in various stages. After communicating with the board, the accepted solutions are evaluated in a quantitative analysis. Quantitative analysis requires the use of engineering methods in which potential solutions discussed in the QDR meetings are analysed against appropriate time-based analysis via different sub-systems. The impact of fire on the property and occupants will be analysed to determine the development of fire. After completing the quantitative analysis, it will be marked against the assessment criteria in which the output of the quantitative analysis will be compared against an acceptance criterion highlighted in the QDR to provide acceptance for certain proposals [28].

Before the quantitative analysis is conducted, various references to schematic drawings and models are signified to the architectural or client requirements which highlight the fire safety strategy. This would be reviewed in order to consider four different aspects:

(1) Building characterization – concerning the layout and geometry of the building and construction aspects that should be explored. It would also look at the degree of fire load present.

(2) Environmental influences – many factors such as wind and snow can influence the safety design of a building and this can affect structural load, smoke ventilation systems and the natural flame development.

(3) Occupant characterization – occupancy type, population within the building and how they are distributed are likely to affect whether or not the fire alarm is triggered manually or detected by the fire detection system.

(4) Management of fire safety – looks at the extent and nature of management within the building premises. Some of the following factors that should be taken into account is the nature or extent of management in buildings which includes:

a. Ownership
b. The number of managers of fire safety responsible for the building
c. Level of resources and authority of the manager of fire safety
d. Level of staffing
e. Level of fire safety training
f. Level of security
g. Level of control over work
h. Effectiveness of communications procedure
i. Frequency of maintenance and testing of fire safety systems
j. Level of liaison with fire brigade
k. Level of contingency planning
l. Level of degraded system planning
m. Level of planning for abnormal occupancies
n. Level of independence of testing and auditing of the management system
o. Level of management of risk
p. Level of management of fire load

All the aspects discussed above are important factors for managing fire safety in buildings, and the implementation of solutions to maintain effectiveness in this code of practice suggests that the strategic opportunities described by fire safety engineers are feasible options.

Certain fire safety objectives must be considered in the early stages of the design process. This aims to clearly identify the fire safety design and how it aligns with the acceptance criteria established. The main aim is the protection of life, which the fire safety legislation enforces; however, the effect of fire on property damage and businesses is also of concern. When these objectives are set out during a qualitative design review session, their importance can be split into three categories:

(1) Life safety
(2) Loss control

(3) Environmental protection

Life safety:

The main objective is to help evacuate occupants to the nearest location of safety when a fire occurs. People who are in the vicinity of a building during a fire are at deep risk of injuries and cause havoc to evacuation procedures. When considering this, occupants should be able to leave buildings in an orderly manner to keep the risk to occupants low. Firefighters that operate on the occasion of a fire should be provided with appropriate protective equipment to ensure that they are well protected and reasonably safe. The structural rigidity of the building in which the likelihood of collapse should not be endangering to people who are close to the location of fire.

Loss control/prevention:

When the case of a fire occurs, the businesses that may be located in the building can see extensive damages to the contents and can cause serious loss to its corporate image. In addition, the structure and fabric of the building and the contents would undergo damages which yield substantial costs for repairs. It is definitely beneficial and desirable to take measure in order to reduce potential large financial losses to corporate partners.

Environmental protection:

When a fire occurs in a building, there is a great release of hazardous materials which can impact on the environment. Moreover, there is a more serious risk of affecting neighboring buildings and facilities which impact the occupants nearby.

Potential fire hazards can arise from a range of different variables within a building. Factors that should be taken into account are:

(1) Ignition sources
(2) Combustible materials
(3) Materials of construction
(4) Nature and activities in the building
(5) General building layout
(6) Any unusual factors

Considering that these factors may influence the fire, this list does not account for all the significant fire hazards. Multiple causes can lead to the development of a fire and the main goal of the fire safety objectives is to prevent such an event from happening or managing it to a suitable level.

When quantitative analysis is conducted after consultation in the QDR meeting, various time-based analysis methods are deployed and are categorized into six sub-systems.

Whilst most buildings are developed and designed in accordance with local code of practice, review and approval for specific design architecture can be considered. It is critical to ensure that fire safety is compiled in the most appropriate way so that it can be reported in a clear and discrete style. It is necessary to clearly specify the fire systems that are implemented throughout the design architecture to ensure that approval is feasible. However, since building designs have typically conformed against traditional code of practice and guidance documents such as BS5588-0, it can be often misled in which variations to the straightforward criteria is considered. As a result, the BS7974 code of practice provides flexibility when designing using performance-related objectives rather than prescriptive solutions. Approving bodies must not simply consider the proposed design against well-defined empirical values and recommendations but also evaluate on the unique methods implemented by fire safety engineers. As a result, evaluation on the report should be conducted based solely on the design, calculation procedures and assumptions made during the study.

When the QDR team has consulted with all important approval bodies, the acceptance criteria must hold true, and the fire safety design must abide with those terms. Identification of the acceptance criteria during meetings shall be collectively agreed in which the measure attempts to reduce the consequences of fire. Possibility of death or injury cannot be eliminated and therefore, the establishment of a criteria to be used to determine whether or not a building has a safe fire safety design can be evaluated. The following methods of determining the boundaries for the acceptance criteria are shown below:

(1) Deterministic (safety factors where appropriate)
(2) Probabilistic (risk-based)
(3) Comparative criteria
(4) Financial criteria

All these methods have shown to give great importance to the safety and effectiveness of fire management in the case that a fire occurs. A further breakdown into each of the factors has been explained.

Deterministic:

The worst possible encounter of a fire scenario should be considered in detail in order to allow for safety factors to become apparent. Certain factors that should be considered include the uncertainty in calculation procedures and the potential consequences in the failure of the

design. The reliability of data should not be questioned and if that could not be achieved, the plan must be revised to ensure all safety measures are feasible.

Life safety criteria:

In the event of a fire, the life safety criteria are produced as per the prescriptive code BS 5588-0 in which occupant exposure to toxic fumes such as irritants, narcotic gases, radiant heat flux, and smoke temperatures should be minimal and under a particular number based on PD 7974-6. Since smoke can most often affect the population, it can be an irritant for people in small, confined areas, which may also cause heavily smoke-logged escape routes. The effect on the eyes, nose, throat, and lungs caused by irritants is toxic and can most likely cause death when exposed for too long. Radiant heat flux is another issue that should be considered as a factor affecting occupants since it can cause intense skin pain and burns after exposure to a naked flame. If they were exposed to lower fluxes, occupants could tolerate this to a greater extent. In general, the longer the person is exposed to high temperatures, the more pain and burning sensation they feel as time passes. Therefore, the longer people are exposed to an environment in close proximity to a fire, the better.

Loss prevention and environmental protection criteria:

Fire can cause damage to property in buildings and that can be grouped into three distinct categories: Building, Contents, and the Environment. These groups have a different degree of fire damage caused by heat and smoke since they do not all combust in the same way. A table consisting of the different property groups is shown here in Table 2-2:

Table 2-2 Property groups found in and around a building

Group	Sub-group
Building	Sub-structure
	Super-structure
	Internal finishes
	Fixtures and fittings
	Services, supply and distribution
Contents	Electrical appliances
	Records
	Production equipment
	Raw materials
	Finished products
	Unique objects
Environment	Water
	Soil
	Air quality
	Neighbouring buildings

Since the consequences of losing property due to fire damage, the direct financial replacement cost is often high. The loss of an asset can often result in tremendous bills that require great reimbursement. Therefore, disruption to companies should be prevented by employing these methods to alleviate losses due to fire.

(1) Selecting materials with resistance to fire
(2) Providing fire protection systems
(3) Contingency planning

The aforementioned preventative measures are brought up to reduce the effects of objects, events, and layouts that could potentially escalate fire damage. A risk assessment can be arranged to ensure minimal property and environmental loss. A list of the acceptable limits within which property and businesses may have damage can be specified in the building scheme. This includes:

(1) Number of specific valuable objects that it is acceptable to damage
(2) Maximum zone of direct fire damage
(3) Maximum zone of smoke and hot gas damage
(4) Maximum zone of water damage
(5) Maximum time periods for recovery from the fire

Probabilistic studies:

A probabilistic risk assessment is carried out with its sole objective to show that the likelihood in which a fire event occurs can impact the occupants in a tolerably small way. This means that the ones injured or lead to death, have large property loss and environmental damages are reduced to a very small number in which the fine margins allow it to still adhere to the criteria.

Comparative studies:

Even though the code of practice in BS7974 allows for some flexibility in the design of fire safety systems, the QDR team may recommend some existing codes in which the fire safety engineers should adhere to. This would help ensure that the level of safety is provided in the best possible way. This approach would use both deterministic and probabilistic techniques and require less extensive analysis. It would be most desirable in which the risk to occupants is similar to types of buildings designed in accordance with existing codes of practice.

When considering the effectiveness of the fire safety strategy, the concern as to the regularity of testing and maintenance procedures is raised. When a large complex building is built, the occupants should be briefed with instructions to manage fire safety in an appropriate manner. These audits are most effective and should be carried out every 1-5 years.

The concepts of using a performance-based approach were introduced in the early 1970s in which flexibility was allowed when designing and applying fire safety and protection systems. In order to provide a framework for an engineering approach, achieving fire safety in buildings and giving guidance to the public was published in BS DD240-1 ‘Draft for Development’, 1997 [30], introduced by British Standards Institution. From 2001, British Standard BS7974, 2019, Application of fire safety engineering principles to the design of buildings [28], was published to replace DD240. It has eight pars 0-8 which were updated in 2002, 2003, 2012, 2016 and the final complete version in 2019. It acts as code of practice, aimed at fire safety engineers (FSE) and practitioners, and was also intended for the stakeholders and regulators but it also allows fire engineers to create effective relevant performance-based fire management strategies. The meetings held involving relevant stakeholders were described as “qualitative design reviews” (QDR) and it can be referred to DD240 for subsequent quantitative analysis.

Overall fire engineering process in BS7974 has three main stages: Qualitative Design Review, Quantitative Analysis and Assessment against Criteria.

For a qualitative assessment of the design, the QDR process is best delivered when many stakeholders are included in the QDR team. Typically, there is at least one fire engineer, architect, services engineer, structural engineer, operational management, approval bodies, insurer and other key members dependent on the size of the project. The purpose of those meetings is to ensure that the design has accounted for possible fire hazards in which the team acknowledges and works out solutions to reduce risk and oversea any solutions that are recommended to reduce the risk.

Financial studies:

Fire safety should be introduced to a project at the feasibility stage of approval. The fire safety management solutions are best considered in project outlines to ensure that necessary precautions are considered in the case of a fire. When QDR is adopted at an early stage of development, the process can help customers improve safety and the cost benefit analysis. Other factors considered during a QDR meeting include business, property, reputation and environmental considerations are part of the criteria beyond Building Regulations. QDR safety margin in fire design is assessed based on an agreed criterion. The QDR process permits an evaluation of the whole building life cycle and integrated safety throughout. After the whole building life-cycle meeting, the QDR process is the fire strategy written.

For the identification of design parameters, the QDR is used to review the early architectural design and to identify the design parameters. It is important for the fire engineer to fully understand the proposed use and functional objectives of the building, as well as any significant hazards or design aspirations that will need to be accounted for when finalising the fire safety design.

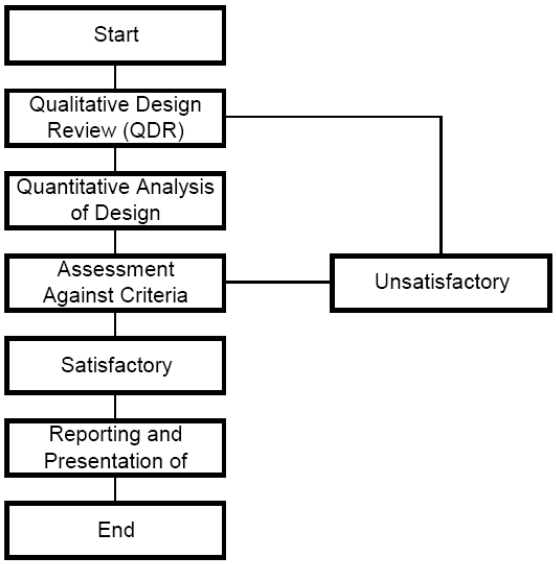

Figure 2-10 BS7974 [28] and ISO basic fire safety design process [33]

Figure 2-10 details described with visual representation of the steps in the BS7974 [28] and ISO 13387-1 [33] document. The overall process in BS7974 included three main stages, Qualitative Design Review, Quantitative Analysis and Assessment against Criteria.

International Fire Engineering Guidelines (IFEG), 2005 [31] , the SFPE Engineering Guide to Performance-Based Fire Protection, 2015 [32], and ISO 13387, 1999, Application of Fire Performance Concepts to Design Objectives [33], provide similar guidance to performance-based fire engineering design to meet the regulatory standards in the current fire safety engineering practice protocol. Amongst the four engineering guidance documents, BS7974 includes the most detailed in regard to the methods of evaluation in comparison to that of IFEG, ISO 13387 and the SFPE Guide. In addition, BS7974 is the only standard that includes risk assessment and probabilistic methods.

The International Fire Engineering Guidelines, the IFE guidelines had their genesis in a document produced by the Australian Building Codes Board (ABCB) in 1996 when they introduced performance-based design. A second edition was published in 2001. The third edition was published in 2005 and was updated to reflect the building legislation in New Zealand, Canada and the United States.

A report with the following key components will be covered with the evaluation methods used and analysis against the criteria at the project completion:

(1) Scope of the Project
(2) Relevant Stakeholders
(3) Principal Building Characteristics
(4) Dominant Occupant Characteristics
(5) General Objectives
(6) Hazards and Preventive and Protective Measures Available
(7) Trial Designs for Assessment
(8) Non-compliance Issues and Specific Objectives or Performance Requirements
(9) Approaches and Methods of Analysis
(10) Acceptance Criteria and Factors of Safety for the Analysis
(11) Fire Scenarios and Parameters for Design Fires
(12) Parameters for Design Occupant Groups
(13) Standards of Constructions, Commissioning, Management, Use and Maintenance

Other than the general fire safety requirements set out in Approved Document B (ADB) which covers the prescriptive standard, it allows for alternative fire safety engineering

solutions by referencing other codes and standards for the design of specific sections. Alternative fire safety engineering approaches set out in BS7974:2001 allows for the applications of fire engineering principles to the design of buildings – Code of Practice directed to the fire design engineer.

2.5 Principle Engineering Calculations

When designing against fire in buildings, the first concern is the magnitude of fire that may occur. In this section fire size is briefly reviewed to establish the learning and problems in recent years.

Fire is usually charaterised firstly by the amount of heat that could potentially be released from the chemical combustion of all building contents and construction materials in a hypothetical scenario of 100% combustion efficiency. This is the ‘fire load. In reality there is always debris from building fires and chemically a fire is not a perfect production process, so considerably less heat is generated than 100%. Furthermore, the furniture and contents of a built space are often arranged around a perimeter, in the center or around a focal point, so there would be more heat potential in some locations than others. This is better charaterised by the fire load density (fire load per unit floor area). Table 2-3 adapted from DD240 part 1, 1997 summarises the fire load densities in a range of occupancies [30].

Table 2-3 Density of Fire Load at Various Occupancies [30]

Occupancies	**Density of Fire Load**			
	Average (MJ/m^2)	**Fractile (MJ/m^2)**		
		80%	90%	95%
Hospital	230	350	440	520
Hotel bedroom	310	400	460	510
Offices	420	570	670	760
Shops	600	900	1100	1300
Dwelling	780	870	920	970

Essentially, this is the effective total amount of energy (per unit area) that a fire could release. The table refers to the measured survey loads, Q, in MJ per m2 of floor area.

The second consideration is a measure of how ferociously the heat is released. This intensity, the heat release rate (HRR) is also imperfect, and in the simplest model, two stages/phases of

fire are usually recognised: growth and fully developed fire. The term “fully developed fire” means approximating to a maximum heat release rate. NFPA 92, 2021 [1] is a well-established reference giving guidance to classify low, medium, and high heat release rates for atriums. This information is extracted and shown in Table 2-4:

Table 2-4 Classification of heat release rates recommended for atria [1]

Atrium Type	**Fire Load (MW)**
Limiting combustible, the minimum fire intensity	2
Minimum fire intensity	5
Maximum fire intensity	25

The maximum HRR is considerably greater than for a domestic building because of the sheer floor area of an atrium and the combustible materials that people accumulate into them. A 5MW fire is usually considered very severe for a single room [1] and a roughly exponential scale is used, as examined below.

Having considered the total amount of heat and the rate at which it is produced, the possible duration of the fire can be hypothesized, but in modern design the priority is the early and immediate fire rather than its lifespan. The more immediate problem, knowing HRR, is what flame size is associated, and how much toxic/hot smoke is produced.

Having considered the maximum HRR from a fire there is very clearly a time delay for any fire to achieve this from the instant of ignition. This growth period is typically a matter of minutes. Figure 2-11 shows a series of six curves of heat release rate, HRR increasing from zero over time and classifying these as slow, medium and fast fire growth.

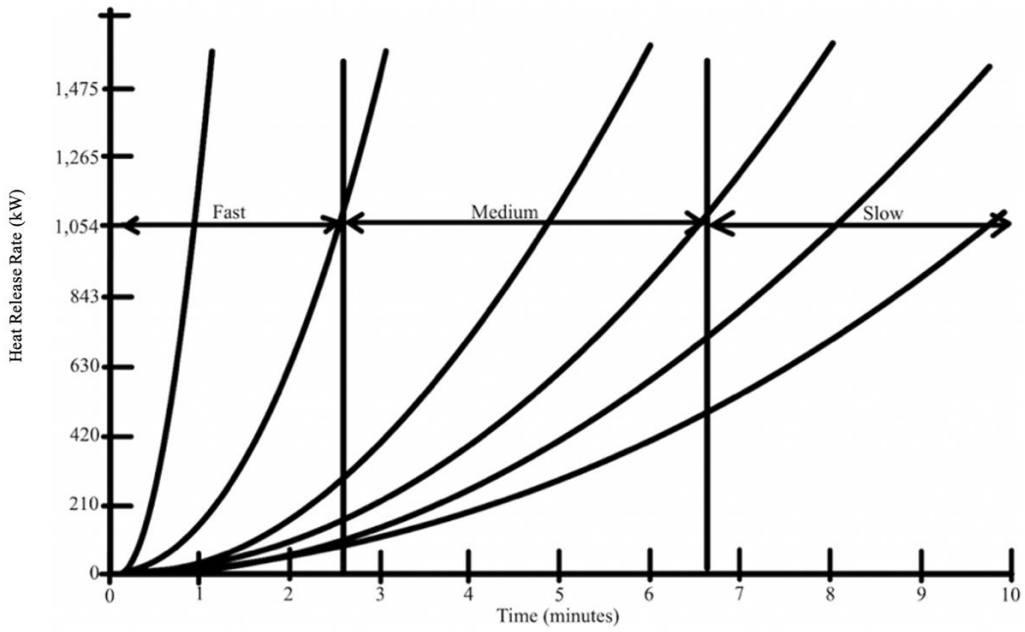

Figure 2-11 t-squared growth rate curves [1]

Experiments have shown that during fire growth, the rate of heat release was found to increase exponentially with time according to an empirical power/index to conceal various complications [1]:

$$\dot{Q} = \alpha t^n \tag{2-1}$$

Here n is a positive exponent. Generally, the exponent is 2 is used for most compartment fires which are often termed "t-squared" fires, (i.e. $\dot{Q} = \alpha t^2$). Most engineers are more comfortable with quadratic equations than some empirical constant such as 2.101 and this preserves a sense that the fire is increasing with a surface area of flame emitting the heat. There is notably an exception, for a high-rack shelving in a warehouse. In this case the flame or fuel bed are three dimensional so n = 3 is a starting point. The special cases are not the main feature of this project, but atria may require their own specific value. This was proposed decades ago by Heskestad in 1972 [36] and has become one of the main/key start points of engineering design.

Following the idea of a time-squared fire shown on Figure 2-11, the time for a fire to grow to a specific size distinguishes slow, medium and fast. For reference a fire achieving a maximum HRR of 1000BTU (1.055MW) was used.

Generalising these timescales, from (2-1) $\alpha = \dot{Q}/t^2$ gives the growth rate parameter irrespective of the lifetime of the fire or the maximum heat release rate that might be achieved.

The growth rate of fire for some common materials found in typical buildings is tabulated in Table 2-5 as stated in NFPA92, 2021, P.57 [1]. The simpler SI unit equivalents, rounded to integers are not common parlance (esp. multiply by 1000).

Table 2-5 Growth Rate of Fire for Common Materials [1]

Growth Rate	**Slow (S)**	**Medium (M)**	**Fast (F)**	**Ultrafast (UF)**
Growth Parameter, α (kJ/s^{-3})	0.0029	0.0117	0.0469	0.1876
Growth parameter in SI units W/s^2	3	12	47	188
Typical Materials	Densely packed wood	Wooden furniture, cotton/polyester spring mattresses	Mail bags, plastic foam, highly stacked wood pallets	Methyl alcohol, fast burning upholstered furniture
Typical Occupancies	Picture gallery	Dwelling, hotel reception, hotel bedroom	Office, school, nursing homes	Shopping and entertainment centers

From the examples in the table above, the reader can easily appreciate the question of where an atrium fire should sit. It is a question of what fuel is distributed in the atrium, how enclosed it is for heat and air transport and its propensity for fire growth.

The fire growth rate of a tea-candle in the centre of a vast, empty space will largely behave the same as in the open on a still-day [37]. However, as the fire size grows and a fire is considered in proximity to boundaries, the space will result in fire development due to the heat feedback to the burning surface and constrained mass flows.

Fire in the atrium is classified as a fast-growing fire, as referenced in Table 2-5 of NPFA 92B, 2005 [16]. Should the space ever be used for a different purpose, this could wildly underappreciate the risks.

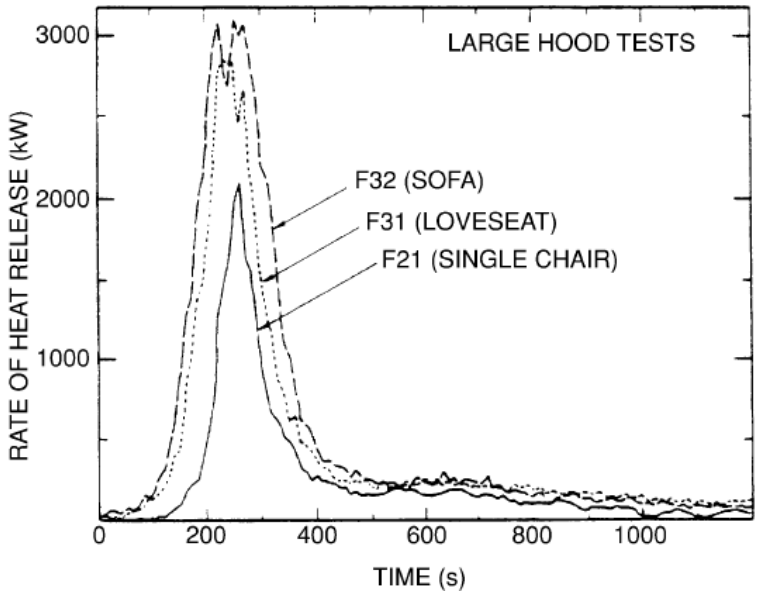

Figure 2-12 Typical rate of heat release against time for upholstered [34]

Figure 2-12 extracted from [34] shows how the HRR of an experimental fire varies over time. The growth stage, and its resemblance to time-squared, is readily visible. This parabolic shape is consistently observed.

Returning to the afore-mentioned lifespan of a fire, if there was a fire load density 4 kJ m-2 is distributed evenly around a floor area 300m2 (i.e., total fire load 1.2 MJ) and burns perfectly at a peak HRR 1 MW, then simple calculation yields a time of 1200 seconds (20 minutes) as the stereotypical lifespan of a fire. This is rule-of-thumb associated with single room fires (i.e., small area, high load density) and has evolved into equation 2-5 found in CIBSE-TM19 [4] for upholstered furniture.

Equation (2-2) is for designated typical furnishings in a fire scene with a fuel bed controlled fire at 20 minutes as referred to Foreground Tactics, Emmanuel Fried stated in 1972 [38].

For upholstered furniture, CIBSE Guide E [3] provides the following equation:

$$\dot{Q} = \frac{q}{1200} \tag{2-2}$$

In buildings there are of course multiple contents and the HRR total for all contents is equated to the total fire load by some empirical combustion efficiency, usually treated as a constant. Because the fuel is not homogenously dispersed or burnt it follows that the heat flux is not homogenous either. The heat flux per unit burning/exposed area is a better measure if intensity.

$$\dot{Q} = \dot{Q}'' A_{fire} \tag{2-3}$$

Equation (2-3) is a time averaged HRR across the lifespan of a fire on a single burning item. It is not representative of a full building fire at its maximum HRR. The chemical combustion of gas generates heat conductively, convectively and as thermal radiation. Radiation dominates fire development at very high temperatures. We denote convective, $\dot{Q}_c$ and radiative $\dot{Q}_r$, components (Tewarson, 2008) [39] and conduction is a slow and small part:

$$\dot{Q} = \dot{Q}_c + \dot{Q}_r \tag{2-4}$$

The convective fraction X_C is the fraction of the net energy produced by the fire and emitted into the surroundings via heated gasses in the plume. A typical assumption for most fires is $X_C \approx 0.6$. In reality these constant changes during the development of the fire.

$$\dot{Q}_c = X_C \dot{Q} \qquad \dot{Q}_r = (1 - X_C)\dot{Q} \tag{2-5}$$

Thermal radiation is represented with the Stefan-Boltzmann formula, for example of thesis in fire engineering design codes, CIBSE-TM19, 1995 [4]. This expression (2-6) is specifically used to represent thermal radiation from a hot smoke layer:

$$Q_r^n = \varepsilon \sigma T^4 \tag{2-6}$$

The emissivity of a smoky volume ε is approximately equal to its absorptivity according to the grey gas model by Hottel and Egbert [40]. Here, the constant 'n' ignores the volume and surface emission of radiation at different electro-magnetic wavelengths as well as the scattering, absorbing, emitting and transmitting nature of rapidly moving multi-phase masses. For example, how effective does dark smoke shield the fuel from thermal radiation from the top of a heated volume? The result is that this is empirically evaluated or guessed to a specific round number. A definitive value does not exist to use for atria.

2.5.1 Smoke characteristics

There are a number of well-established design formulae that lead from the HRR to the volumetric production rate of smoke. Smoke is accepted widely as the greatest danger to

building occupants because of its toxicity. The effects upon visibility and irritants are also significant during evacuation of a building-fire. The first priority in fire safety engineering is preservation of life, and in relation to atria this means designing around an increasing volume of smoke in a large volume so that the smoke is away from people.

In 1972 Alpert [41] examined the plume and ceiling jet produced from pool fires. This study has been updated and applied to a wide range of fuels [42]. In these studies, the HRR and geometry of the compartment were the only parameters, and the empirical constants obtained correlated strongly to ceiling jet temperature and velocity.

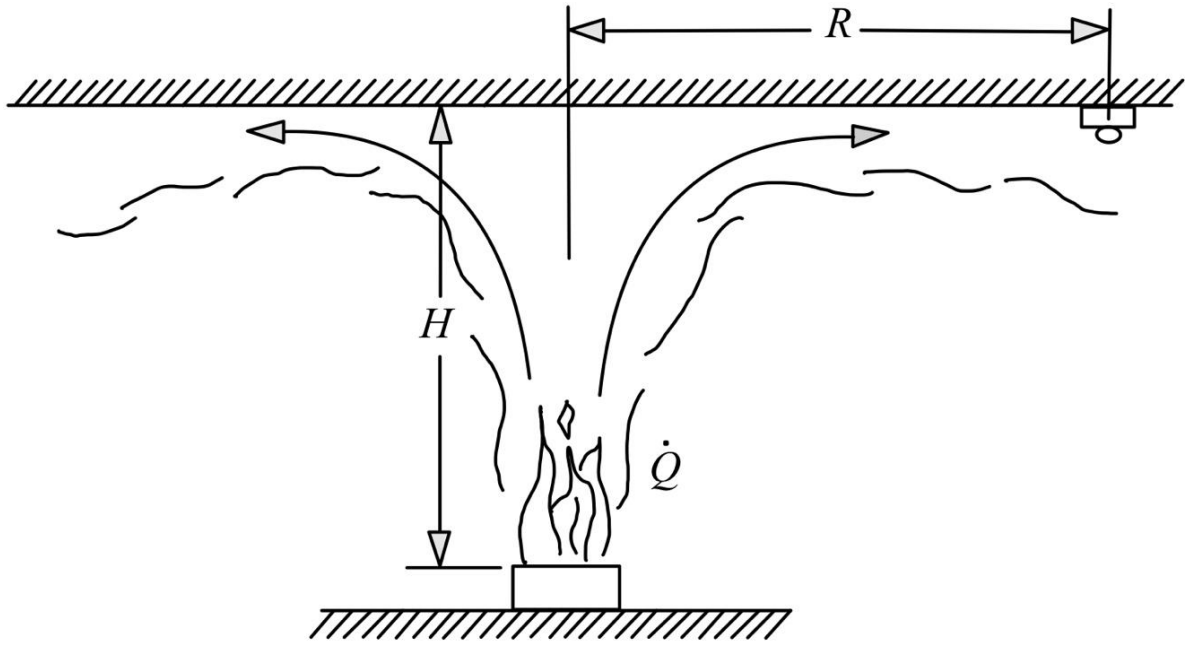

Figure 2-13 Ceiling jet flow beneath an unconfined ceiling

Smoke spread out radically at the ceiling beneath an unconfined ceiling and forms the ceiling jet in Figure 2-13.

$$U = \begin{cases} 0.947\left(\frac{\dot{Q}}{h}\right)^{\frac{1}{3}} for \dots \frac{r}{h} \leq 0.15 \\ 0.197\frac{\left(\frac{\dot{Q}}{h}\right)^{\frac{1}{3}}}{\left(\frac{r}{h}\right)^{\frac{5}{6}}} for \dots \frac{r}{h} > 0.15 \end{cases} \quad (2\text{-}7)$$

Alpert's equation for ceiling jet temperature mentioned in CIBSE-TM19 1995 [4].

$$T - T_0 = \begin{cases} \dfrac{16.9\dot{Q}^{\frac{2}{3}}}{h^{\frac{5}{3}}}, & r \leq 0.18h \\ \dfrac{5.38\left(\dfrac{\dot{Q}}{r}\right)}{h}, & r > 0.18h \end{cases} \quad (2\text{-}8)$$

The reader will note the assumed symmetric plume which explains clearly why each formula has two parts. The first line in each case represents a largely vertical buoyant jet within the scope of a ceiling 'footprint'. The second line then corresponds to horizontal flow outside this footprint. The 'junction' of the two formulae is the least understood range. Another frequent observation is the need for different limits 0.15 and 0.18 because the temperature distribution does not equal the velocity distribution. This is obviously because temperature and velocity are different physical properties of hydrodynamic flow, which is not simply laminar.

For example, an atrium 30m tall has a detector placed on the ceiling (controversial in itself) and a 1MW fire occurs on the floor. The axis of the fire and fire plume is 25m horizontally from the point of detection. Then this detection point is outside the footprint and the flow is horizontal. The equations (2-7, 8) give $U_{jet} = 3.05ms^{-1}$, $\Delta T = 5.83$K which signifies walking-speed smoke spread but such a low temperature the smoke would not remain buoyant and would 'sink'.

In 2011 these expressions were updated using better optimization software and allowing for a virtual source of plume and the convective part of HRR.

$$U = 0.2526 \frac{{\dot{Q}_C}^{1/3}}{(z_H - z_V)^{1/3}} \left(\frac{r}{z_H - z_V}\right)^{-1.0739} \qquad \frac{r}{z_H - z_V} > 0.246 \quad (2\text{-}9)$$

$$T = T_0 + 6.721 \frac{{\dot{Q}_C}^{2/3}}{(z_H - z_V)^{5/3}} \left(\frac{r}{z_H - z_V}\right)^{-0.6545} \qquad \frac{r}{z_H - z_V} > 0.134$$

From the same example

If the fire has an equivalent diameter of 2m the Heskestad correlation gives the virtual origin 0.72m below the floor.

$$z_v = 0.083\dot{Q}^{\frac{2}{5}} - 1.02D \quad (2\text{-}10)$$

Then $\frac{r}{z_H - z_V} = 0.81$ and $U = 0.879$, $\Delta T = 1.95K$ the smoke is spreading less than a third the speed predicted by the older correlation.

Once the smoke has spread under the ceiling of an atrium, then it begins to fill the volume. This has been compared to filling an upside-down bathtub, but the smoke thickens as it is stirred and expanded so a better term is inspissation as used in the dairy industry.

The fire safety engineer asks the two important questions: how hot the smoke and how much clear height is there under the smoke for an evacuating human to be certain their head are not in the hot toxic cloud.

Smoke Temperature

In CIBSE-TM19 1995 [4], Equation (2-11) is the average temperature of collected smoke layer. This follows from the textbook definition of specific heat capacity, $\mathrm{Q} = mc_P\Delta T$ with the useful simplification that smoke is 99% clear air entrained by the fire plume. So, the specific heat capacity of air is usually assumed. Since the layer is freely expanding at atmospheric pressure the constant-pressure constant is used. Furthermore, the specific heat capacity is treated as a constant with respect to temperature.

The temperature of collected smoke is given by:

$$T_{smoke} = T_0 + \frac{\dot{Q}_P}{\dot{m}c_P} \tag{2-11}$$

Equation (2-8) assumes a high Reynolds number so that the mass fluxes are rapidly distributed $\dot{Q}/\dot{m} \approx Q/m$ and that no heat has been lost (adiabatic condition). The formulation has been further refined [4] for convective losses from the smoke (i.e., assuming temperatures are relatively low so that radiation is negligible).

$$T_g = T_0 + \frac{\dot{Q}}{c_P\dot{m} + h_c A_W} \tag{2-12}$$

The density and temperature of smoke can be simply related using the ideal gas law. Because we are concerned with air at atmospheric pressure, the ideal gas law can be expressed in Quintiere's book [43].

$$\rho = \frac{353}{T} \tag{2-13}$$

From (2-13) a smoky layer at 20°C has density 1.20 kg m^{-3} but at 200°C this has reduced to 0.75 kg m^{-3}. In relation to the temperature of the plume, the volume flow rate of smoke, $\dot{V}$ ($m^3\ s^{-1}$), can be described [4]:

$$\dot{V} = \frac{\dot{m}}{\rho_0} + \frac{\dot{Q}_p}{\rho_0 c_p T_0} \tag{2-14}$$

How to evaluate the smoke production rate for (2-14) is the subject of the next section.

Smoke Production

Having established the temperature and volumetric production rate of smoke, the next design consideration is the depth of smoke and the mass production rate. The smoke production rate depends on many parameters, such as the building shape, small and large area, etc. Most importantly the smoke production rate depends upon the hydrodynamic way that the smoke enters an atrium.

(1) Flow from smoky layer in a compartment, out of a window/door into an atrium
(2) Spill plumes
(3) Plumes from fire beds within the atrium volume

Equation (2-15) is described in BRE258 (1994) [26] as the mass flow rate of smoking gases passing from another room, through a vertically opening door/window into an atrium.

$$\dot{m} = \frac{c_e P W h^{\frac{3}{2}}}{\left[w^{\frac{2}{3}} + \frac{1}{c_d} \left(\frac{c_e P}{2} \right)^{\frac{2}{3}} \right]^{\frac{3}{2}}} \tag{2-15}$$

The ventilation parameter $Wh^{\frac{3}{2}}$ is clear in the numerator of (2-15) and c_e is an entrainment constant for the plume, c_d is the discharge constant for the vertical opening (w, for window).

In different atrium shapes and ventilation directions, the most general agreement exists in which the air comes from ‘adjacent surroundings’ and is ultimately exhausted to the outside or at least surrounding rooms or possibly the roof.

Moving to models of spill plumes, the four equations (2-15) to (2-18) are formulations from different authors. Equation (2-16) is for the smoke production in spill plumes referenced from the CIBSE Guide E, 2010 [3] based on the experiments from Morgan and Marshall, 1975 [12] which come from Law, 1986 [13]:

$$\dot{m} = 0.23 Q_p^{\frac{1}{3}} w_o^{\frac{2}{3}} (z_o + h_o) \tag{2-16}$$

Where z_o is the vertical height of the plume above the spill-edge, w_o is the width of the opening. And h_o is the height of the opening.

Equation (2-17) from CIBSE Guide E, 2010 [3] is for the smoke production in spill plumes from a balcony and channelling which also originated from Law, 1986 [13]:

$$\dot{m} = 0.36 Q_p^{\frac{1}{3}} l_c^{\frac{2}{3}} (z_b + 0.25 h_b) \tag{2-17}$$

The same 1/3 power laws are seen between (2-16) and (2-17) but a different geometric problem was considered, resulting in different values for the constant and an opening width in one equation.

Equation (2-18) is the mass flow in spill plumes by Thomas, 1987 [14] and is included in BRE 368, 1999 [2]:

$$\dot{m} = 0.58 \rho \left(\frac{g \dot{Q}_c L^2}{\rho c T_o} \right)^{\frac{1}{3}} (h_b + \Delta) \left[1 + \frac{0.22 \, (h + 2\Delta)}{L} \right]^{\frac{2}{3}} \tag{2-18}$$

Equation (2-19) uses the Poreh method set out in BRE 368, 1999 [2] for mass flow in a spill plume.

$$\dot{m} = \dot{Q}_w^{\frac{1}{3}} C \left[h_b + D_b + \frac{\dot{m}_w}{C Q w^{\frac{1}{3}}} \right] \tag{2-19}$$

Equation (2-20) is the smoke entering an atrium reservoir by Heskestad's model as given in Klote & Milke, 1992 [15] and demonstrated in NFPA 92B, 2005 [16] .

$$\dot{m} = C (E W^2)^{\frac{1}{3}} (z_o + 0.3h) \left[1 + \frac{0.63 \, (z_o + 0.6h)}{W} \right]^{\frac{2}{3}} \tag{2-20}$$

Equation (2-21) is used for the plume mass flow rate by Zukoski et al [44].

$$\dot{m}_p = C m \dot{Q} f^{\frac{1}{3}} z^{\frac{5}{3}} \tag{2-21}$$

Where $z^{\frac{5}{3}}$ was obtained as a result of integration of $z^{\frac{2}{3}}$

Equation (2-22) is the entrained mass flow rate at and above the mean flame height.

$$\dot{m} = 0.071\dot{Q}^{\frac{1}{3}}z^{\frac{5}{3}} + 0.0018\dot{Q} \tag{2-22}$$

Equation (2-23) and (2-24) are the mass flow rates in the plumes for fire beds near a wall or corner fire by Zukoski [44] respectively.

$$\dot{m}_{C,wall} = 0.045\dot{Q}^{\frac{1}{3}}z^{\frac{5}{3}} \tag{2-23}$$

$$\dot{m}_{C,corner} = 0.028\dot{Q}^{\frac{1}{3}}z^{\frac{5}{3}} \tag{2-24}$$

The choice of which equation to apply (2-14) to (2-23) then depends upon the fire bed location. The empirical constants are obtained from limited data over many years and are largely incomparable because of the variations of fuel and parameters did not describe such as the fire growth.

Equation (2-25) CIBSE-TM19, 1995 [4] for ceiling jet velocity enables modellers to estimate how long it will take for a smoke-reservoir to fill up. The estimated depth of the smoke layer will be predicted by thus equation:

$$d = \left[\frac{\dot{m}T}{38W_c(T - T_0)^{\frac{1}{2}}}\right]^{\frac{2}{3}} \tag{2-25}$$

Equation (2-25) is a ratio of the thermal mass of the smoke to the ventilation parameter.

Entrainment for fires at different location:

The axisymmetric plume is also known as the non-restricted plume or the free plume, which means smoke entrainment, is not affected by walls or obstacles and the air can come from any direction [1]:

$$\dot{m} = 0.071\dot{Q}_c^{\frac{1}{3}}z^{\frac{5}{3}} + 0.0018\dot{Q}_c \tag{2-26}$$

Alpert & Ward's equation for ceiling jet temperature [45]:

$$T_{pl} = T_{\mathbf{0}} + 6.81\,\frac{\left(K\frac{\dot{Q}}{R}\right)^{\frac{2}{3}}}{h} \tag{2-27}$$

2.5.2 Ventilation system features

The correlation between ceiling jet velocity, volume flow rate fan, stack effect, wind effect in CIBSE-TM19, 1995[4], entrainment coefficient by Morton et al., 1956 [46] and grid sensitivity used in fire modelling FDS, 2021 [5] are described as follow.

In CIBSE-TM19, 1995 [4], Hinkley's correlation Equation (2-28) is used for calculating ceiling jet velocity, Equation (2-29) is for volumetric flow rate of fan.

$$u = 0.7\left(\frac{g\dot{Q}\rho T}{\rho_0 c_p T_0^2 W_c}\right)^{\frac{1}{3}} \tag{2-28}$$

$$\dot{V}_e = \frac{\dot{m}_P}{\rho_g} \tag{2-29}$$

Equation (2-30) is for stack effect in relation to the pressurization of stairways and other protected shafts [4]

$$\Delta P = 3460\left(\frac{1}{T_0} - \frac{1}{T_g}\right)h \tag{2-30}$$

Equation (2-31) expresses the kinematic pressure of wind in relation to smoke movement within a building [37].

$$P_w = \frac{1}{2}C_w\rho_0 v^2 \tag{2-31}$$

Equation (2-32) is the horizontal rate of entrainment of surrounding fluid or entrainment velocity implied by the plume theories of Morton et al., 1956 [46]:

$$\alpha_E = U_E W \tag{2-32}$$

2.5.3 Correlation for smoke filling in atria

Since equation (2-15) the leading question was the rate of supply of smoke into the cloud collected within the reservoir of an atrium. The smoke can thicken as well as collect as a volume; it also expands and contracts with temperature. As a result, engineers sought a way to

predict the floor-smoke 'clearance' height so that persons in an atrium would not be exposed to the heat/toxins. Referring to the smoke filling equation in NFPA 92, 2021 [1]:

$$\frac{z}{H} = 1.11 - 0.28\, ln\left(\frac{t\dot{Q}^{\frac{1}{3}}H^{-\frac{4}{3}}}{\frac{A}{H^2}}\right) \tag{2-33}$$

The volumetric flow of smoke exhaust should be:

$$\dot{V} = \frac{\dot{m}}{P_0} \times R\left(T_0 + \frac{K_s \chi Q}{\dot{m} C_p} + 273\right) \tag{2-34}$$

Except *A*, *H*, *Q* and *t*, other variables in Equation (2-33) are both parameters. Therefore, *A*, *H*, *Q* and *t* are independent variables in function of smoke mass flow rate (kg s^{-1}) m (*A*, *H*, *Q*, *t*). Furthermore, smoke mass flow rate (kg s^{-1}) m and HRR Q are both independent variables in. Equation (2-34) is the function of volumetric flow of smoke exhaust is V (m, Q).

Except A, H, $\dot{Q}$ and t, other variables in Equation (2-33) are both parameters. Therefore, A, H, $\dot{Q}$ and t are independent variables in function of smoke mass flow rate (kg s^{-1}) m (A, H, $\dot{Q}$ t). The function of volumetric flow of smoke exhaust is $\dot{V}$(m, $\dot{Q}$).

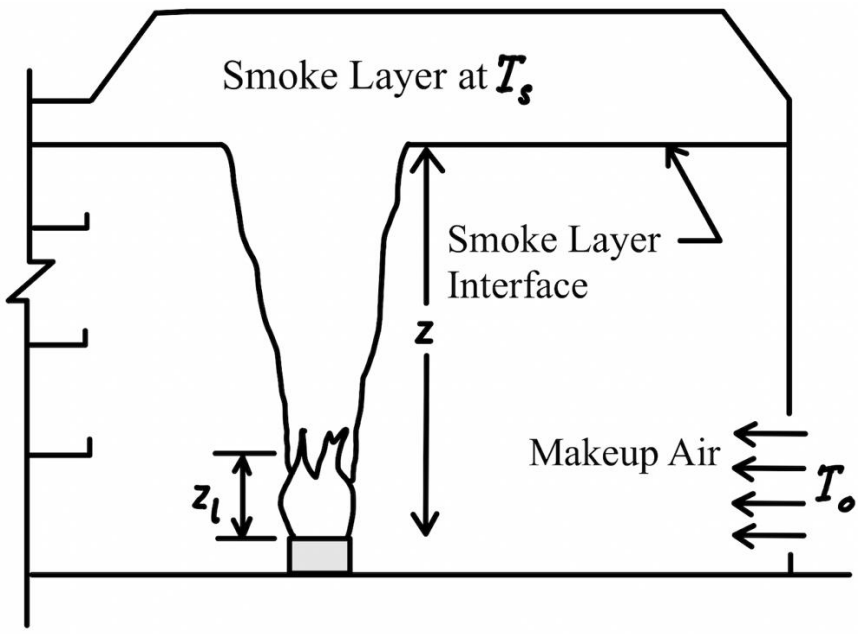

Figure 2-14 Entrainment of Air

Figure 2-14 shows the smoke layer formed at the ceiling from the fire source and fuel of combustion continues by the makeup of air from inlet.

z is the distance from base of fire to smoke layer interface. z_l is the flame height. $\dot{m}$ is the exhaust mass flow rate. R is the gas constant. T_s is the smoke layer temperature. T_0 is the ambient or outdoor temperature.

K_S is 1 for steady smoke exhaust. ρ_S is the smoke density, P_0 is the atmospheric pressure. $\dot{V}$V is the volumetric flow of smoke exhaust. χ is the convective fraction (dimensionless). H is the ceiling height above the fire. T is the time of each interaction. A is the cross-sectional area of the atrium.

2.6 Main problems studied, and methods used

2.6.1 High-rise buildings

According to the Hazard Fires in tall buildings, 2022 [47] based on their risk management planning and local procedure, buildings no matter it is residential, commercial or mixed use are categorized into three common terms:

(1) Medium-rise buildings, buildings between 11m and 18m to the highest occupied floor, or in some area's buildings with 4 storeys or more
(2) High-rise buildings referred as buildings over 18m to the highest occupied floor, or in some areas buildings with 7 storeys or more
(3) Supertall buildings – any building over 300m

Learning from the fire in a block of student accommodation in Bolton in 2019, the UK government launched a consultation for lowering the 18m height for 'high-rise' to 11m [48].

Emporis [49], the global provider of building data, defines buildings as high-rise building and skyscrapers according to the height of "between 35 and 100 meters tall" and "at least 100 meters tall" respectively. Some well know stunning atrium in award winning buildings are skyscrapers which are not within this study. Therefore, the high-rise with common atrium form in rectangular and linear is selected common height in the Analysis of Atrium's Architectural Aspects in Office Buildings under Tropical Sky Conditions [20].

2.6.2 Correlation in NFPA92

For the modern atrium, the design is generally based on climatic conditions, architectural experiments, the expected level of thermal comfort, and the functions of the building, achieving energy efficiency as well. A study found that there are four different shapes of atrium that form the main category of atria forms, and the centralised and linear atria are the most common generic forms in use in the hot region. Based on the study of energy efficiency, the aspect ratios of 1:2, 1:3 and 1:4 have similar thermal comfort.

The constant used in Equation in NFPA92, 2021 [1] based on research by Heskestad, 1977 [50], Nowlen, 1987 [51], Mulholland et. al., 1981 [52] and Hagglund, 1985 [53] and review by Chow and Li, 2005 [54]. All these referrals are over 33 to 44 years ago, comparing to the modern atria, those are usually having a much larger volume and dimension length.

After reviewing the current correlations for the smoke control systems, the equations using the height of atrium to the cross-sectional area become the focus of the study.

NFPA92 and SFPE Handbooks are widely used by fire engineers in the industry for the design for smoke management system in an atrium.

In 1977, Heskestad carried out a series of 49 fire tests with enclosed fire in various room geometries, ceiling configuration, fire type and detector spacing for mapping up the environmental conditions of investigation of the response time of different types of fire detectors.

Nowlen test carried out in the enclosure of 18.29mx12.19mx6.10m (L:W:H = 3:2:1). With fuel type Propylene burners, heptane pool, methanol pool and PMMA solid slabs with Peak fire intensity 500KW, 1000kW and 2000KW steady state mode and growing fire mode in 1987.

Mulholland G., Handa, T, Sugawa O., and Yamamoto H. at el. Smoke filling an enclosure in 1981 with heat fluxes ranging 11 to 32Kw. The filling of an enclosure by smoke generated by diffusion flame was studied by measuring the smoke extinction coefficient and temperature versus height during the filling process.

Hägglund et al carried out fifteen experiments in a dimension of 5.62m x5.62mx6.15m enclosure in 1985, fire sizes range from varied from 0.25m×0.25m to 0.75 m × 0.75 m, thermal power 70 kW-630kW. The main purpose of the experimental work was to measure the smoke filling times and temperatures of the descending smoke layer. Therefore, the tests were stopped shortly after the smoke layer had reached the floor level.

The use of hand calculations based on a specific formula can be used to determine the distance from the base of fire to smoke layer interface. For this specific scenario, the equation from NFPA 92B will be used to determine the smoke height for an atrium with the dimension 20m x 20m x 30m. Multiple atrium sizes will be used in this research and the results will be based on the following method from section 3.2. The following atrium sizes all have the same length and width, but the difference is in the height which ranges from 30 to 60 meters tall.

Since the 1970s, atriums have been a welcoming element in architectural design. The risk of smoke control had to be addressed for such a large space due to its size and volume, which are not within the normal range. In 1985, the NFPA Standards Council established two subcommittees to prepare documents for this issue. The basic code NFPA 92 first appeared in 1988 and 1991 in two documents as NFPA 92A and NFPA 92B, respectively. The two separate documents were combined into one in 2012.

The correlation for calculation of the height of the first indication of smoke with no smoke operating in steady fire under Equation 5.4.2.1b of NFPA is considered in this study because this equation starts from the beginning of NFPA 92B in 1991 and is still used in the 2021 edition. The parameter in this equation considers the ratio of the height of the smoke layer interface above the fire surface, z, to the ceiling height above the fire surface. The position of the smoke layer interface at any time can be determined from this correlation, which is based on experimental data from investigations with A/H2 ratios in the range from 0.9 to 14.

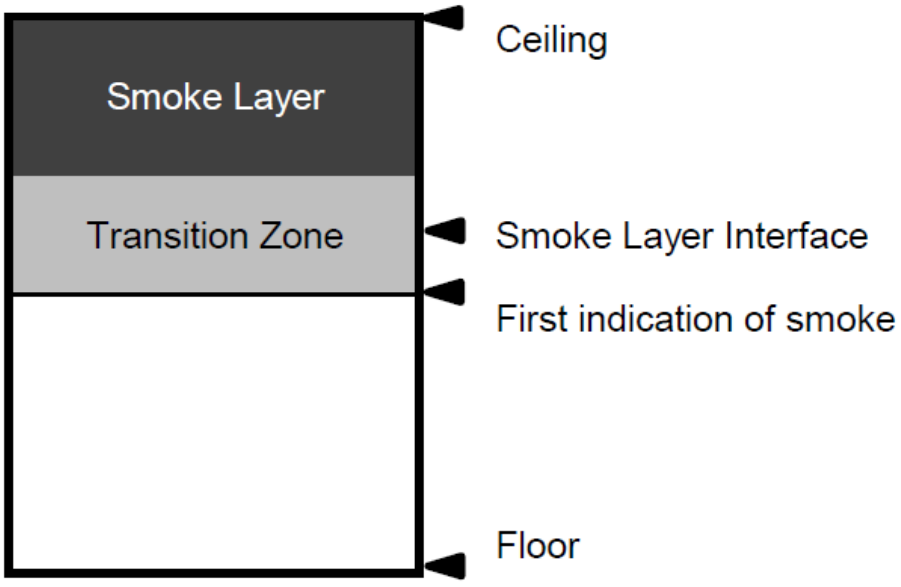

Figure 2-15 First Indication of Smoke and Smoke Layer Interface in NFPA92

First indication of smoke layer in Figure 2-15 described in NFPA92 which is the level of height does not pose a significant threat as the smoke layer interface.

This equation is also referred by Klote, 1994, NIST paper NISTIR 5516, Method of Predicting Smoke Movement in Atria with Application to Smoke Management, for calculation of smoke layer filling by a steady fire [55].

Figure 2-16 Atrium in HSBC Main Building

Figure 2-16 is a sample of rectangular atrium design used in commercial buildings popularly adopted by architects for commercial premises, shopping centres, etc.

2.6.3 Fire plume

Fire plume is the buoyant stream of heated air and combustion products rising above a fire. The main physical parameters that influence fire plume development include the building geometry, air supply by ventilation, fire load and location of the fire.

Equation (2-35) is the mean flame height of the plume by Heskestad, 1984 [56] used in SFPE Handbook, 2016 [11]. Equation (2-8), (2-27), (2-28) and (2-29) is the axisymmetric, corner, wall and spill plume. Equation (2-27) is the Alpert & Ward, 1984 [45] equation for ceiling jet. Equation (2-8) is the Alpert's equation for jet temperature used in CIBSE-TM19, 1995 [4].

The fire plume forms when the fire produces hot temperature combustion products and rise from the fire surface due to the buoyancy effect. When there is fresh air entrained from the

surrounding, the combustion products that are rising will be mixed and cooled down. This mixture of hot gases rising forms the fire plume. The fire plume typically carries away approximately 40 to 70 percent of the total energy generated by the fire.

A fire plume consists of three regions: the persistent flame, an intermittent flame and a buoyant plume. The plume is perceived as an inverted cone rising to the ceiling and expects a ceiling jet when it encounters the boundaries.

Flame height is a fundamental parameter that must be considered in a fire. The equation by Heskestad for the mean flame height in SFPE Handbook, 2016 [11] is based on an experimental measurement dependent on the heat release:

$$L = 0.235\dot{Q}^{\frac{2}{5}} - 1.02D \tag{2-35}$$

In general, there are four plume equations which include the Zukoski plume [44], the Heskestad plume [56], the McCaffery plume [57] and the Thomas plume [58] which has been derived from many practical experiments. The results will be explored and compared.

2.7 Summary of results

Smoke layer height and velocity are the focus of this study. Therefore, the correlation been used from the born of Code and guidelines widely used by fire safety engineer related simply the area and height is selected for investigation.

Selection of atrium shape is based on the shape adapted in most atria which are rectangular and square, Environmental Design of Atrium Buildings in The U.K., 1990 [59]. Also, from the recent study of energy savings and architectural aspect of rectangular and linear atrium are common forms [19]. Mostly minimum 1-storey and tallest 11-storey, majority of atrium height is less than 5-storeys in Asia [19]. One of an icon building in Hong Kong is the HSBC Main Building built in 1985 which has a spectacular 55 metres height atrium.

Hong Kong has an impressive 55m rectangular atrium in the main banking hall of HSBC's headquarters (Figure 2-16). So, for this study, I will examine atria up to 60m (i.e. rounding this number) in 10m increments.

Atria height to compare: 10m, 20m, 30m, 40m, 50m, 60m. There is no apparent reason to pursue this for every 1m of building height to understand the effects and consequences of fires.

CHAPTER 3: Research Methodology

3.1 Numerical methodology

Fire Dynamics Simulator (FDS), Version 6.7.5 developed by National Institute of Standards and Technology (NIST) has been used to perform the numerical analysis [5]. The numerical model is validated against experimental data and a parametric study gas been performed by changing the relevant geometrical features, e.g., height and width, of the atrium that is used as a benchmark.

3.1.1 Mesh size

The cell size (dx) for a given simulation can be related to the characteristic fire diameter (D^*), i.e., the smaller the characteristic fire diameter, the smaller the cell size should be in order to adequately resolve the fluid flow and fire dynamics. [5]

Equation (3-1) refers from the FDS User Guide used a D^*/dx ratio between 4 and 16 to resolve fires in various scenarios accurately [5]. These values were also used to resolve plume dynamics adequately along with other geometrical characteristics of the models. For the mesh resolution, this study will examine the mesh and determine the most suitable one for the rest of the simulations. The three types of mesh that will be referenced are coarse, moderate, and fine.

Once the FDS simulation has completed, the results are compiled into an Excel table for analysis. Since the increments are small, the processed data indicates the time interval per 15 seconds, up to 180 seconds.

The characteristic fire diameter (D*) relationship is given in the following formula:

$$D^* = \left(\frac{\dot{Q}}{\rho_0 c_P T_0 \sqrt{g}}\right)^{\frac{2}{5}} \tag{3-1}$$

FDS has been performed to determine the distance from base of fire to smoke layer interface. Given that there is a 5 MW steady fire in an atrium with the following dimensions: 41 m

length x 23 m width x 23 m height, the following step will be required to perform FDS successfully. The same method used previously will be applied for this scenario.

Table 3-1 Simulations Parameter

HRR (kW)	5,000
Fire Size (m)	1.44 x 1.44
Burning surface (m^2)	2.07
HRR per unit area (kW m^{-2})	2,411.27
D*	1.826
Mesh resolution	$64 \times 64 \times 64$
Computation size	30.4cm

Table 3-1 shows the values and boundary conditions used in the numerical simulations of the fires in the atria. A 5MW fire was used as a base case to perform a grid sensitivity analysis.

3.1.2 Grid sensitivity analysis

In a previous study by Cai and Chow, 2012 [60], the authors suggested that the open boundary conditions could be studied properly with a computing domain which is 7.2m in length, 4.8m in width and 4.8m in height. Thus, this scheme in the Cartesian coordinate system was used in the grid sensitivity analysis of this case.

Since the Grid Sensitivity is an important aspect to consider, the atrium with the dimensions: 20m length, 20m width and 20m height will be evaluated with various D*/dx ratios. A cubic atrium has been used to evaluate the differences between grid mesh. Based on the FDS User Guide [5], a D*/dx ratio of 3, 6 or 9 resolve fires in various scenarios relatively accurately. Therefore, three FDS simulations with each grid type will be analysed.

Table 3-2 FDS Domain and Mesh Properties

Scenario	D*/dx	Cell size (cm)	Total number of cells
G1	3	60.9	32,768
G2	6	30.4	262,144
G3	9	20.3	1,000,000

Table 3-2 describes the three different scenarios G1, G2 and G3 studied, with uniform mesh

distributions. The grids had different cell sizes including 0.609 m, 0.304 m and 0.203 m. The mesh size for 20cm in length, width and height was 32, 64 and 100 when the D*/dx value was 3, 6 and 9 respectively.

The fire occurred in the centre position of an atrium with dimensions of 20m length, 20m width, and 20 m height, in which z is the height of the smoke layer interface.

From these results, a correlation coefficient test could be made to determine which mesh grid is most accurate for the theoretical z curve. The table below will conduct this test, and the results will be illustrated. The mesh with the strongest correlation coefficient shall be used for the remaining FDS simulations.

Table 3-3 Correlation Coefficient to the NFPA92 correlation in the mathematical model

NFPA92	G1	G2	G3	Optimized-Value
1.000	0.945	0.973	0.958	1.000

From Table 3-3, evidence shows that G2 is preferred and performs a greater fit with the NFPA value. This suggests that G2 would be the most suitable FDS mesh size and will be used to conduct future FDS simulations when altering the height of the atrium.

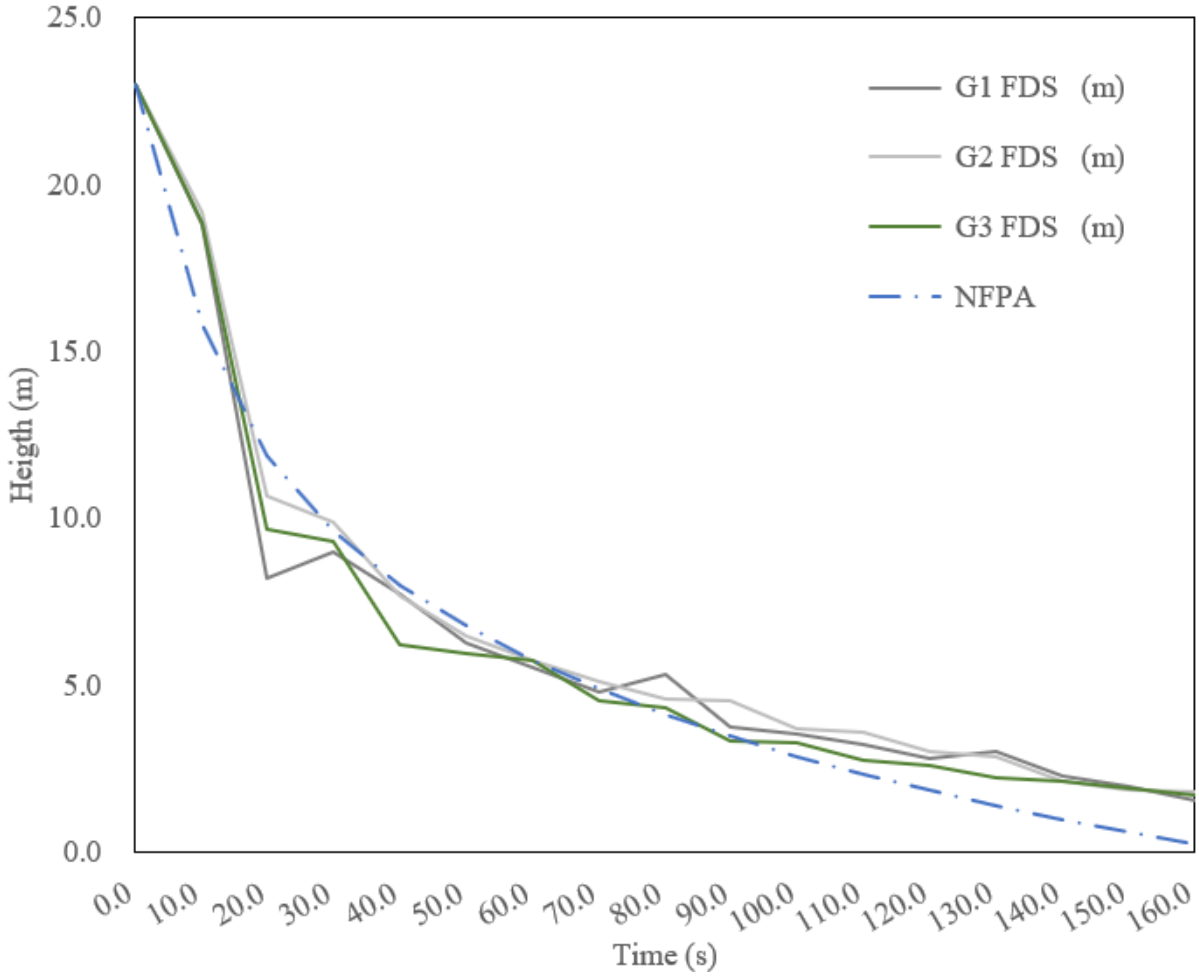

Figure 3-1 Height of smoke above the floor over time using a 5MW HRR and comparing the NFPA92 calculation with three different grid resolutions G1, G2 and G3 FDS.

In Figure 3-1, the curves represent the results for all three simulations on FDS with different grid sizes. It can be observed that the curves derived from the grid resolution of G2 and G3 have an identical shape to the NFPA curve. The curve derived from the grid resolution of G2 has a similar shape as that of the NFPA curve; however, there were significant fluctuations in this scenario. FDS simulations for G3 were carried out, and the fluctuations still existed, suggesting a pattern of unsteadiness. By changing the grid resolution from G1 to G3, a change in the functional analysis has been seen when compared to the theoretical height.

3.2 Validation

An experimental study has been selected for comparison between the full-scale experimental data against the FDS simulated results. This provides a suitable platform for validation to determine how suitable FDS is and how it can be used to support external research. A research article from Guan-Yuan Wu, and Ruu-Chang Chen [61], presents an investigation on

the scenarios of the natural smoke filling times in an atrium due to a located floor fire. The investigation was based on K.S. Yang's experiment [62] as well as Zukoski [44], Thomas [58] and McCaffrey's [57] models. Therefore, a unique comparison between FDS and the findings of Zukoski, Thomas and McCaffrey will be considered.

3.2.1 Introduction to the experimental study

K. S. Yang [62] conducted an experiment in a large-spaced building by Fire Prevention Laboratory in Guei-Jen, Tainan. The dimension of the laboratory is 41 m x 23 m with a height of 23 m. This experiment was executed on a full-scale basis, the aim is to compare and analyse the functions in terms of both prescription and performance-based design for smoke control. By adjusting the amount of smoke exhaust, the velocity of smoke descent and the smoke exhaust performance were evaluated. With both natural ventilation and smoke exhaust equipment closed, the interface height of the smoke layer and time were obtained when oil burners with heat release rate of 5.0 MW were placed under natural smoke filling scenario.

3.2.2 Results from the experimental study

The results of this study have been identified and extracted into the following figure. Their experiment determined the height of the smoke above the base of fire. This is a suitable comparison since the mathematical model and FDS utilize the same variables that will be compared against.

The experimental results are illustrated in Figure 3-2:

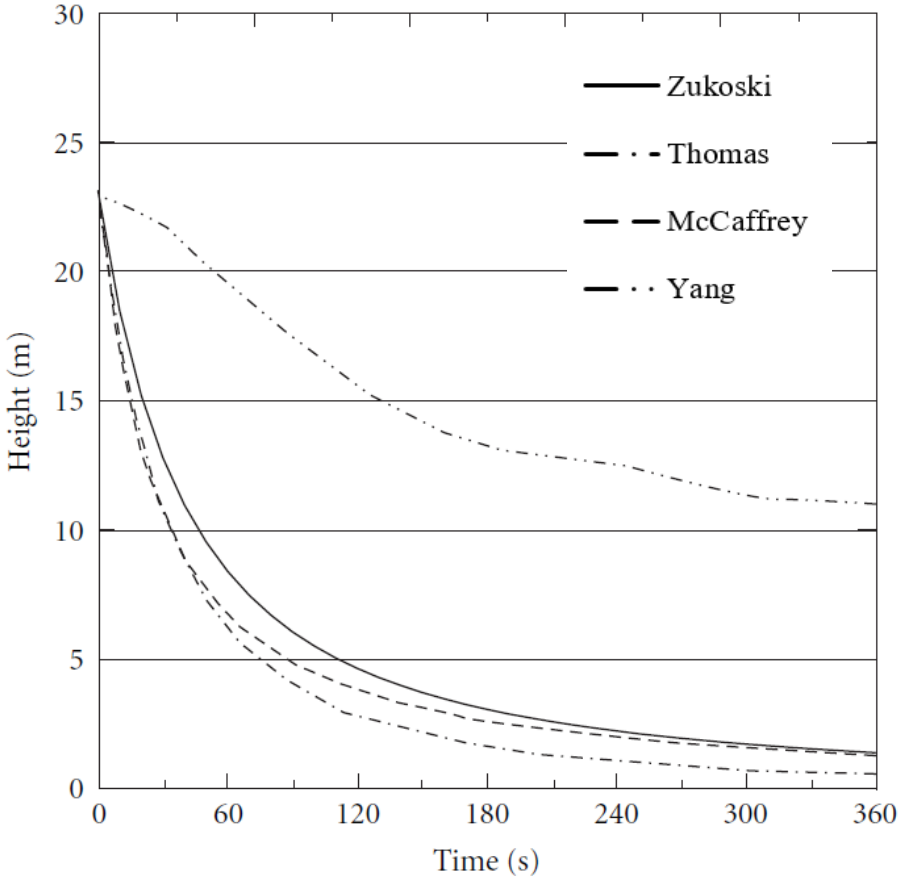

Figure 3-2 Height of Smoke Layer against time in 5 MW steady fire in a closed space with dimensions: 41 m length × 23 m width × 23 m height. Predictions are compared from four different authors (Extracted from Yang's experiment [62])

Figure 3-2 shows the interface height of the smoke layer of the experimental data carried out in a building of 41m length x 23m width x 23m height with a steady fire of 5MW compared to McCaffrey, Zukoski and Thomas models.

3.2.3 Analysis of the results

Yang's experiment [62] requires further analysis since the results were not given in the form of a table, therefore, the graph has to be analysed with MATLAB [65]. To deduce the specific values from their experiment, the following steps are required. The same process has been repeated to determine the results for all Zukoski, Thomas and McCaffrey's research.

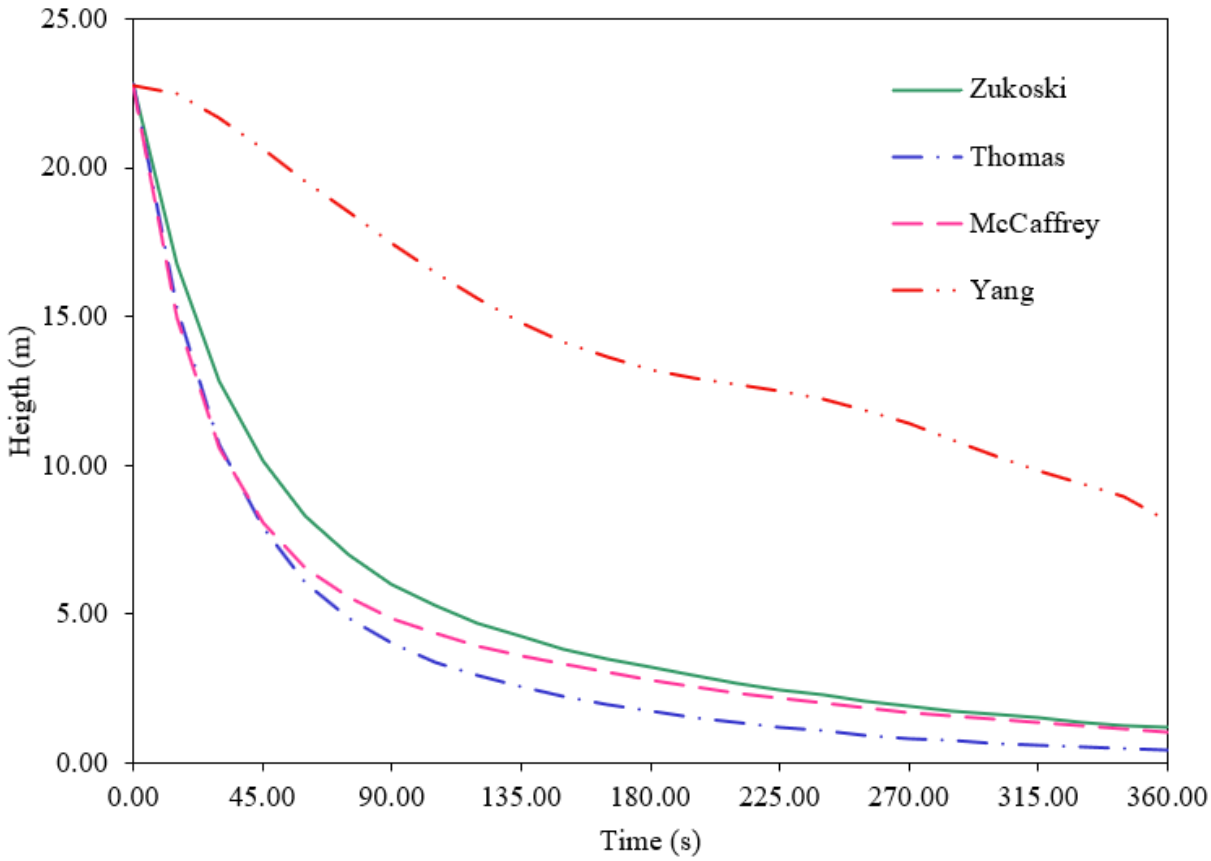

Figure 3-3 Smoke height above ground versus time from Zukoski, Thomas, McCaffrey and Yang using different methodologies

There is agreement amongst the empirical works of Zukoski, Thomas, McCaffrey, and Yang, as shown in Figure 3-3.

3.2.4 Calculating the value of NFPA92 Theoretical Z

With reference to Equation 2-35, empirical correlation based on this formula used in NFPA92 to determine the distance from the base of fire to smoke layer interface, theoretical Z [1].

Given that the dimensions used in the experimental design were 41 m length x 23m width and 23m height, a 5MW steady fire was placed in the atrium, using these dimensions to determine the value of Z.

In order to validate our proposed theoretical model, the experimental data [62] extracted from MATLAB were used to compare the calculated height of smoke layer (based on the proposed theoretical model and 5 MW steady fire in 41 m long x 23 m wide x 23 m High space).

Table 3-4 Comparison of the NFPA92 and experimental data from Yang

	NFPA92	Yang	Difference
Time (s)	Height (m)	Height (m)	(%)
0.0	23.0	22.8	-1.0
15.0	21.6	22.5	4.2
30.0	17.1	21.7	26.5
45.0	14.5	20.6	42.1
60.0	12.7	19.6	54.2
75.0	11.2	18.5	64.4
90.0	10.1	17.5	73.4
105.0	9.1	16.5	81.8
120.0	8.2	15.6	90.0
135.0	7.5	14.8	98.7
150.0	6.8	14.2	108.9
165.0	6.2	13.6	121.1
180.0	5.6	13.2	136.2

From Table 3-4, there is a large discrepancy of between the NFPA and Yang [62], ranging from 4% to 136%. The difference is more obvious upwards with time. However, the slopes of the two curves were quite similar after 45s. The smoke layer is dropping only 3 metre from the top at the first 60s and then descending each 1m at the interval of 15s up to 135s, then slow down to 0.6m onwards to 13.2m at 180s which is more than half of atrium height in the experiment. Whereas the smoke layer from NFPA drops quickly at the beginning 60s nearly to the half of the atrium height and then less than one fourth at 180s. It could be understood that the theoretical calculation did not meet the reality conditions and had a quite big difference too.

To further establish a connection between the results from Yang's study, an FDS Simulation has been conducted with the dimensions and HRR of Yang's design.

3.2.5 Smoke layer height by performing an FDS simulation

Given that there is a 5 MW steady fire in an atrium with the following dimensions: 41 m length x 23 m width x 23 m height, the following step will be required to perform FDS successfully.

Before creation of the input file of FDS simulation, the first thing is to determine the characteristic fire buoyant diameter and cell size ratio in simulation.

The cell size (dx) for a given simulation can be related to the characteristic fire diameter (D^*), i.e., the smaller the characteristic fire diameter, the smaller the cell size should be in order to adequately resolve the fluid flow and fire dynamics. Reference from the FDS User Guide used a D^*/dx ratio is between 4 and 16 to resolve fires in various scenarios accurately. These values were used also to resolve plume dynamics adequately along with other geometrical characteristics of the models. For the mesh resolution, in this study coarse, moderate and fine mesh is adopted to simulate the results.

Table 3-5 List of Grid Size

FDS Simulation	Domain Dimension			Fire Source			D*			Mesh Input			FDS Domain Cell No
Case	Width (m)	Length (m)	Height (m)	Fire Q (MW)	Location of Fire Load	Fire Size (m x m)	D* (m)	D^*/ dx	D* / 4 Coarse Cell Size (cm)	Mesh (I)	Mesh (J)	Mesh (K)	Total Number of Cells
Experiment	41	23	23	5	Centre	1.44x1.44	1.826	6	30.4	135	76	76	779,760

Table 3-5 listed the grid size used to perform the simulations of the 5MW steady fire load in the 41m width x 23m length x 23m height atrium.

Since the increments are very tight, the processed data indicates the time interval per 15 seconds up to 180 seconds.

The results gathered from FDS can be compared against the results from Yang's Experimental study. A comparison table in compiled below:

Table 3-6 Comparison of the FDS and Experimental data (Yang)

	FDS	Experimental Data (Yang)	Difference
Time (s)	Height (m)	Height (m)	(%)
0.0	23.0	22.8	-1.0
15.0	21.5	22.5	4.6
30.0	15.4	21.7	40.7
45.0	13.5	20.6	53.1
60.0	12.8	19.6	52.2
75.0	10.5	18.5	76.5
90.0	9.2	17.5	89.0
105.0	7.6	16.5	116.8
120.0	6.6	15.6	135.5
135.0	6.7	14.8	121.0

150.0	6.6	14.2	114.7
165.0	5.2	13.6	159.7
180.0	5.2	13.2	155.3

Also, Table 3-6 shows that there is a large discrepancy of between the FDS and Experimental data (Yang) [62] ranging from 4% to 160%. The difference is more obvious upwards with time. It shows the percentage is higher than the NFPA.

Furthermore, Table 3-7 is another comparison of the difference between the Theoretical smoke height (NFPA) value and the FDS value from the data analysed of which the highest difference is less than 20% and some of them are very closed to no difference.

Table 3-7 Comparison of Theoretical smoke height (NFPA) and FDS

t (s)	NFPA	FDS	Difference
Time (s)	Height (m)	Height (m)	(%)
0.00	23.00	23.00	0.00
15.00	21.60	21.53	-0.34
30.00	17.14	15.41	-10.10
45.00	14.53	13.49	-7.18
60.00	12.68	12.84	1.33
75.00	11.24	10.47	-6.83
90.00	10.06	9.23	-8.28
105.00	9.07	7.61	-16.14
120.00	8.21	6.62	-19.34
135.00	7.45	6.70	-10.10
150.00	6.77	6.59	-2.70
165.00	6.16	5.24	-14.88
180.00	5.60	5.18	-7.45

In order to evaluate the performance of the proposed theoretical model, the comparison of NFPA z (height of smoke layer), experimental data [62], and data obtained from Zukoski [44], Thomas [58] and McCaffrey [57] Models.

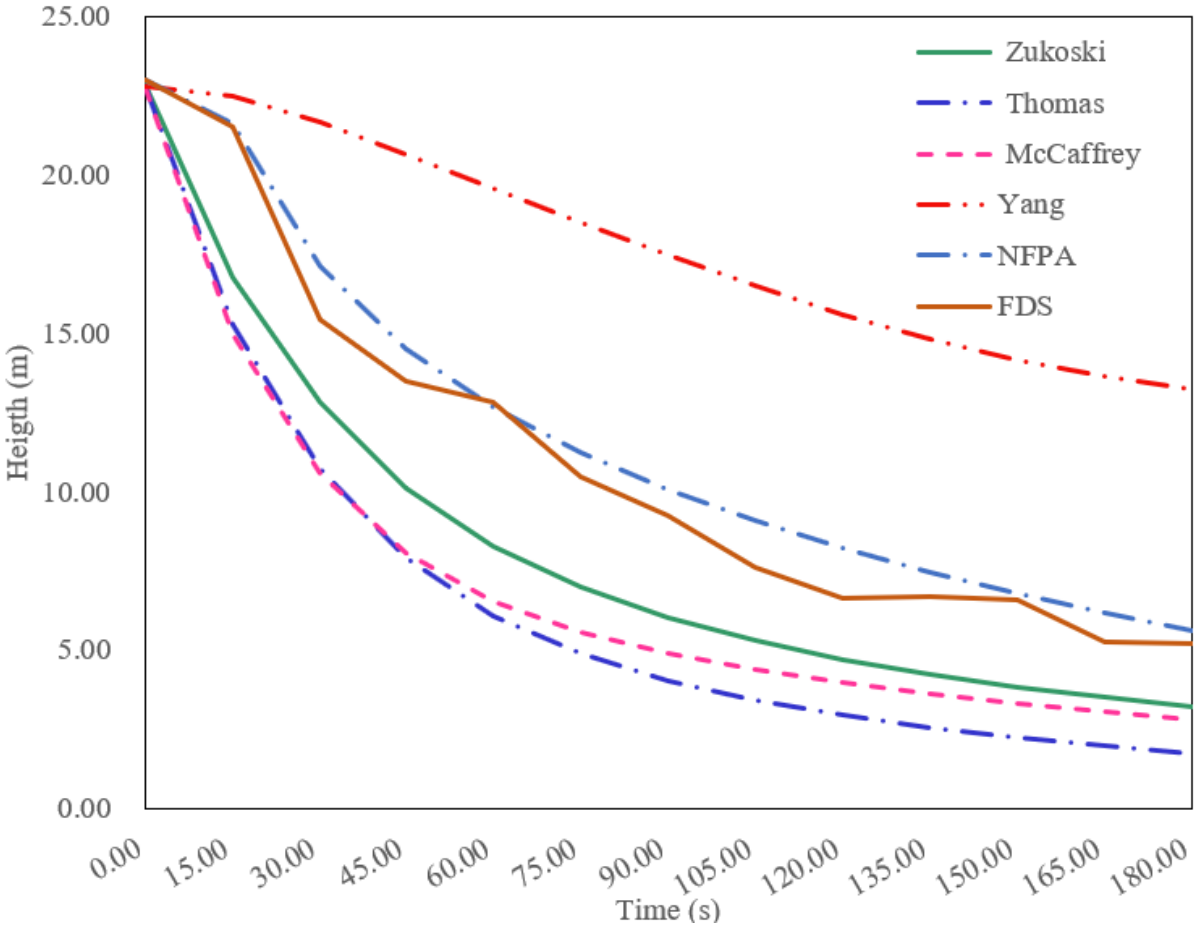

Figure 3-4 The comparison of height of smoke layer based on NFPA, FDS, Experimental data from Yang, and data obtained from Zukoski, Thomas and McCaffrey's studies

Figure 3-4 compares theoretical and experimental data on smoke filling for a 5 MW fire in a 23-metre-tall atrium. The clear height under the smoke decreases over time as the atrium fills. Thomas's formula predicts the fastest rate of descent of smoke. The NFPA correlation is the slowest of the empirical relationships. Yang's experiments are consistently slower because they are based on human observation of smokiness rather than simulation. The FDS simulation is far better resolved than the empirical works, far less subjective than the experiments, and reveals much more irregularity and fine detail.

It is found that the accuracy of the proposed theoretical model was similar to Zukoski model and better than Thomas and McCaffrey model.

3.2.6 Comparison of fire sources

Since the original source used in Yang's experimentation is not known, the fuel source could be questioned. As a result, by researching some typical experimental designs with combustion in real life scenarios, the most common type of fuel used is Methanol and N-Heptane. Both

types of pool fires have been justified as a suitable source for combustion in experimental studies, thus, the use of these substances as a source for combustion can be accepted. Furthermore, Polyurethane can also be considered for combustion since it is a cause of natural fires.

Therefore, further FDS simulations have been carried out to determine whether Propane is a justified fuel to be used alongside the comparison of Yang's experimental design [62]. The use of the three types of combustibles (Methanol, N-Heptane and Polyurethane) has been compared with Propane to determine whether different fire sources affect the value for the distance from base of fire to smoke layer interface. Below are the various comparisons between each source with the original FDS simulation consisting of a Propane flame and the new simulations.

3.2.7 Effect of fuel

A. Methanol

The use of Methanol as a fuel source for combustion arose from an experimental design which used Methanol pool fires. To vary the FDS programme to use a Methanol flame, an alternation to the script is required. Although stating the fuel in the FDS simulation will automatically use this fuel source, the soot yield must be considered as a factor since incomplete combustion happens in real life fires. The soot yield value has been considered as 0.001 upon reading a literature review from Węgrzyński and Vigne (2017) [66]. Radiative fraction has been referenced from the FDS User Guide. The following revised script for the flame source is attached below:

```
&REAC ID='methanol reaction',
      FUEL='METHANOL',
      SOOT_YIELD=0.001,
      RADIATIVE_FRACTION=0.16/
```

Figure 3-5 Revised coding for the FDS simulation

Figure 3-5 is being the input code of methanol as reaction fuel for the combustion in the FDS simulation.

Comparison between Methanol and Propane fuel as the source for combustion:

After completion of the simulation with Methanol, a comparison has been made in which Propane and Methanol has been used to determine whether a significant difference between different fuel sources can be identified.

Table 3-8 Comparison of the difference between using Methanol and Propane as a fuel source

	Propane	Methanol	Difference
Time (s)	Height (m)	Height (m)	(%)
0.0	23.0	23.0	0.0
15.0	21.5	19.9	-7.7
30.0	15.4	13.4	-13.0
45.0	13.5	12.7	-5.7
60.0	12.8	13.5	5.0
75.0	10.5	9.5	-9.2
90.0	9.2	9.3	0.3
105.0	7.6	9.4	23.9
120.0	6.6	7.7	17.0
135.0	6.7	7.5	11.9
150.0	6.6	6.9	5.1
165.0	5.2	6.6	26.5
180.0	5.2	5.7	9.6

Based on the result of this simulation, the consistency between the use of methanol and propane can be seen. The difference in data is not significant, and it seems that the use of methanol aligns with the results when using a propane flame. However, there is a little bit of uncertainty.

B. N-Heptane

The use of N-Heptane is another comparison that could be made with Propane since it was also a source that has been used in real life experimental studies. As a result, an FDS simulation with this fuel source has been conducted. The reference for both soot yield and CO yield from NISTIR 7031 has been considered due to incomplete combustion which would happen in real life scenarios. The altered script for this FDS simulation is attached below:

```
&REAC ID='N-HEPTANE REACTION',
      FUEL='N-HEPTANE',
      CO_YIELD=0.007,
      SOOT_YIELD=0.00108,
      RADIATIVE_FRACTION=0.45/
```

Figure 3-6 Revised coding for FDS when using N-Heptane as the fuel source

Comparison between N-Heptane and Propane fuel as the source for combustion:

The simulation using N-Heptane as the fuel source can once again be compared to the one with propane as the fuel source. A comparison table has been made below.

Table 3-9 Comparison between using N-Heptane and Propane as a fuel source

	Propane	N-Heptane	Difference
Time (s)	Height (m)	Height (m)	(%)
0.0	23.0	23.0	0.0
15.0	21.5	20.5	-4.7
30.0	15.4	15.6	1.1
45.0	13.5	13.1	-3.1
60.0	12.8	11.7	-9.3
75.0	10.5	9.6	-8.1
90.0	9.2	7.9	-14.1
105.0	7.6	7.4	-2.2
120.0	6.6	6.4	-3.5
135.0	6.7	5.5	-18.3
150.0	6.6	6.8	3.5
165.0	5.2	6.3	20.1
180.0	5.2	4.3	-16.5

As can be seen from Table 3-9, the similarities between both N-Heptane and Propane as a fuel source for consideration is very similar. It could also be said that the N-Heptane is more like Propane than when Methanol was used. A consideration as to why this may be true is because N-Heptane and Propane fall into the same category of organic compounds - alkanes. Since they are both classified as alkanes, they both undertake combustion in a similar way.

C. Polyurethane

Another type of substance that can be considered as a combustible fuel is Polyurethane since it is a natural cause of fire. This matter is originally a solid which can be used for comparison with Propane. The code used to run it in the FDS program is shown below:

```
&REAC ID='POLYURETHANE_REAC',
      FYI='SFPE HANDBOOK, GM27',
      FUEL='REAC_FUEL',
      C=1.0,
      H=1.7,
      O=0.3,
      N=0.08,
      CO_YIELD=0.042,
      SOOT_YIELD=0.198/
```

Figure 3-7 Revised coding for FDS when using Polyurethane as the fuel source

Comparison between Polyurethane and Propane fuel as the source for combustion:

When considering these two types of substances for combustion, their chemical properties are considerably different in structure. While propane is a short chain of hydrocarbons, polyurethane is considered a polymer that is branched and complex. Therefore, the outcome of this simulation may differ.

Table 3-10 Comparison between using Polyurethane and Propane as the fuel source

	Propane	Polyurethane	Difference
Time (s)	Height (m)	Height (m)	(%)
0.0	23.0	23.0	0.0
15.0	21.5	21.5	0.0
30.0	15.4	15.5	0.7
45.0	13.5	14.5	7.3
60.0	12.8	12.9	0.1
75.0	10.5	10.0	-4.7
90.0	9.2	9.0	-3.0
105.0	7.6	7.6	0.2
120.0	6.6	6.9	4.0
135.0	6.7	6.9	3.2
150.0	6.6	6.7	1.8
165.0	5.2	6.1	17.2
180.0	5.2	5.5	5.3

When looking at Table 3-10 in detail, it seems that out of all the comparisons made between each type of fuel, Polyurethane data adhered to the Propane data stronger than the other sources. As a result, even though the chemical structure may seem more branched and complex, the overall combustion still yields similar results in FDS.

3.2.8 Overall comparison with all the different types of fuel sources 5MW

When comparing the three different types of fuel sources to Propane (the original source used in the first FDS simulation), the results yielded very similar data. This is shown on Figure 3-8. Therefore, when considering the various types of fuel sources, it can be said that Propane could also be considered as a suitable choice. There seemed to be no outstanding fuel sources which would defy against the data gathered from the Propane FDS simulation and thus, question the reasoning towards using this as the fuel source for comparison against Yang's experimental design. Below is a comparison between all the types of fuel sources used in FDS as well as the data from Yang's experimental design.

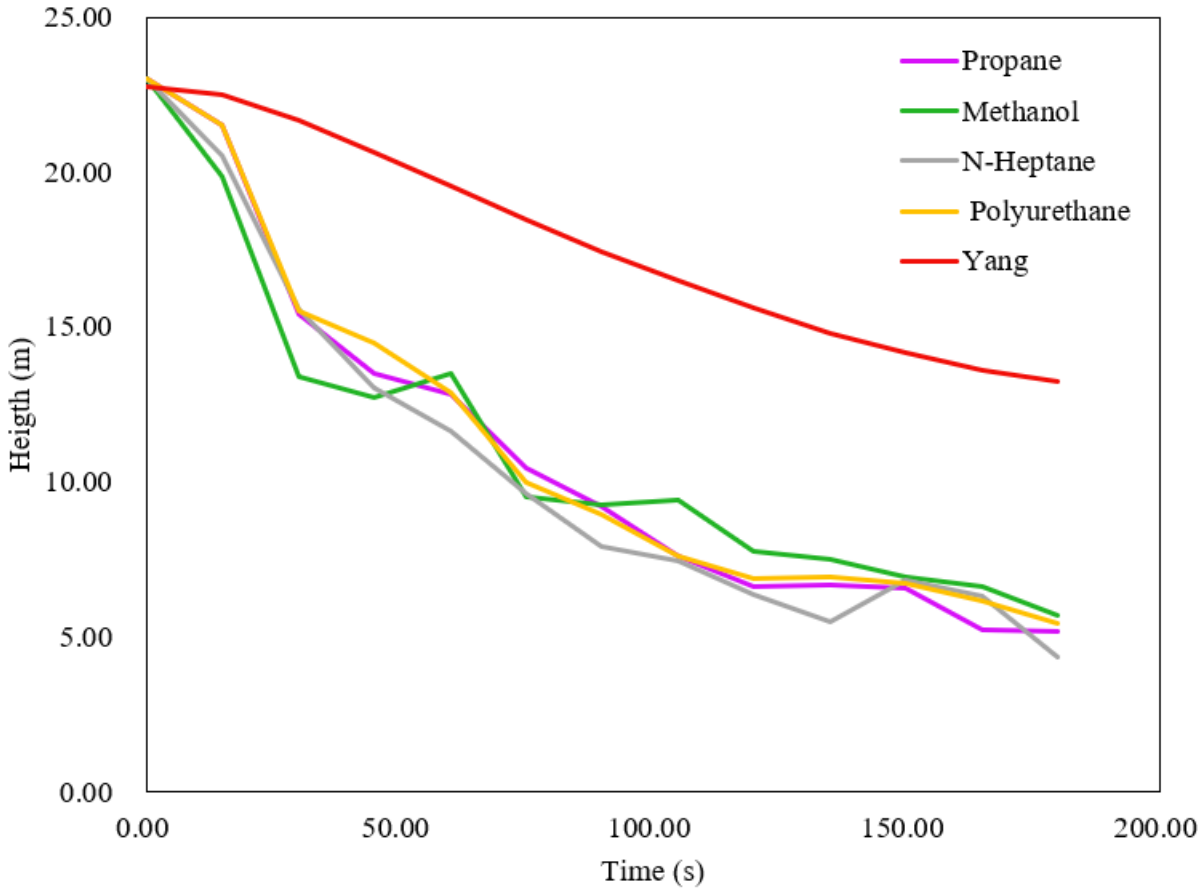

Figure 3-8 Complete comparison between all the fuel sources of 5MW used in FDS against Yang's Experimental design

3.2.9 5MW heat release rate N-Octane flame FDS comparison

Whilst reviewing the literature related to Yang's experimental design, the fuel source was unknown and not stated in the article. As the author of the experiment stated, his guest 95 Non-Leaded Gasoline was used. As a result, this translates to using N-Octane in for the FDS simulation. A 5MW Heat Release Rate was used to determine how FDS compares to the actual results noted from the real-life experimentation. Below is the graph of the original data set from Yang, the NFPA and the FDS simulated graph.

The N-Octane graph seems to be relatively like the NFPA result and distant from Yang's experimental design. This could suggest that external variables may conflict with the outcome of the experiment. Problems such as ventilation may be an issue in the real-life experiment and affect the outcome of the smoke plume. In addition, the data from FDS suggests a relatively stable curve and is quite close to the NFPA in the beginning.

3.2.10 Comparison of N-Octane against alternative fuel sources

When using the FDS program, different fuel sources have been used to determine whether significant differences could be seen. Therefore, N-Octane has been input into the graph below to compare it against the other fuel sources.

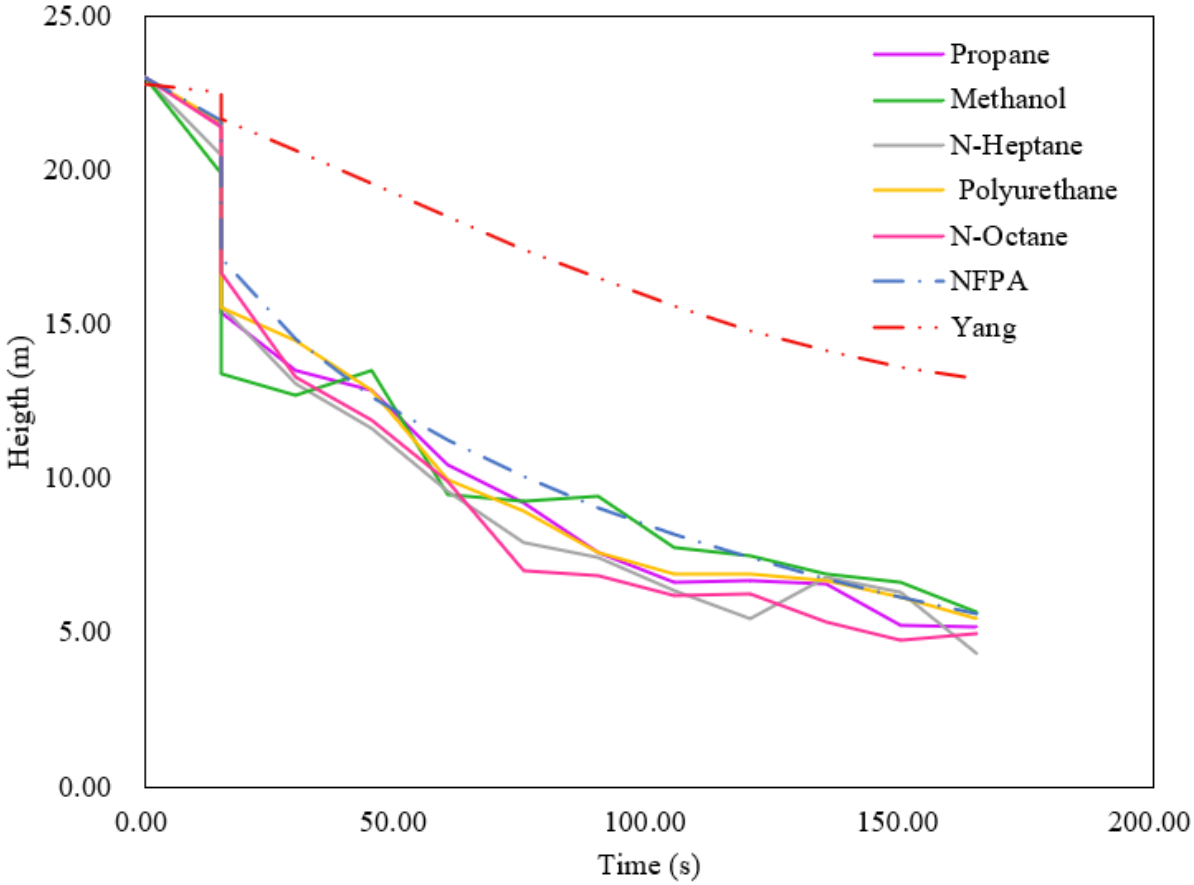

Figure 3-9 A comparison between all the fuel sources and N-Octane of 5MW from the FDS simulation against Yang's Experimental design and NFPA

When different fuel sources have been used in the FDS program, the differences are relatively minor and still follow the trend suggested by the NFPA as shown in Figure 3-9. However, Methanol seems to be most like the NFPA line, but it consists of some fluctuations. The N-Octane curve is not the smoothest but better than that of Methanol. On the other hand, the smoothest graph is from Polyurethane. In conclusion, the external variables may have contributed to Yang's experiment causing it to differ from the FDS simulated results. The use of various fuel sources has not significantly impacted the data collected.

3.2.11 Comparison between different fuel sources when a HRR of 4.9MW

A series of FDS simulations have been conducted in which a HRR of 4.9MW has been used for analysis. The fuel sources that have been considered are Propane, Methanol, N-Heptane and Polyurethane. The same experimental design has been used in which the atrium sizes and soot yields have been kept consistent.

By analysing the data from FDS simulations, the following conclusions have been compared against the last set of data in which 5.0 MW HRR has been used.

The first fuel source that has been considered is Propane in which a HRR of 4.9MW has been selected. When considering this comparison, an illustrated graph has been produced to visually analyse the data. A comparison can also be drawn against the smoke layer height from NFPA values.

When considering the results from the FDS simulation, the curve from Propane (4.9MW) adheres closely to the original line (Propane 5.0MW). The outcome of this suggests that altering the HRR by 0.1MW seems to not have a strong effect on the distance from the base of fire to smoke layer interface. When comparing the results against the curve from the NFPA values, the start and end are remarkably similar.

Originally, the FDS simulation using Methanol (5.0MW) resulted in a very unstable curve. This time the simulation will run with Methanol as the fuel source producing a HRR of 4.9MW.

From the result, it could be seen that the original line for Methanol (5.0MW) was relatively unstable and had fluctuations in the 30 to 105 second region. The results seem to be more stable and provide more of a slope. In addition, when compared to the NFPA, the 4.9MW line seems to be closer in that regard.

N-Heptane has been considered as a more stable line providing a gentle curvature when the FDS simulation was conducted with a 5MW HRR. However, towards the end of the 180 s, the height suddenly went up and as a result disrupted the curve.

From the results, the 4.9MW HRR seems to show a greater descent from 15 to 30 seconds. However, the time period from 135 to 180 seconds seems to have a bit more consistency without the jump seen previously in the 5.0MW line.

By using Polyurethane as a fuel source, the 5MW test seemed to provide a slightly smoother curve when compared to Methanol. However, there is still a slight dip when compared to the likes of N-Heptane (5MW).

A drop from 21 to 11 meters from 15 to 30 seconds has been seen in the FDS simulation which suggests a greater downward slope. This affects the data by disrupting the slope that should have theoretically been formed. Therefore, by decreasing the HRR from 5.0MW to 4.9MW, this does not seem to improve the previously gathered data.

After conducting all four simulations with a HRR of 4.9MW, a graph has been produced to compare all the different fuel sources with reference to the NFPA value. This is illustrated in Figure 3-10.

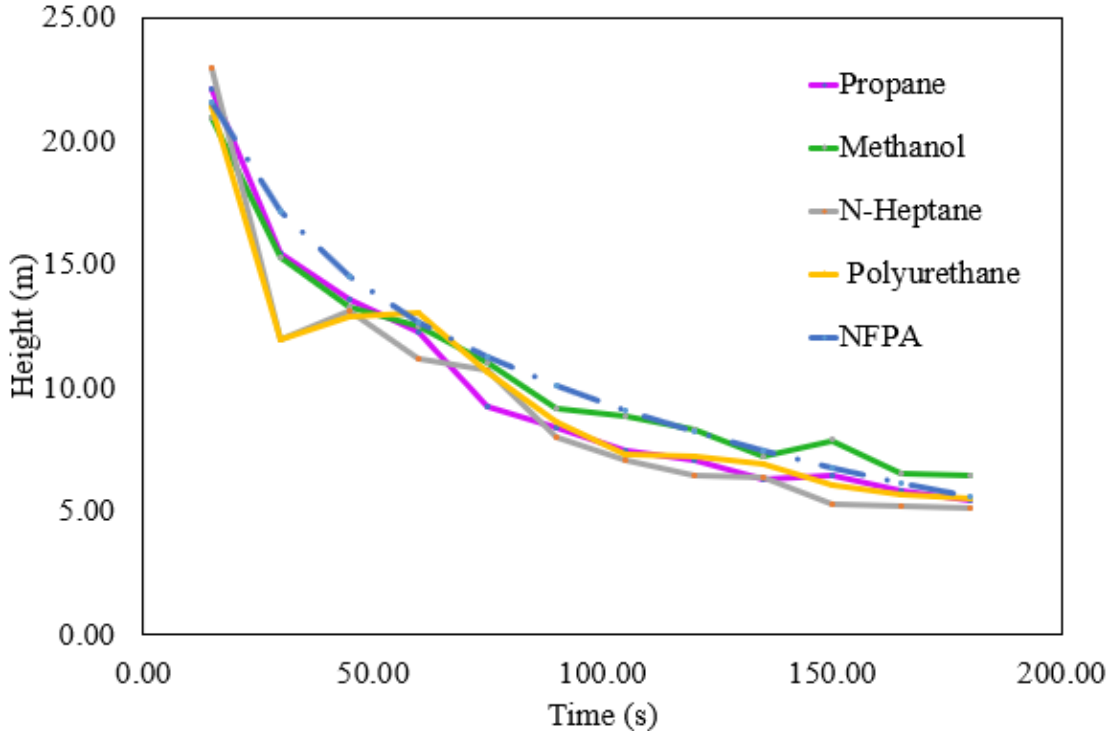

Figure 3-10 A comparison between all the different fuel sources when a HRR of 4.9MW is considered against NFPA

3.2.12 Determining the effect of changing the heat release rate to 4.5MW

From the 4.9MW HRR simulation, it seemed to yield interesting results in which both Polyurethane and N-Heptane seemed to be unstable at the beginning. The dip was seen between 15-30 seconds before gradually increasing back to its theoretical curve shape. However, after all the FDS simulations, the later part of the results was terribly similar to the data gathered from the 5.0MW HRR FDS simulations. All of the different fuel sources seemed to follow the same trend of decreasing as time passes.

Then a HRR of 4.5MW used to simulate to find the effect of changing the fire load. Furthermore, the heat efficiency rating is also considered as a factor. The following fuel sources will be studied: Propane, N-Heptane, Methanol and Polyurethane.

Reflecting from the previous results, the smoothest line that has been produced is the one from 5.0MW. This is followed with the more unsteady line produced by the 4.9MW results table. The completed FDS simulation using 4.5MW has been compared with the previous two results.

When comparing the differences between the HRR, the 4.5MW line was the most unstable at the beginning since the gradient from 15 to 30 seconds dropped significantly. When the 4.5MW line is compared against the others, it seems to go along the same path as time passes from 60 to 180 seconds. Out of all the lines, the 5.0MW data seems to fit the curve and become steadier as the simulation goes on.

N-Heptane was discussed previously, in which the 5MW flame produced one of the most stable curves when compared against the other fuel sources. Whilst this may be stable, at the end, between 140-180 seconds, there was a slight rise in height, thus affecting the shape of the curve. When 4.9MW was explored, the results suggested a huge jump from 15 to 30 seconds, which was not expected. This unsteadiness caused fluctuations and affected the data.

The 4.5MW line seemed to be most steady and when compared against the others, provide the most stable curve. The drop previously seen most exaggerated between 15 to 30 seconds from the 4.9MW flame has now resulted in gentle decrease similar to that of the NFPA. The 4.5MW line seemed to be in closer proximity to the NFPA values although the gap increases from 100 seconds onward.

Methanol has been previously explored in which the 5MW flame was most unstable when compared against the 4.9MW HRR. The 4.9MW flame provided a better and more stable result and seemed to have less stutter.

When comparing the 4.5MW HRR data against the other two data, it seems to highlight the smoothness of the 4.9MW line. The line generated for a HRR of 4.5MW did not yield data that provided a gentle slope. Between 45 to 120 seconds, there was a slight negative parabola shape. From 120 to 180 seconds, there was another slight increase in height.

Polyurethane has produced a relatively consistent result in the other two sets of simulations in which the 5MW graph seemed to be quite smooth. The polyurethane curve for 4.5MW seemed to be most suitable and considerably more stable than the other sets of data. However, there seems to be a slight upward movement for 120 seconds, but it quickly decreases back to its stable curve structure. Another line that can also be considered quite stable is the 5MW one.

A comparison between all the different fuel sources with a HRR of 4.5MW has been plotted into Figure 3-11.

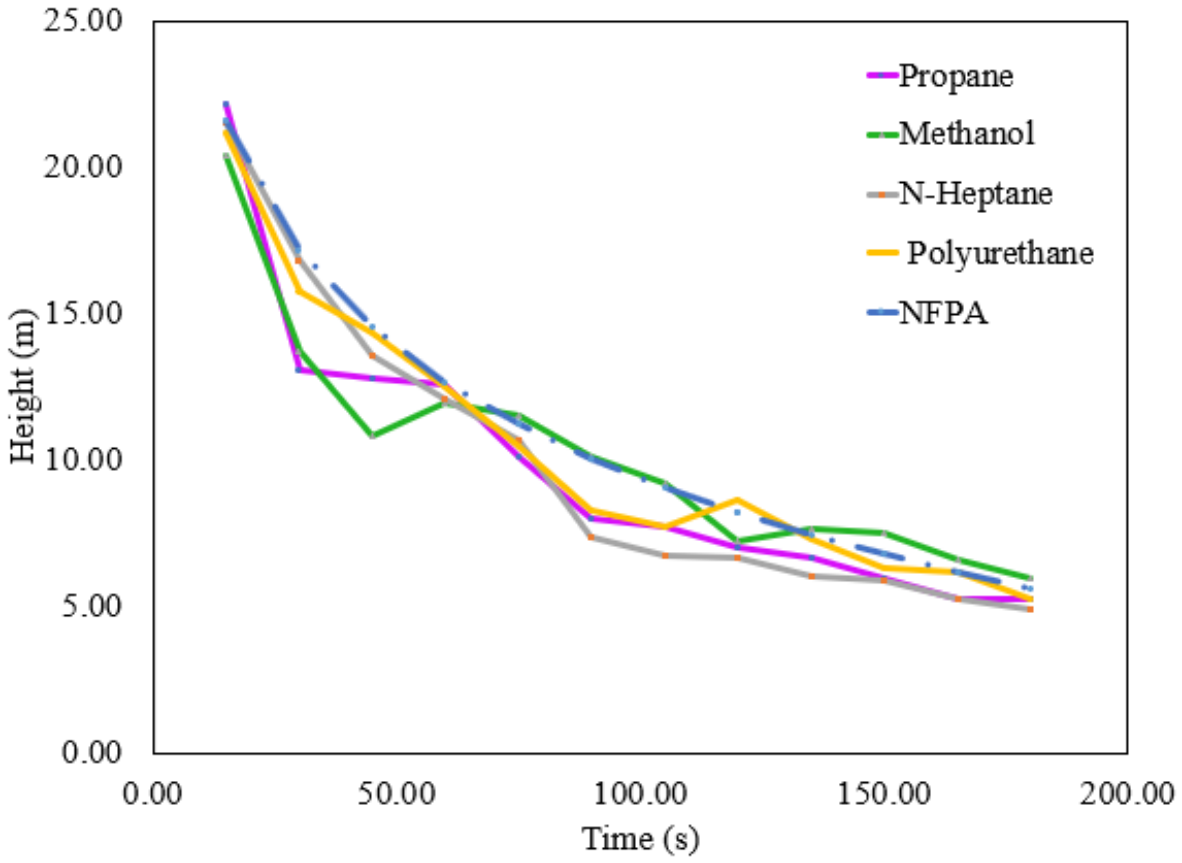

Figure 3-11 A comparison between all the different fuel sources when a HRR of 4.5MW is considered against NFPA

In conclusion, when comparing all the different fuel sources, the consensus lies around the idea of either N-Heptane or Polyurethane as a more stable source that can be used. On the other hand, Methanol has provided some unsteady results which may be deemed unsuitable.

3.2.13 Comparison of velocity and temperature among different fire load in various tall atrium

Fire load is the critical parameter that directly affects the temperature and is an important factor influencing the direction of plume flows. FDS simulation for 2MW, 5MW, and 25MW, referred to NFPA 92, 2021 [1] and NISTIR 5516, 1994 [55] for steady design fire sizes for atria.

Table 3-11 Steady design fire sizes for atria

Fuel loading	Design fire (MW)
Low (Minimum fire for fuel-restricted atrium)	2
Typical (Minimum fire for atrium with combustibles)	5
High (large fire)	25

The fire source consisted of fuel of 1m in length by 1m in width for 2MW fire load, 1.44m in length by 1.44m in width for 5MW fire load and 2.73m in length by 2.73m in width for 25MW for 25MW fire load for the simulation. Velocity and temperature in different height in various tall atria at 100s are considered.

Fire load - 2MW

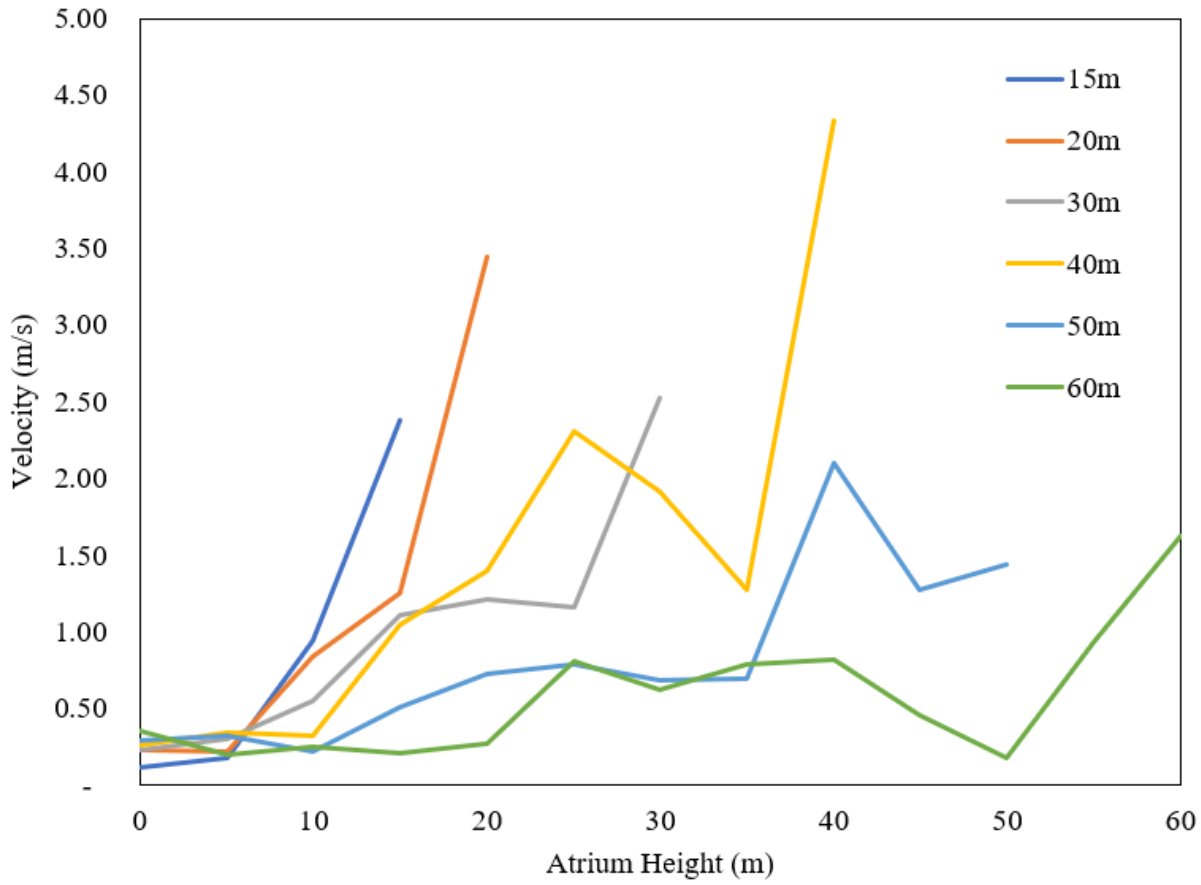

Figure 3-12 Velocity at different height in various tall atrium at 100s (2MW)

As shown in Figure 3-12, with the fire load of 2MW, the velocity in atrium of various heights less than 30m has a trend of upward at 100s at all measuring height from low to top. At 40m tall atrium, velocity drops from 25m and returns sharply upward at 35m to the roof. It happens in 60m too, it drops from one third of the atrium height and rebounds at the 50m to the top.

For the plume centerline temperature, the Heskestad flame height of a 2MW fire load with a fire diameter of 1.265m is 3.62m. Therefore, data below 3.62m is excluded.

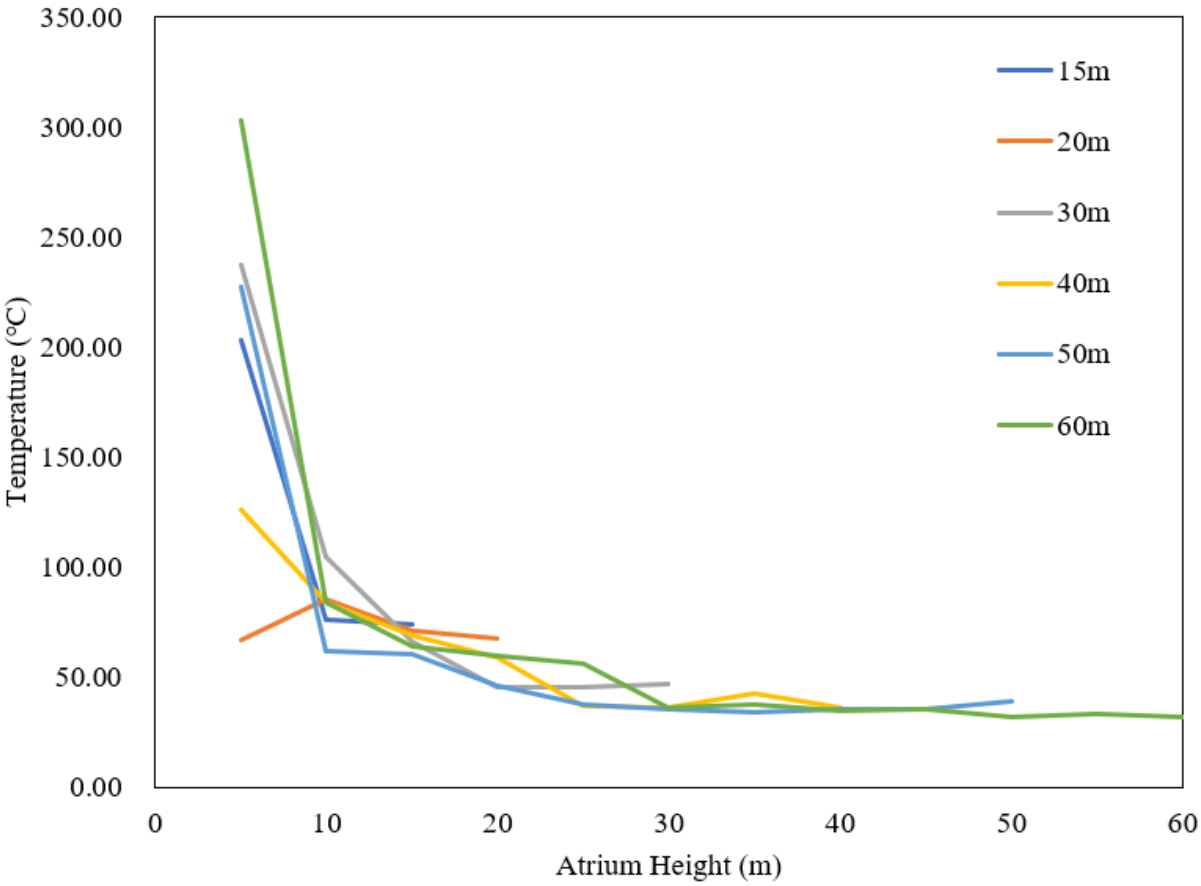

Figure 3-13 Plume Centreline Temperature at different height in various tall atrium at 100s (2MW)

Figure 3-13 shows that with the 2MW fire source, the plume centreline temperature of various atrium drops with the increase of height when the plume moved upwards to the top of atrium almost in all different height of atrium at 100s.

Fire load - 5MW

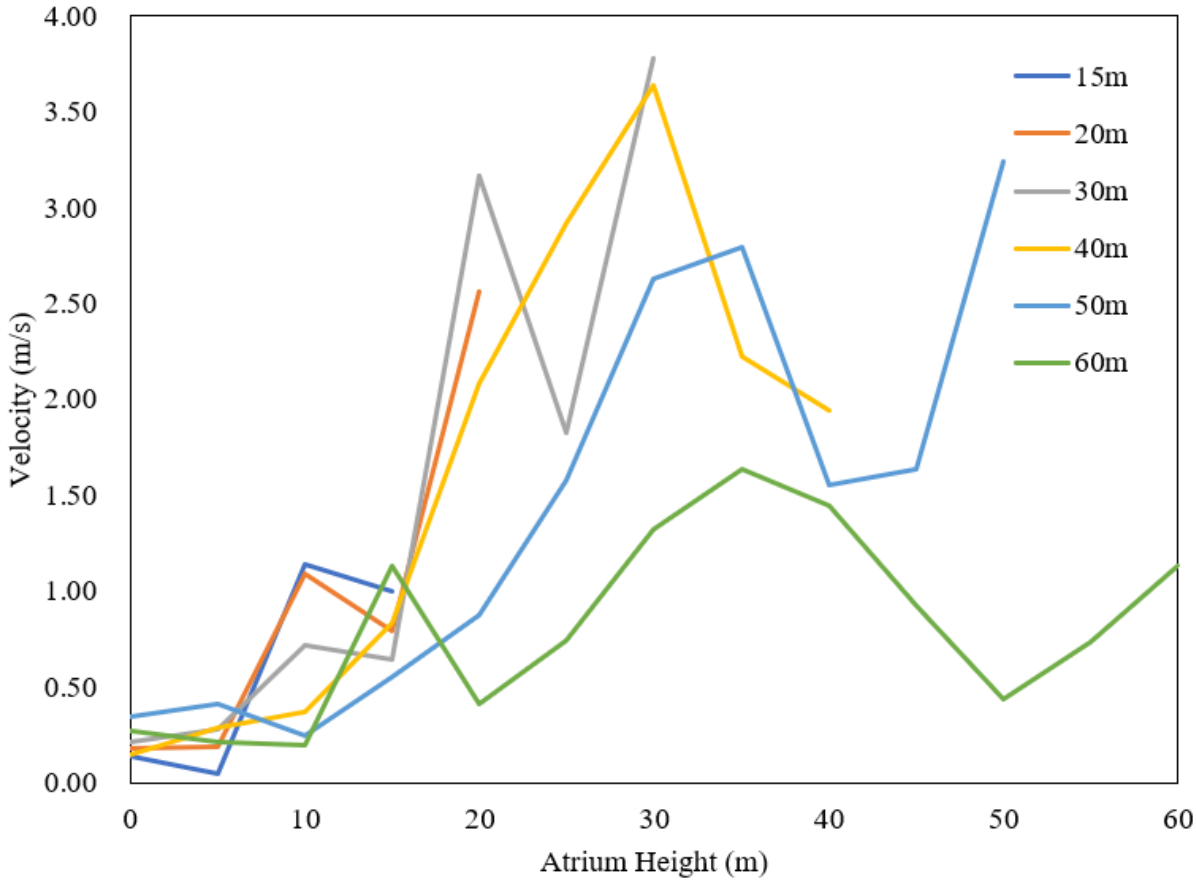

Figure 3-14 Velocity at different height in various tall atrium at 100s (5MW)

In the 5MW simulations, the velocity of atrium at 15m and 20m has a trend of upward at 100s at all measuring height from low to top. At 30m tall atrium, velocity drops sharply from 10m below the roof and rebounds at 5m upper level and move upward from 5m below the roof. It happens in 50m too, it drops from two third of the atrium height and rebounds at 10m below the roof to the top. In the 60m tall atrium, the velocity is going up and down which can be considered as buoyancy effect which due to the loss of energy to the ambient temperature in large space.

Figure 3-14 shows that not all the atriums have the highest velocity at the ceiling level and does not show that the height of the atriums has a positive relationship with the velocity.

For the plume centerline temperature, the Heskestad flame height of a 5MW fire load with a fire diameter of 1.826m is 5.23m. Therefore, data below 5.23m is excluded.

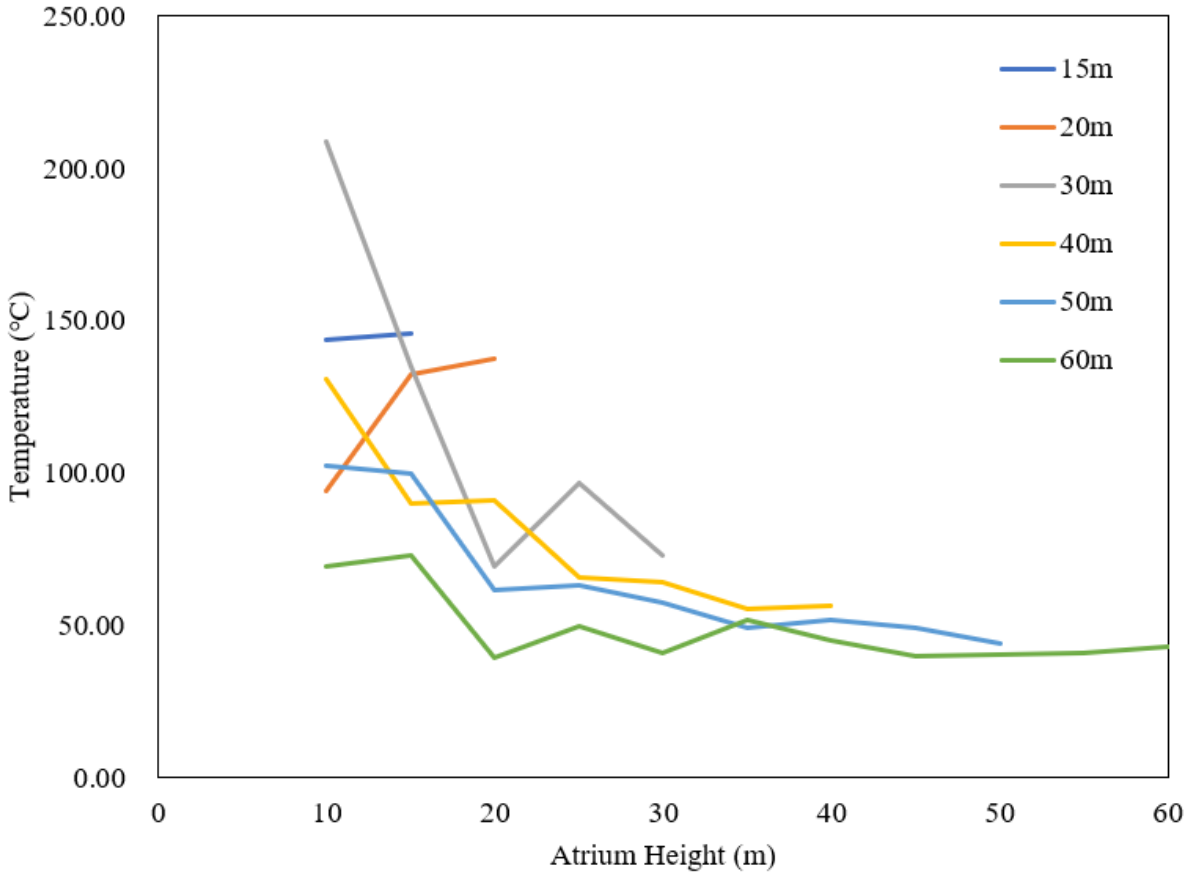

Figure 3-15 Plume Centerline Temperature at different height in various tall atrium at 100s (5MW)

Figure 3-15 shows the plume centerline temperature in all atria, the temperature goes upwards at the 15m and 20m tall atrium. At the time of 100s, the temperature is all below 68℃ at the atrium more than 40m of which the smoke detectors are normally installed. So, fire alarm will not be activated at the level of temperature. The smoke layer is found to quickly drop to below 20% in the higher atria at 180s.

Fire load - 25MW

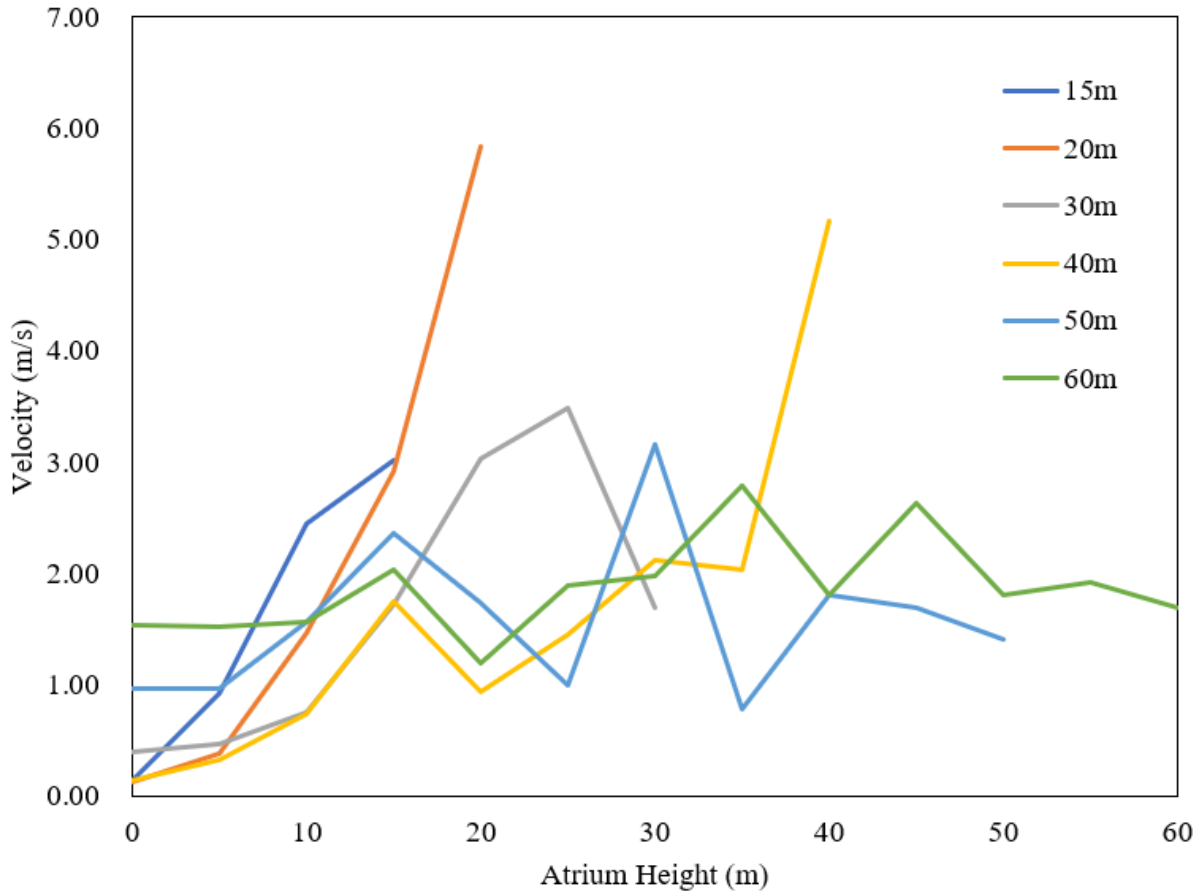

Figure 3-16 Velocity at different height in various tall atrium at 100s (25MW)

Figure 3-16 shows the velocity in the 15- and 20-metre atriums increased upward at 100s at all measuring heights from low to top under the 25-MW fire source. At a 30-metre-tall atrium, velocity drops from 25m. For the 40-, 50-, and 60-metre-tall atriums, velocity is moving up and down.

For the plume centerline temperature, the Heskestad flame height of a 25MW fire load with a fire diameter of 3.475m is 9.95m. Therefore, data below 9.95m is excluded.

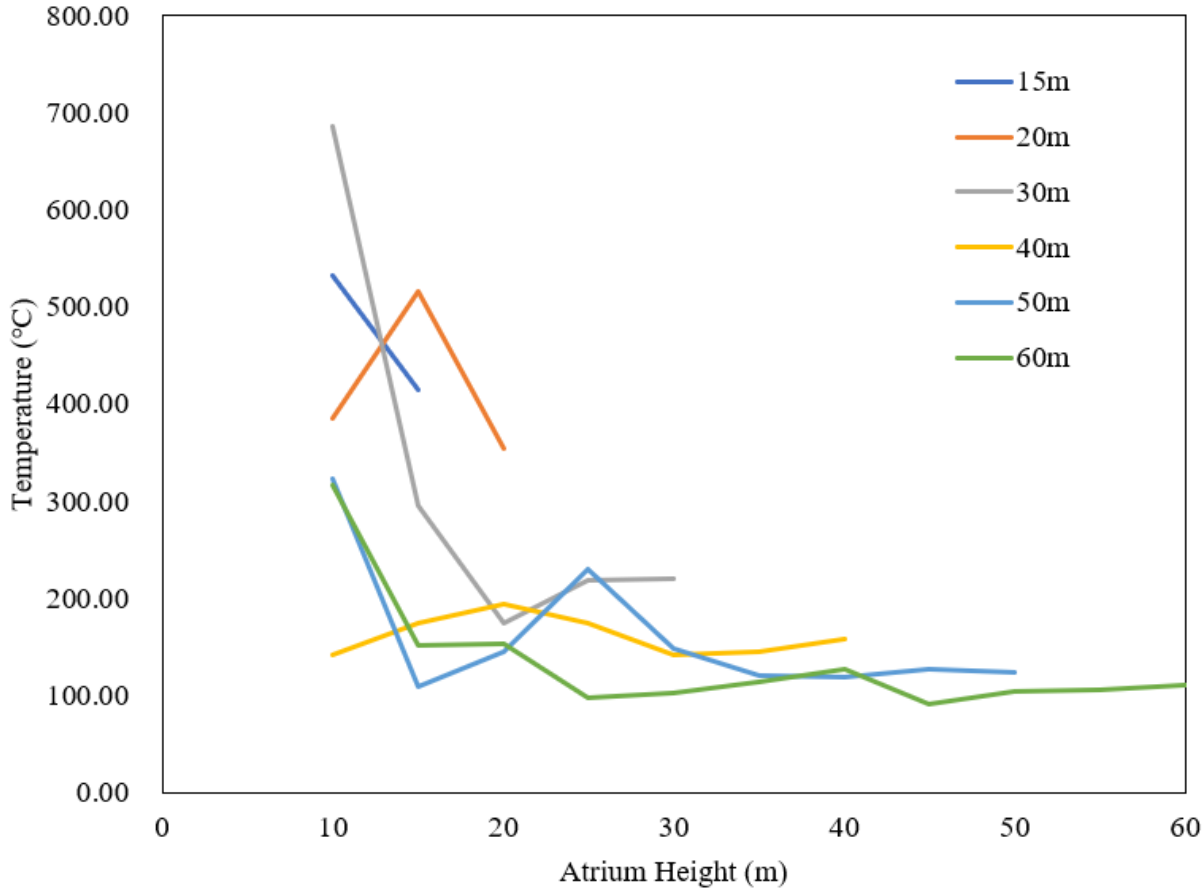

Figure 3-17 Plume Centreline Temperature at different height in various tall atrium at 100s (25MW)

From the plume centerline temperature distribution in Figure 3-17, there is a hotter smoke layer at the middle of the height of the atrium in the 20m, 30m, 40m, 50 m, and 60m atriums at 100s of the 25 MW fire source.

Stratification happens in the 60m tall atrium, the smoke spread to the surrounding instead of moving upwards at 25m and 35m layer between the floor and ceiling.

3.2.14 Combined graph of velocity and temperature in various tall atrium at 100s at the fire load of 5MW

The following are the combined graph of the velocity and temperature plot onto the same graph with two y-axis variables to demonstrate the relation at 100s in various height of atrium with fire load of 5MW.

15m tall atrium

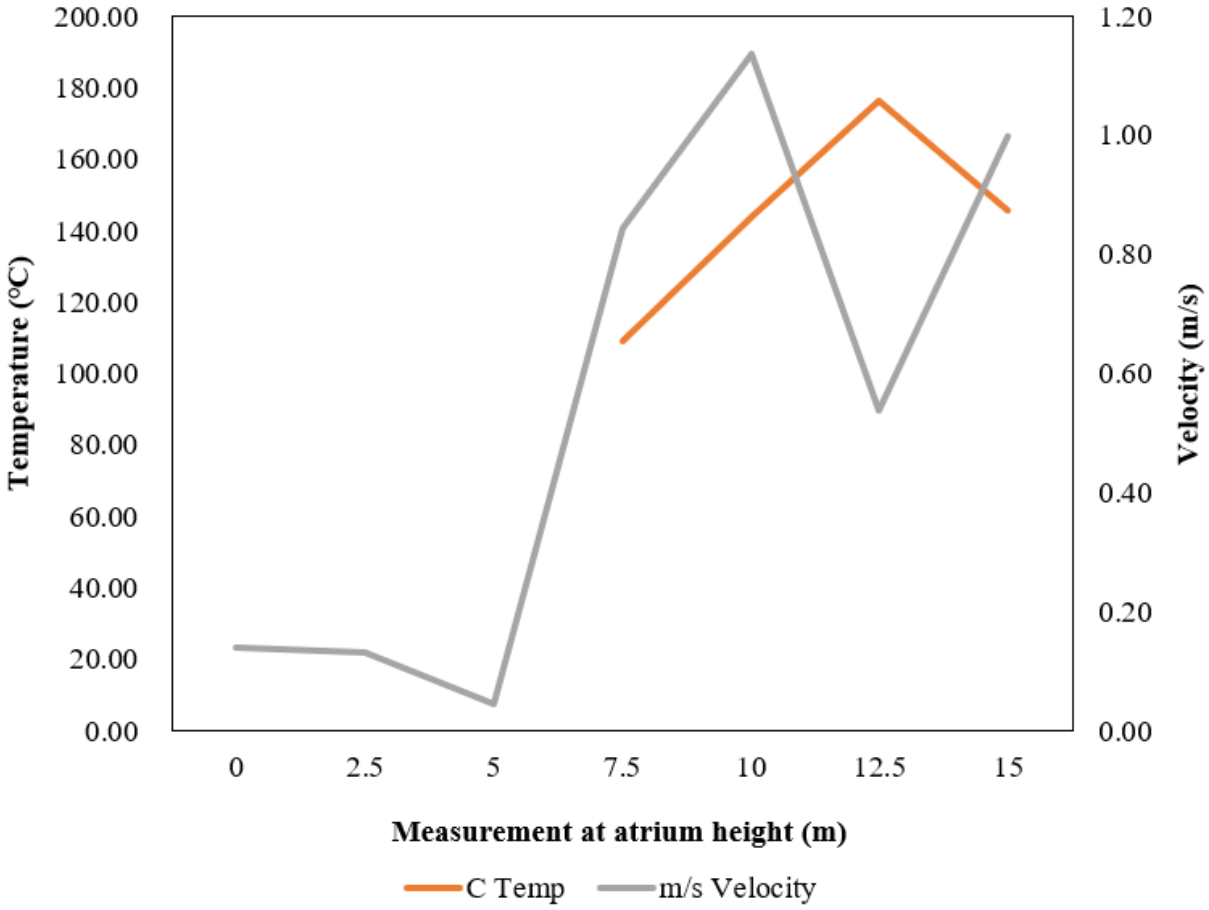

Figure 3-18 Combined temperature and velocity in 15m atrium at 100s at 5MW fire load

The velocity in the 15-metre atrium at 100s shown in Figure 3-18 has the highest value at 10m, drops to a lower value at 12.5m and then rebounded to the ceiling at 15m. The highest temperature is at 12.5m and lowers when the velocity rebound at the same time.

20m tall atrium

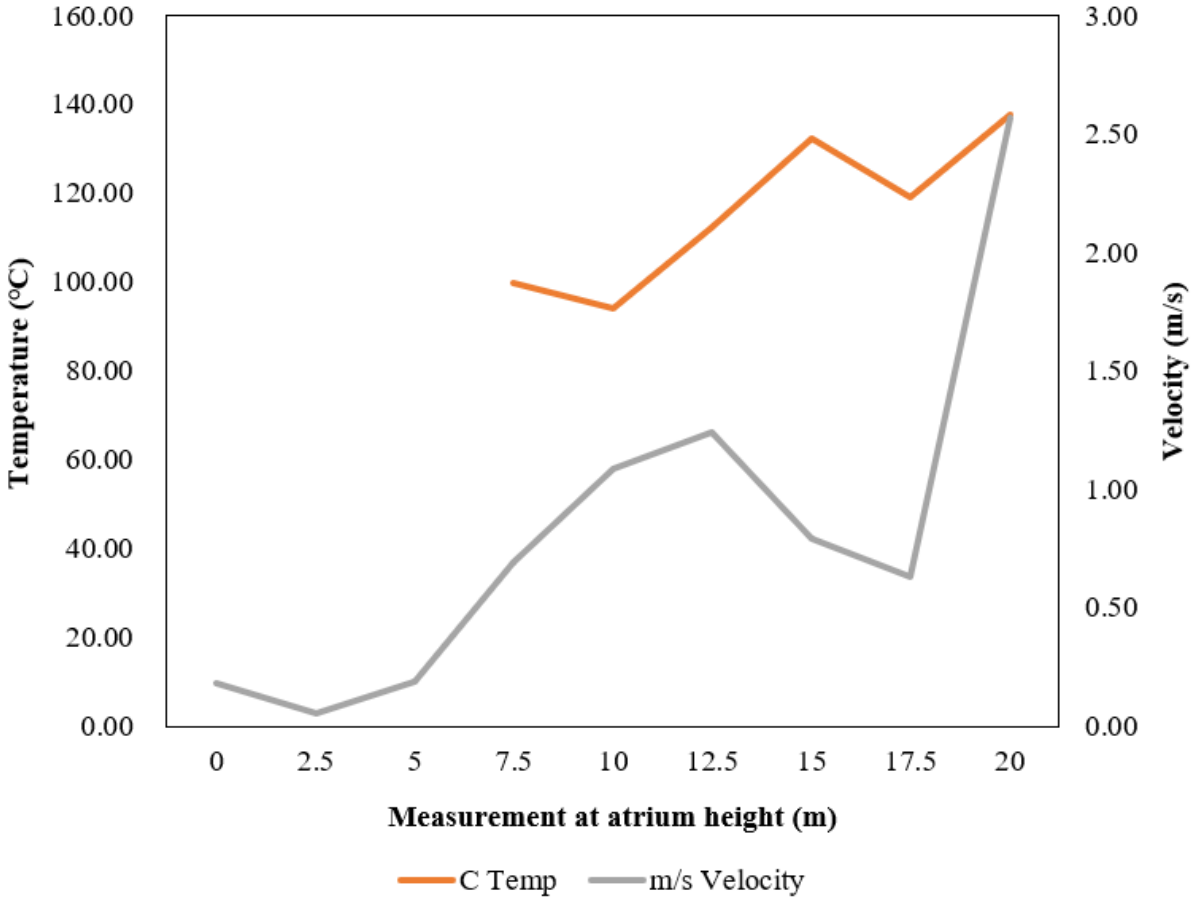

Figure 3-19 Combined temperature and velocity in 20m atrium at 100s at 5MW fire load

Comparing to Figure 3-18, the highest velocity and temperature in 20m cubic atrium at 100s is both at the ceiling level after dropped down from 12.5m to 15m and then rebound at 17.5m height in Figure 3-19.

30m tall atrium

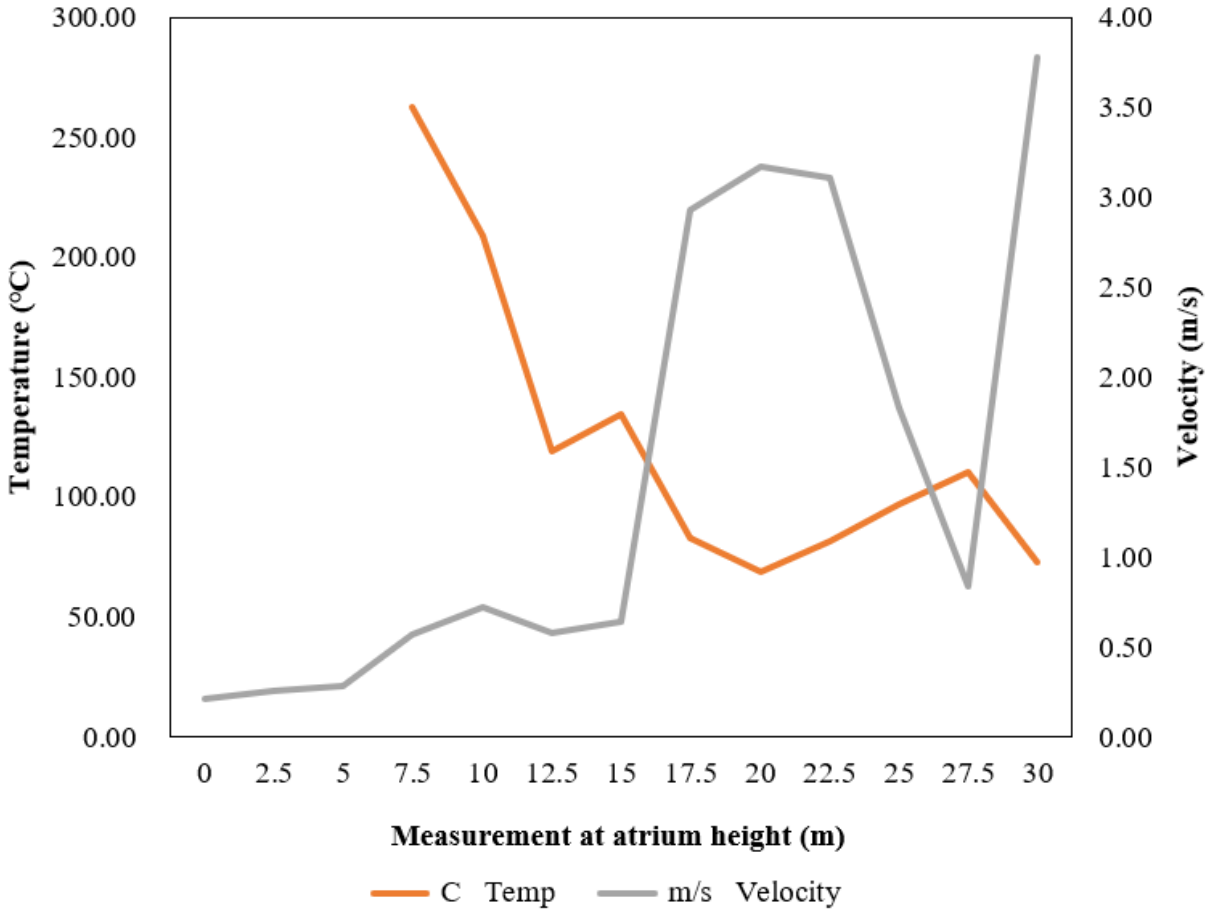

Figure 3-20 Combined temperature and velocity in 30m atrium at 100s at 5MW fire load

Figure 3-20 shows that the highest velocity in 30m tall atrium at 100s is same as Figure 3-19 at the ceiling level. On the contrary, the temperature is the lowest at the ceiling level which keeps almost all the way down from the low height to the higher level.

40m tall atrium

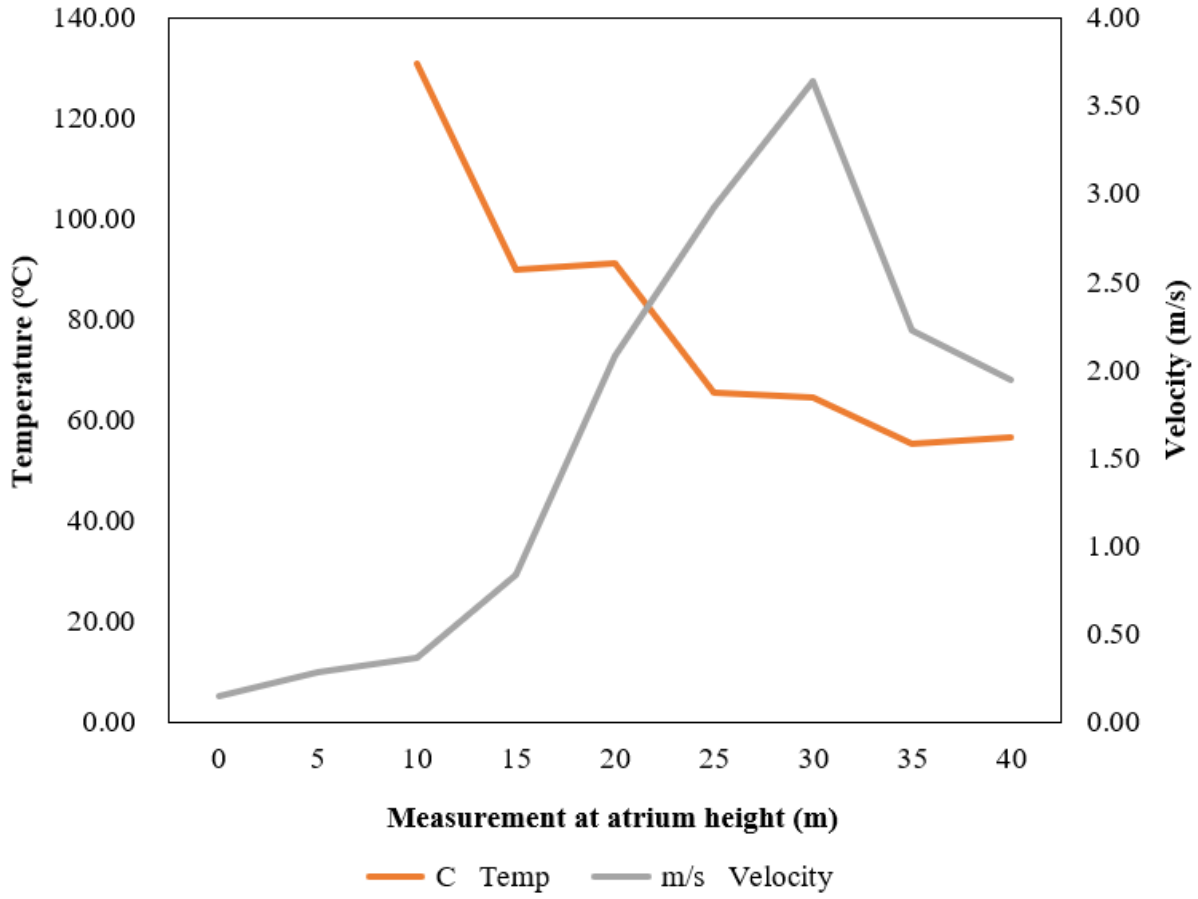

Figure 3-21 Combined temperature and velocity in 40m atrium at 100s at 5MW fire load

Same as Figure 3-20, in the 40m tall atrium, the lowest temperature is at the ceiling level. But the highest velocity value is at the 30m and drop down when it rises to the ceiling Figure 3-21.

50m tall atrium

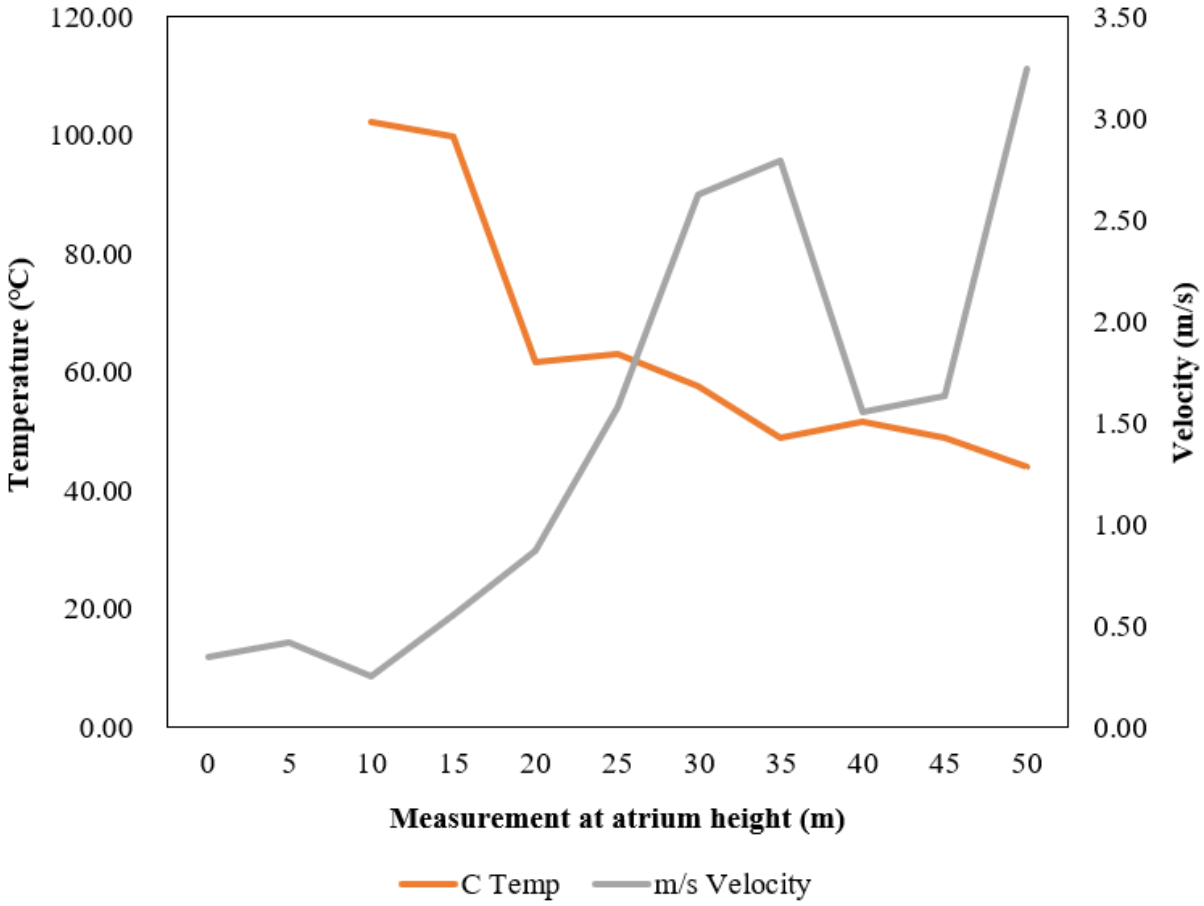

Figure 3-22 Combined temperature and velocity in 50m atrium at 100s at 5MW fire load

Same as Figure 3-20 and Figure 3-21, in the 50m tall atrium, the lowest temperature is at the ceiling level. But for the highest velocity is at the ceiling after the second highest velocity at 35m and rebound at 45m as shown in Figure 3-22.

60m tall atrium

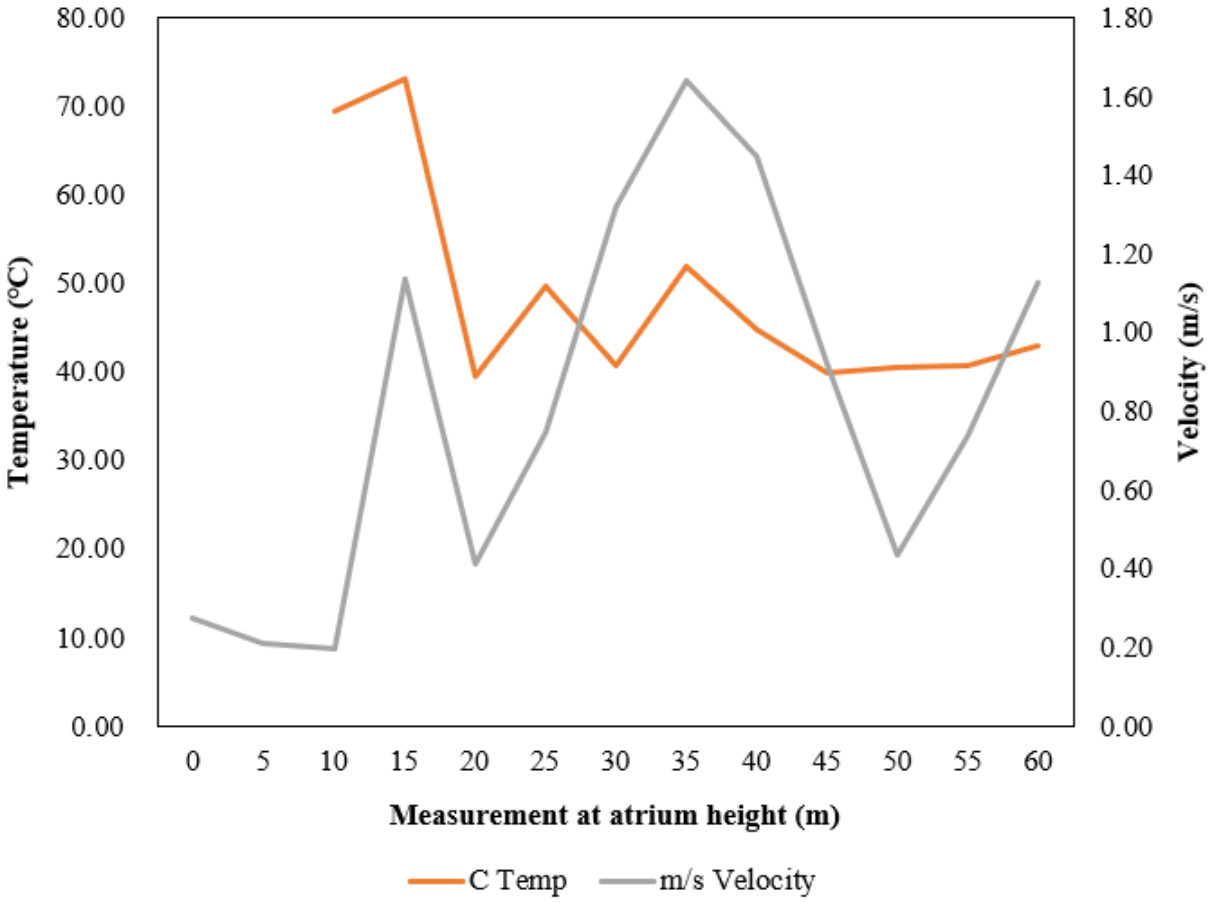

Figure 3-23 Combined temperature and velocity in 60m atrium at 100s at 5MW fire load

Same as Figure 3-20, Figure 3-21 and Figure 3-22, in the 60-metre-tall atrium, the lowest temperature is at the ceiling level but starts flat at 45-metre height. The highest velocity is at 35m and starts to drop to 50m before rebounding to the ceiling. Except for the 15-metre-tall atrium, the 60-metre-tall atrium has the lowest velocity outcome and is the most fluctuating in Figure 3-23.

Conclusion

The highest velocity in 2MW fire load is at 40m tall atrium with the value of 4.33m/s, in 5MW fire load is in 30m tall atrium with 3.78m/s and 5.84m/s in 20m tall atrium happened in 25MW fire load. The peak velocity is affected by the atrium size and height. The velocity is decreased inversely with the height of atrium and fire load due to buoyancy effect in smaller fire size is not obvious.

3.2.15 Smoke height comparison

The data gathered from FDS has been analysed and have been placed into a graph below for comparison between the NFPA [1], Zukoski [44], Thomas [58] and McCaffrey [57]. The experimental data from Yang [62] has been disregarded since the results conducted in a real-life scenario have multiple conflicting factors that may have affected the results. This comparison between three other curves is suitable since an Octane fuel source has been used and this was also considered in the other researcher's study.

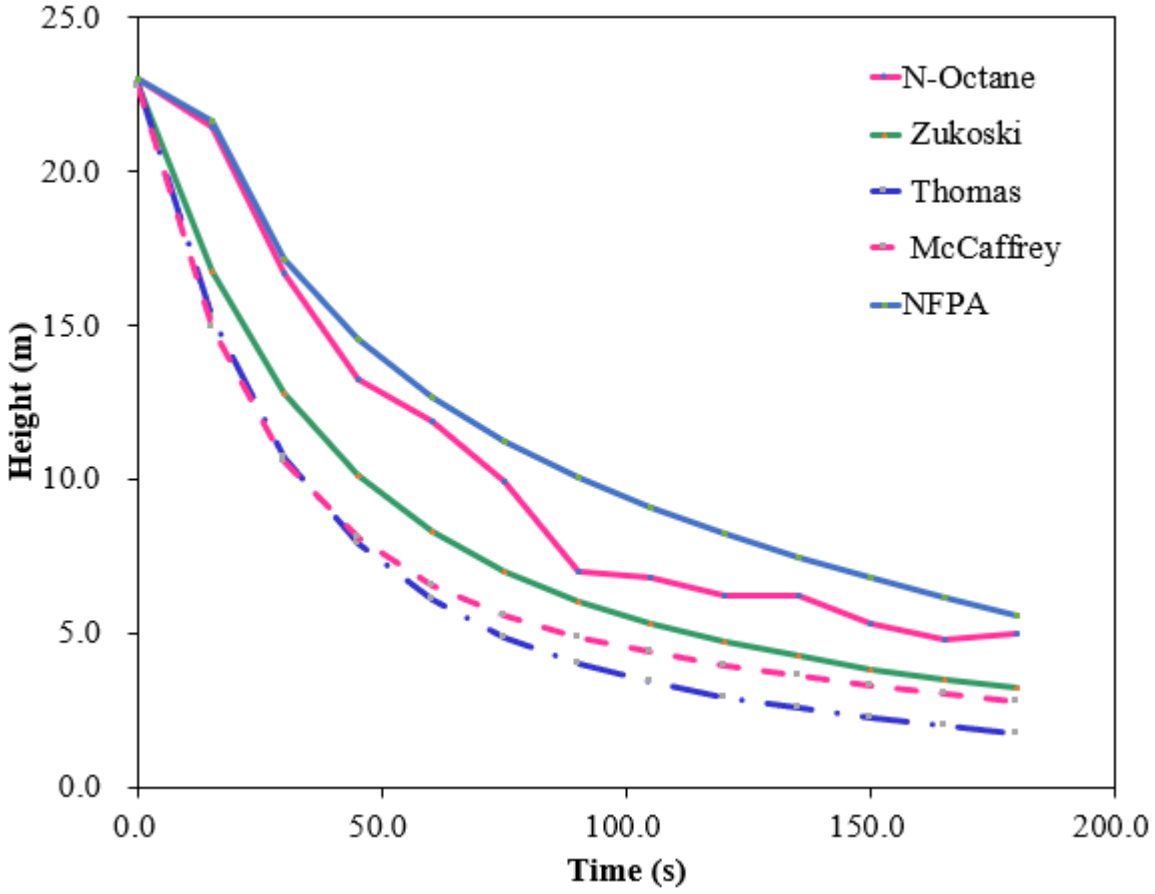

Figure 3-24 Comparison between FDS (N-Octane), NFPA, Zukoski, Thomas and McCaffrey of 5MW fuel source

Based on the findings from Figure 3-24, the results from the FDS 5.0MW HRR test seemed to align with the results from Zukoski, Thomas, and McCaffrey as well as the NFPA. From the initial point, the gradient of all four lines is very similar, and the Zukoski curve seems to be gentler as time goes on. Thomas has the greatest difference among the curves to NFPA. The NFPA from the new mathematical equation is considered to be in the middle of the rest of the equations and relatively close to Zukoski's curve at the end of the experiment. McCaffrey's

results seem to be more aligned with the NFPA than the rest, suggesting a stronger relationship with them. However, with the minor fluctuations from FDS, it is safe to suggest that the comparison between all four of these lines is similar, and the results suggest no significant difference between them. This helps strengthen the argument that the smoke filling equation from NFPA 92B, 2005 [16] is reliable and can predict the smoke layer height to a certain extent for non-ventilated, natural atriums.

3.3 Aspects of the smoke layer calculation considered

Given that the atrium features a 5MW steady fire that has the following dimensions: 20m length x 20m width x 30m height, the values shall be substituted into the following formula. This formula calculates the distance above the base of the fire to the first indication of smoke as stated in NFPA92, 2021, Page 92-12, Equation 5.4.2.1b [1]:

$$\frac{Z}{H} = 1.11 - 0.28\, ln\left(\frac{tQ^{\frac{1}{3}}H^{-\frac{4}{3}}}{\frac{A}{H^2}}\right) \tag{3-2}$$

3.3.1 Applying the formula to determine the smoke height

The constant 0.28 has been used to determine the NFPA smoke layer height as expressed in the equation (3-2) for various type of tall and long atrium. The following calculation in Table 3-12 is a sample of result of the smoke layer height from the input data for the equation (3-2) of a 20m tall atrium. This table has the substituted values which will be compared alongside the FDS simulated results.

Table 3-12 Determining the smoke height value using the constant in correlation (3-2)

Calculations of NPFA									
T (s)	Z (m)	Q (kW)	1.11	Constant	$Q^{1/3}$ (kW)	$H^{4/3}$ (m)	A (m^2)	H^2 (m^2)	H (m)
0.00	20.00	5000.00	1.11	0.28	17.10	54.29	400.00	400.00	20.00
15.00	13.50	5000.00	1.11	0.28	17.10	54.29	400.00	400.00	20.00
30.00	9.62	5000.00	1.11	0.28	17.10	54.29	400.00	400.00	20.00
45.00	7.35	5000.00	1.11	0.28	17.10	54.29	400.00	400.00	20.00
60.00	5.74	5000.00	1.11	0.28	17.10	54.29	400.00	400.00	20.00
75.00	4.49	5000.00	1.11	0.28	17.10	54.29	((400.00	400.00	20.00
90.00	3.47	5000.00	1.11	0.28	17.10	d54.29	400.00	400.00	20.00
105.00	2.61	5000.00	1.11	0.28	17.10	54.29	400.00	400.00	20.00
120.00	1.86	5000.00	1.11	0.28	17.10	54.29	400.00	400.00	20.00
135.00	1.20	5000.00	1.11	0.28	17.10	54.29	400.00	400.00	20.00
150.00	0.61	5000.00	1.11	0.28	17.10	54.29	400.00	400.00	20.00
165.00	0.08	5000.00	1.11	0.28	17.10	54.29	400.00	400.00	20.00

3.3.2 Limitations related to the use of empirical correlations

In the current investigation related to smoke layer calculations, various formulae have been reviewed in order to determine the air flow velocity in an atrium during a fire. Even though these equations have been utilized for various applications, certain limitations can be identified and will be explored below.

(1) Limitation of Smoke Layer Calculation Equation (3-2)

a. The atrium must have a uniform cross-sectional area with respect to height

b. The A/H^2 must be in the range of $0.9 \leq x \leq 14$

c. $\frac{z}{h} > 0.2$

d. This equation shall only be used when a steady fire source is explored, unsteady fires will not apply to this formula

e. Natural ventilation is explored, therefore, no smoke exhaust shall be installed and operated

(2) Rate of smoke mass production in an axisymmetric plume

The mass flow rate of smoke production can be calculated using the following equations:

$$z_l = 0.166 Q_c^{\frac{2}{5}}, \tag{3-3}$$

$$m = 0.071 Q_c^{\frac{1}{3}} z^{\frac{5}{3}} + 0.0018 Q_c \quad for\ z > z_l \tag{3-4}$$

$$m = 0.032 Q_c^{\frac{3}{5}} z \quad for\ z \leq z_l \tag{3-5}$$

Limitations:

a. The plume must be axisymmetric
b. These equations cannot be used when the temperature rise above ambient ($T_p - T_o$) is less than2.2℃.

(3) Air flow volume

$$V = \frac{m}{\rho_s} \tag{3-6}$$

Limitations:

a. An assumption is made in which the smoke volume produced in the selected time interval is instantly and uniformly distributed over the atrium area
b. Since the fire is placed in the centre of the atrium – it is assumed to be an axisymmetric flame

General limitations:

a) If the plume makes contact with all the walls before reaching the atriums full height, it may disorientate the findings

In this specific scenario, it is assumed that no heat is loss from the smoke layer to the atrium boundaries.

3.4 Synthesis

A numerical methodology is selected for simulation of atrium smoke filling in various tall and long atria. Statistical analysis for selecting the appropriate cells, grid sensitivity, validation with experimental data from Guan-Yuan Wu and Ruu-chang Chen's research is natural smoke filling time in an atrium of the same fuel source and compared against Zukoski, McCaffrey's models along with the smoke layer height from the substitution of NFPA formula.

After the series of simulation, the data collected from FDS will be compared with the NFPA to investigate whether the constant 0.28 as specified in the correlation is suitable for the list of tall and long atria.

Table 3-13 lists out the FDS setup and the boundary conditions for the series of simulations of different tall and long atriums.

Table 3-13 FDS setup and boundary condition

Tall atrium Geometry	Square atrium with common length and width of 20m in different heights of 15m, 20m, 30m, 40m, 50m and 60m, Sectional aspect ratio (SAR) 0.75, 1.00, 1.50, 2.00, 2.50 and 3.00 respectively.
Dimension / SAR / Volume	20m (L) x 20m (W) x 15m (H) / 0.75 / 6000 m3
	20m (L) x 20m (W) x 20m (H) / 1.00 / 8000 m3
	20m (L) x 20m (W) x 30m (H) / 1.50 / 12000 m3
	20m (L) x 20m (W) x 40m (H) / 2.00 / 16000 m3
	20m (L) x 20m (W) x 50m (H) / 2.50 / 20000 m3
	20m (L) x 20m (W) x 60m (H) / 3.00 / 24000 m3
Long atrium geometry	Rectangular atrium with common width and height of 20m in different length of 15m, 20m, 30m, 40m, 50m and 60m, Plan Aspect Ratio (PAR) 1.33, 1.00, 0.66, 0.50, 0.40 and 0.33 respectively.
Dimension / PAR / Volume	15m (L) x 20m (W) x 20m (H) / 1.33 / 6000 m3
	20m (L) x 20m (W) x 20m (H) / 1.00 / 8000 m3
	30m (L) x 20m (W) x 20m (H) / 0.66 / 12000 m3
	40m (L) x 20m (W) x 20m (H) / 0.50 / 16000 m3
	50m (L) x 20m (W) x 20m (H) / 0.40 / 20000 m3
	60m (L) x 20m (W) x 20m (H) / 0.33 / 24000 m3
Computation cell size	30.4cm
Characteristic fire diameter D*	1.826m
Mesh Grid	64x64x64
Location of ignition source	Centre fire
Fuel type	Propane
Heat release rate	Steady fire 5MW
Fire size	1.44m x 1.44m
Fire diameter	1.625m
Burning surface	$2.07m^2$
Heat release rate per unit area	$2,411.27kWm^{-2}$
Ambient temperature	25℃
Ventilation	Natural ventilation
Vent size	1m x 1m
Vent location	Top of atrium
Simulation time	180 sec

Empirical correlation (3-2), smoke heights, the convective portion of heat release rate, mass flow rate, smoke density, air flow velocity, and limitations of the selected equation are included in this research.

The smoke layer height limit is set at 0.2 of Z/H which is the ratio of the height of the smoke layer to the height of the atrium as specified in the NFPA correlation. This is also the minimum design smoke layer depth of the smoke layer for a smoke management system, either twenty percent of the floor-to-ceiling height or based on engineering analysis in NFPA 92, 2021, Clause 4.5.1.3 [1].

3.5 Summary of results

The results of this study refer to the numerical methodology (FDS) which will be used for simulation of tall and long atria in different heights and lengths.

It involved an in-depth study of numerical methodology (FDS) to accurately simulate atrium smoke filling, validation of numerical methodology with past experimental studies and other theoretical results, and empirical correlation related in the smoke layer height calculation. The research on FDS included mesh size, and grid sensitivity analysis for selecting the appropriate cell size for simulation. Data collected from the various fire scenarios are to be compared with the calculated results of the empirical correlations. To achieve the objectives of this study, the results are to be analysed and used to find out whether the constant in the correlation is applicable to the tall and long atria and review for any adjustments that need to be made for matching with the modern atria.

CHAPTER 4: Parametric Study

A parametric study is performed to study the effect of geometry and HRR on smoke characteristics including the smoke layer height, hot temperature and velocity on smoke layer formation. To limit the scope of the research, the natural fire scenario in high-rise atria is considered. As indicated in NFPA92, the 5MW centre fire load is selected for the simulation of tall atria with common cross-section area and long atria with common height and width. Tall atria of 15m, 20m, 30m, 40m, 50m, and 60m in height and long atria of 15m, 20m, 30m, 40m, 50m, and 60m in length are selected. Snapshot collected from Smokeview of each simulation performed at the time interval of 0s, 10s, 50s and 100s are recorded to investigate the effect of geometry and HRR on smoke characteristics.

The results from the chosen atria fire simulations will be validated using empirical correlations and past experimental data at the same fire load.

4.1 Effect of geometry and HRR on smoke characteristics

The use of computational fluid dynamics (CFD) as a tool for the design of smoke control systems and fire protection in large spaces has become more frequent as accuracy and computational speeds have increased. Currently, the Fire Dynamic Simulator (FDS) has been used to study two full-scale experiments conducted in Murcia (Spain) for a 1.36 MW and 2.34 MW pool fire burning inside a 20 m cubic atrium under natural ventilation conditions. Fire protection is mainly focused on life safety, smoke being one of its main concerns.

According to a recently published UK fire statistic, smoke alone has caused 42% of fatalities in building fires, whereas an additional 17% of deaths were caused by the joint action of smoke inhalation and burn. At this point, some new architectonic trends with large-volume spaces like atria, underground car parks, stadiums or tunnels, present singularities and different problems related to their ventilation and the calculation of these systems, due to their complex and non-conventional design.

Moreover, these constructions do not allow engineers to carry out prescriptive designs.

Therefore, alternative techniques lead to performance-based design (PBD) which should be supported by knowledge and understanding of fire phenomena, such as the use of numerical models or empirical correlations, among others.

Regarding the performance of numerical simulations for fire safety designs, it is sometimes necessary to carry out some simplifications and assumptions for the geometry and the materials, for example, the complexity of some fire scenarios may pose challenges. However, these must be rigorously conducted as they can affect the results by delivering unrealistic predictions.

4.1.1 Parametric study altering atrium height

A list of tall atria with different height by FDS setup with boundary conditions and measuring devices is simulated for studying the factor affected by the geometry in Table 4-1.

Table 4-1 List of Tall Atria Geometries for 5MW Fire Load Centre Located Test

Atrium Geometry				
Case	**Length m**	**Width m**	**Height m**	**Volume m^3**
FDS-5MW-L20W20H15	20	20	15	6,000
FDS-5MW-L20W20H20	20	20	20	8,000
FDS-5MW-L20W20H30	20	20	30	12,000
FDS-5MW-L20W20H40	20	20	40	16,000
FDS-5MW-L20W20H50	20	20	50	20,000
FDS-5MW-L20W20H60	20	20	60	24,000

A single type of atrium configuration will be considered in which the height of the atrium will be altered. Throughout all four FDS simulations, a medium grid size has been selected since it is most suitable as established previously. The varied height will be examined, and the smoke flow will be observed based on the FDS results.

Snap shots of Smokeview from FDS showing the smoke layer, temperature contours and velocity flow from centre of fire recorded at 0s, 10s, 50s and 100s of various tall and long

atria are displayed and compared.

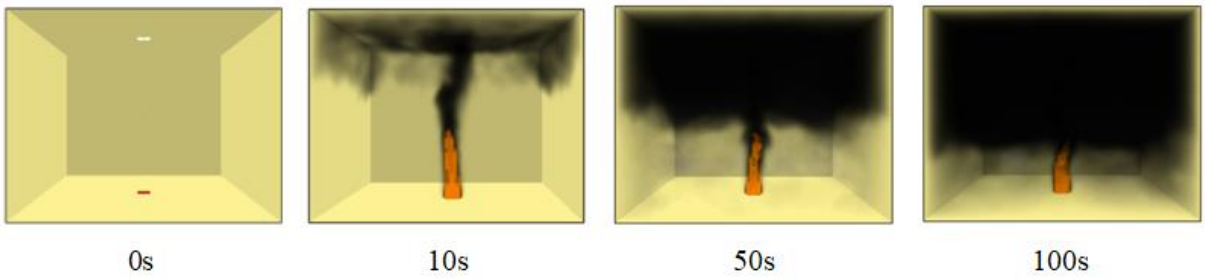

Figure 4-1 Descent of smoke layer height in FDS simulation case FDS-5MW-L20W20H15: 15m Height with 20m Length x 20m Width atrium, (5MW) at 0s, 10s, 50s and 100s

Figure 4-1 shows that after 10s a smoky layer has developed and the ceiling jet, wall jets and recirculation can be seen. The depth of the initial layer is around 25% of the volume. After 50s the smoke has thickened and occupies approximately 50% of the volume. The jets are no longer visible in these slices. At 100s the layer is fully developed and occupies 70% of the volume. Some of the smoke has evidently become distributed into the lower layer.

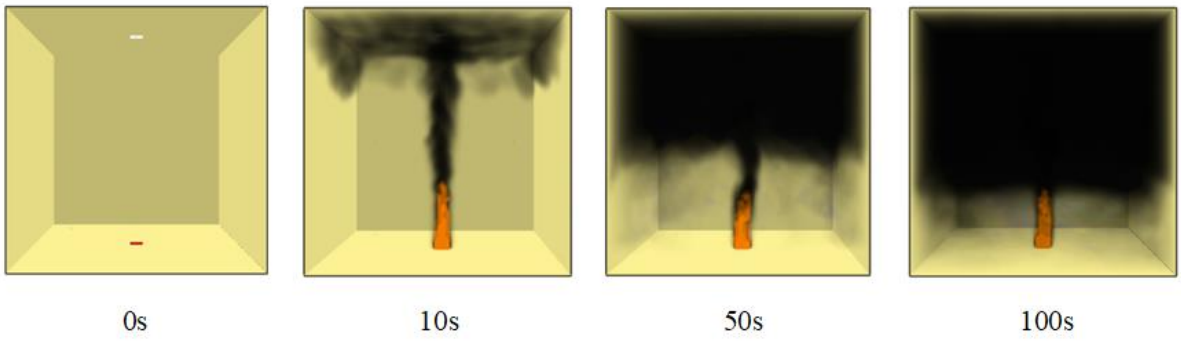

Figure 4-2 Descent of smoke layer height in FDS simulation case FDS-5MW-L20W20H20: 20m Height with 20m Length x 20m Width atrium, (5MW) at 0s, 10s, 50s and 100s

Figure 4-2 like the 15m atrium shown on Figure 4-1, the smoke layer in 20m atrium comes down to nearly half of the height of the atrium at the beginning of 40s and to the remaining 20% at around 120s. The additional 5m height appears to have had little effect upon the smoke filling.

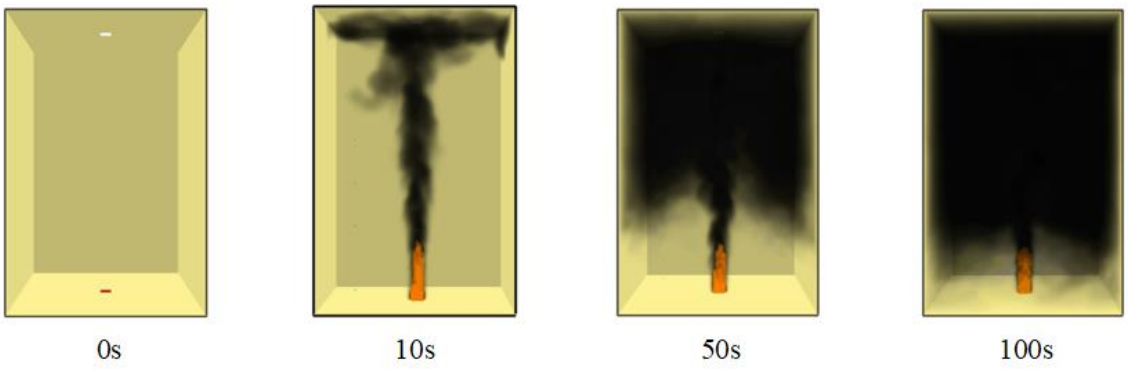

Figure 4-3 Descent of smoke layer height in FDS simulation case FDS-5MW-L20W20H30: 30m Height, with 20m Length x 20m Width atrium, (5MW) at 0s, 10s, 50s and 100s

Figure 4-3 compared to Figure 4-1 and Figure 4-2 smoky layer in 30m atrium is clearly less developed at 10s. After 50s the smoke appears to have filled a larger fraction of the volume but has the appearance of stronger wall jets and less recirculation, providing a slightly less dense region surrounding the plume. After 100s the appearance is the same smoke clearance height even though the smoky volume fills a much larger volume.

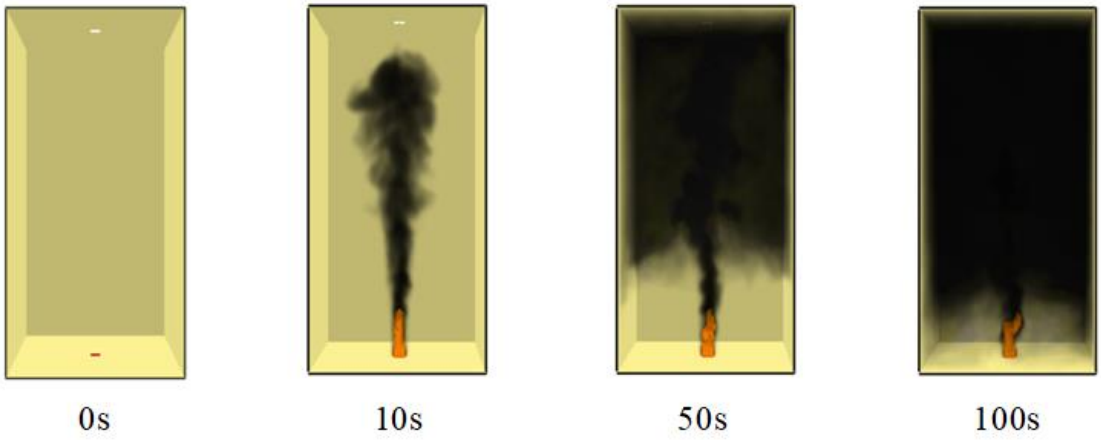

Figure 4-4 Descent of smoke layer height in FDS simulation case FDS-5MW-L20W20H40: 40m Height with 20m Length x 20m Width atrium, (5MW) at 0s, 10s, 50s and 100s

On Figure 4-4, the smoke in 40m atrium has so far to travel vertically that it no longer reaches the ceiling in the first 10s. After 50s the smoky volume is notably less dense. The smoke however fills most of the volume very effectively within 100s. In the last picture it can be seen that the main mechanism for transporting smoke into the lower volume is from residual

wall jets. The smoke travelling vertically down the walls has lost so much heat and gained so much momentum it reaches the floor.

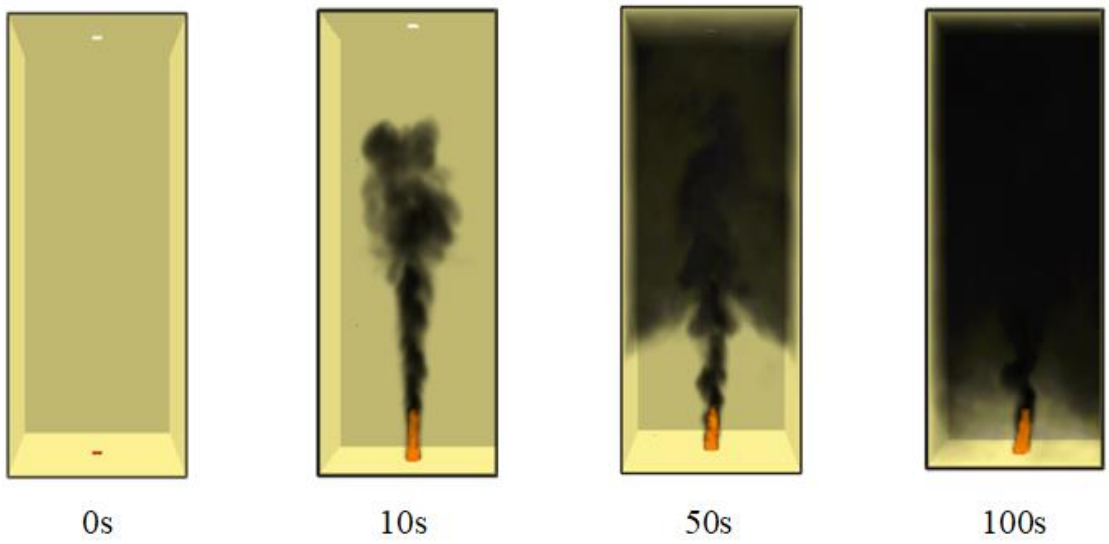

Figure 4-5 Descent of smoke layer height in FDS simulation case FDS-5MW-L20W20H50: 50m Height with 20m Length x 20m Width atrium, (5MW) at 0s, 10s, 50s and 100s

The smoke layer in 50m atrium comes down to nearly two-third of the height of the atrium at the beginning of 50s and to around 20% at 60s in Figure 4-5.

Comparing to Figure 4-1 to Figure 4-4, the plume is still discernible at 50s and partially at 100s. Atrium smoke reservoir-filling is evidently dominated by boundary flows.

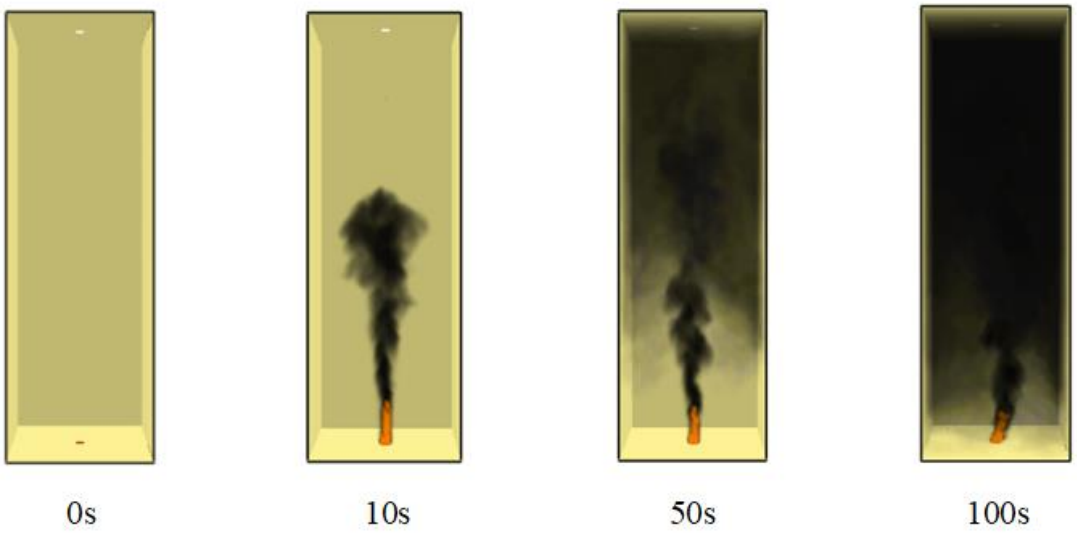

Figure 4-6 Descent of smoke layer height in FDS simulation case FDS-5MW-L20W20H60: 60m Height with 20m Length x 20m Width atrium, (5MW) at 0s, 10s, 50s and 100s

Figure 4-6 shows that the smoke layer in 60m atrium comes down to nearly half of the height of the atrium at the beginning of 50s and to less than 20% at around 100s.

Figure 4-1, 4-2, 4-3, 4-4, 4-5 and 4-6 show the series of FDS simulations of smoke filling in the tall atrium at 15m, 20m, 30m, 40m, 50m and 60m. For the atrium held with 15m and 20m tall, the tenable conditions would not be held at 100s because the layer drops to below and near 2m. For the range of taller atria, 30m to 60m, the smoke is thinner and thinner ascend with height. The density of smoke at 60m is relatively lighter than the lower atria. The smoke layer is found to quickly drop to below 20% in the higher atria.

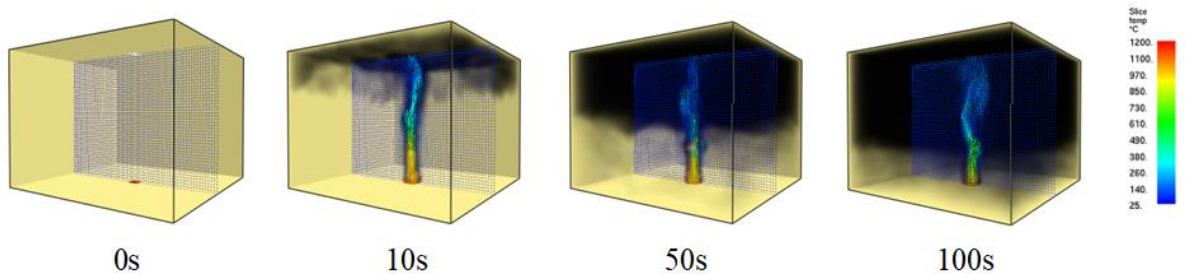

Figure 4-7 Smoke temperature in FDS simulation case FDS-5MW-L20W20H15: 15m Height with 20m Length x 20m Width atrium, (5MW) at 0s, 10s, 50s and 100s

Figure 4-7 shows the highest temperatures ranging from 1039℃, 1150℃, 937℃, 578℃, 400℃, 296℃ and 241℃ at 15m, 12.5m, 10m, 7.5m, 5m, 2.5m and 0m heights of the atrium, respectively. The first of these high temperatures has a few suggestive of flame temperatures and the fire bed. The latter ones suggest there is no combustion near the fire roof.

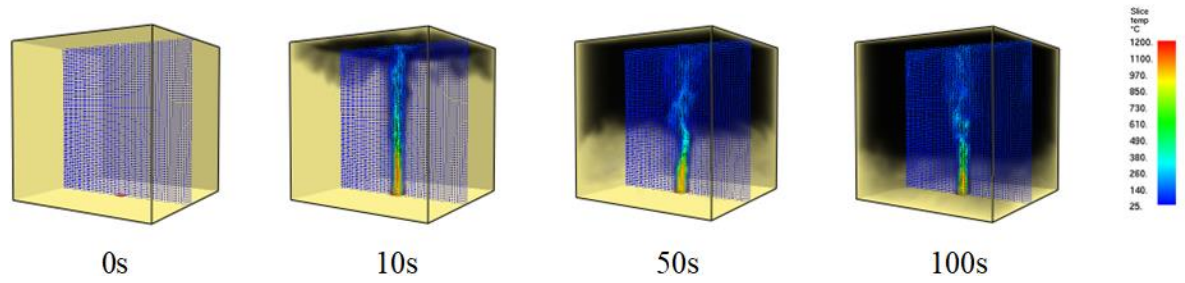

Figure 4-8 S Smoke temperature in FDS simulation case FDS-5MW-L20W20H20: 20m Height with 20m Length x 20m Width atrium, (5MW) at 0s, 10s, 50s and 100s

Figure 4-8 shows that the highest temperature ranging from 167℃, 200℃, 258℃, 318℃, 436℃, 621℃, 965℃, 1169℃ and 1010℃ at 20m, 15m, 12.5m, 10m, 7.5m, 5m, 2.5m and 0m height of atrium.

In the pictures (Figures 4-6 to 4-8), the fire begins in a narrower jet shape but broadens over time.

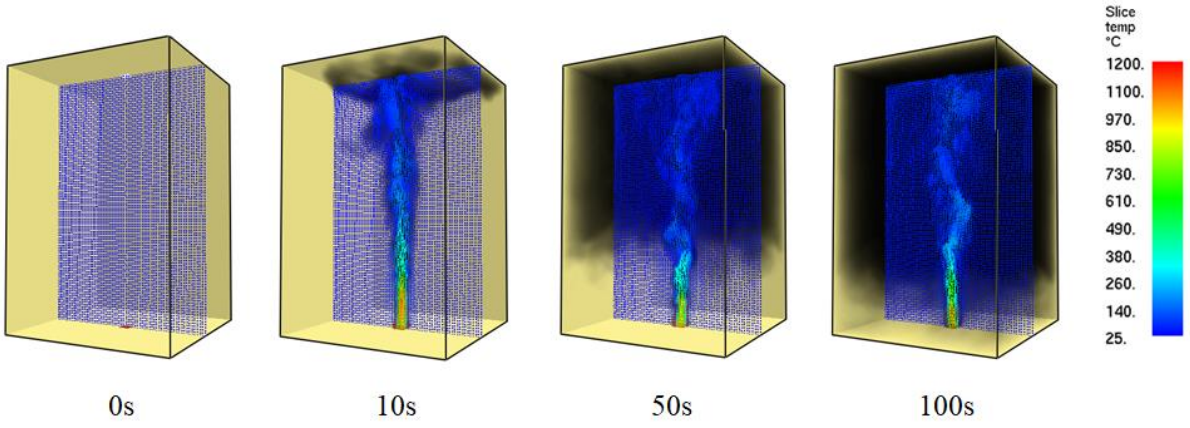

Figure 4-9 Smoke temperature in FDS simulation case FDS-5MW-L20W20H30: 30m Height with 20m Length x 20m Width atrium, (5MW) at 0s, 10s, 50s and 100s

Figure 4-9 shows that the boarder flame shape corresponds to a more looping/convective plume shape. Clearly the velocity, and hence Reynolds number, have increased.

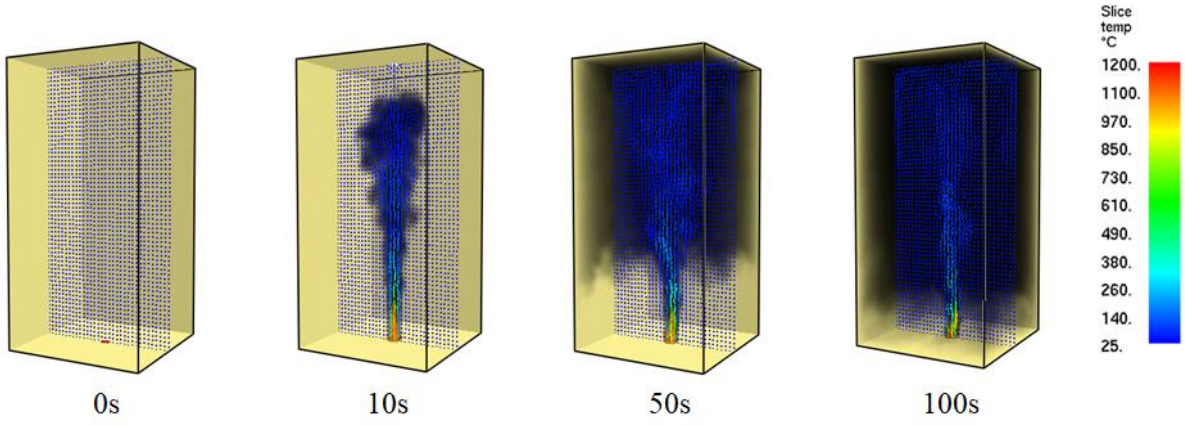

Figure 4-10 Smoke temperature in FDS simulation case FDS-5MW-L20W20H40: 40m Height with 20m Length x 20m Width atrium, (5MW) at 0s, 10s, 50s and 100s

Figure 4-10 shows that due to the increase of height, the smoke temperature at the 10s is diluted with the cooler ambient temperature and the temperature rise is mainly at the centre in the latter two.

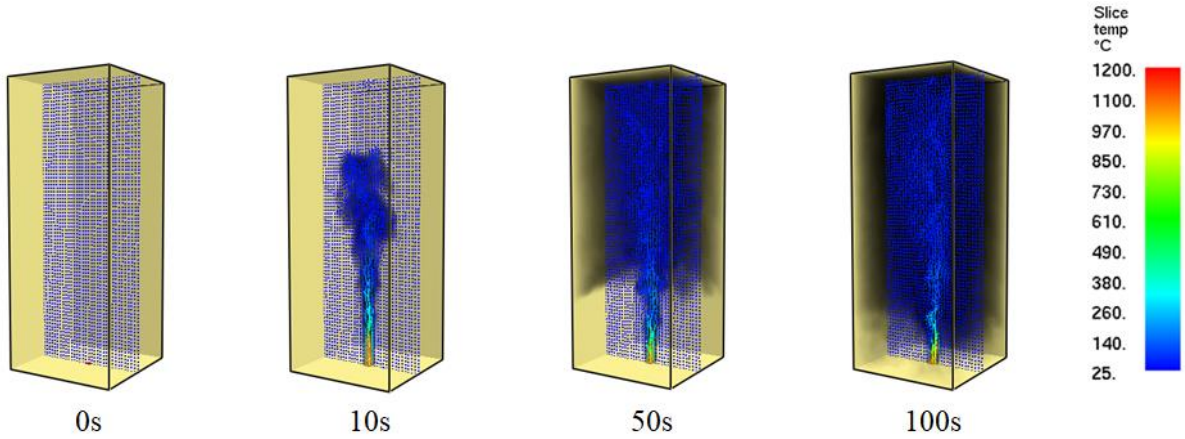

Figure 4-11 Smoke temperature in FDS simulation case FDS-5MW-L20W20H50: 50m Height with 20m Length x 20m Width atrium, (5MW) at 0s, 10s, 50s and 100s

Figure 4-11 also shows that with a 10 metre increase of height, the smoke temperature at the first 10s is dispersing at the lower part of atrium with the cooler ambient temperature and the temperature rise is mainly at the centre in the latter two.

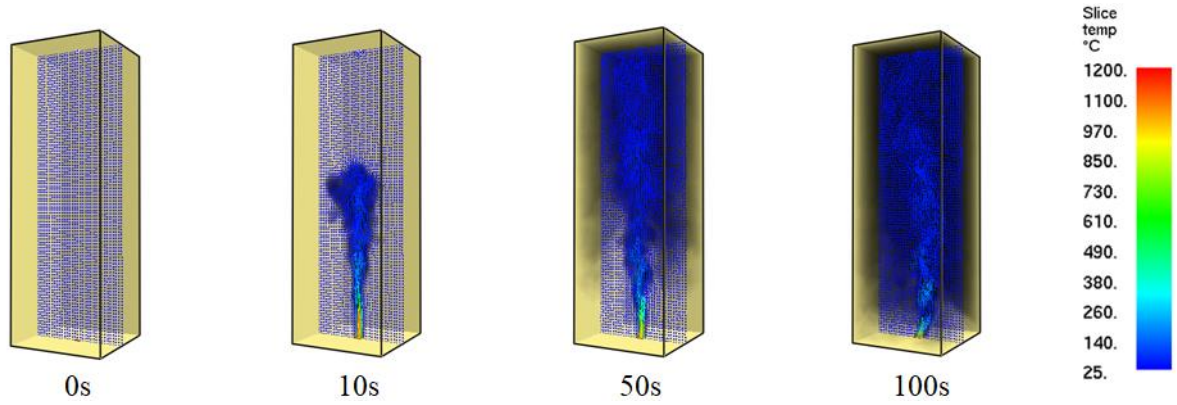

Figure 4-12 Smoke temperature in FDS simulation case FDS-5MW-L20W20H60: 60m Height with 20m Length x 20m Width atrium, (5MW) at 0s, 10s, 50s and 100s

Figure 4-12 also shows that the smoke temperature at the first 10s is already dispersing irregularly at the lower part of atrium. At the 50s, the smoke layer temperature does go upward but decreased when the filling up the whole volume when touching the ceiling. The smoke temperature of the upper region is hotter than the lower middle colder region. The fire load is not large enough for mixing the whole boundary completely so stratification at the middle of atrium is found at the latter.

Temperature of smoke layer are shown in Figure 4-7, 4-8, 4-9, 4-10, 4-11 and 4-12 in various tall atria.

4.1.2 Parametric study altering atrium length

Table 4-2 List of Long Atria Geometries for 5MW Fire Load Centre Located Test

Atrium Geometry				
Case	**Length m**	**Width m**	**Height m**	**Volume m^3**
FDS-5MW-L15W20H20	15	20	20	6,000
FDS-5MW-L20W20H20	20	20	20	8,000
FDS-5MW-L30W20H20	30	20	20	12,000
FDS-5MW-L40W20H20	40	20	20	16,000
FDS-5MW-L50W20H20	50	20	20	20,000
FDS-5MW-L60W20H20	60	20	20	24,000

A single type of atrium configuration will be considered in which the length of the atrium will be altered. Throughout all six FDS simulations, a medium grid size has been selected since it is most suitable as established previously. The varied length will be examined, and the smoke flow will be observed based on the FDS results.

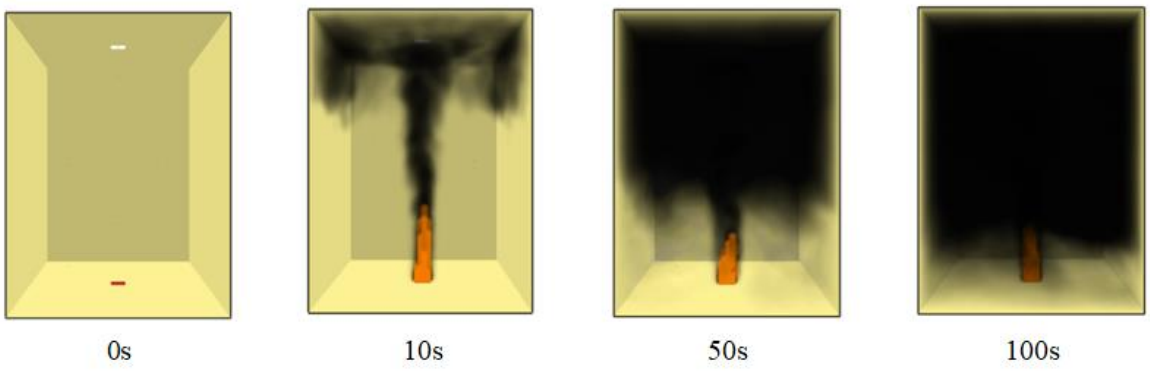

Figure 4-13 Descent of smoke layer height in FDS simulation case FDS-5MW-L15W20H20: 15m Flat Atrium with 20m Width x 20m Height atrium, (5MW) at 0s, 10s, 50s and 100s

On Figure 4-13, after 10s a smoky layer in 15m long atrium has developed and the ceiling jet, wall jets and recirculation can be seen. After 50s the smoke has thickened and occupies more than 50% of the volume. The jets are no longer visible in these slices. At 100s the layer is fully developed and occupies over 80% of the volume. Some of the smoke has evidently become distributed into the lower layer.

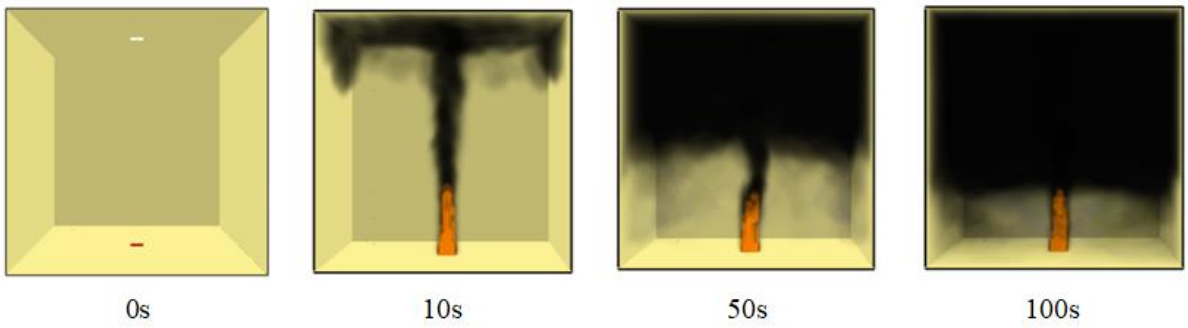

Figure 4-14 Descent of smoke layer height in FDS simulation case FDS-5MW-L20W20H20: 20m Cubic Atrium with 20m Width x 20m Height atrium, (5MW) at 0s, 10s, 50s and 100s

Figure 4-14 is similar to Figure 4-13, the smoke layer in 20m long atrium comes down to nearly half of the height of the atrium at the beginning of 50s and to less than 30% at around 100s. The additional 5m length appears to have not much effect upon the smoke filling.

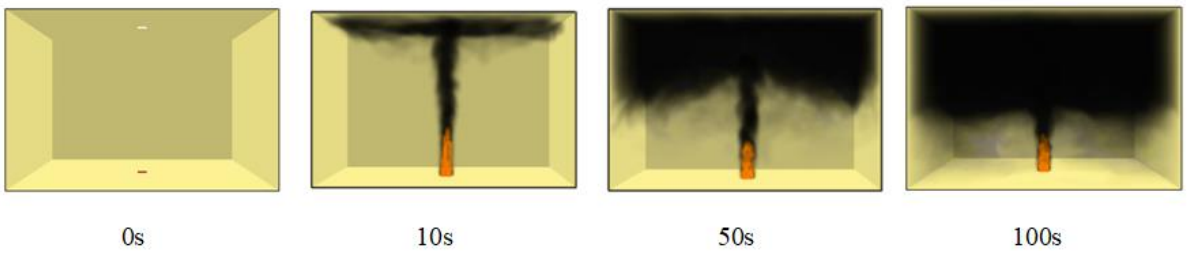

Figure 4-15 Descent of smoke layer height in FDS simulation case FDS-5MW-L30W20H20: 30m Flat Atrium with 20m Width x 20m Height atrium, (5MW) at 0s, 10s, 50s and 100s

Figure 4-15 shows the smoke layer in a 30-metre-long atrium comes down to nearly half of the height of the atrium at the beginning of the 50s and to the remaining 40% at around the 100s.

Figure 4-15 compared to Figure 4-13 and Figure 4-14, the smoky layer in 30m long atrium is clearly less developed at 10s but reached the ceiling. After 50s the smoke appears to have filled an approximately 40% of the volume, providing a slightly less dense region surrounding the plume. After 100s the smoke clearance height is remaining 40% at 100s.

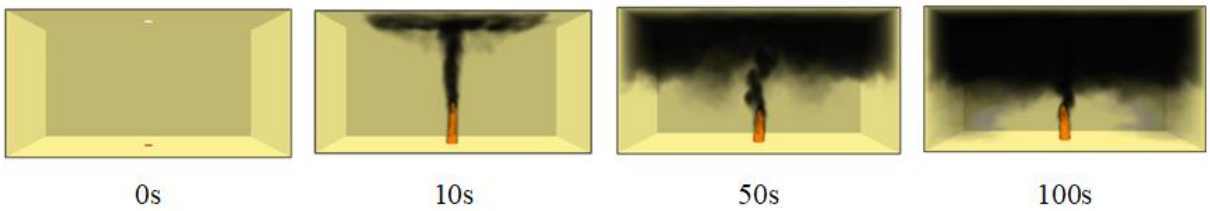

Figure 4-16 Descent of smoke layer height in FDS simulation case FDS-5MW-L40W20H20: 40m Flat Atrium with 20m Width x 20m Height atrium, (5MW) at 0s, 10s, 50s and 100s

Figure 4-16 shows that the smoke layer in 40m long atrium comes down to nearly one-third of the height of the atrium at the beginning of 50s and to the remaining 30% at around 100s.

It also shows light smoky layer is developed at 10s and dispersed at the ceiling. The less dense smoke descends around one-third of the height of the atrium at the beginning of 50s. After 100s the smoke layer height dropped to the level below 50% of the volume.

Figure 4-17 Descent of smoke layer height in FDS simulation case FDS-5MW-L50W20H20: 50m Flat Atrium with 20m Width x 20m Height atrium, (5MW) at 0s, 10s, 50s and 100s

Figure 4-17 shows light smoky layer in 50m long is developed at 10s. The smoke descends around one-third of the height of the atrium at the beginning of 50s, but the density is lighter than Figure 4-13 to Figure 4-15. After 100s the smoke layer height dropped to the level below 60% of the volume.

Figure 4-18 Descent of smoke layer height in FDS simulation case FDS-5MW-L60W20H20: 60m Flat Atrium with 20m Width x 20m Height atrium, (5MW) at 0s, 10s, 50s and 100s

Figure 4-18 compares to the shorter atrium Figure 4-13 to Figure 4-17; the light smoky layer in 60m long atrium is developed at 10s and horizontally dispersed at ceiling. The smoke descends slowly to the boundary and is around one-third of the height of the atrium at the beginning of 50s. After 100s the smoke layer height dropped to the level below 50% of the volume.

Figure 4-13, 4-14, 4-15, 4-16, 4-17 and 4-18 show the series of FDS simulations of smoke filling the long atrium at 15m, 20m, 30m, 40m, 50 m, and 60m in length. For the atrium with a 15- and 20-metre height, the tenable conditions would not be held at 100s because the layer drops to less than 20% of the atrium height. For the range of longer atria, 20m to 60m, the smoke spreads at the top and descends a flat, and the density of the smoke is thicker than the smoke layer at the tall atrium.

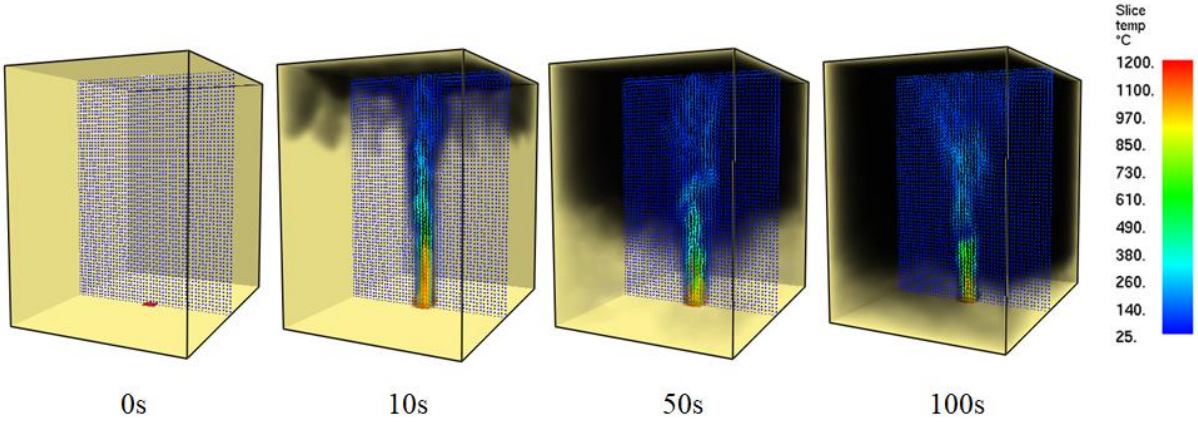

Figure 4-19 Smoke temperature in FDS simulation case FDS-5MW-L15W20H20: 15m Flat Atrium with 20m Width x 20m Height atrium, (5MW) at 0s, 10s, 50s and 100s

Figure 4-19 shows the first few suggestive of flame temperatures and sites of active combustion near the ceiling in 15m long atrium. The latter ones suggest there is no combustion near the fire bed.

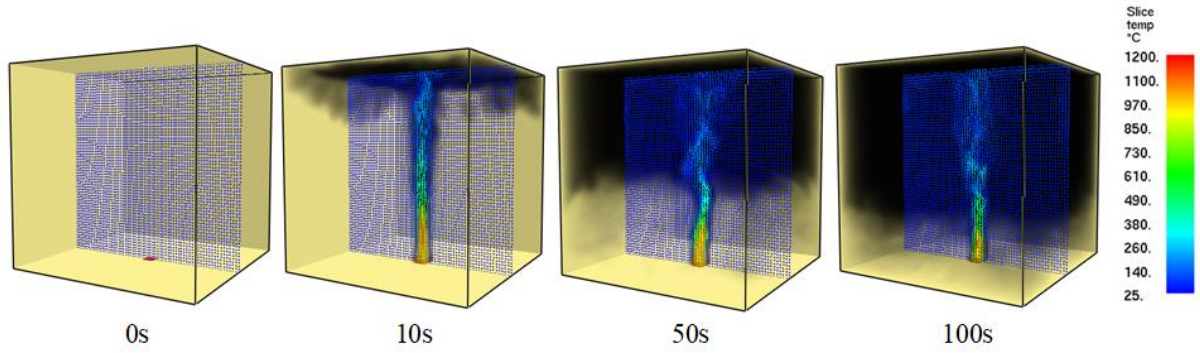

Figure 4-20 Smoke temperature in FDS simulation case FDS-5MW-L20W20H20: 20m Cubic Atrium, with 20m Width x 20m Height atrium, (5MW) at 0s, 10s, 50s and 100s

Figure 4-20 shows the smoke layer in 20m long atrium is formed at ceiling at 10s and the smoke layer temperature becomes unsteady at the middle height of atrium at 50s and then diluted by the surrounding air at 100s.

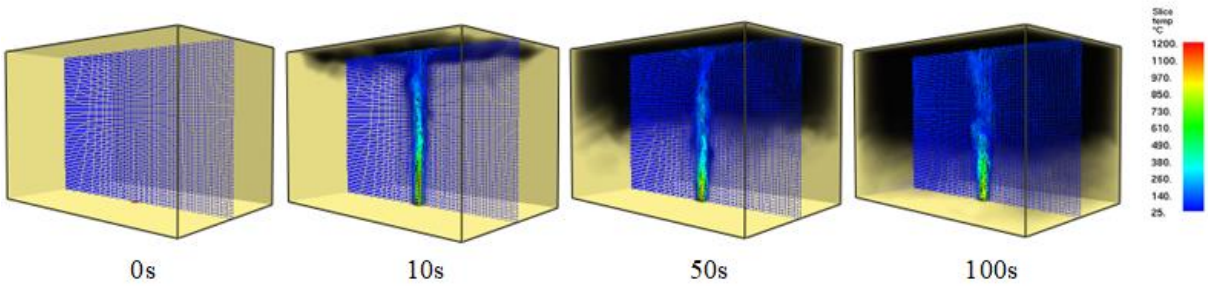

Figure 4-21 Smoke temperature in FDS simulation case FDS-5MW-L30W20H20: 30m Flat Atrium with 20m Width x 20m Height atrium, (5MW) at 0s, 10s, 50s and 100s

Figure 4-21 shows that the smoke temperature in 30m long atrium is steadily grow upward to the ceiling and then become broaden at the later stage when cooling effect from the ambient air at the ceiling level.

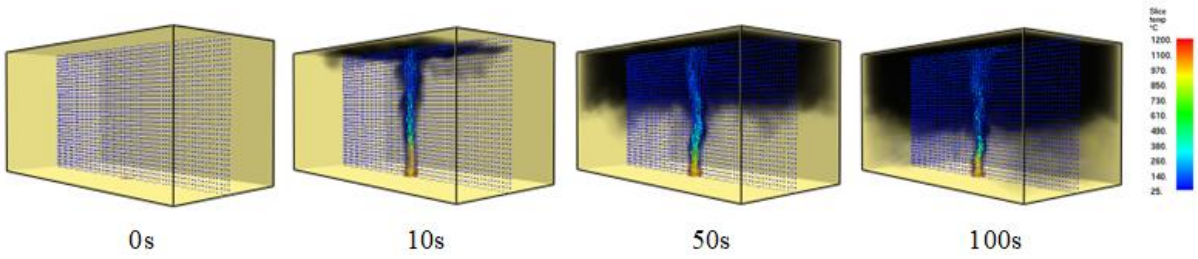

Figure 4-22 Smoke temperature in FDS simulation case FDS-5MW-L40W20H20: 40m Flat Atrium with 20m Width x 20m Height atrium, (5MW) at 0s, 10s, 50s and 100s

Figure 4-22 shows that the smoke generated at the first 10s starts to spread out at the lower level near the fire source in 40m long atrium. The smoke temperature in atrium becomes unsteadily when the smoke layer drops downwards to the fire sources.

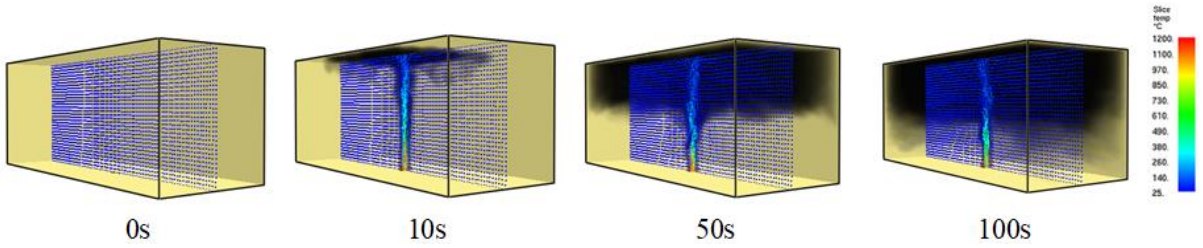

Figure 4-23 Smoke temperature in FDS simulation case FDS-5MW-L50W20H20: 50m Flat Atrium with 20m Width x 20m Height atrium, (5MW) at 0s, 10s, 50s and 100s

Figure 4-23 shows that the smoke in 50m long atrium generated at the first 10s starts to spread out at ceiling. The smoke temperature in atrium is higher at the middle of atrium around the fire source shown in 100s.

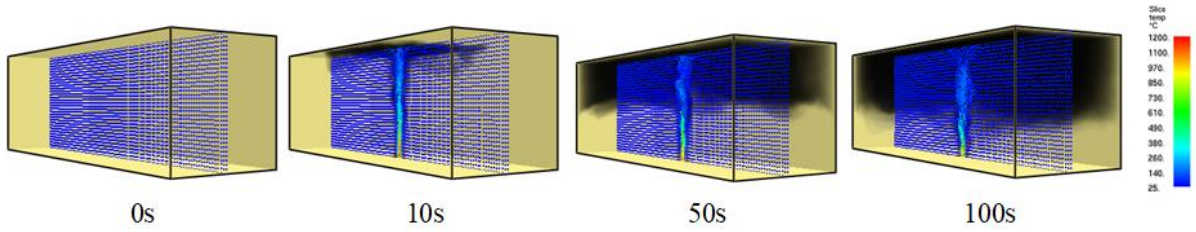

Figure 4-24 Smoke temperature in FDS simulation case FDS-5MW-L60W20H20: 60m Flat Atrium with 20m Width x 20m Height atrium, (5MW) at 0s, 10s, 50s and 100s

Figure 4-24 shows that the smoke in 60m long atrium reaches the ceiling at the first 10s. The smoke temperature in 60m long atrium is higher at the middle of atrium around the fire source shown in 100s which is more obvious than in the 50m atrium.

Figure 4-19 to 4-24, due to the height is the same in all atria, so the smoke temperature rises quickly in the shorter atrium and ceiling jet is obvious. For the longer atrium 40m, 50m and 60m, the smoke layer takes longer time to spread to the boundary of the atrium and the smoke temperature decreases with the length of atrium and broadens over time at the top of atrium.

4.2 Effect of geometry and HRR on velocity

The velocity of smoke layer in various tall atria:

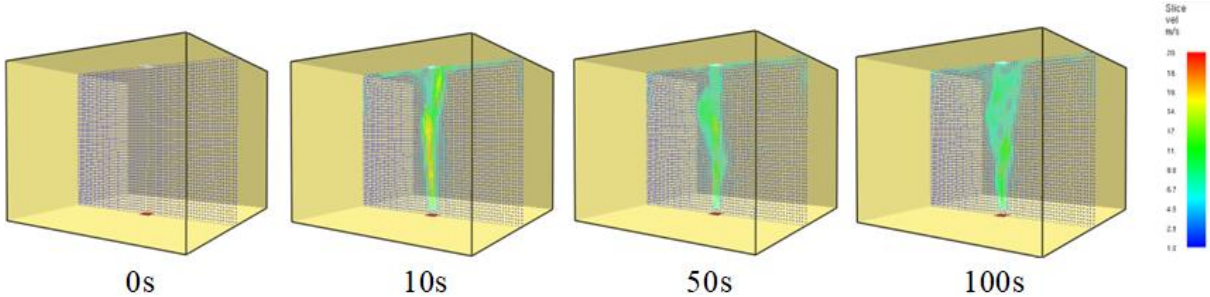

Figure 4-25 Smoke velocity in FDS simulation case FDS-5MW-L20W20H15: 15m Height with 20m Length x 20m Width atrium, (5MW) at 0s, 10s, 50s and 100s

Figure 4-25 shows the mixing of air in 15m tall atrium is quick at the second 10s and the smoke layer descents with the increasing of smoke velocity in the latter.

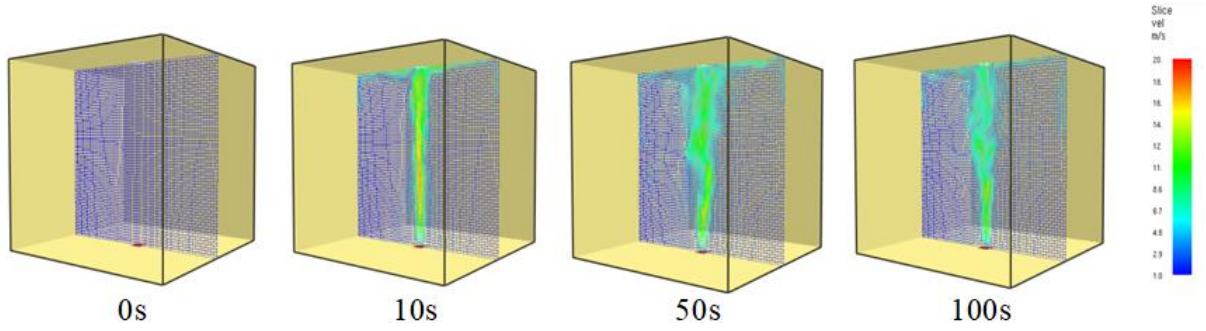

Figure 4-26 Smoke velocity in FDS simulation case FDS-5MW-L20W20H20: 20m Height with 20m Length x 20m Width atrium, (5MW) at 0s, 10s, 50s and 100s

Figure 4-26 shows the mixing of air in 20m tall atrium is more evenly in the cubic atrium and the velocity is quite steady at the latter.

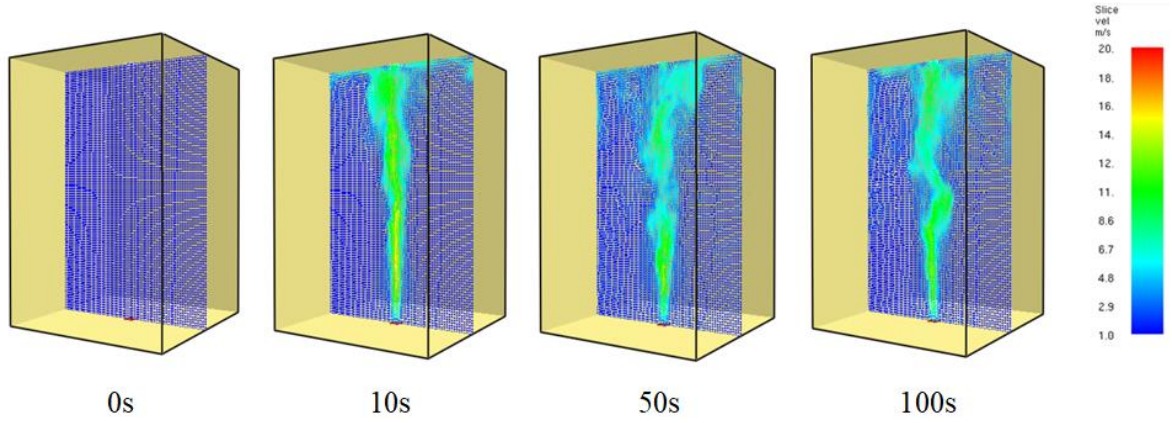

Figure 4-27 Smoke velocity in FDS simulation case FDS-5MW-L20W20H30: 30m Height with 20m Length x 20m Width atrium, (5MW) at 0s, 10s, 50s and 100s

Figure 4-27 shows the velocity of smoke layer in 30m tall atrium becomes unsteady with the increase of height and is obvious in the mixing of air at the middle height of atrium and is fluctuated at the latter.

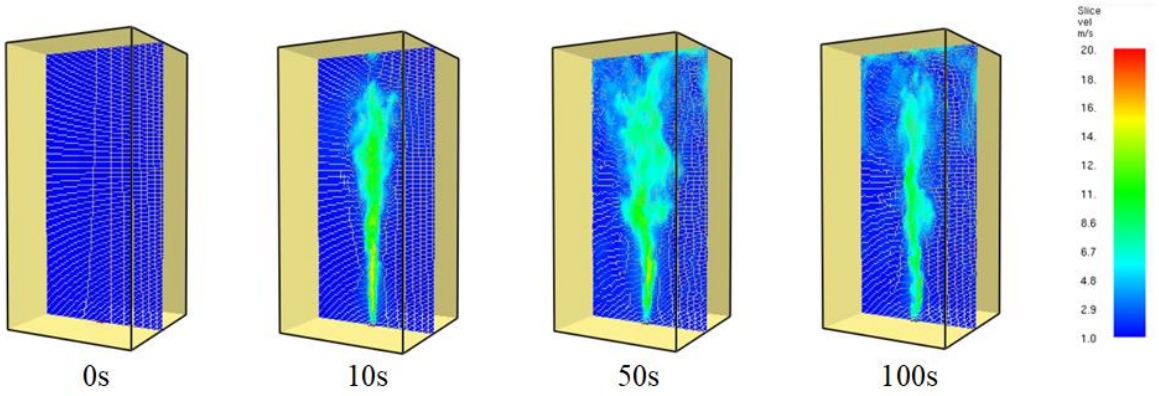

Figure 4-28 Smoke velocity in FDS simulation case FDS-5MW-L20W20H40: 40m Height with 20m Length x 20m Width atrium, (5MW) at 0s, 10s, 50s and 100s

Figure 4-28 shows the velocity of smoke layer in 40m tall atrium becomes unsteady with the increase of height and the mixing of air at the middle height of atrium is dispersing and loss of momentum at the latter due to the HRR is not sufficient for supporting the upwards movement at the latter.

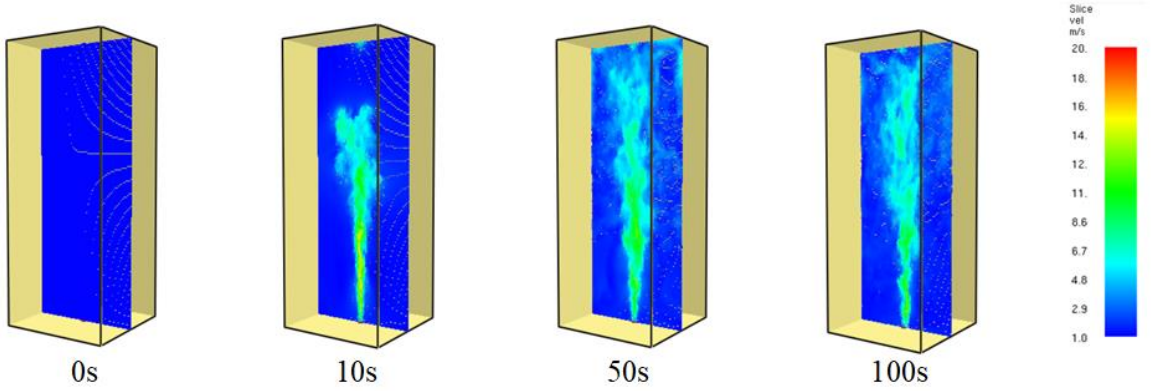

Figure 4-29 Smoke velocity in FDS simulation case FDS-5MW-L20W20H50: 50m Height with 20m Length x 20m Width atrium, (5MW) at 0s, 10s, 50s and 100s

Figure 4-29 shows the velocity of smoke layer in 50m tall atrium is lowering at the middle height of atrium and is dispersing at the upper region and loss of momentum at the latter due to the HRR is not sufficient for supporting the upwards movement at the latter.

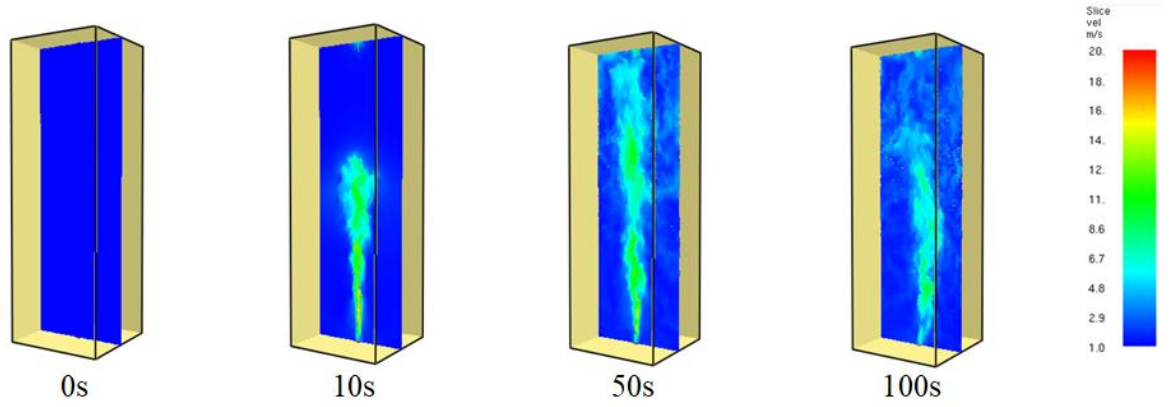

Figure 4-30 Smoke velocity in FDS simulation case FDS-5MW-L20W20H60: 60m Height with 20m Length x 20m Width atrium, (5MW) at 0s, 10s, 50s and 100s

Figure 4-30 shows the velocity of smoke layer in 60m tall atrium is lowering at the middle height of atrium and is dispersing at the upper region and loss of momentum at the latter due to the HRR is not sufficient for supporting the upwards movement at 50s and with a low velocity at the ceiling in the latter. On the last 100s picture, the plume cools as it rises and encounters a warm layer and has lost its jet like appearance of which a stratification may be found at the middle of atrium.

Velocity of the smoke layer referred to Figure 4-25, 4-26, 4-27, 4-28, 4-29 and 4-30. The highest value at the top of atrium among the tall atria is fluctuated as the highest values among the atria are not in ascending or descending order.

The velocity of the smoke layer in various long atriums:

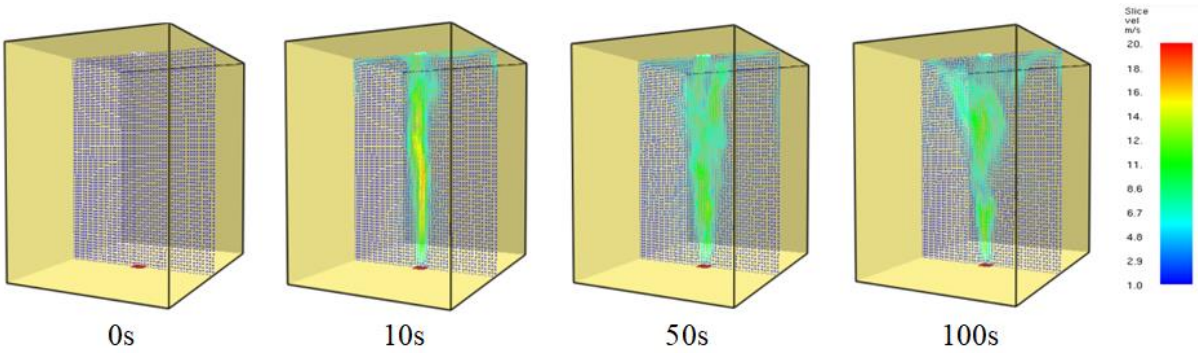

Figure 4-31 Smoke velocity in FDS simulation case FDS-5MW-L15W20H20: 15m Flat Atrium with 20m Width x 20m Height atrium, (5MW) at 0s, 10s, 50s and 100s

The 100s picture on Figure 4-31 depicts a very clear ceiling ‘footprint’ for the plume on the ceiling in 15m long atrium. The change in direction of the velocity can be discerned and the stagnation point of the flow.

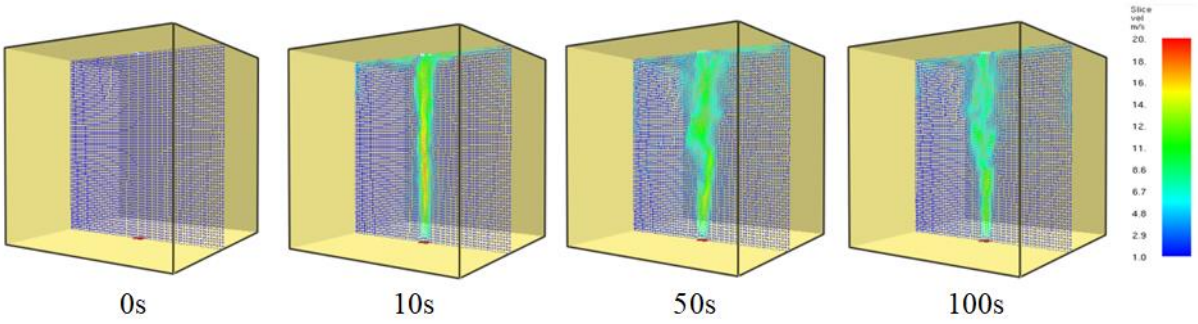

Figure 4-32 Smoke velocity in FDS simulation case FDS-5MW-L20W20H20: 20m Cubic Atrium with 20m Width x 20m Height atrium, (5MW) at 0s, 10s, 50s and 100s

Figure 4-32 shows a clearly radial pattern for horizontal mass flow near the ceiling in a 20-metre cubic atrium. There is also a range near the ceiling/wall where velocity turns downward to form wall jets. The corners of the ceiling appear as dead spaces with little velocity.

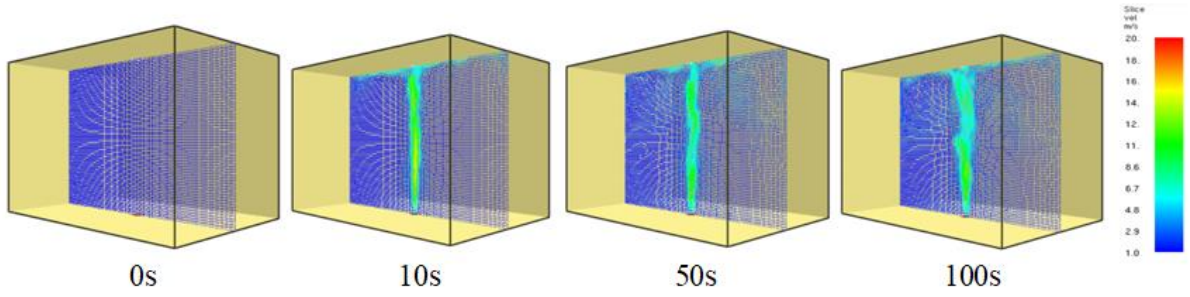

Figure 4-33 Smoke velocity in FDS simulation case FDS-5MW-L30W20H20: 30m Flat Atrium with 20m Width x 20m Height atrium, (5MW) at 0s, 10s, 50s and 100s

Figure 4-33 shows a ceiling jet at 30m long atrium when the smoke layer reaches the highest level. Due to the length extending to 30m, the high velocity is found near the fire plume and instead of the ceiling like Figure 4-32.

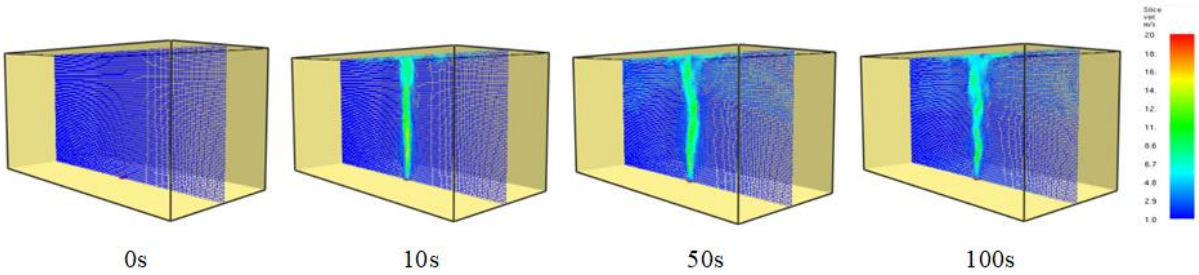

Figure 4-34 Smoke velocity in FDS simulation case FDS-5MW-L40W20H20: 40m Flat Atrium with 20m Width x 20m Height atrium, (5MW) at 0s, 10s, 50s and 100s

Figure 4-34 shows a narrower plume and the ceiling jet is less obvious in 40m long atrium. The velocity of smoke drops when the smoke layer descends to near the ground floor level at 100s.

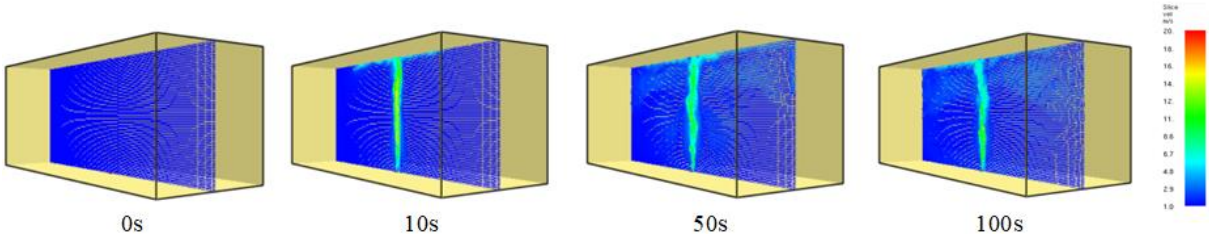

Figure 4-35 Smoke velocity in FDS simulation case FDS-5MW-L50W20H20: 50m Flat Atrium with 20m Width x 20m Height atrium, (5MW) at 0s, 10s, 50s and 100s

On Figure 4-35 the ceiling jets appear to be confined to a region of the ceiling with a radius comparable to the plume height in 50m long atrium.

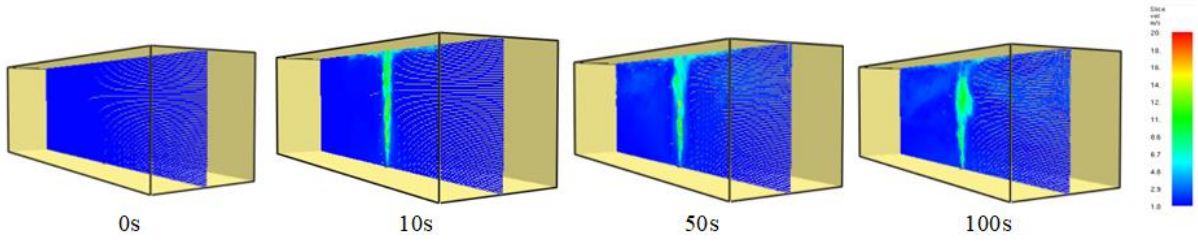

Figure 4-36 Smoke velocity in FDS simulation case FDS-5MW-L60W20H20: 60m Flat Atrium with 20m Width x 20m Height atrium (5MW) at 0s, 10s, 50s and 100s

Figure 4-36 shows the smoke velocity in 60m long atrium increase at the beginning 10s to the ceiling. But at the 50s, velocity is unsteady at the higher level and then loss of momentum at the middle of atrium at 100s when the ambient air diluted with the smoke layer.

The velocity of the smoke layer is referred to in Figures 4-31, 4-32, 4-33, 4-34, 4-35 and 4-36. The highest value at the top of the atrium among the long atria descends from 7.58m/s to 2.41m/s inversely with the length of the atrium.

4.3 Summary of results

A parametric study on different height and long atria is performed by a CFD model, FDS. Simulation with six each tall and long atria was performed to determine the effect on the smoke layer height and velocity. Twelve scenarios were simulated and found that smoke filling time was less than the results from the hand calculation.

4.3.1 Validation with experimental data

The results from the FDS 5.0MW HRR test align with the results from Zukoski and McCaffrey as well as the NFPA. From the initial point, the gradient of all four lines is very similar and the Zukoski curve seems to be gentler as time goes on McCaffrey's results seem to be aligned to the NFPA more than the rest suggesting a stronger relationship between them. However, with the minor fluctuations from FDS, it is safe to suggest that the comparison between all four of these lines is similar and the results suggest no significant difference between them. This helps strengthen the argument in which the smoke filling equation from NFPA 92B is reliable and can predict the smoke layer height to a certain extent for non-ventilated, natural atriums.

4.3.2 Experimental data from different atrium heights

Comparison between the calculated results from the proposed theoretical model with the values in FDS simulation, the conclusion is as follows.

FDS can only use the rectangular mesh for the simulation. When the fire occurs in the middle of the Atrium, in 0s, 10s, 50s and 100s, the simulation results of the FDS correspond with calculated results. For FDS, the impact of the simulated results is decided by the meshing accuracy, therefore, the meshing process needs more refined in order to obtain a more accurate result. Furthermore, since the smoke is not spreading evenly during the FDS simulation, more devices for smoke interface height measurement should be placed at different locations to obtain more data to calculate the average value. In conclusion, reducing the mesh size and placing more devices at different locations will improve the accuracy of

simulation results; the error in comparison of theoretical value and simulation measured value will also be reduced.

4.3.3 Stratification in tall atria

The data collected from FDS simulation that the temperature and velocity in taller atrium drop quickly at the height. 30m and 60m height are selected which show the stratification.

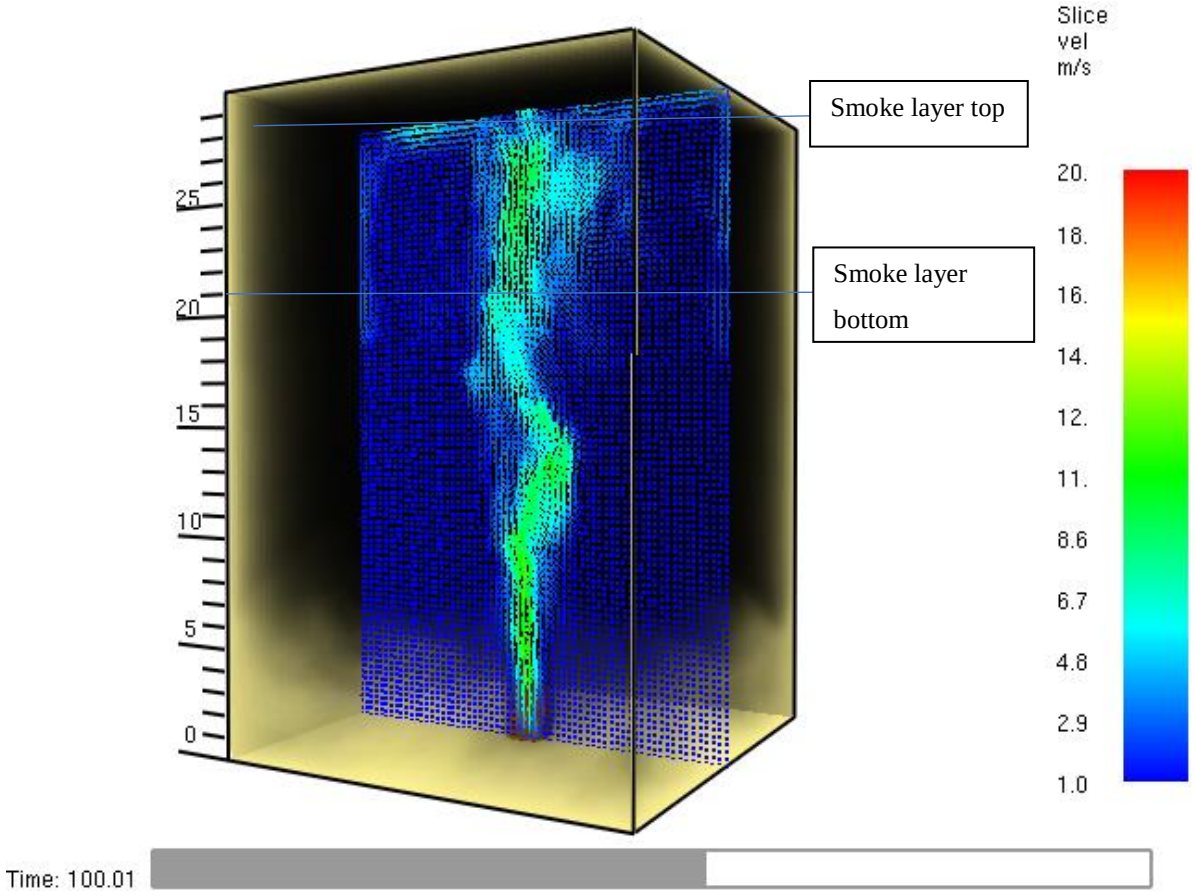

Figure 4-37 Peak and trough of velocity in 30m tall atrium 20m width x 20m length (5MW) at 100s

Figure 4-37 shows the peak and trough of velocity in the 30m tall atrium with 20m width and 20m length under the 5MW fire load at 100s. The temperature and velocity of the smoke layer at the top are higher than those of the layer of heat between 15m and 21m. In this case, stratification may occur as the air entrainment takes place at the middle height of the atrium smoke layer, cooling down the smoky plume and halting the upward movement.

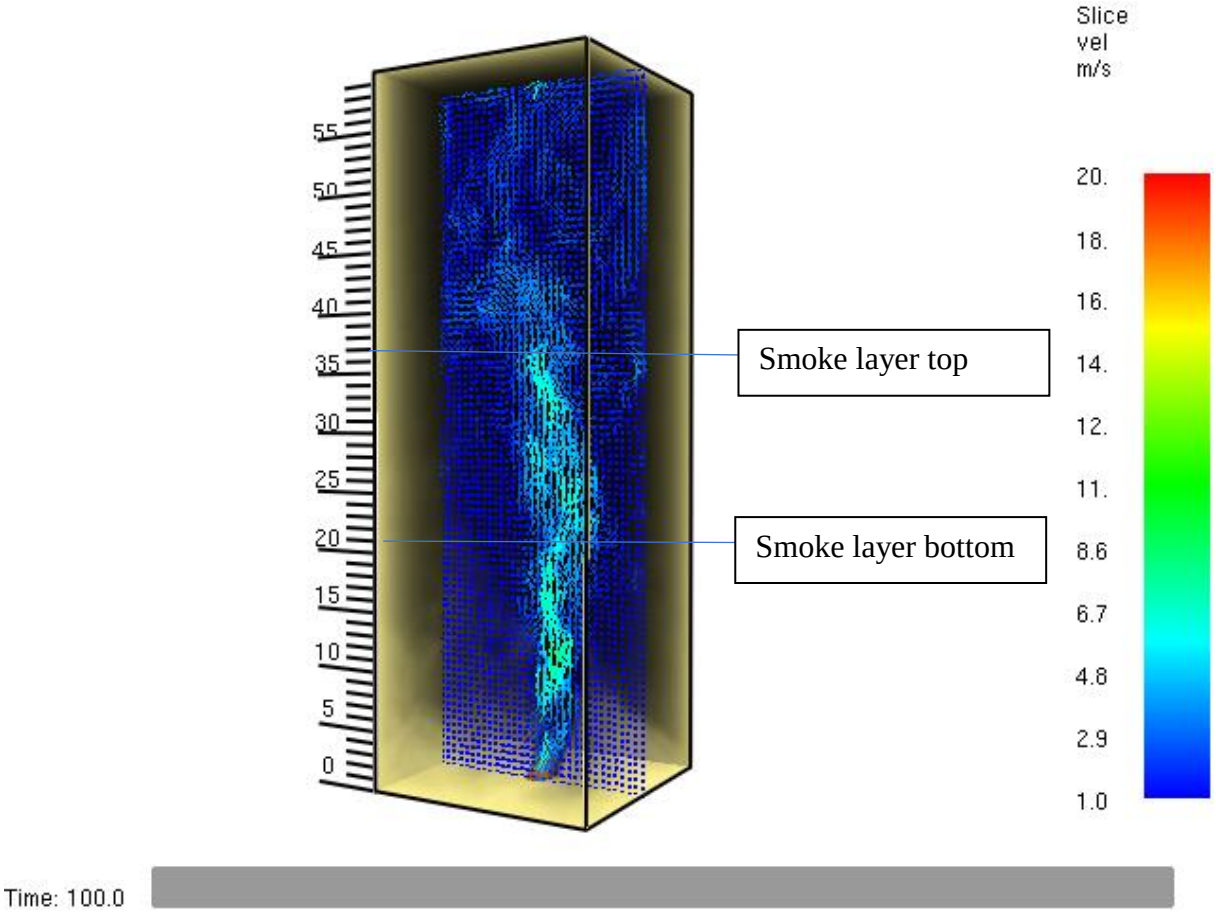

Figure 4-38 Velocity in 60m tall atrium with 20m width x 20m length (5MW) at 100s shown in Figure 4-30

Figure 4-38 shows the velocity of smoke layer in the 60m tall atrium with 20m width and 20m length under the 5MW fire load at 100s. Velocity of the smoke layer over 37m is very low and nearly static at the top of ceiling when the cooler air at the ceiling mixed with the upward smoke layer and cool it down at the middle of atrium. So the layer of smoke state at the middle of atrium and well stirred at the bottom of atrium at 100s.

The following figure presenting Figure 4-38:

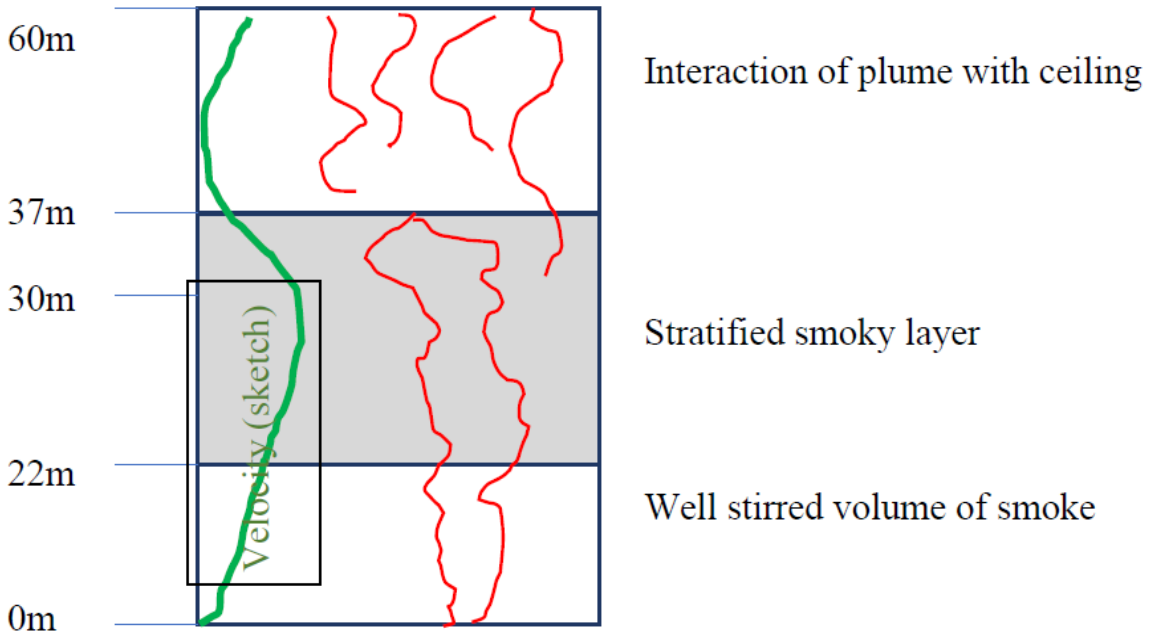

Figure 4-39 Stratification at tall atrium 60m height x 20m width x 20m length in (5MW) at 100s

Figure 4-39 shows the two-dimensional stratification phenomenon at a 60m tall atrium of Figure 4-38.

Smoke layer height, mass flow, temperature and velocity in the 30m and 60m tall atrium at 100s are being evaluated. FDS plot data show that in the 60m atrium, there is a layer of higher temperature and velocity beneath the ceiling and close to the middle height of atrium. The temperature is found unable to activate the smoke detector which is under 68℃ during the whole period of simulation.

Temperature and velocity of smoke from the burner on the vertical upside give a buoyancy effect. However, the thickness of smoke will cool down at the upside of the tall atrium at a certain level. Then the smoke will drop because the velocity does not support this upward.

BRANZ Study Report SR15 Fire safety in atrium buildings, 1988 [68] already indicated that the first three minutes is important as the whole atrium may be smoke logged within this limit of time. In the 60m atrium, the smoke layer height is 6m at 180s which is around 10 percentage of atrium height. Therefore, stratification happened at this situation and the fire protection system does not activate to prevent loss of property and lives.

For the plume centerline temperature, the Heskestad flame height of a 5MW fire load with a fire diameter of 1.826m is 5.23m. Therefore, data below 5.23m is excluded.

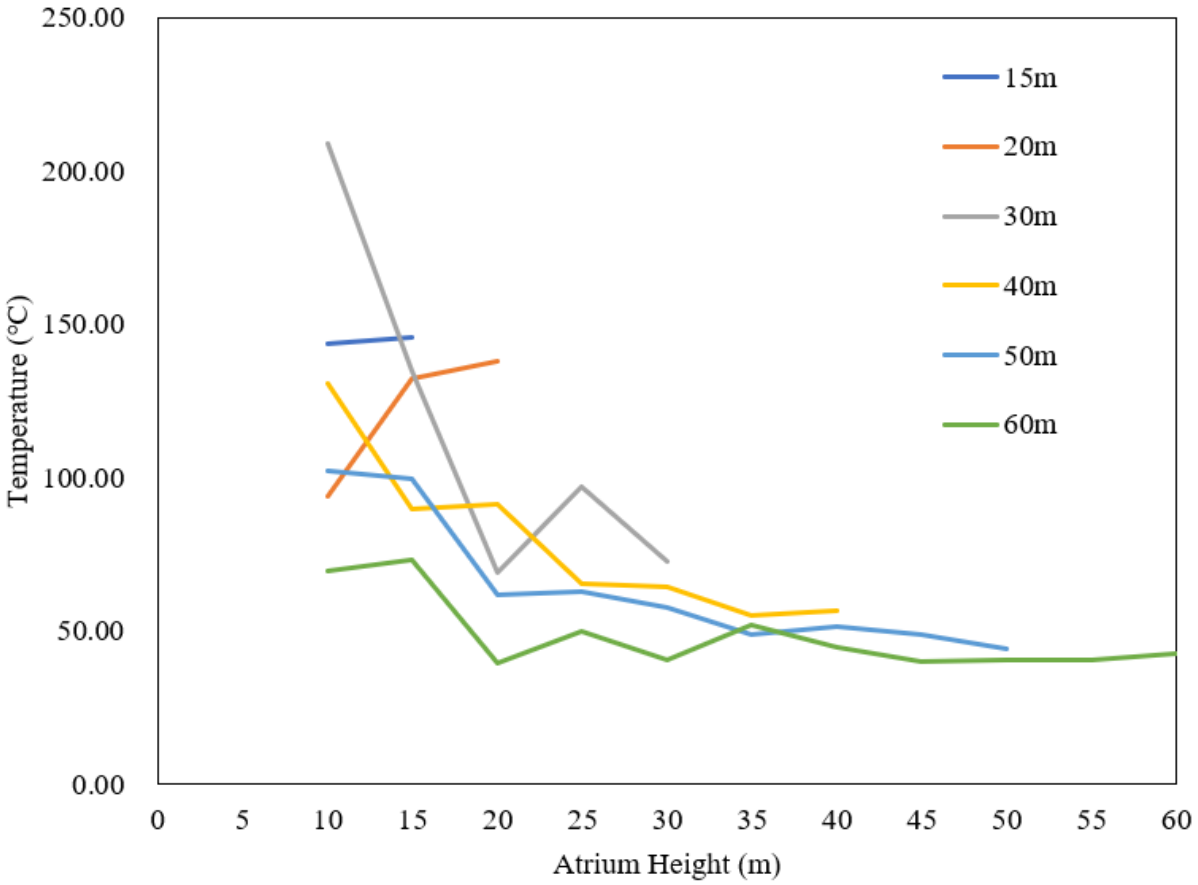

Figure 4-40 Plume Centreline Temperature at different height in various tall atrium height of 15m, 20m, 30m, 40m, 50m and 60m with 20m width x 20m length at 100s (5MW)

Figure 4-40 shows the plume centreline temperature in various height tall atria. Temperature goes upwards at the 15m and 20m tall atrium. At the time of 100s, the temperature is all below 68℃ at the atrium more than 40m of which the smoke detectors are normally installed. So, fire alarm will not be activated at the level of temperature.

The smoke layer is found to quickly drop to below 20% in the higher atria at 180s.

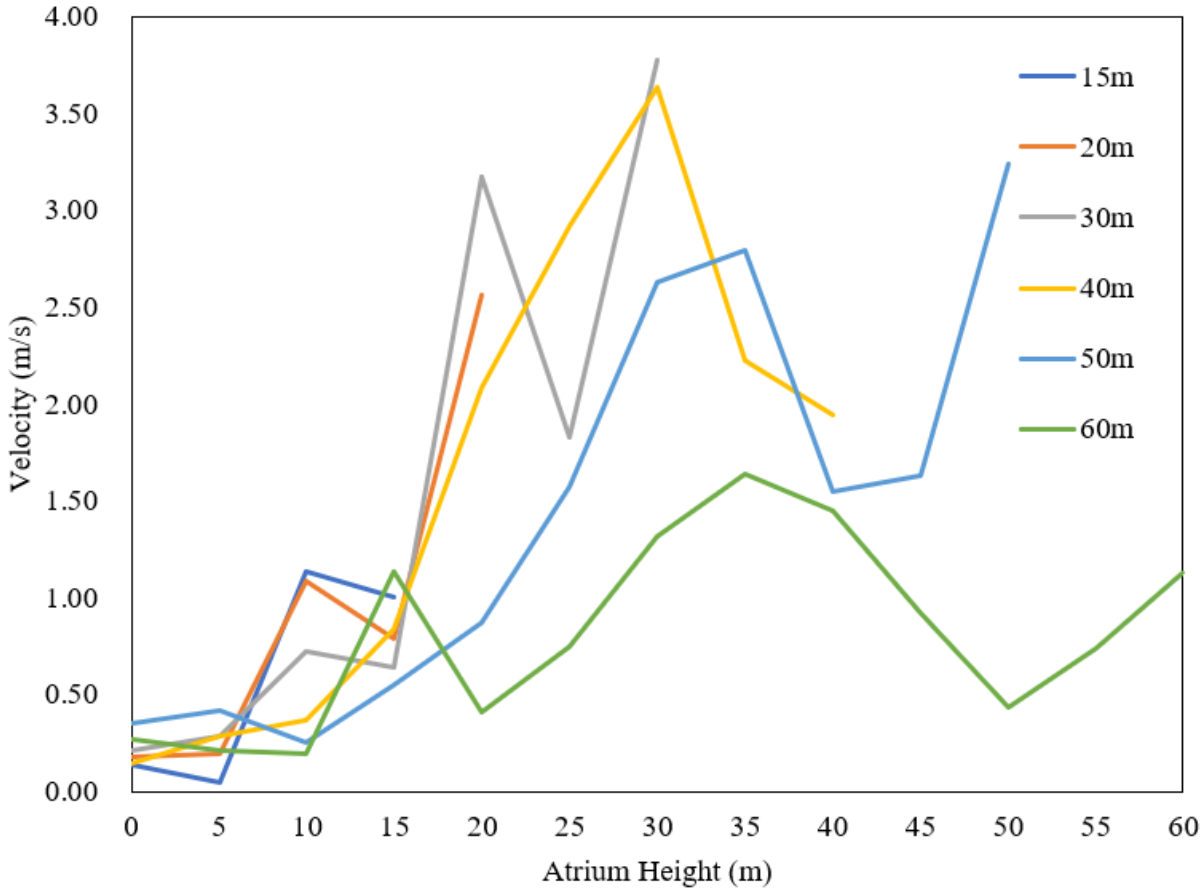

Figure 4-41 Velocity at different height in various tall atrium height of 15m, 20m, 30m, 40m, 50m and 60m with 20m width x 20m length at 100s (5MW)

From Figure 4-41, in the 50m height atrium, the cooling upside remains so it is rising. In the 60m straight atrium the ceiling level is cooler, so the smoke cannot go straight upward.

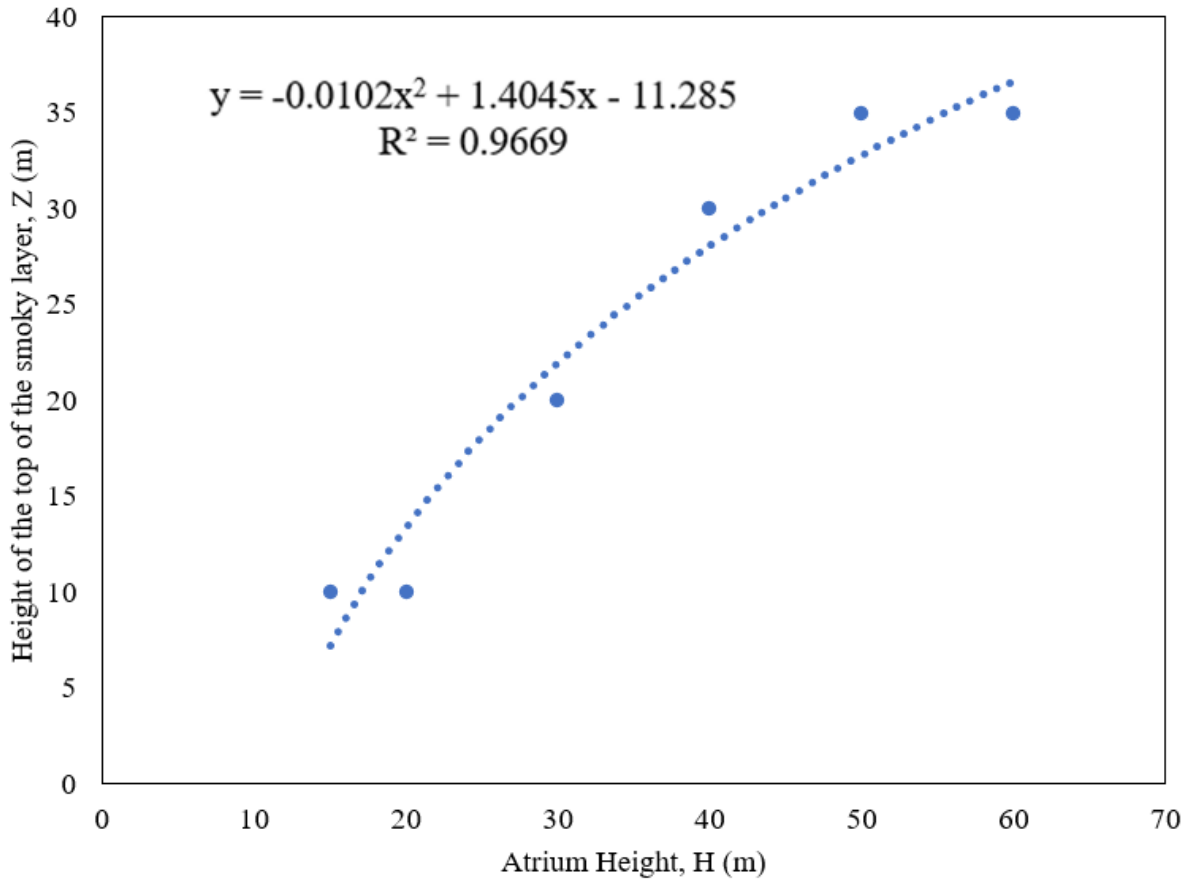

Figure 4-42 Height of top of smoky layer at different height in various tall atrium of 15m, 20m, 30m, 40m, 50m and 60m with 20m width x 20m length at 100s (5MW)

Figure 4-42 shows the best fitted trend line is quadratic polynomial with R^2 value of 0.9669 covering the sets of oscillating values from the results of the height of top of smoky layer at different height in various tall atria at 100s at 5MW fire load.

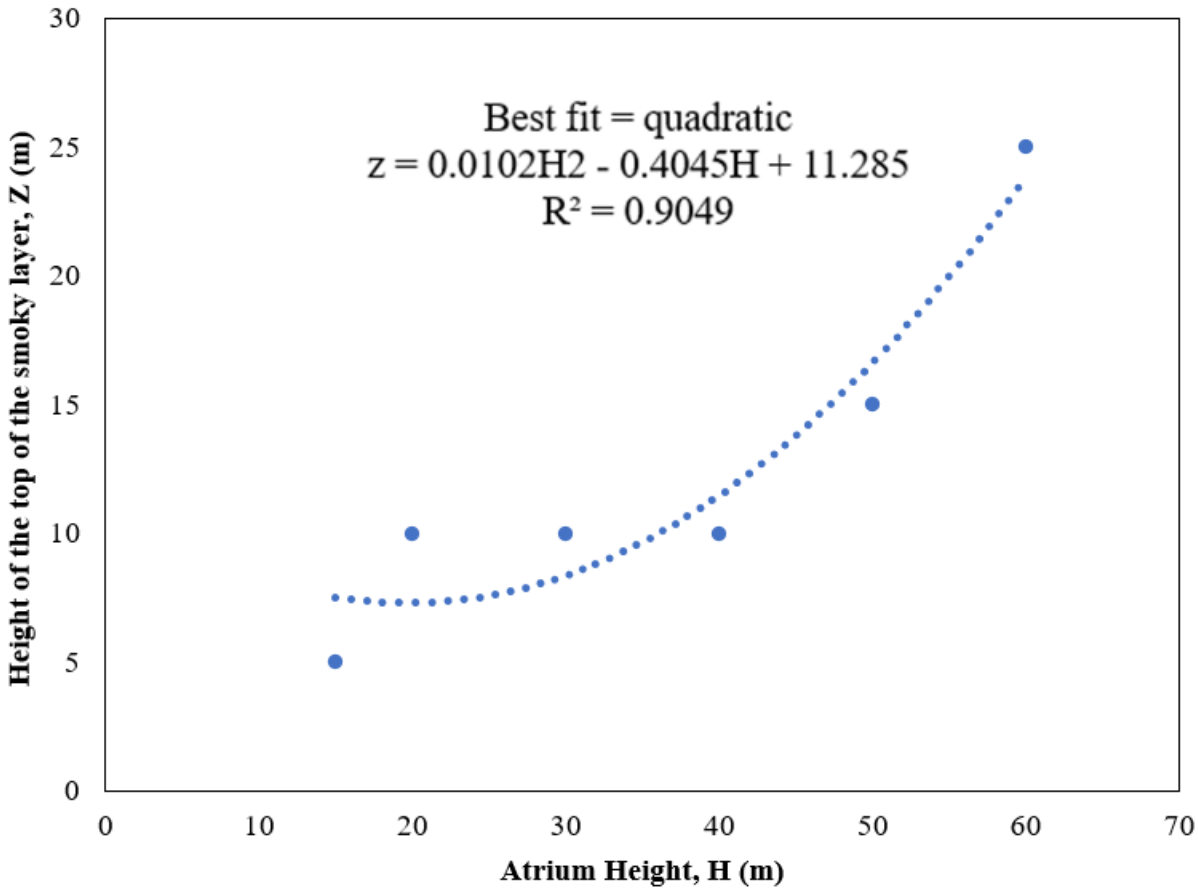

Figure 4-43 Height of clear space at different height in various tall atrium of 15m, 20m, 30m, 40m, 50m and 60m with 20m width x 20m length at 100s (5MW)

Figure 4-43 shows the best fitted trend line is a quadratic polynomial with R^2 value of 0.9049 covering the sets of oscillating values from the results of the height of clear space at different heights in various tall atria at 100s at a 5MW fire load. Clear space starts from 11m and increases quadratically with atrium height, which is a 90.5% correlation.

From the simulated results, stratifications were found in the tall atrium. The following correlation in CIBSE Guide E, 2010 [3] calculates the maximum height of rise of an axisymmetric plume for stratification, which is applicable to 20m or less atria.

$$Z_m = 5.54 Q_p^{\frac{1}{4}} \ (dT/dZ)^{-\frac{3}{8}} \qquad (4\text{-}1)$$

Therefore, a simple equation is not reached because of the effects of stratification. The future work should look to develop a simple relationship for stratification height.

CHAPTER 5: Evaluation of Empirical Correlations

5.1 Proposed physical trends to causes

Modern building architecture is currently extensively open-space concepts in atria and other spaces. Atria become more and more complicated when it comes to their geometry and thus design guides and hand calculations are not able to accurately predict fire and smoke development. Use of performance-based design can be used to address those issues.

According to Chapter 2.2 regarding the brief review of atria and Chapter 2.3 for types and configuration of atrium, performed FDS in different height and long atrium for re-assessment.

Dimensions of the tall atrium used are 15m, 20m, 30m, 40m, 50m and 60m with a common 20m length and 20m width.

Dimensions of the long atrium used are 15m, 20m, 30m, 40m, 50m and 60m with a common 20m width and 20m height.

5.1.1 Calculation of plume centreline velocity by the Heskestad's equation in different height atrium from 15m, 20m, 30m, 40m, 50m and 60m with the smoke layer interface NFPA and FDS results.

The air flow velocity can be calculated from the mass flow rate equation. It is assumed that a 1 m x 1 m vent is placed at the center of the roof of an atrium (20 m length x 20 width x 20 m height). Using the FDS default measuring device provided in the spreadsheet, the mass flow rate of a vent can be measured using the following equation for the flow velocity in z direction at the roof of the atria.

$$Q_c = \chi Q \tag{5-1}$$

$$T_s = T_o + \frac{K_s Q_c}{m C_p} \tag{5-2}$$

$$\rho_s = \frac{P_{atm}}{R(T_s + 273)} \tag{5-3}$$

$$Volumetric\ flow\ rate = \frac{m}{\rho_s} \times \frac{1}{Cross - sectional\ Area} \tag{5-4}$$

It is assumed that T_0 is 25℃, P_{atm} is 101300 Pa, Q is 5MW and χ is 0.7

Sample calculation is in Appendix 1.

Using Heskestad's equation as below to calculate the velocity at the smoke layer interface in different atrium height: 15m, 20m, 30m, 40m, 50m and 60m in respect of the time after ignition:

$$u_o = 1.03\left(\frac{\dot{Q}_c}{z - z_o}\right)^{\frac{1}{3}} \tag{5-5}$$

The virtual source z_o is evaluated using (2-6).

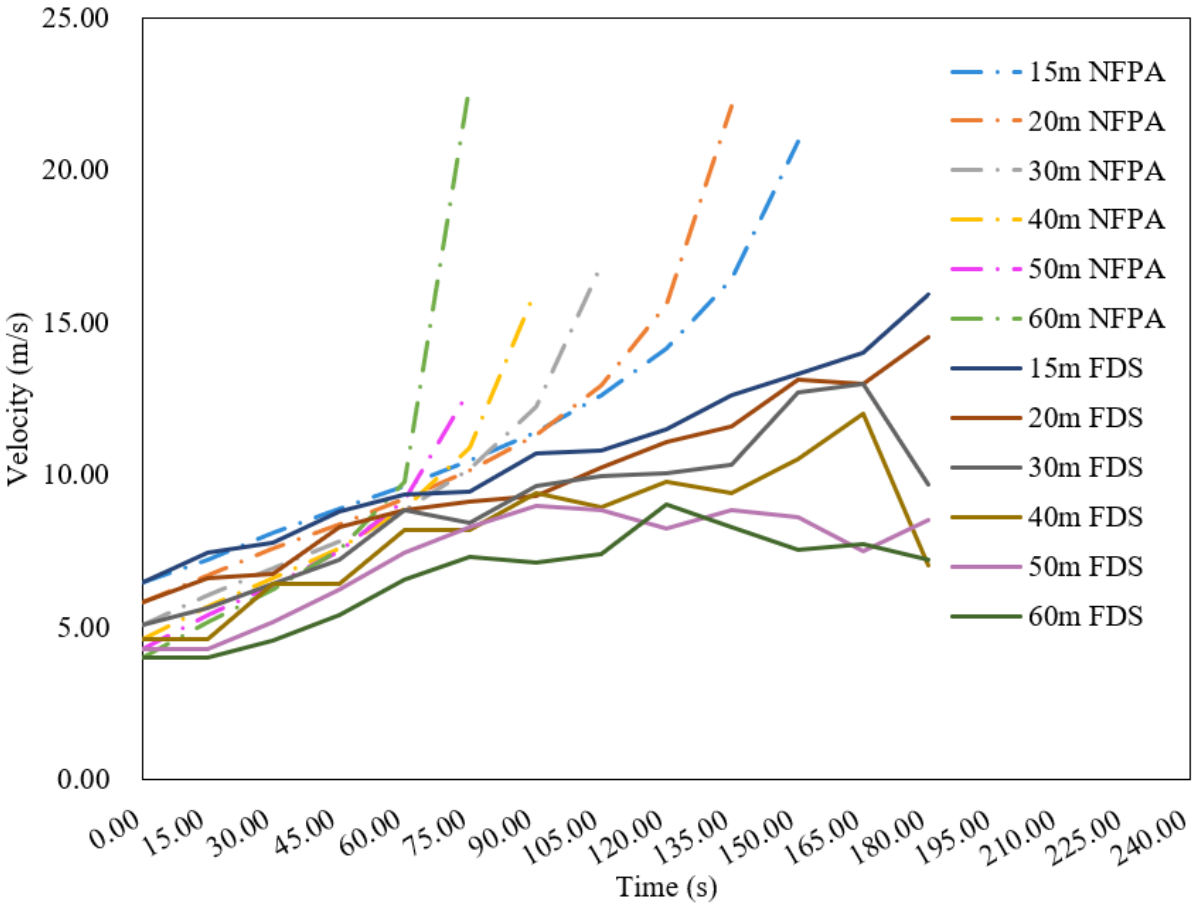

Figure 5-1 Velocity of descending smoke layer by NFPA and FDS comparing it against different atrium height of 15m, 20m, 30m, 40m, 50m and 60m with 20m width x 20m length

Figure 5-1 reflects the velocity at the smoke layer interface from NFPA and FDS simulations of a range of tall atrium at 15m, 20m, 30m, 40m, 50m and 60m in respect of the running time of FDS simulation measured at the bottom of smoke on centreline [5].

All the curves show the smoke descending increasingly rapidly but the FDS simulations show that there is a slowdown and settling for the tallest atria after the first couple of minutes.

The deviations between NFPA and FDS are mainly that NFPA has overstated the prediction of the velocity of the descending smoke layer in all cases. This error is apparently very large after one minute. This is most likely because the empirical formulae did not account for the cooling of smoke in larger atria.

5.1.2 Comparison of smoke layer height in same volume atria in 5MW

The tall and long atria share the same volume as the dimensions of the 15m, 20m, 30m, 40m, 50m and 60m. The following Figure 5-2 is the comparison of the descending smoke layer height of the same volume but different geometry at the same dropping time period in the 5MW fire load measured at the bottom of the smoke on the centreline.

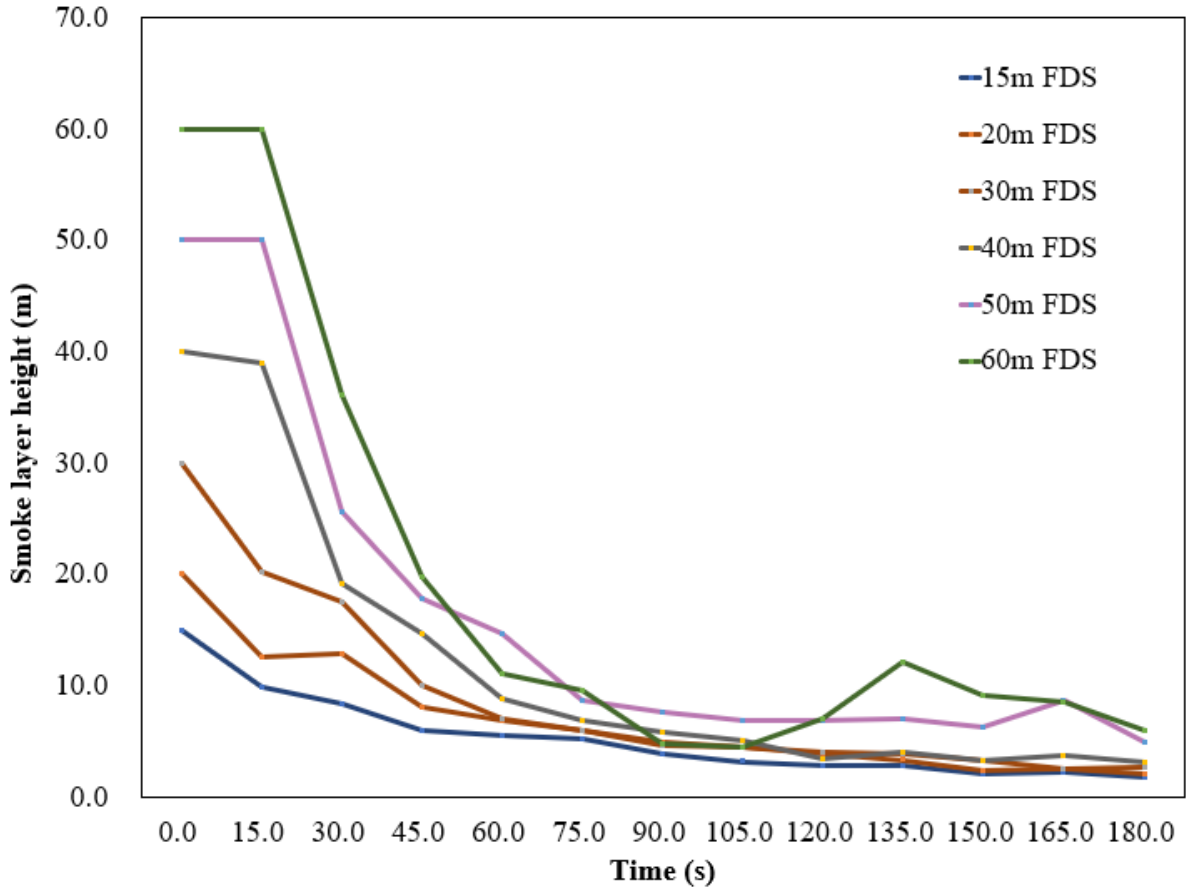

Figure 5-2 Descending smoke clearance height in tall atria in height of 15m, 20m, 30m, 40m, 50m and 60m with 20m width x 20m length

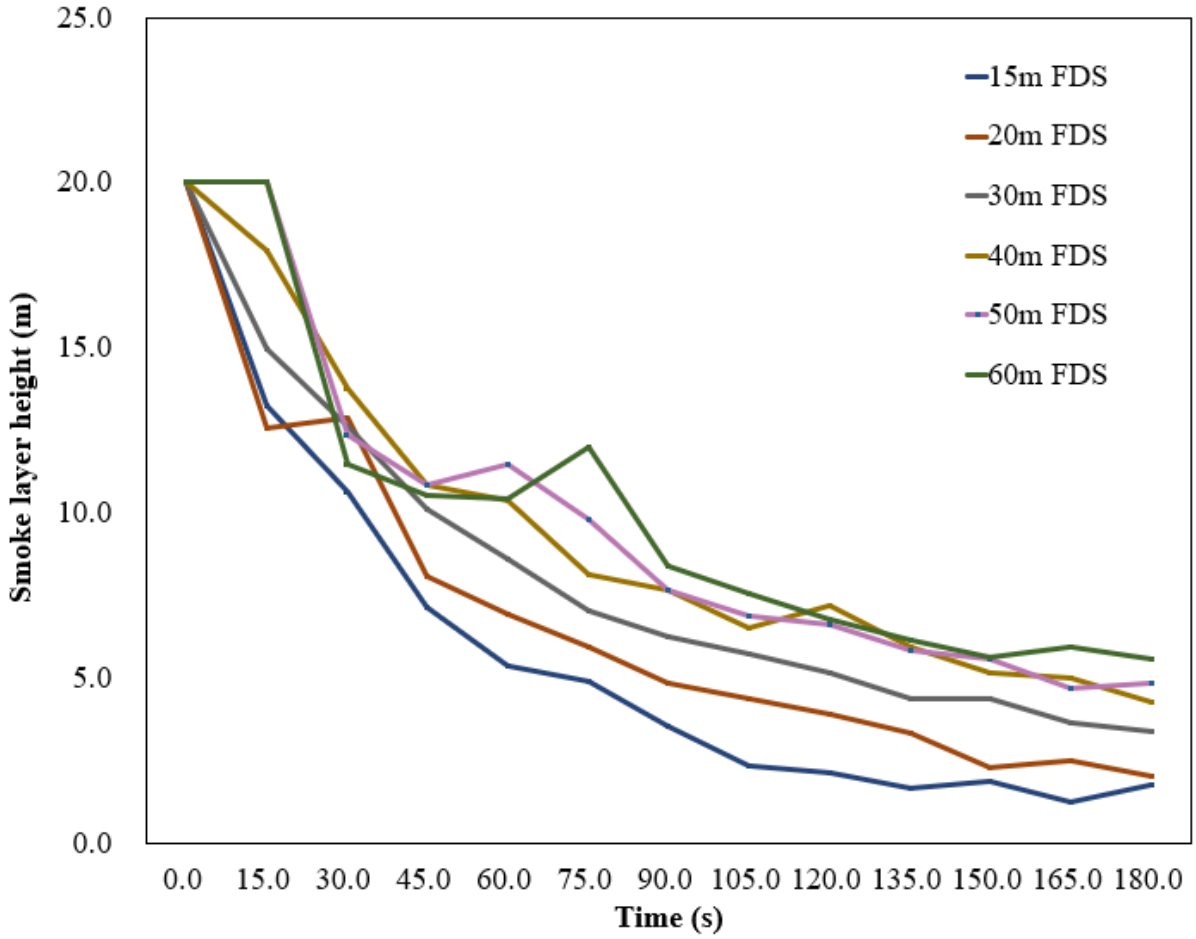

Figure 5-3 Descending smoke clearance height in long atria length of 15m, 20m, 30m, 40m, 50m and 60m with 20m width x 20m height

Figure 5-2 and 5-3 show that increasing atrium height up to 60m only has an appreciable difference on smoke depth for the first minute. After this time the volumes are filled with different density of smoke, which is not visible on this graph. It appears to show that a longer atrium attenuates the filling time. As before, the smoke density and optical opacity are not easily deduced from this one graph. The smoke layer in the tall atria drops quicker than the long atria although they are of the same volume.

5.1.3 Comparison of smoke layer temperature in tall atrium

The temperature calculated from the results of the theoretical smoke layer height is not applicable to high atrium as the smoke drops quickly to 1.17m at 75s, relatively higher than the smoke layer height collected from FDS data.

Because of algebraically calculation, the trend is only upwards with the height of the atrium. Overall, the smoke layer temperature of the NFPA has been found much higher than the

simulation results. Based on the comparison, it shows that the constant used in the correlation is not suitable in the taller atrium.

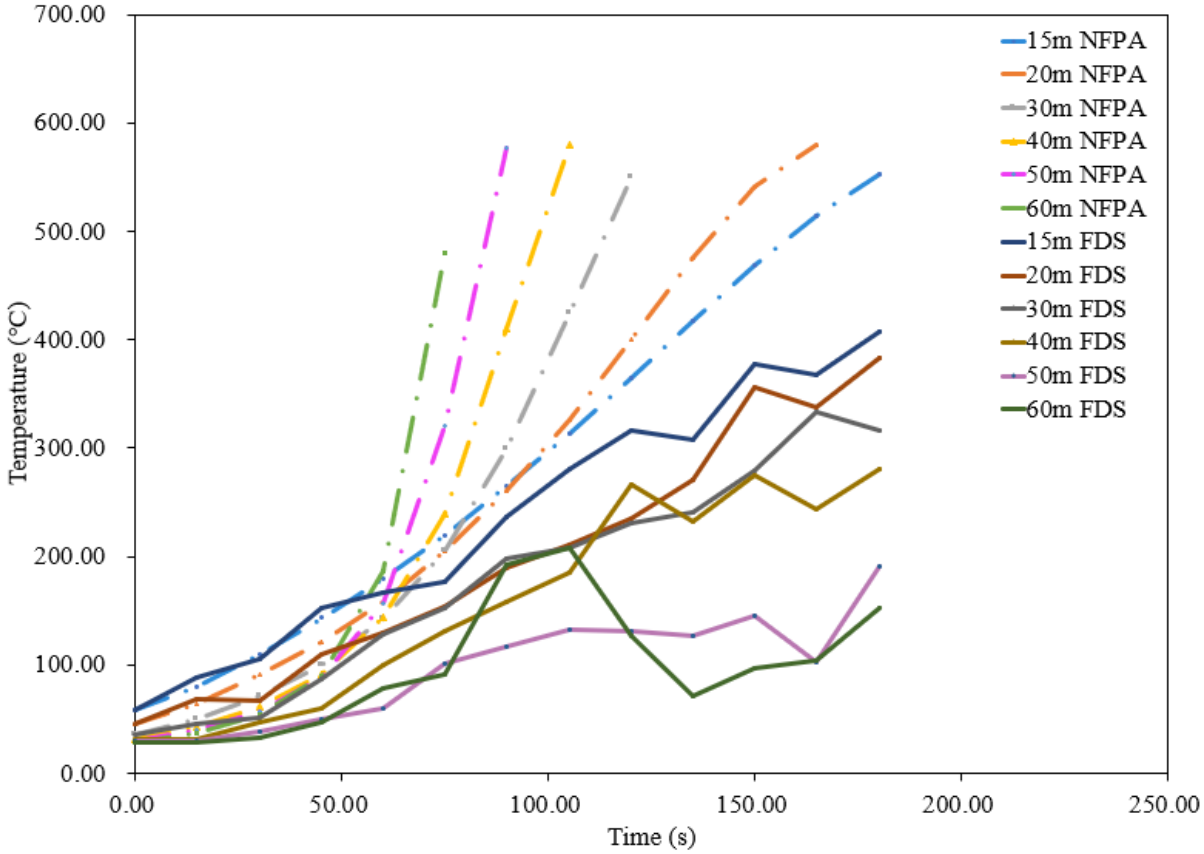

Figure 5-4 Centreline smoke layer temperature (at the base of the smoky layer) in tall atrium – NFPA against FDS height of 15m, 20m, 30m, 40m, 50m and 60m with 20m width x 20m length (5MW)

Figure 5-4 shows clearly that the FDS and NFPA curves disagree increasingly over time. FDS gives significantly lower temperatures. This is because the flow structure is complicated, and the heat is consequently distributed more widely throughout the smoky volume.

5.1.4 Comparison of smoke layer temperature in long atrium

For the long atrium, although the volume of the atrium is same as the tall atrium, the smoke layer temperature is much less than in the tall atrium as the dropping of smoke is not as quick as the tall atrium. The temperature data from NFPA and FDS are similar at the longer atrium especially at the longest atrium. It also shows that the constant using the correlation is appropriate at the longer atrium.

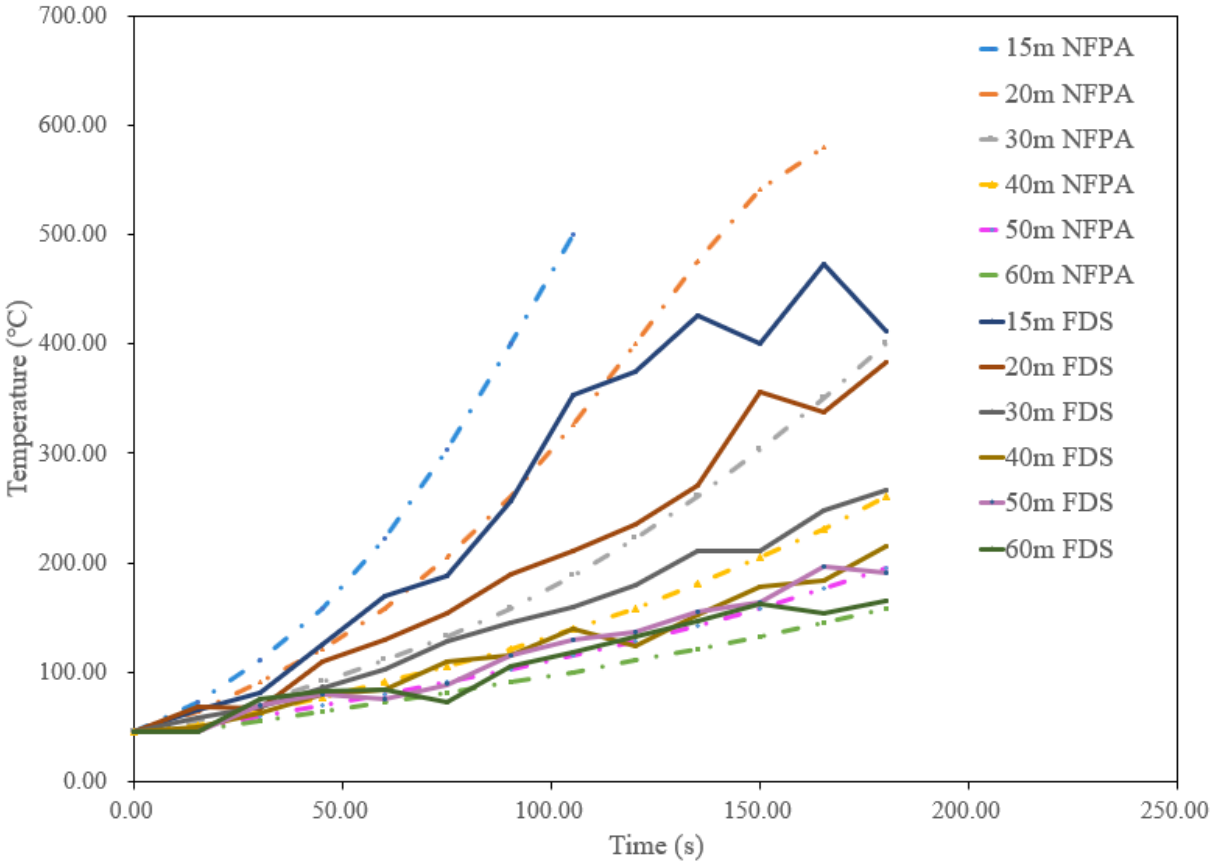

Figure 5-5 Smoke layer temperature in long atrium length 15m, 20m, 30m, 40m, 50m and 60m with 20m width x 20m height by NFPA against FDS performed in 180s (5MW)

NFPA and FDS show a general agreement in order of magnitude in Figure 5-5, but FDS is still markedly lower for the shorter atria.

First step used NFPA92 calculation

$$T_s = T_o + \frac{K_s Q_c}{m C_p} \tag{5-6}$$

From Figure 5-5, an overall comparison of the long atrium, the results from FDS simulation for 50m and 60m long atrium have the closest matching with the NPFA data. In the early 75s, the predicted smoke layer temperatures in 30m and 40m atrium also closed to the FDS data but found deviate after the 90s and expanded greater difference at longer period in 30m long atrium. For the shorter atrium, 15m and 20m, there is a significant difference between the FDS data. The quite satisfactory correlation between the simulation and the NFPA results for the longer atria.

Therefore, it reflects that the constant 0.28 is still the most suitable value for the longer atriums of 50 and 60m. Whereas in the 30m and 40m should have a lower constant for shifting to the descending slop of the shorter atrium.

5.2 Development of empirical calculations

The use of hand calculations based on a specific formula from NFPA 92 can be used to determine the distance from the base of fire to the smoke layer interface. The smoke layer height can be evaluated through the use of hand calculation by using the formula from NFPA 92, (2021), Equation 5.4.2.1b [1] as above Equation (3-2) :

$$Z = \left[1.11 - 0.28\, ln\left(\frac{tQ^{\frac{1}{3}}H^{-\frac{4}{3}}}{\frac{A}{H^2}}\right)\right] \times H \tag{5-7}$$

Based on equation (5-7), the variables that must be considered include time, the heat release rate of the flame, and the cross-sectional area of the atrium and the height of the atrium.

The data collected from the FDS simulation were compared and found out that the constant used in the empirical correlation does not satisfy various atrium heights and are segmented into two ranges of atrium height. Below shows the results using the constant used in the NFPA correlation and the possible improvement of using the newly found appropriate constant to accommodate the different atrium heights.

5.2.1 Investigating the smoke depth from an axisymmetric plume and how variations in atrium height affect the smoke generated – High Atrium

When considering both methods used to generate a value for the smoke height layer, the value for smoke depth can be evaluated by both hand calculation and by FDS [5]. In Figure 5-6 there is a comparison that has been done to investigate how different atrium sizes affect the development of smoke depth. The following atrium heights have been used: 15m, 20m, 30m, 40m, 50m and 60m. The transient phase and steady phase will also be considered since they form a crucial part of this exploration.

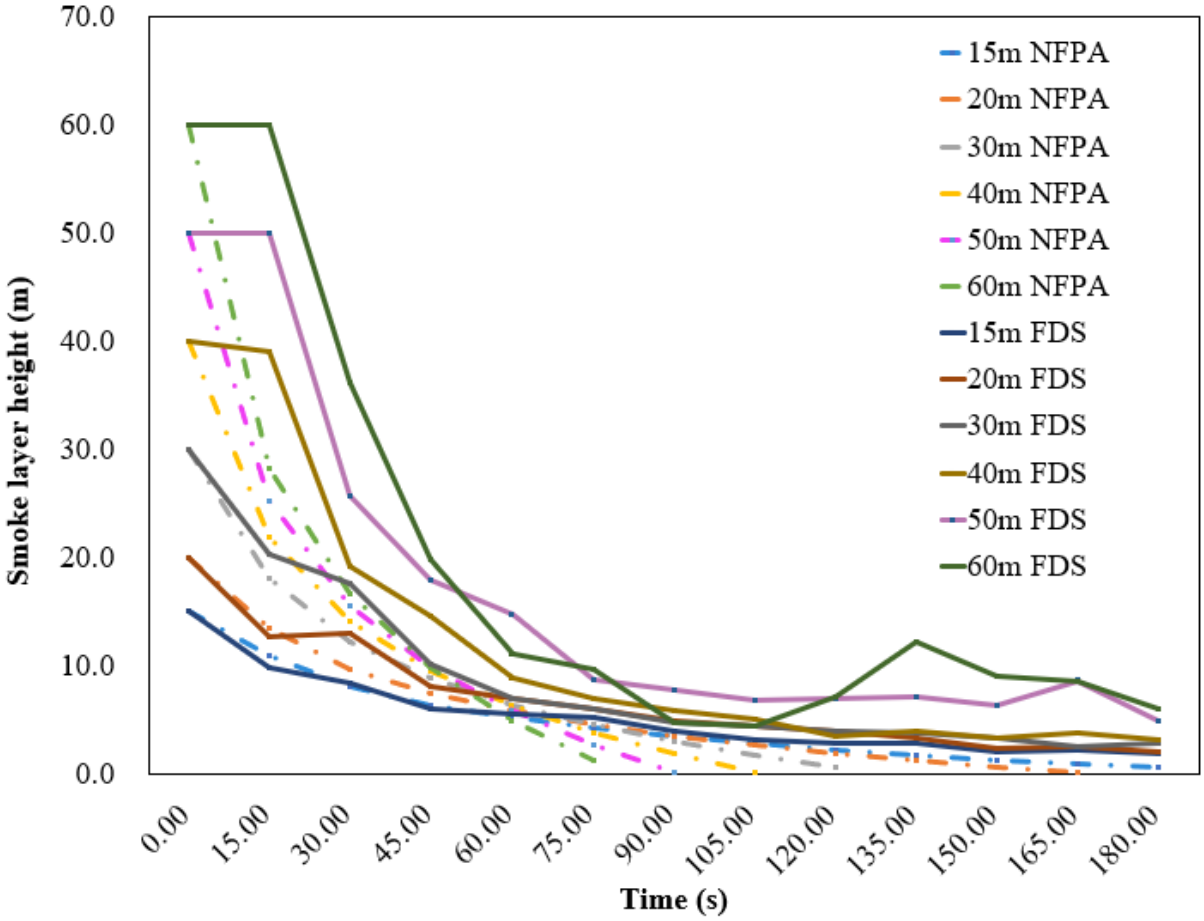

Figure 5-6 FDS and NFPA92 for the smoke layer height at different atrium heights of 15m, 20m, 30m, 40m, 50m and 60m with 20m width x 20m length (5MW) using Constant 0.28

A graph depicts the smoke layer height when a range of different atrium heights are considered. Using FDS to identify the smoke layer height and compare it against different atrium heights. From the above-mentioned graph, the gradient for each graph was significantly different, ranging from the least significant gradient drop from 15m and the steepest gradient at 60m. Since the mathematical approach utilized a logarithmic equation, this is expected and the result for when t=0 cannot be identified. Moreover, the value for smoke layer height should not be able to go under 0 and therefore, raises an issue that shall be investigated. As a result, the transient and steady phase cannot be properly identified in this situation of the NFPA correlation.

After investigating the properties of a logarithmic graph, the constant (0.28) alters the stretch of the graph and thus altering it to approximately 0.21 will help prevent the overlap shown in Figure 5-6 at 60 seconds. In addition, this constant can be revised to obtain positive values from 0-180 seconds instead of dropping below 0.

Table 5-1 Results table for the mean square error (MSE) comparison of applying different constants of varying atrium heights

Atrium Height (M)	Constant								
	0.20	**0.21**	**0.22**	**0.23**	**0.24**	**0.25**	**0.26**	**0.27**	**0.28**
15	9.15	6.68	4.61	2.95	1.69	0.83	0.37	0.32	0.26
20	12.43	8.48	5.34	2.99	1.46	0.72	0.79	1.66	2.04
30	28.17	18.73	11.40	6.18	3.07	2.08	2.69	4.21	7.70
40	48.76	34.66	24.71	18.92	17.28	18.71	20.91	25.13	49.88
50	48.28	36.71	32.14	34.59	45.54	58.61	81.88	102.71	162.24
60	85.26	71.04	67.53	74.75	95.71	113.47	89.86	105.66	123.08

The results show that the better fit of the constant for the range of atrium are 0.25 for 20-30m and 0.24 for 40m tall atrium.

5.2.2 Constant 0.25 for atrium range from 20m to 30m

Figure 5-7 shows the updated smoke layer height of NFPA compared with FDS comparison for using the improved constant 0.25 for the 20m and 30m tall atrium:

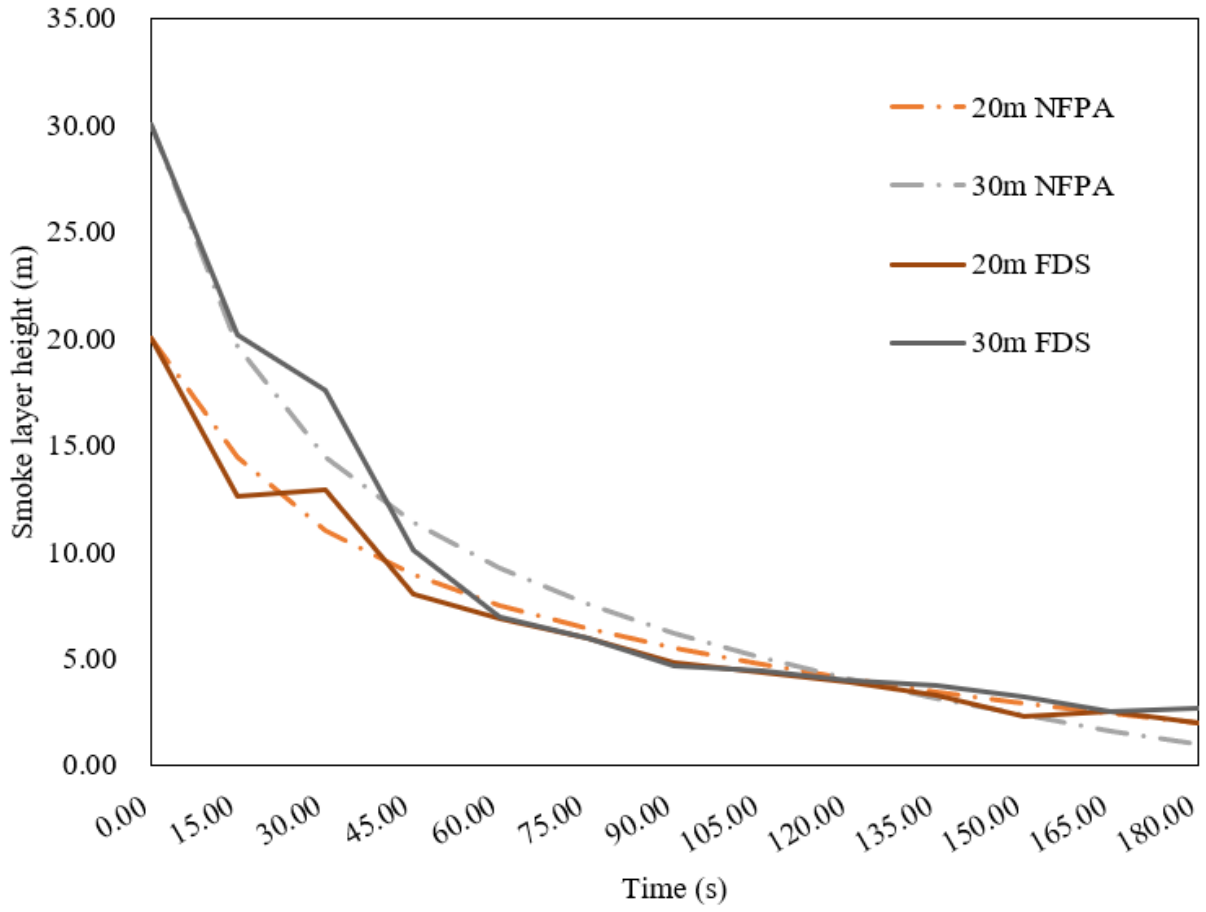

Figure 5-7 Improved correlation between smoke layer height and time when the atrium height of 20m and 30m with 20m width x 20m length (5MW) is altered using constant 0.25

5.2.3 Constant 0.24 for 40m atrium

Figure 5-8 shows the updated smoke layer height of NFPA compared with FDS comparison for using the improved constant 0.24 for the 40m tall atrium:

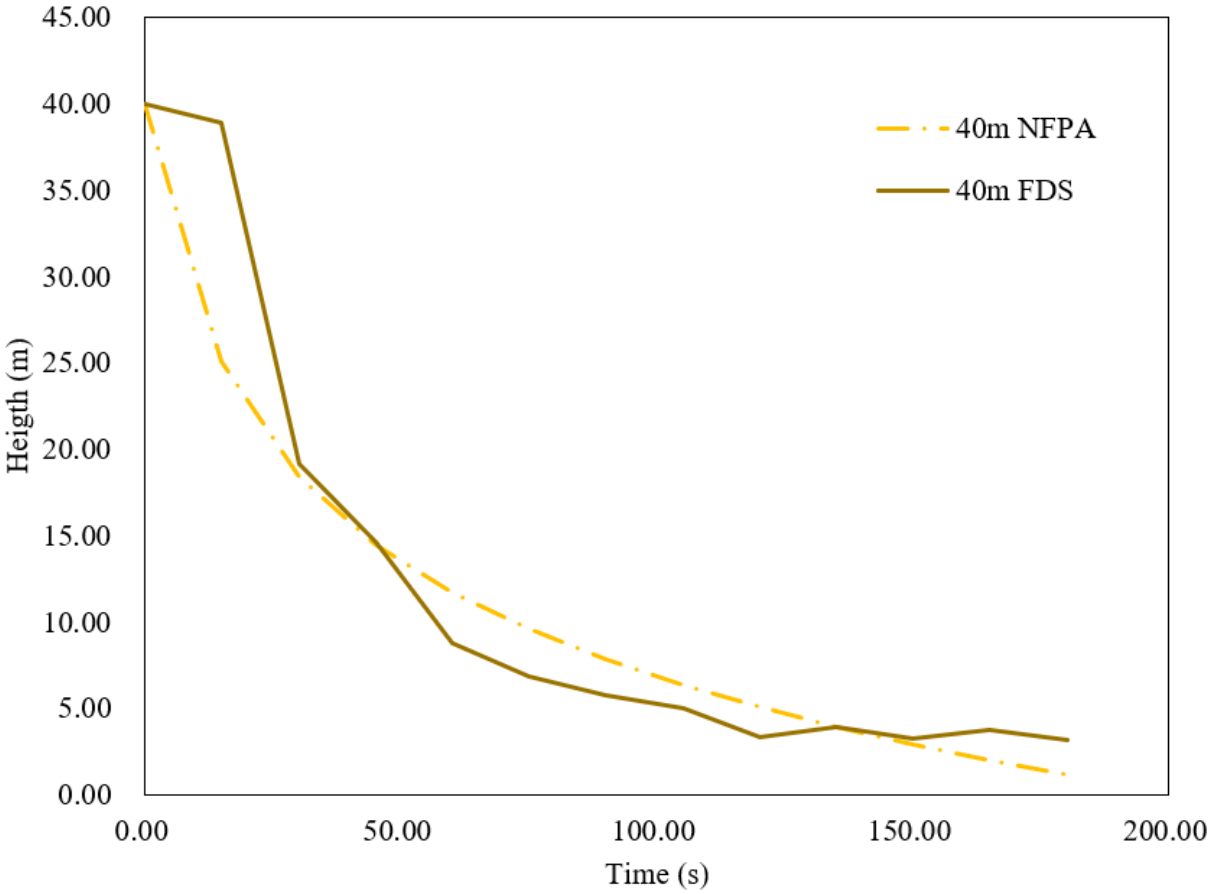

Figure 5-8 Improved correlation between smoke layer height and time when the atrium height of 40m with 20m width x 20m length (5MW) is altered using constant 0.24

5.2.4 Constant 0.22 for atrium range from 50m to 60m

Figure 5-9 shows the updated smoke layer height of NFPA compared with FDS comparison for using the improved constant 0.22 for the 50m and 60m tall atrium:

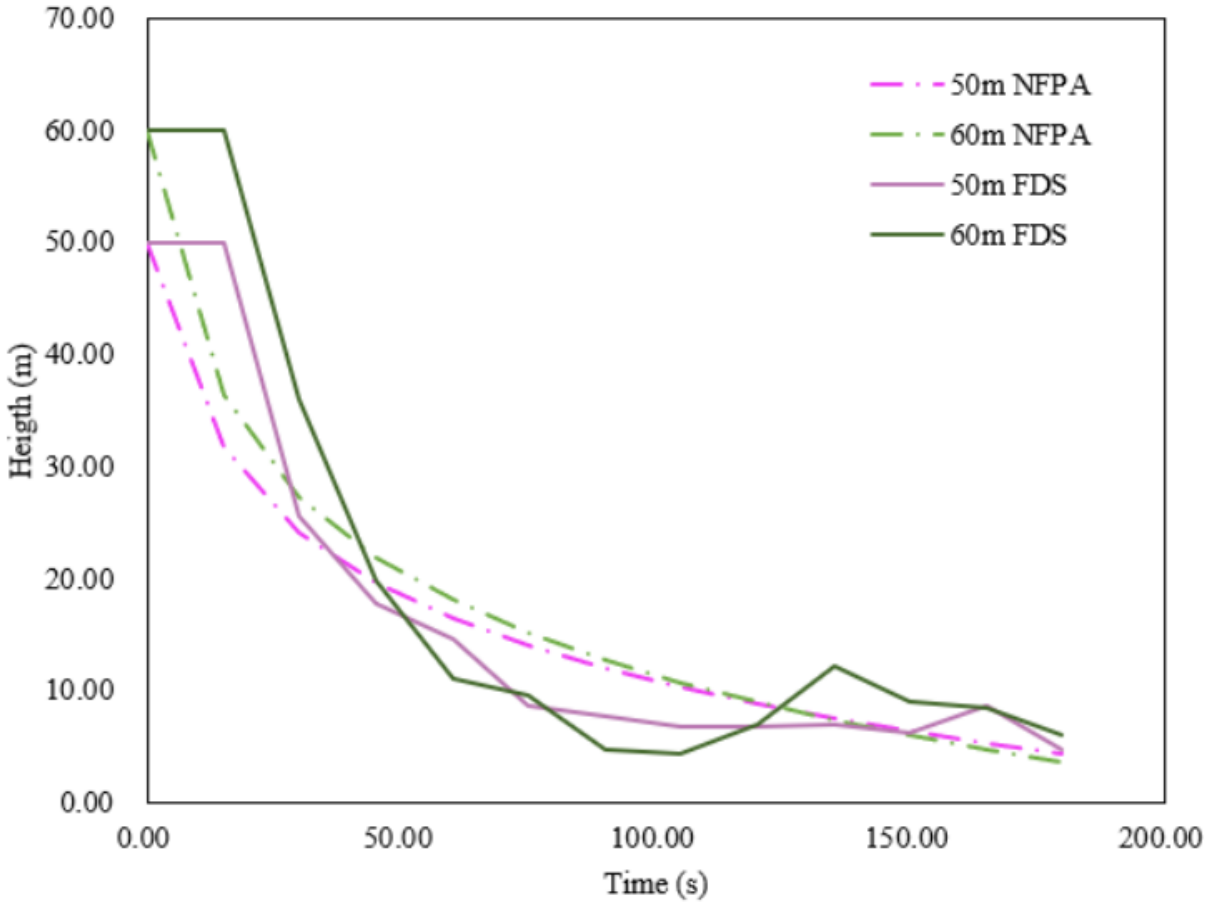

Figure 5-9 Improved correlation between smoke layer height and time when the atrium height of 50m and 60m with 20m width x 20m length (5MW) is altered using constant 0.22

From Figure 5-7 to Figure 5-9, it is evident that the overlapping issue has been resolved and the smooth curve generated by the formulae can be applicable for all atrium heights. Once the constant has been altered to the new constants, the stretch of the logarithmic graph is not as evident and causes no overlap. These figures are a better comparison that could be used against the data from FDS.

As the NFPA results become unrealistic on the range of higher atrium, an adjustment of constant starts from 0.20 to 0.27 to investigate the better fitted new constants to cover the range of atrium height from 15m to 60m.

From the results identified from the FDS simulations, the data seems more promising since the transient and steady phases can be properly identified. In addition, the values do not reach a negative number, and this is expected since the height of the smoke layer interface cannot go under 0. The shape of this curve seems to be like Zukoski [44], Thomas [58] and McCaffrey's [57] data, since it also has a transient and steady phase. A diagram of these phases has been shown below.

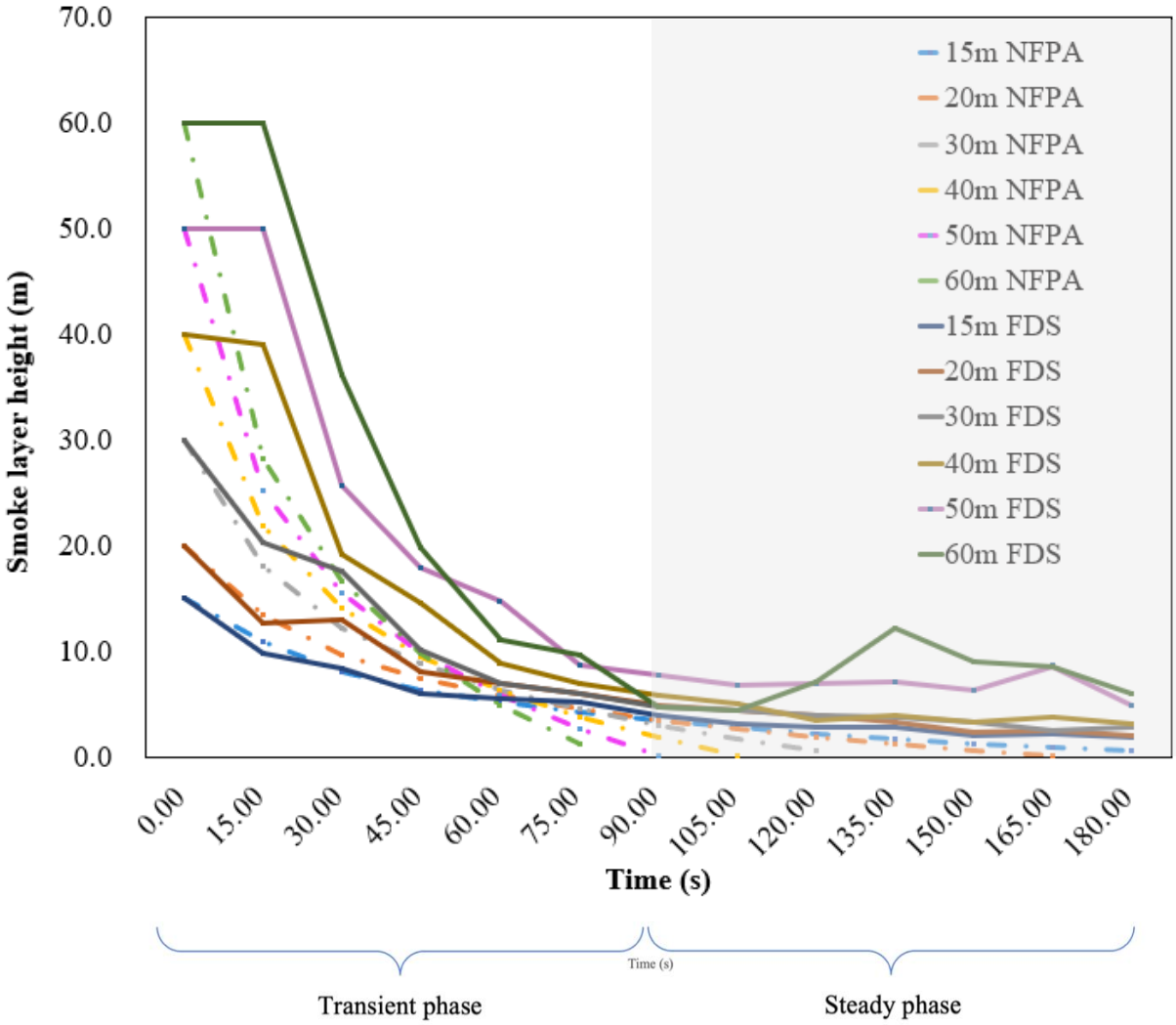

Figure 5-10 Identifying the transient and steady phase from NFPA and FDS data for tall atrium height of 15m, 20m, 30m, 40m, 50m and 60m with 20m width x 20m length (5MW) with constant 0.28

From Figure 5-10, there are some lines that go beyond 0. The values for smoke layer height cannot be lower than 0. Therefore, 0.28 is obviously not suitable for the lines explored by the NFPA results in this situation.

By adjusting the constant from the formulae for the smoke layer height from NFPA correlation, the data seems to be more aligned with the FDS and provides a stronger correlation between the FDS model and the calculated model. Even though the steady phase is not as prominent in the NFPA result, the trend still follows and seems to be relatively close to that of the FDS data. The original crossover from the calculated data was likely due to the constant (0.28) and the stretch of the logarithmic graph. By eliminating this problem, the

results can be considered as a more accurate representation of the data. There is good agreement between the calculated and FDS results.

Table 5-2 Results table for the correction of constant for various atrium heights

Correction of Constant for different atrium height with 20m width and 20m length

Atrium Height (M)	Traditional Constant	New Constant	Section Aspect Ratio (SAR) (H/W)
15	0.28	0.28	0.75
20	0.28	0.25	1.00
30	0.28	0.25	1.50
40	0.28	0.24	2.00
50	0.28	0.22	2.50
60	0.28	0.22	3.00

5.2.5 Investigating the smoke depth from an axisymmetric plume and how variations in atrium length affect the smoke generated – Long Atrium

When considering both methods used to generate a value for the smoke height layer, the value for smoke depth can be evaluated by both hand calculation and by FDS [5]. Below is a comparison that has been done to investigate how different atrium lengths affect the development of smoke depth. The following atrium lengths have been used: 15m, 20m, 30m, 40m, 50m and 60m. The transient phase and steady phase will also be considered since they form a crucial part of this exploration.

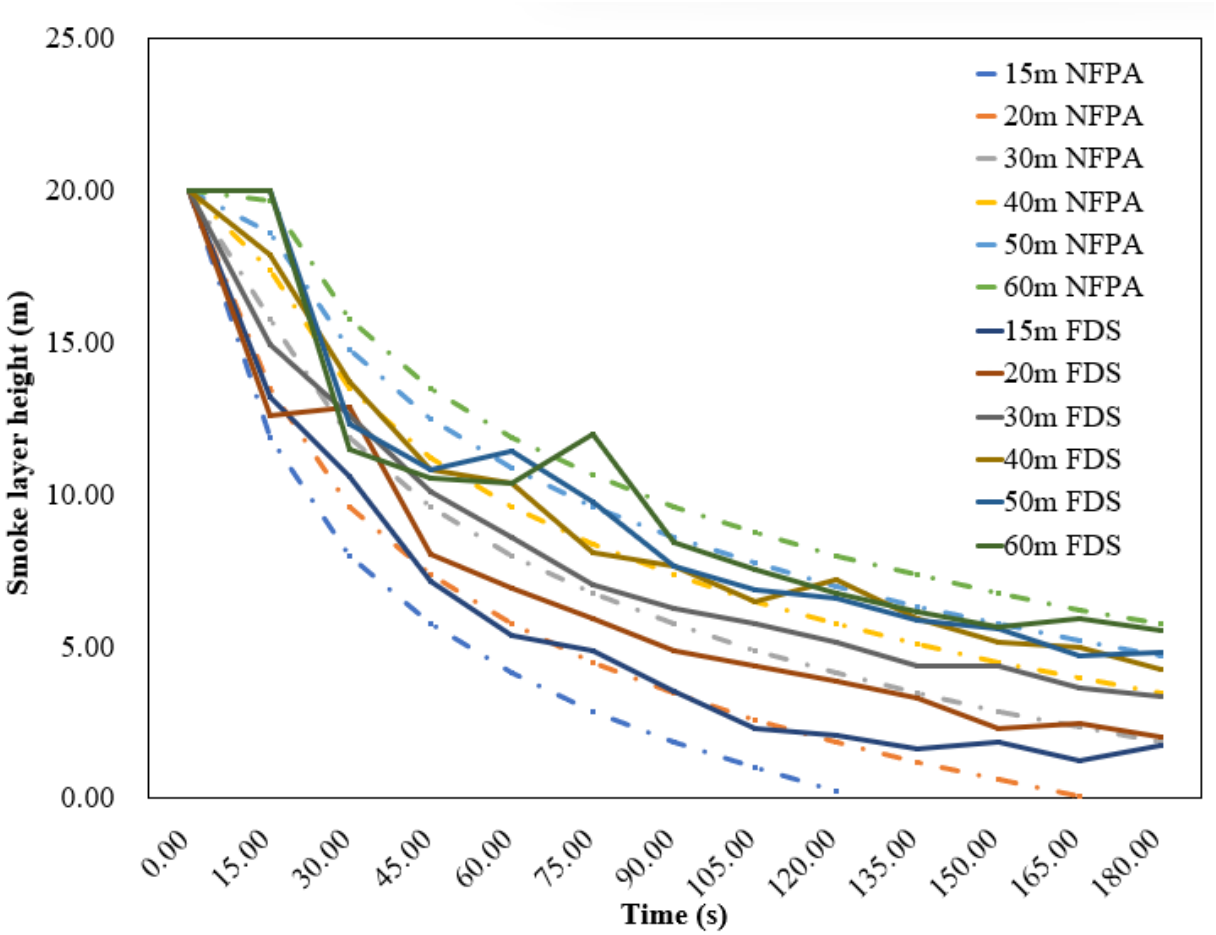

Figure 5-11 Combined NFPA92 and FDS to identify the smoke layer height and comparing it against different atrium lengths of 15m, 20m, 30m, 40m, 50m and 60m with 20m width x 20m height (5MW) using Constant 0.28

Figure 5-11 presents the smoke layer height when a range of different atrium lengths are considered. Using FDS to identify the smoke layer height and comparing it against different atrium lengths. From Figure 5-11, because the floor area has been changed according to length; atrium 15m in length with a ratio of 0.75 to a height of 20m, the smoke layer height drops more steeply than the other ratio. In general, the slope becomes flattered at the longer length ratio by using the equation with a constant of 0.28 for the hand theoretical height of NFPA correlation.

For the smoke layer height from FDS results, the longer atria do not have the same sloping as the shorter atria. It becomes obvious when the length is increased.

From the combined graph, the results from NPFA do not match the data collected from FDS. Therefore, the adjustment of the constant has been done with other constant figures, to find the more appropriate constant.

Table 5-3 Results table for the mean square error (MSE) comparison of applying different constants of varying atrium lengths

Atrium Length (M)	Constant								
	0.20	**0.21**	**0.22**	**0.23**	**0.24**	**0.25**	**0.26**	**0.27**	**0.28**
15	11.39	7.70	4.75	2.54	1.08	0.36	0.39	1.16	2.67
20	10.84	8.32	5.30	2.83	1.53	0.78	0.80	1.58	3.13
30	13.59	9.81	6.66	4.13	2.22	0.94	0.28	0.24	1.19
40	12.63	9.33	6.54	4.25	2.48	1.21	0.46	0.21	0.48
50	17.79	14.19	11.01	8.27	5.95	4.07	2.62	1.59	0.96
60	21.21	17.64	14.43	11.60	9.13	7.04	7.04	3.97	2.77

From Table 5-3, constant 0.25 and 0.27 are better fitted at 15-20m and 30-40m respectively than 0.28 as specified in the NFPA 92 (2021).

5.2.6 Constant 0.25 for atrium length range from 15m to 20m

Figure 5-12 shows the updated smoke layer height of NFPA compared with FDS comparison for using the improved constant 0.25 for the 10m and 20m long atrium:

Figure 5-12 is an improved graph for the NFPA.

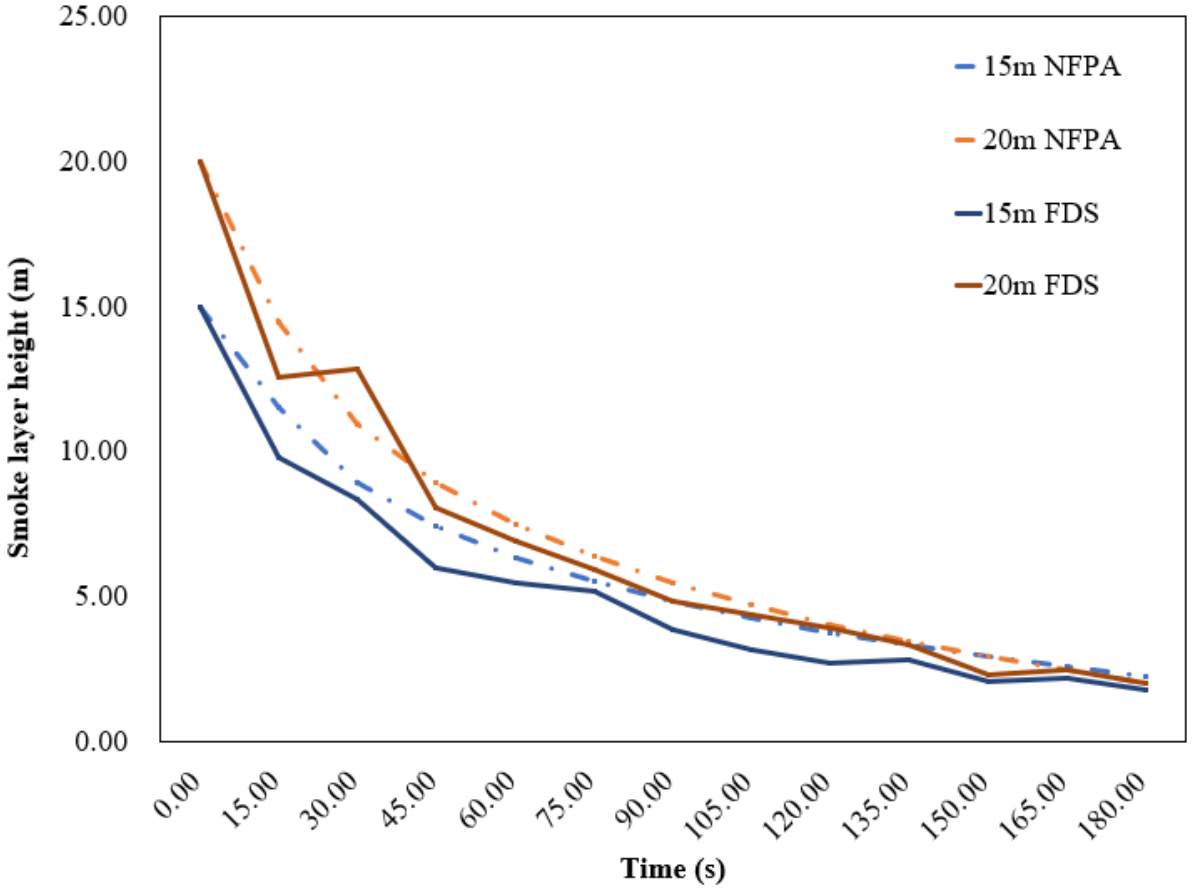

Figure 5-12 Improved correlation between smoke layer height and time when the atrium length of 15m and 20m with 20m width x 20m height (5MW) is altered for using constant 0.25

From Figure 5-12, it is evident that the overlapping issue has been resolved and the smooth curve generated by the formulae applied to all atrium lengths. Once the constant has been altered to 0.25, the stretch of the logarithmic graph is not as evident and causes no overlap. This figure is a better comparison that could be used against the data from FDS.

5.2.7 Constant 0.27 for atrium length range from 30m to 40m

Figure 5-13 shows the updated smoke layer height of NFPA compared with FDS comparison for using the improved constant 0.27 for the 30m to 40m long atrium:

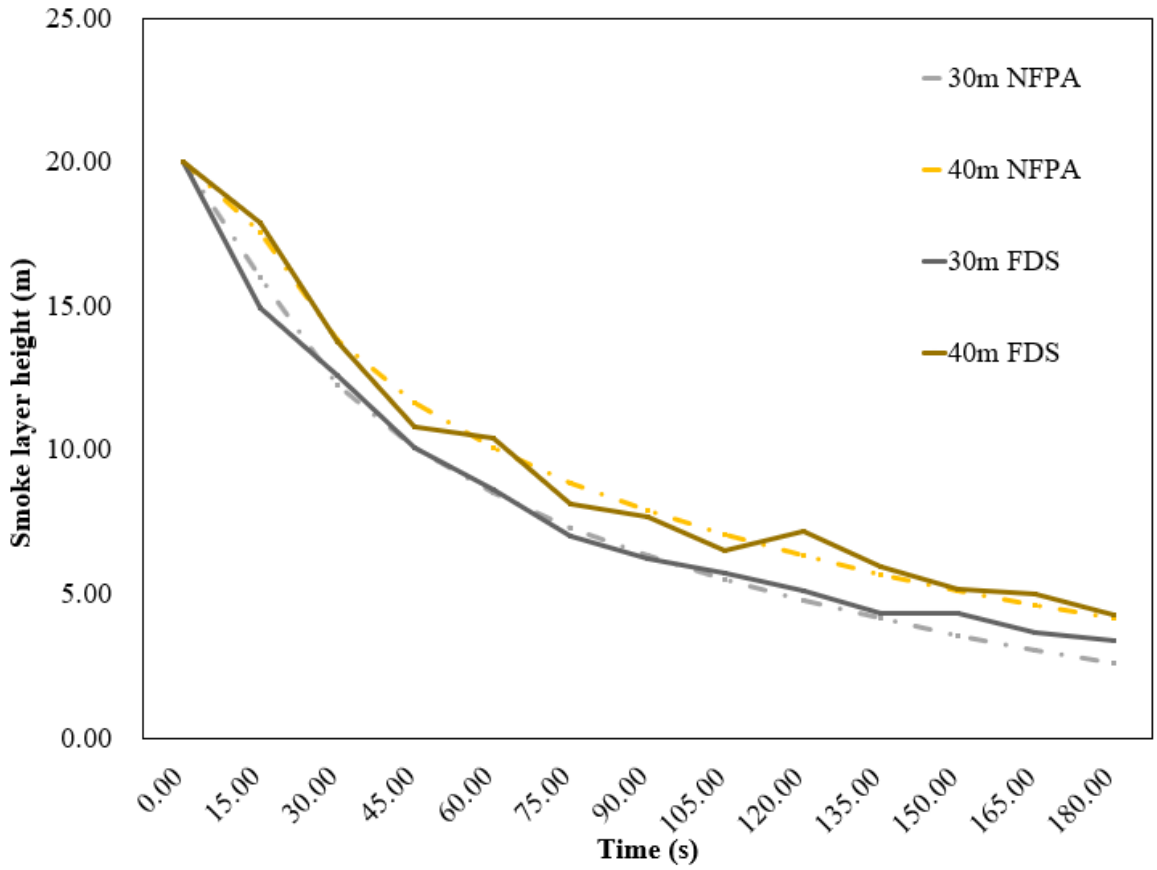

Figure 5-13 Improved correlation between smoke layer height and time when the atrium length of 30m and 40m with 20m width x 20m height (5MW) is altered for using constant 0.27

From Figure 5-12 and Figure 5-13, it is evident that the issue of quickly dropping at a shorter length atrium has been resolved and the smooth curve generated by the formulae can be applicable for all atrium lengths. Once the constant has been altered to 0.25 and 0.27, the stretch of the logarithmic graph is better matched with the data from FDS.

The results from the FDS simulations indicate more promising since the transient and steady phases can be properly identified. In addition, the values do not reach a negative number, and this is expected since the height of the smoke layer interface cannot go under 0. The shape of this curve seems to be like Zukoski [44], Thomas [58] and McCaffrey's data [57] since it also has a transient and steady phase. A diagram of these phases has been shown in Figure 5-14.

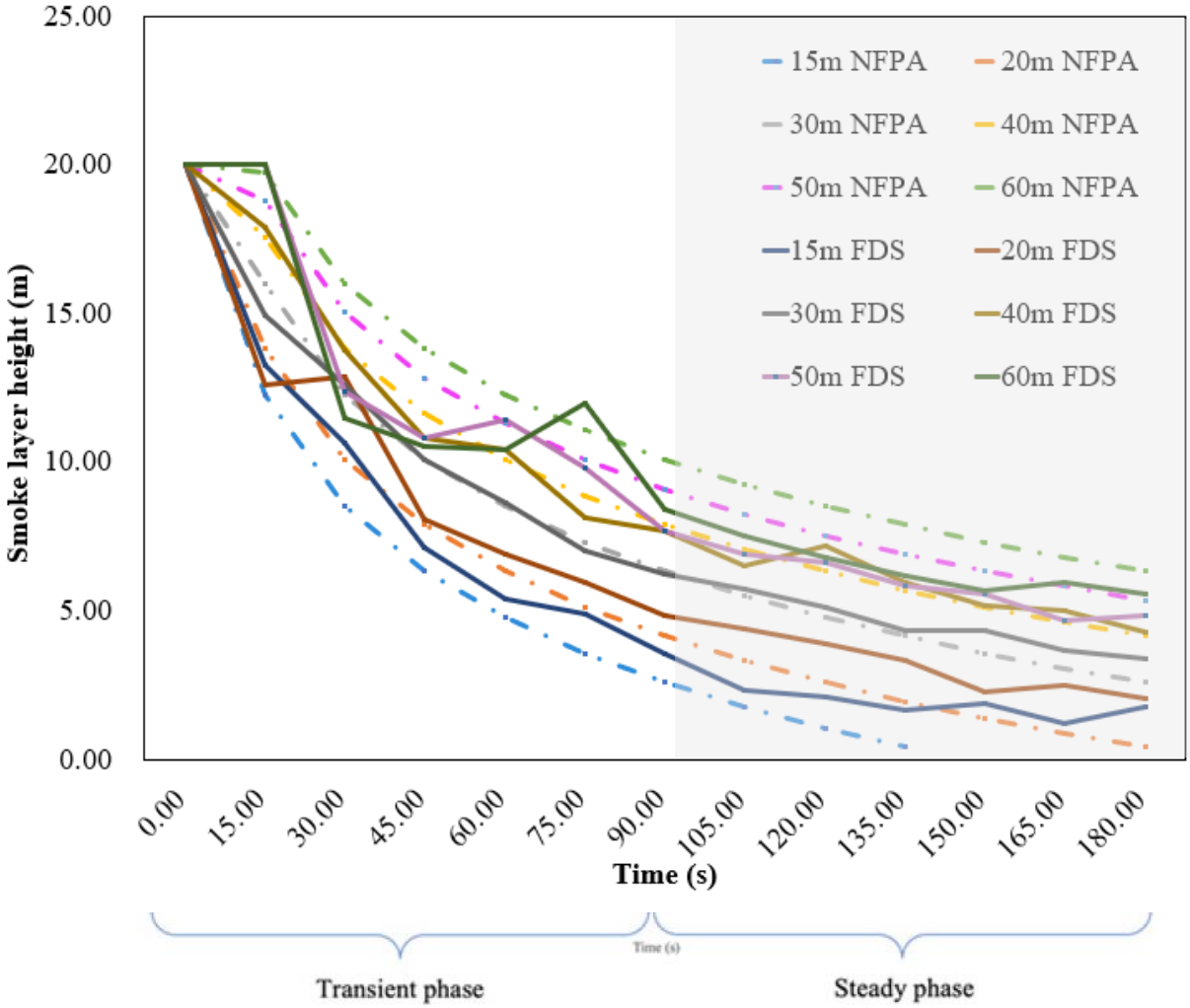

Figure 5-14 Identifying the transient and steady phase from NFPA and FDS data for long atrium length of 15m, 20m, 30m, 40m, 50m and 60m with 20m width x 20m height (5MW) using Constant 0.27

Figure 5-14 shows that by adjusting constant 0.27, the lines 30m and 40m atrium are now at positive value and found suitable when compared with the FDS results.

By adjusting the constant from the formulae for the NFPA with constants 0.25 and 0.27, the data seems to be more aligned with the FDS and provides a stronger correlation between the FDS model and the calculated model. Even though the steady phase is not as prominent in the theoretical z result, the trend still follows and seems to be relatively close to that of the FDS data. The original steep drop from the calculated data was likely due to the constant (0.28) and the stretch of the logarithmic graph. By eliminating this problem, the results can be considered a more accurate representation of the data. There is a better agreement between the calculated and FDS.

The above alternation is due to the constant used in the original equation based on research by Heskestad, 1977 [66], Nowler, 1987 [51], Mulholland et. al., 1981 [52], and Hagglund, 1985 [53] and review by Chow and Li, 2005 [54]. Together with an experiment with dimensions of 6m cubic by Hagglund, 1985 [53], all these referrals are over 33 to 44 years ago, compared to the modern atria which have a much larger volume and dimension length. The new constants of 0.25 and 0.27 fit better in the lower range of length atria than the original 0.28.

For the minimum smoke clear height is either twenty percent of the floor-to-ceiling height or 2 metres above the ground level as referred to the requirement by NFPA92, 2021 [1].

Table 5-4 Minimum smoke clear height (twenty percent of atrium height)

Atrium Length	Atrium Height	20% Minimum Smoke Clear Height (m)
15	20	4.00
20	20	4.00
30	20	4.00
40	20	4.00
50	20	4.00
60	20	4.00

Table 5-4 is minimum smoke clear height according to the requirements in NPFA92 for the mandatory height in the tenable conditions for the occupants in the fire scenarios.

Table 5-5 Minimum smoke clear height to atrium height (NFPA)

	Smoke Layer Height / Atrium Height (%)					
T (s)	15m	20m	30m	40m	50m	60m
0.00	100.00	100.00	100.00	100.00	100.00	100.00
15.00	64.99	72.18	82.32	89.51	95.09	99.65
30.00	47.66	54.85	64.99	72.18	77.76	82.32
45.00	37.52	44.71	54.85	62.04	67.62	72.18
60.00	30.33	37.52	47.66	54.85	60.43	64.99
75.00	24.75	31.94	42.08	49.27	54.85	59.41
90.00	20.19	27.39	37.52	44.71	50.29	54.85
105.00	16.34	23.53	33.67	40.86	46.44	51.00

120.00	13.00	20.19	30.33	37.52	43.10	47.66
135.00	10.06	17.25	27.39	34.58	40.16	44.71
150.00	7.42	14.62	24.75	31.94	37.52	42.08
165.00	5.04	12.23	22.37	29.56	35.14	39.70
180.00	2.87	10.06	20.19	27.39	32.96	37.52
195.00	0.86	8.06	18.19	25.38	30.96	35.52
210.00	0.00	6.20	16.34	23.53	29.11	33.67
225.00	0.00	4.48	14.62	21.81	27.39	31.94
240.00	0.00	2.87	13.00	20.19	25.77	30.33
255.00	0.00	1.35	11.49	18.68	24.26	28.81
270.00	0.00	0.00	10.06	17.25	22.83	27.39
285.00	0.00	0.00	8.71	15.90	21.48	26.03
300.00	0.00	0.00	7.42	14.62	20.19	24.75

The atria all have the same height of 20m. According to the 20% requirement, as shown in Table 5-5, the atrium height defines the clear smoke height in Table 5-6. The time for filling up the atrium height has changed inversely with the atrium length.

Table 5-6 Minimum smoke clear height to atrium height (NFPA) with constant 0.25

	Atrium Length (m)					
t (s)	15m	20m	30m	40m	50m	60m
0.00	20.00	20.00	20.00	20.00	20.00	20.00
15.00	13.00	14.44	16.46	17.90	19.02	19.93
30.00	9.53	10.97	13.00	14.44	15.55	16.46
45.00	7.50	8.94	10.97	12.41	13.52	14.44
60.00	6.07	7.50	9.53	10.97	12.09	13.00
75.00	4.95	6.39	8.42	9.85	10.97	11.88
90.00	4.04	5.48	7.50	8.94	10.06	10.97
105.00	3.27	4.71	6.73	8.17	9.29	10.20
120.00	2.60	4.04	6.07	7.50	8.62	9.53
135.00	2.01	3.45	5.48	6.92	8.03	8.94
150.00	1.48	2.92	4.95	6.39	7.50	8.42
165.00	1.01	2.45	4.47	5.91	7.03	7.94
180.00	0.57	2.01	4.04	5.48	6.59	7.50

195.00	0.17	1.61	3.64	5.08	6.19	7.10
210.00		1.24	3.27	4.71	5.82	6.73
225.00		0.90	2.92	4.36	5.48	6.39
240.00		0.57	2.60	4.04	5.15	6.07
255.00		0.27	2.30	3.74	4.85	5.76
270.00			2.01	3.45	4.57	5.48
285.00			1.74	3.18	4.30	5.21
300.00			1.48	2.92	4.04	4.95

Referring to Table 5-6, the minimum requirement of 2 metre above ground level, the time for reaching this level is longer than the one stated 20 of the height. So, the difference could be a risk issue in the selection of fire safety design.

As the new values 0.25 and 0.27 are different from the original form below, using 0.28 in NFPA92, 2021, Equation 5.4.2.1b [1] for the smoke layer height as in Chapter 3 equation (3.3).

New constants 0.25 and 0.27 are investigated by calculating the Mean Square Error (MSE) of FDS and NFPA for various atrium lengths.

From Table 5-3, the 0.25 constant could be the better selection for covering the 15-20m long atrium and 0.27 is for the 30-40m long atrium.

Constant 0.28 has the lowest mean square error at 50m and 60m. However, it does have a better match with FDS data in Figure 5-5, but not the shorter and longer length atria.
Although in Table 5-3, it shows that 0.28 has the lowest value for 50-60m length atrium, it may not be the optimum value as there is no data for the constant 0.29 and 0.30, or perhaps better fitted would be found in the higher constant. Therefore further work is required to prove where the optimum really lies.
From the above-mentioned graph, because the floor area has been changed according to length; atrium 15m in length with a Section Aspect Ratio (SAR) of 0.75 and Plan Aspect Ratio (PAR) of 1.33 to a height of 20m, the smoke layer height drops more steeply than the other ratio. In general, the slope becomes flattered at the longer length ratio by using the equation of constant 0.28 for the theoretical hand z.

For constants 0.25 and 0.27 have the lowest values at 15-20m and 30-40m respectively. Therefore, these two constants best fit the stated long atria.

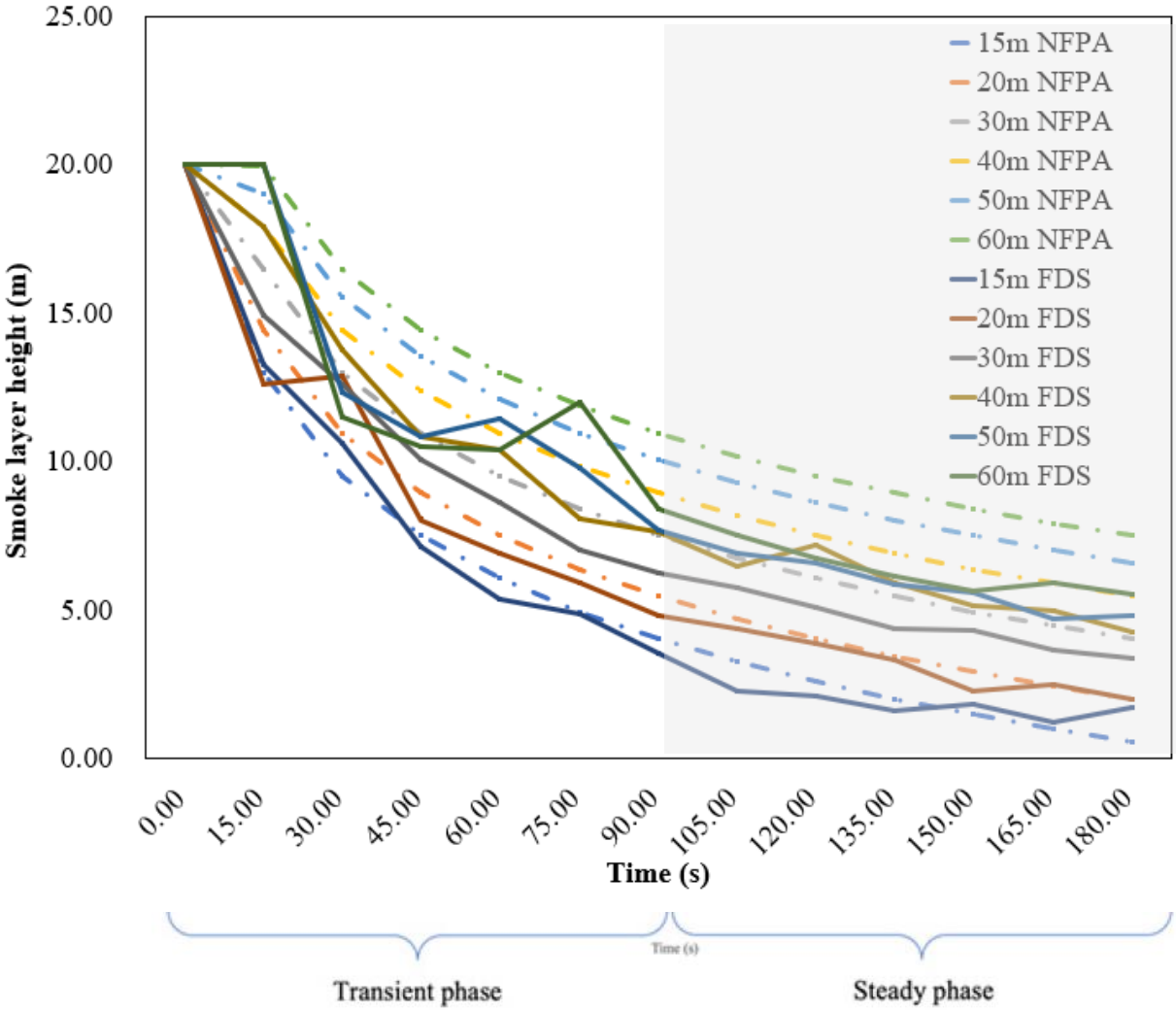

Figure 5-15 FDS and NFPA for the smoke layer height at different atrium lengths of 15m, 20m, 30m, 40m, 50m and 60m with 20m width x 20m height (5MW) using Constant 0.25

By adjusting the constant from the formulae for the theoretical height, the data seems to be more aligned with the FDS and provides a stronger correlation between the FDS model and the calculated model. Even though the steady phase is not as prominent in the theoretical height result, the trend still follows and seems to be relatively close to that of the FDS data. The original steep drop from the calculated data was likely due to the constant (0.28) and the stretch of the logarithmic graph. By eliminating this problem, the results can be considered a more accurate representation of the data. There is a better agreement between the calculated and FDS height.

Table 5-7 Results table for the correction of constant for various atrium lengths

Correction of Constant for different atrium length with 20m width and 20m height

Atrium Length (M)	Traditional Constant	New Constant	Plan Aspect Ratio (PAR) (W/L)
15	0.28	0.25	1.33
20	0.28	0.25	1.00
30	0.28	0.27	0.66
40	0.28	0.27	0.50
50	0.28	0.28	0.40
60	0.28	0.28	0.33

The original constant is found to be appropriate for linear atrium PAR below 0.4 which can be applied to the 50m and 60m length atrium.

5.3 Summary of results

In this chapter, the NFPA empirical correlation (2-33) has been reviewed and updated with new knowledge of what determines the value of the constant.

Traditional value of constant = 0.28

Table 5-8 New Constant for Tall and Long Atrium

Tall Atrium	
Atrium height (M)	New Constant
15	0.28
20	0.25
30	0.25
40	0.24
50	0.22
60	0.22

Long Atrium	
Atrium Length (M)	New Constant
15	0.25
20	0.25
30	0.27
40	0.27
50	0.28
60	0.28

In Table 5-8 the effects of atrium geometry have been studied using state-of-art computer simulation technology and the value of the constant is clearly affected significantly. The trends shown are plotted in Figure 5-16 and Figure 5-17.

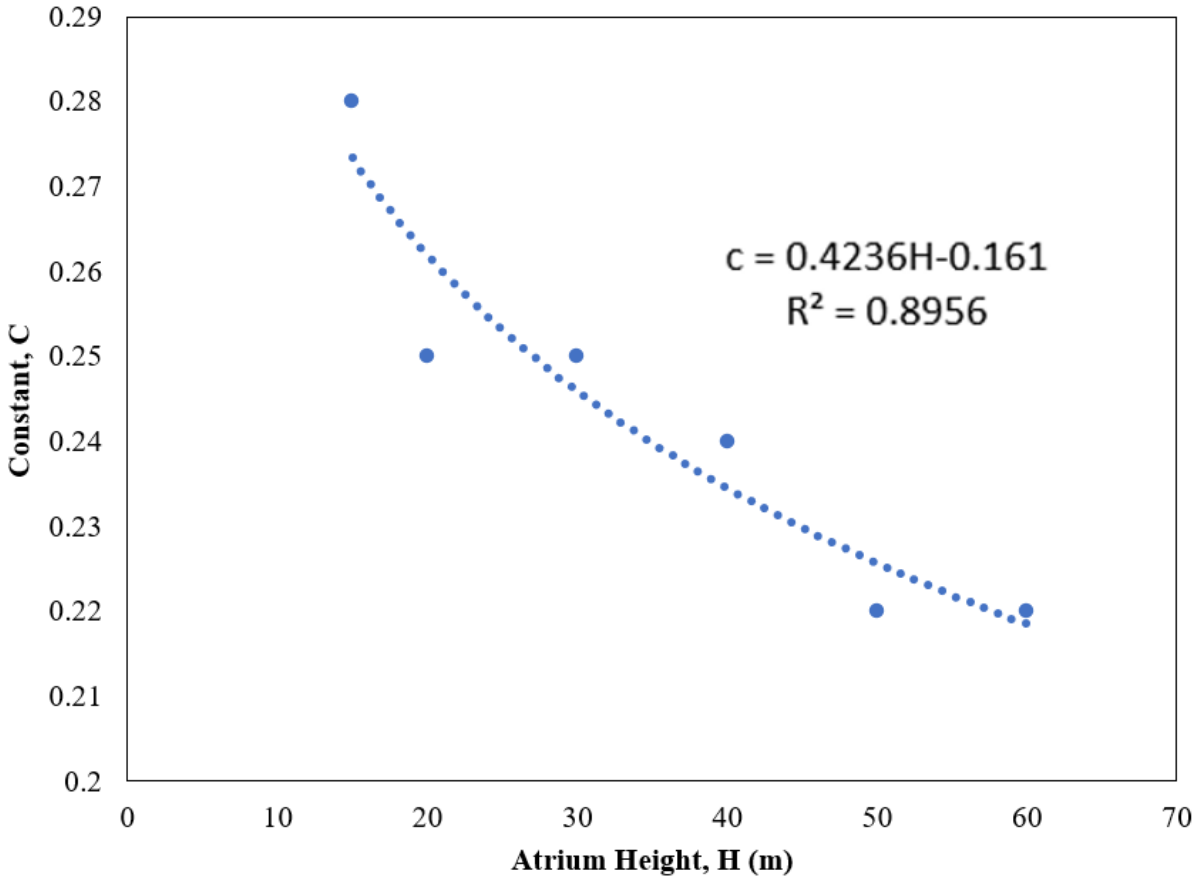

Figure 5-16 R-value of new constant in tall atrium by Power Law

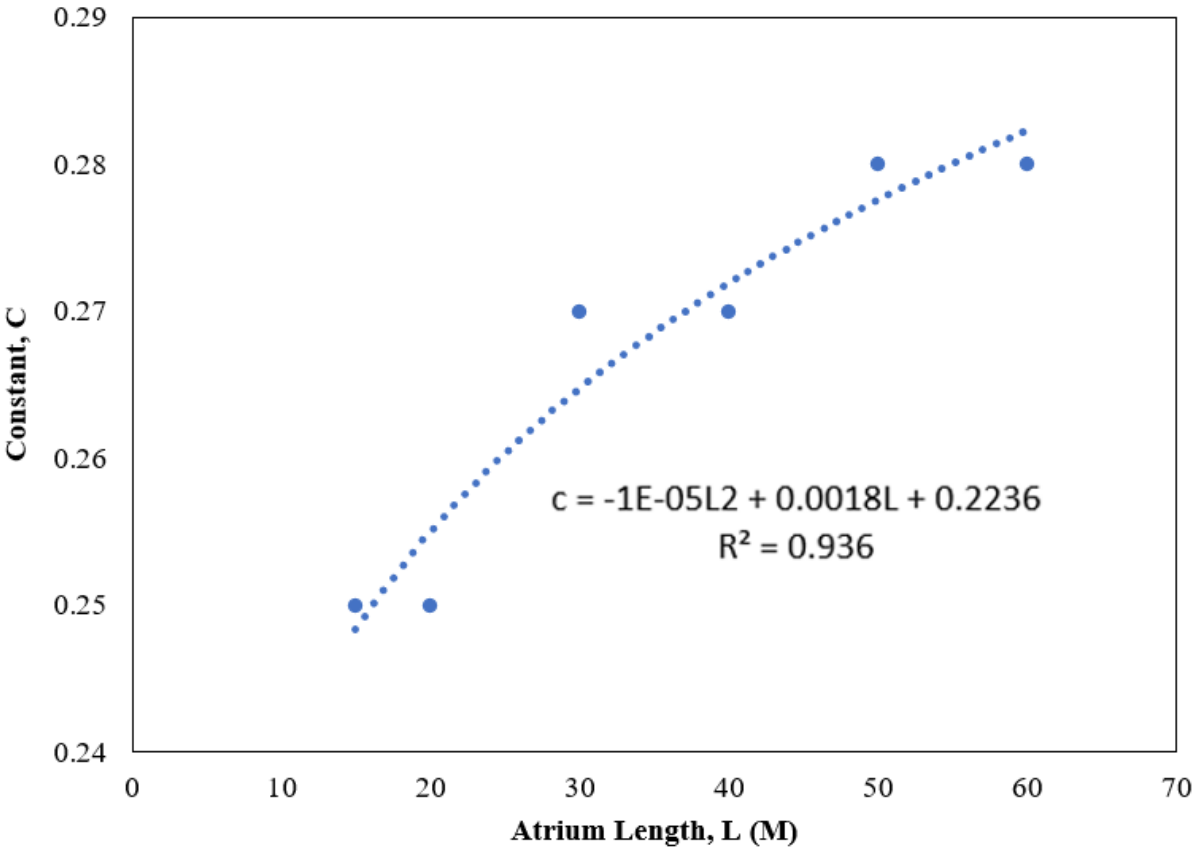

Figure 5-17 R-value of new constant in long atrium by Polynomial

Figure 5-16 shows that the constant decreases with height by up to 20% with height and there is a 90% correlation to a best fit line. Figure 5-17 shows the constant increases in atrium length, a 94% correlation. This is because the larger volume atrium takes longer to fill, but because the smoky layer begins to stratify in the tallest atria.

Because the effect of length and height is small (less than 1%), it is reasonable to treat the constant still as a constant rather than to suggest some power law.

For this reason, the thesis should simply produce tables for the constant as a function of height and length.

When there is a situation for a given length and height, we have two values. For example - a 50m tall atrium (c=0.22) 15m long (c=0.25).

We have two choices. Either we simulate all possible permutations of height and length. Or else we make a reasoned choice to err on the safe side during design.

Assuming the latter, we assume the smoke clear height is the worst result, meaning the smallest value of the constant in the formula.

Power Law is being considered better fit as it has a higher R-value in the tall atrium. Polynomial is the best fit for long atrium.

From the results from the calculated and the FDS simulation, this study finds that the constant is not universally applicable to the high and long atrium.

For the tall atrium, 15m, 20m, 30m, 40m, 50m and 60m, the constant in correlation decreased and inverted as the height increased.

For the high atrium, the constants 0.25 and 0.24 are better fitted at 20-30m and 40m respectively than 0.28 as specified in the NFPA 92, 2021.

For the long atrium, the constants 0.25 and 0.27 are better fitted at 15-20m and 30-40m respectively than 0.28 as specified in the NFPA 92, 2021.

Table 5-9 Constant for different atrium heights and lengths

Atrium Type	Constant
Traditional	0.28
Tall	
15m	0.28
20-30m	0.25
40m	0.24
50-60m	0.22
Long	
15-20m	0.25
30-40m	0.27
50-60m	0.28

The new constants in Table 5-9 show that the trend in tall is inversely to the height of the atrium. For the long atrium, the smaller value is found to be better fitted to the shorter length atrium.

From equation 5-7, a larger value for the constant corresponds to a larger value Z. So, to err on the conservative side of safety the smaller value should always be used.

CHAPTER 6: Conclusions and Future Work

This chapter presents the conclusions of the research described in the thesis and the results fed into practice. The aim and objectives of the research are reviewed, and their achievement addressed.

Chapter 2 was a review of the engineering design process as well as literature to set the context of this study. The engineering design process used today follows a small number of design codes and guides which employ empirical and semi-empirical relationships dating back decades around the world. The development and refinement of these formulas has always followed experimental studies to consider specific cases and reinvigorate the data as building materials evolve. However, the studies are usually 'one-project deep' and have not taken advantage of the modern computational fluid dynamics software that has emerged in the last generation. Furthermore, some data was observational, such as where smoke is humanly visible. A CFD study would be more objective and quantified. It is the first result of this study to identify this technology's absence and examine a way to update any of the formulae. Thus, a methodology was selected, enlightened by the literature survey.

It was found that atria are a massively changing sub-field of study; with new materials and sheer scale. So, it was decided to examine one of those 'old' design formulae, atrium smoke filling, in comparison to CFD. The relationships, data of previous studies in from literature including NFPA and Yang were compared to FDS, Fire Dynamics Simulator simulations. The aims of the project were narrowed to atria in line with the problems being studied in the literature.

Having selected FDS as the working tool for simulations, chapter 3 reports on the validation work of the modelling for application to atria. A mesh resolution study was performed and the results of validation were good.

A parametric approach has been used in chapter 4 to examine how the scale of atria affects the established design criteria and formulae. The CFD simulations considered Different heat release rates and different fuels. The focus in tall atrium was stratification; the physical understanding of this phenomenon is a function of the weight and mobility of the smoke and depends on temperature and pressure.

In chapter 5, new values were found for the ‘constants’. Ultimately a simple table was produced for what value constant to use when the atrium dimensions are varied.

Finally, this chapter 6 is a discussion of all the results and future work.

Newly developed constants were found for tall and long atria. The new constants can be fed into practice by replacing the traditional one. In future work, deeper analysis of mechanisms in well-ventilated conditions, other new proposals to try different methods, other complex types of atria were to be evaluated in conditions.

This thesis investigated the possibility of adjusting the constant in the NFPA correlation for the expected smoke layer height in the modern tall and long atrium. It proves the importance of the updated technology of computer simulation for fire dynamics in verification of past experiment data may not be applicable to architectural buildings nowadays. The findings are the constants 0.25 and 0.24 have a more appropriate value for the tall atrium with 20-30m and 40m respectively. For the constants 0.25 and 0.27 would be the better fitted values for 15-20m and 30-40m respectively in the long atrium. Both of which the constant in the NFPA 92 (2021) is 0.28. Not much difference between using the traditional constant 0.28 in short atrium of 15m height and longer atrium of 50-60m length. However, further study is required for investigating the optimum constant value of 50-60m length atrium.

The results also proved that this simple conventional equation is valuable for the determination of a preliminary study in fire safety of atrium after adjusting the constant according to its aspect ratio or geometric dimensions. A change of height and length of a large in sized atrium has a close relationship with the constants studied and evaluated.

The results are reliable, reproducible, and verifiable. It is selected based on the appropriate use of sampling that provides confidence in the research conclusions.

Exercise a degree of due care appropriate to the importance of the safety design and the confidence placed in the research by the analysis and when planning, conducting, and reporting taken into consideration. Focus on matters that ensure the new constant can achieve reliable results.

6.1 Fulfilment of the aims of this study

By numerical tools, FDS and correlations are used in legal statutory requirements and industry-standards to predict smoke behavior in the atria and analyses the physical mechanisms of smoke filling and characteristics in various dimensions of atria.

Also evaluated the effect of geometry and HRR on the smoke filling processes in the atria and exhibited the limitations of current methodologies for smoke filling when applied in the atria. A way to achieve compatible results of the measurement outcomes in order to justify prior codes based on knowledge of the past and improve the nowadays environment.

Finally, a holistic methodology is developed with improved practical implementation for smoke filling calculations in the atria.

To achieve the five aims, objectives are listed below with a designed research methodology to seek the gaps in the current knowledge and to realize the research aim:

(1) Literature review of empirical correlations for atria, plus types and configuration of atria;
(2) Literature review of design process;
(3) Literature review of experimental work on atria fires and smoke properties;
(4) Literature review of previous empirical correlations, with an emphasis on accurately estimating smoke layer, smoke-filling time and smoke production rate;
(5) Development of a numerical methodology using CFD to accurately simulate atrium smoke-filling;
(6) Data from past experimental data and fuel sources collected and compared with FDS for validation and verification;
(7) Parametric analysis of the effect of atrium geometric characteristics and HRR on smoke layer formation;
(8) Evaluation of empirical constants currently used in NFPA 92 for smoke layer height based on cross-sectional area; and
(9) Development of empirical calculations.

A literature review was conducted into the design process and the relationships used. It was found that dated empirical correlations are widespread and that modern CFD was hardly considered as a method. CFD shows a wealth of information on the fine structure of plume and smoky layer and can provide ‘why?’ explanations for the formula that were created by simple observation.

In this thesis, the addressed queries are recognized by using graph representations and graph matching.

Discussions of different tall and long atria are provided and presented for evaluation. Proposed new a constant to solve the gap in the current knowledge and improve the accuracy of the correlation.

Comparisons of the tall atria height of 15m, 20m, 30m, 40m, 50m and 60m with 20m width x 20m length and long atria length of 15m, 20m, 30m, 40m, 50m and 60m with 20m width x 20m height with 5MW centre fire with the correlation in NFPA 92 have been done. The new constant of the tall and long atria was introduced for solving the graph matching problem. Comparison of the results from theoretical correlations among different geometrical dimensions has been realized and is much relied on the developmental computation technology applied in the simulation of fire scenarios, which has been a vital part of the research methodology. Also, the original constraints on the correlation have been considered.

The new constant may enlarge the potential application to the fire safety design process.

The list of factors that affect the atrium fire safety design is height, length and the constant specified in the empirical correlation.

6.2 How results can be fed into practice

The purpose of this study is to align the equation coping with the new trends of atrium design. This is achieved by adjusting the constant of the original correlation in the code of practice – industry standard guidebook which provided a more appropriate logical order that helps the fire safety design to stay on track and achieve the goals which will close the present gap.

Provide a reference to management of the need for safety design, as well as those required by the standards as necessary for continued improvement and fulfilling the legal statutory and international parties' requirements.

The safety objectives are being met. The result could be proactive in preparing the design for fire safety.

The newly developed methodology of calculating the smoke layer height would be fed into the fire safety design with respect to the different SAR or PAR architectural geometry of the atria. In other words, fire engineers would have another reference to performing a design process.

This makes the design process more accountable when comparing the numerical analysis and demonstrating to stakeholders including the clients and architects in the QDR meetings. That means the evaluation of fire safety design can be more easily understood and effective and tends to be more illustrative.

6.3 Future work

The main results of this study use a comparison of simulated results to empirical trends observed on a smaller scale. The tall and long atrium in the research study indicated SAR from 0.75 to 3 and PAR from 0.33 to 1.33 and a recommendation is for further work on another ratio in parametric evaluation. Different, more complicated geometries have also been left for the future. Future work concerns the deeper analysis of mechanisms in well-ventilated conditions and other new proposals to try different methods.

The model investigated may be fine enough for extra tall and low atria, which are the current premises built, mainly in Asia. The other complex type of atrium is to be evaluated conditions.

The ultra-tall and thin atrium mentioned is in fact a very low aspect ratio for which the awarding buildings are designed and used nowadays.

From the validation process, the type of fuel, size of fire, smaller or close to 5MW could apply.

Nevertheless, this research has already designed and run numerical experiments to compare the performance of the newly proposed constant based on the existing correlations. As such, it seems to have improved the calculation method as specified in the codes.

Concerning the results for both tall and long atria, the newly developed constant could be exploited to try to achieve a better solution.

References

[1] National Fire Protection Association. (2021). *NFPA 92: Standard for Smoke Control Systems.*

[2] Morgan, H. P., Ghosh, B. K., Garrad, G., Pamlitschka, R., De Smedt, J.-C., & Schoonbaert, L. R. (1999). *Design methodologies for smoke and heat exhaust ventilation (BR 368).* Garston, Liverpool, United Kingdom: IHS BRE Press.

[3] CIBSE. (2010). *Fire Safety Engineering: CIBSE Guide E* (3rd ed.). London, United Kingdom: Chartered Instituition of Building Services Engineers.

[4] CIBSE. (1995). *CIBSE Technical Memoranda TM19: Relationships for Smoke Control Calculations.* London, United Kingdom: The Chartered Instituition of Building Services Engineers.

[5] McGrattan, K., Hostikka, S., Floyd, J., McDermott, R., & Vanella, M. (2020). *Fire Dynamics Simulator User's Guide. Sixth Edition.* Gaithersburg, Maryland, United States of America: National Institute of Standards and Technology. doi:http://dx.doi.org/10.6028/NIST.SP.1019

[6] Our World in Data. Institute for Health Metrics and Evaluation, Global Burden of Disease (2019), https://ourworldindata.org/grapher/fire-deaths-by-age?country=~OWID_WRL

[7] Marty Ahrens and Ben Evarts, (2021), *Fire Loss in the United States during 2020 - NFPA*. https://www.nfpa.org/-/media/Files/News-and-Research/Fire-statistics-and-reports/US-Fire-Problem/osFireLoss.pdf.

[8] International Building Code (IBC), (2021), *US International Code Council (ICC)*

[9] *ISO 23932-1:2018 Fire safety engineering - General principles - Part 1: General*, International Organization for Standardization

[10] British Standard BS 9999. (2017), *Fire Safety in the Design, Management and Use of Buildings. Code of Practice*; British Standard: London, UK

[11] Morgan J. Hurley, John R. Hall, Kazunori Harada, Erica Kuligowski, Milosh Puchovsky, Jose Torero, John M. Watts, and Christopher Wieczorek ed. (2016). *SFPE handbook of fire protection engineering.* 5th ed. New York, United States: Springer, New York.

[12] Thomas, P. H., Morgan, H. P., & Marshall, N. R. (1998). *The Spill Plume in Smoke Control Design*. Fire Safety Journal, 30(1), 21-46.

[13] Law, M. (1986). *Translation of Research into Practice: Building Design in Fire Safety Science: Proceedings of the First International Symposium.* Berkeley, California , United States of America.

[14] Thomas, P. H. (1987). *On the upward movement of smoke and related shopping mall problems* (Vol. 12). Fire Safety Journal.

[15] Klote, J. H., & Milke, J. A. (1992). *Design of smoke management systems.* Atlanta, Georgia, United States of America: American Society of Heating, Refrigerating and Air-Conditioning Engineers.

[16] National Fire Protection Association. (2005). *NFPA 92B Guide For Smoke Management Systems in Malls, Atria, and Large Areas* (2005 ed.). Quincy, Massachusetts, United States of America: NFPA.

[17] Littlefair, P.J. (2002). *Daylight prediction in atrium buildings.* Solar Energy, 73, 105-109.

[18] Moosavi, Leila et al. *Thermal performance of atria: An overview of natural ventilation effective designs.* Renewable & Sustainable Energy Reviews 34 (2014): 654-670.

[19] Lan Wang, Qiong Huang, Qi Zhang, Hong Xu, Richard K.K. Yuen, (2017), *Role of atrium geometry in building energy consumption: The case of a fully air-conditioned enclosed atrium in cold climates*, China, Energy and Buildings, Volume 151, 2017

[20] Yunus, J., Ahmad, S.S. and Zain-Ahmed, A. (2010), *Analysis of atrium's architectural aspects in office buildings under tropical sky conditions.* 2010 International Conference on Science and Social Research (CSSR 2010)

[21] Fatma Abass, Lokman Hakim Ismail And Mohmed Solla, B. (2016), *A Review of Courtyard House: History Evolution Forms, And Functions.* ARPN Journal of Engineering and Applied Sciences, VOL. 11, NO. 4

[22] Danielski, I., Krook, M., & Weimer, K. (2018). *Atrium in residential buildings – a design to enhance social interaction in urban areas in Nordic climates.* In Cold Climate HVAC 2018 : Sustainable Buildings in Cold Climates (pp. 773–789). https://doi.org/10.1007/978-3-030-00662-4_65

[23] Bednar, M. J. (1986). *The new atrium*. New York City, New York, United States of America: McGraw-Hill Inc.

[24] Nasrollahi, et al. (2015). *Appropriate geometrical ratio modeling of atrium for energy efficiency in office buildings.* Journal of Building Performance (2015)

[25] Su, Y., Yi, R., Shao, L., & Riffat, S. (2009). *Daylighting performance of atriums in subtropical climate.* International Journal of Low-Carbon Technologies, 4(4), 230-237.

[26] Hansell, G. O., & Morgan, H. P. (1994). *Design approaches for smoke control in atrium buildings (BR 258).* Borehamwood, England, United Kingdom: Fire Research Station.

[27] British Standard Institution (1997), *BS 5588-7:1997 Incorporating Amendments Nos. 1 and 2 Fire precautions in the design, construction and use of buildings — Part 7: Code of practice for the incorporation of atria in buildings*. British Standard Institution

[28] British Standard BS 7974. (2019), Application of Fire Safety Engineering Principles to the Design of Buildings. Code of Practice; British Standard: London, UK

[29] National Fire Protection Association (2006), NFPA 5000, Building construction and safety code, Quincy, MA, USA.

[30] British Standards Institution. (1997). *DD240 (DD240 part 1: 1997) Fire safety engineering in buildings. Guide to the application of fire safety engineering principles.* London, United Kingdom: British Standards Instituition

[31] The International Fire Engineering Guidelines (IFEG), (2005), Australian Building Codes Board (ABCB), the Canadian Codes Centre of the National Research Council of Canada (NRC), the United States International Codes Council (ICC) and MBIE (in its former capacity as the Department of Building and Housing)

[32] National Fire Protection Association, et al. SFPE Engineering Guide to Performance-based Fire Protection Analysis and Design of Buildings, (2000) National Fire Protection Association

[33] ISO 13387:1999 Application of Fire Performance Concepts to Design Objectives. International Organization for Standardization

[34] Kransny, J., Parker, W., & Babrauskas, V. (2001). *Fire behavior of upholstered furniture and mattresses.* Park Ridge, Illinois, United States of America: Noyes Publications.

[35] Zalok, E. (2011). *Validation of methodologies to determine fire loads for use in structural fire protection.* Quincy, Massachusetts, United States of America: Fire Protection Research Foundation; National Fire Protection Association

[36] Heskestad. G. (1972), Similarity Relations for the Initial Convective Flow Generated by Fires, FM Report 72-WA/HT- 17, Factory Mutual Research Corporation, Norwood. MA.

[37] The Hong Kong Institution of Engineers, The Association of Registered Fire Service Installation contractors of Hong Kong Ltd (FSICA) (2009). *HKIE CPD Training Course (II).*

[38] Fried, E. (1972). *Fireground Tactics* (1st ed.). Chicago, Illinois, United States of America: H. Marvin Ginn Corporation.

[39] Tewarson, A. (2008). Generation of Heat and Gaseous, Liquid and Solid Products in Fires. *SFPE Handbook of Fire Protection Engineering*, 3-109 to 3-203.

[40] Hottel, H.C.; Egbert, R.B.: The radiation of furnace gases. Trans. ASME 63 (1941)

[41] Alpert, R.L. (2016). Ceiling Jet Flows. in The SFPE Handbook of Fire Protection Engineering, (5th edition) *SFPE handbook of fire protection engineering.* 5th ed. New York, United States: Springer, New York

[42] Alpert, R. L. (2011). *The Fire-induced Ceiling-jet Revisited.*

[43] Karlsson, B., & Quintiere, J. G., Second Edition (2022). *Enclosure fire dynamics.* Boca Raton, Florida, United States of America: CRC Press.

[44] Zukoski, E. E., Kubota, T., & Cetegen, B. M. (1980-81). Entrainment in fire plumes. *Fire safety journal, 3*(2), 107-121.

[45] Alpert, R. L., & Ward, E. J. (1984). *Evaluating unsprinklered fire hazards* (Vol. 7). Boston, Massachusetts, United States of America: Society of Fire Protection Engineers. doi:https://doi.org/10.1016/0379-7112(84)90033-X

[46] Morton, B. R., Taylor, G. I., & Turner, J. S. (1956). *Turbulent gravitational convection from maintained and instantaneous sources.* London, United Kingdom: The Royal Society. doi:https://doi.org/10.1098/rspa.1956.0011

[47] Developed and maintained by the NFCC, Hazard Fires in tall buildings, (2020) https://www.ukfrs.com/guidance/search/fires-tall-buildings

[48] New measures to improve building safety standards, (2020), https://www.gov.uk/government/news/new-measures-to-improve-building-safety-standards

[49] Emporis GmbH, (2022), https://www.emporis.com/building/standard/3/high-rise-building

[50] Heskestad G. & Delichatsios M.A., (1977). *Environments of fire detectors − phase 1: Effect of fire size, ceiling height and materials, Volume I − Measurements (NBS-GCR-77-86), Volume II − Analysis (NBS-GCR-77-95),* National Bureau of Standards, Gaithersburg MD

[51] Nowlen S.P. (1987). *Enclosure environment characterization testing for the base line validation of computer fire simulation codes, NUREG/CR-4681, SAND 86-1296*, Sandia National Laboratories

[52] Mulholland G., Handa, T, Sugawa O., and Yamamoto H., (1981). *Smoke filling in an enclosure Paper 81-Ht-8,* The American Society of Mechanical Engineers

[53] Hagglund B., Jansson R. and Nireus K. (1985). *Smoke filling experiments in a 6 × 6 × 6 meter enclosure, FOA Rapport C20585-06*, Forsavrets Forskningsanstalt, Sweden

[54] Chow, W. K., & Li, J. (2005). *Review on design guides for smoke management system in an atrium* (Vol. 7). International Journal on Engineering Performance-Based Fire Codes, Volume 7, Number 2, p65-87.

[55] Klote, J. K. (1994). *Method of predicting smoke movement in atria with application to smoke management, NSTIR 5516.* Gaithersburg, Maryland, United States of America: National Institute of Standards and Technology.

[56] Heskestad, G. (1984). Engineering relations for fire plumes. *Fire Safety Journal, 7*, 25-32.

[57] McCaffrey, B. J. (1983). Momentum implications for buoyant diffusion flames. *Combustion and Flame, 52*, 149-167. doi:10.1016/0010-2180(83)90129-3

[58] Thomas, P.H., Hinkley, P.L., Theobald, C.R. and Simms, D.L., "Investigations into the Flow of Hot Gases in Roof Venting", Fire Research Technical Paper No. 7, Department of Scientific and Industrial Research and Fire Offices' Committee Joint Fire Research Organization, London, U.K., 1963.

[59] Environmental Design of Atrium Buildings in the U.K. (1990), Conference Proceeding By ASHRAE, 1990

[60] N. Cai, W.K. Chow (2012). Air flow through the door opening induced by a room fire under different ventilation factors. Procedia Engineering.

[61] Wu, G., & Chen, R. (2010). The Analysis of the Natural Smoke Filling Times in an Atrium. *Journal of Combustion*, vol. 2010, Article ID 687039, https://doi.org/10.1155/2010/687039

[62] Yang, K. S., (2004), The Full-Scale Hot Smoke Test and Validation of Passive Smoke Management System in Large Space Building, M.S. thesis, Architecture Research Institute, Taiwan

[63] Zukoski, E. E., (1978), "Development of a Stratified Ceiling Layer in the Early Stages of a Closed -room Fire," Journal of Fire Materials, g, p. 54

[64] McCaffrey, B.J., Quintiere, J.G., and Harkeleroad, M.F., (1981) “Estimating room temperatures and the likelihood of flashover using fire data correlations”, Fire Technology, Vol. 17, No. 2, pp. 98-119

[65] The Math Works, Inc. (2021). MATLAB (Version 2021b) [Computer software]. https://www.mathworks.com/

[66] Węgrzyński, W., Vigne, G., (2017), Experimental and numerical evaluation of the influence of the soot yield on the visibility in smoke in CFD analysis, Fire Safety Journal

[67] Baum, Howard & McCaffrey, BJ. (1989). Fire Induced Flow Field - Theory And Experiment. Fire Safety Science. 2. 129-148. 10.3801/IAFSS.FSS.2-129.

[68] Bastings D. 1988. Fire Safety in Atrium Buildings. Building Research Association of New Zealand, BRANZ Study Report SR15.

[69] American Society of Heating, Refrigerating and Air, & -Conditioning Engineers. (2015). *2015 ASHRAE Handbook - Heating, Ventilating, and Air-Conditioning Applications (SI Edition).* Atlanta, Georgia, United States of America: ASHRAE.

[70] Chow, W. K. (1999). *Atrium smoke filling process in shopping malls of Hong Kong* (Vol. 9). Journal of fire protection engineering. doi:10.1177/104239159800900403

[71] Chow, W. K., & Hung, W. Y. (2001). A Review on Architectural Aspects of Atrium Buildings. *Architectural Science Review*, *44*(3), 285-295. doi:10.1080/00038628.2001.9697484

[72] Chow, W. K., Huo, R., Jin, X. H., & Li, Y. (2005). Experimental studies on natural smoke filling in atrium due to a shop fire. *Building and Environment, 40*, 1185-1193

[73] Heskestad, G. (1984). *Engineering relations for fire plumes* (Vol. 7). Boston, Massachusetts, United States of America: Society of Fire Protection Engineers. doi:https://doi.org/10.1016/0379-7112(84)90005-5

[74] Heskestad, G. (1995). *"Fire Plumes," in SFPE Handbook of Fire Protection Engineering* (2nd ed.). NFPA and SITE.

[75] ISO 16730. (2008). *Fire safety engineering — Assessment, verification and validation of calculation methods* (1st ed.). Geneva, Switzerland: International Organization for Standardization. doi:https://doi.org/10.1007/s10694-014-0432-3

[76] Jin, T. (1981). *Journal of Fire and Flammability* (Vol. 12). Tokyo, Japan: Fire Protection Equipment and Safety Center of Japan.

[77] Khan, M. M., Tewarson, A., & Chaos, M. (2016). Combustion Characteristics of Materials and Generation of Fire Products. *SFPE Handbook of Fire Protection Engineering*, 1143-1232.

[78] Klote, J. H., & Milke, J. A. (2002). *Principles of smoke management.* Atlanta, Georgia, United States of America: American Society of Heating, Refrigerating and Air-Conditioning Engineers.

[79] Lash, D., & Sharples, S. (2007). Daylight in Atrium Buildings: A Critical Review. *Architectural Science Review, 50*(4), 301-312. doi:10.3763/asre.2007.5037

[80] Novozhilov, V. (2012). A Brief Note on the Smoke Filling Equation. *Fire Safety Journal, 47*, 16-17.

[81] NUREG-1824, & EPRI 1011999. (2007). *Verification & validation of selected fire models for nuclear power plant applications.* Palo Alto, California, United States of America: U.S. Nuclear Regulatory Commission and Electric Power Research Institute.

[82] Poreh, M., Morgan, H. P., Marshall, N. R., & Harrison, R. (1998). *Entrainment by Two-Dimensional Spill Plumes* (Vol. 30). Fire Safety Journal.

[83] SFPE G.06. (2011). *Engineering guide : guidelines for substantiating a fire model for a given application.* Bethesda, Maryland, United States of America: Society of Fire Protection Engineers.

[84] Troitzsch, J. H. (2000). Flammability And Fire Behaviour Of TV Sets. *Fire Safety Science, 6*, 979-990. doi:10.3801/IAFSS.FSS.6-979

[85] Wong, W. K., & Chow, W. K. (1993). *Application of the Zone Model FIRST on the Development of Smoke Layer and Evaluation of Smoke Extraction Design for Atria in Hong Kong* (Vol. 11). Journal of Fire Sciences. doi:10.1177/073490419301100405

[86] Wu, P., Zhou, J., & Li, N. (2021). Influences of atrium geometry on the lighting and thermal environments in summer: CFD simulation based on-site measurements for validation.

[87] McGrattan, K., Floyd, J., Forney, G., Baum, H. and Hostikka, S. (2005), Improved Radiation and Combustion Routines for a Large Eddy Simulation Fire Model, Fire Safety Science. Proceedings. Seventh (7th) International Symposium. International Association for Fire Safety Science (IAFSS), Boston, MA

Appendix 1: Sample Calculation of The Heskestad's equation [1]:

Determining the Air Flow Velocity for an atrium with the size 20m length x 20m width x 30m height given that it has run for **15 seconds** with 5MW centre fire load, then calculating the **NFPA** results.

1. Identify the limiting elevation using the equation below in NFPA 92, 2021, Equation 5.5.1.1d [1]:

$$z_l = 0.166 Q_c^{\frac{2}{5}} \tag{3-3}$$

$Q_c = 3500$ kw
$z_l = 4.342$ m

2. Since $z = 17.986$ when $t = 15$, the NFPA 92, 2021, Equation 5.5.1.1e used to determine the mass flow rate is [1]:

$$m = 0.071 Q_c^{\frac{1}{3}} z^{\frac{5}{3}} + 0.0018 Q_c \quad for\ z > z_l \tag{3-4}$$

$m = 139.396$ kg/s

3. Using the mass flow rate to find out the smoke layer temperature, assume T_o is 25℃ in NFPA 92, 2021, Equation 5.5.5 [1]

$$T_s = T_o + \frac{K_s Q_c}{m C_p} \tag{5-6}$$

$T_s = 50.108$ ℃

4. Determine the smoke density assuming that P_{atm} is 101300 Pa NFPA 92, 2021, Equation 5.8b [1]

$$\rho_s = \frac{P_{atm}}{R(T_s + 273)} \tag{5-3}$$

$\rho_s = 1.076$ Kg/m^3

5. Calculating the volumetric flow rate of smoke exhaust with the following formula:

$$Volumetric\ flow\ rate = \frac{m}{\rho_s} \times \frac{1}{Cross{-}sectional\ Area} \quad (5\text{-}4)$$

Volumetric flow rate $= 129.581$ m^3/s

6. Calculating the plume centreline velocity with the following formula:

Calculation Virtual Origin of Pool Fire by Equation in SFPE, 2016, Equation 13.32 [11]:

$$z_0 = -1.02D + 0.083Q^{\frac{2}{5}} \quad (2\text{-}6)$$

D = 1.625 m
$z_0 = 0.847$ m

The equation used to determine the plume centreline velocity SFPE 2016, Equation 13.23 at the NFPA 17.986 m [11]:

$$u_o = 1.03\left(\frac{\dot{Q}_c}{z - z_o}\right)^{\frac{1}{3}} \quad (4\text{-}6)$$

$u_o = 6.065$ m/s